ELECTROANALYSIS OF ALUMINIUM

A thesis submitted in partial fulfilment of the requirements for the degree of

DOCTOR OF PHILOSOPHY IN CHEMISTRY

at the

University of Canterbury

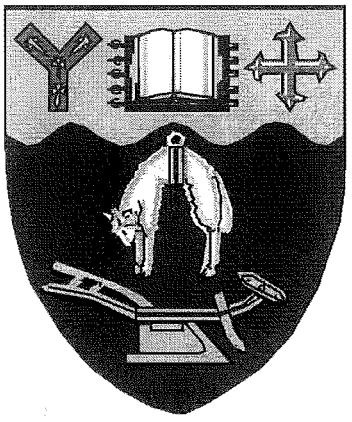

by

Brendon O'Sullivan.

1997

Dedication

A doctoral degree is a large undertaking for anyone. For me it has been a 'rite of passage', in both my personal and professional life. Now that it is complete the people I think most of are the students who shall follow me. Who can say why they do it? Is it courageous ambition or naive stupidity? Either way it is certain that there will continue to be people who commit 3-6 years (or more) of their lives to the gaining of a higher degree. I hope that they may all be at least as fortunate and as tenacious as I have been.

i want to know everything,
i want to be everywhere,
i want to fuck everyone in the world
and i want to do something that matters.

Trent Reznor (Nine Inch Nails)
from 'The Downward Spiral'
1994, nothing/TVT/interscope records,
TIME-WARNER

Acknowledgments

We knocked the bastard off.

- E. Hillary, Nepal, 1953.

Undoubtedly the people from whom I have received the most assistance are my supervisors, H. Kipton J. Powell and Alison J. Downard. Kip has been a courteous and polite guide. Alison's contribution came at a critical time in the project and her interest and enthusiasm since have been unfailing.

Helen Devereux and Richard Blaikie are generously thanked for providing free access and guidance to the screen printing equipment in the Micro-electronics laboratory of the Electrical and Electronic Engineering Department of the School of Engineering, University of Canterbury, - and to think I only broke one screen!

Financial assistance from the Chemistry Department in granting a teaching assistant scholarship and from the Evans fund in covering my costs in attending a conference in Melbourne are gratefully acknowledged.

Finally I would like to thank all the students who, as fellow in-mates, were fun to be around: Peter for being kooky, Kathryn D. for keeping me up to date on Shortland St., Alisa who showed me up in aerobics, Quentin who shared my taste in music, Azmi who hated my music but shared my passion for food, Martin for his love of both classical music and deviant cinema, Samson for his giggle, Parveen who was patient with my explanations, and, last but not least, the gossipy old women of room 753, Steve and Kathryn H..

Abbreviations

4-nitrocatechol	4-ncat
cyclic voltammetric scan rate	ν
standard deviation	σ
electrode rotation rate	ω
atomic absorption spectrometry	AAS
adsorptive stripping voltammetry	AdSV
also known as	aka
analytical reagent grade	AR
anodic stripping voltammetry	ASV
British Drug Houses	BDH
chrome azurol S	CAS
chemically modified electrode	CME
1,2-dihydroxyanthraquinone 3-sulfonic acid	DASA
3,4-dihydroxybenzylamine	DHB
differential pulse voltammetry	DPV
flow injection analysis	FIA
glassy carbon	GC
inductively coupled plasma	ICP
internal diameter	i.d.
International Union of Pure and Applied Chemistry	IUPAC
mass spectrometry	MS
methyl iso-butyl ketone	MIBK
outer diameter	o.d.
optical emission spectrometry	OES
parts per billion	ppb
parts per million	ppm
potentiometric stripping analysis	PSA
poly(vinyl chloride)	PVC
rotating disk electrode	RDE
relative standard deviation	RSD
saturated calomel electrode	SCE
screen printed electrode	SPE
triply distilled water	TDW

Contents

CHAPTER 3: SOLUTION EQUILIBRIUM STUDIES 29

Abstract

The aim of this project was the development of new analytical methods for the measurement of reactive (toxic) aluminium in natural waters (i.e. soil solutions, rivers and lakes).

Indirect electrochemical methods were used. These involve the formation of a complex between a metal and a redox-active ligand. The coordination chemistry of two redox-active ligands and aluminium was studied using the techniques of solution thermodynamics.

After complex formation with aluminium a shift in the ligand's redox potential is observed. Three ligands were studied voltammetrically. A theoretical model taken from the literature describing the shifts in ligand redox potential was shown to be inappropriate and the shifts were shown to result from the direct electrode reaction of aluminium-coordinated ligand. The effect of variation in complex stoichiometry was also studied.

Shifts in ligand redox potentials may be exploited in the development of analytical applications. A flow injection analysis (FIA) system was constructed which allowed the amperometric measurement of aluminium after formation of a complex with the reagent 4-nitrocatechol. Incorporation of a micro-column of oxine-derivatised gel into the manifold eliminated the effect of interfering cations and allowed the selective measurement of reactive aluminium in natural waters.

A problem was encountered with electrode fouling in the amperometric system. Two novel FIA strategies were developed to overcome this.

Screen printing technology was used to fabricate chemically modified electrodes for the analysis of aluminium. General advantages of the application of this technology were revealed. The particular electrodes made here were suitable for 'in-field' measurement of reactive aluminium in natural samples. The oxine micro-column was used in conjunction with the screen printed electrodes allowing selective measurement of reactive aluminium. This gives flexibility in the linear working range and eliminates the effect of interfering cations.

Chapter 1

INTRODUCTION

ELECTROANALYSIS OF ALUMINIUM.

1.1 THE ALUMINIUM CYCLE.

Aluminium[1] is prevalent in the natural environment. During the formation of the earth this element moved out of the mantle and into the crust to the extent that it is the most common metal there and the third most common element after oxygen and silicon [Favero and Jobstraibizer, 1996]. Although this aluminium is present in some 714 minerals belonging to various classes, most of it is contained in a dozen or so silicates and (hydr)-oxides. The silicates range from the feldspars (tetrahedral coordination of aluminium only) to the partially weathered micas to the fully weathered clay minerals (mixed or octahedral only coordination of aluminium).

In highly crystalline forms aluminium is generally unavailable (unreactive) for chemical and biological reactions but as minerals are weathered their burden of aluminium is gradually released. The cycling of aluminium between solid and aqueous forms in the environment is summarised schematically in Fig. 1.1.

Three distinct pools are recognised for the release of aluminium into natural waters. (1) weathering of crystalline minerals which gradually converts them into amorphous materials. This occurs through carbonic acid and/or strong acid dissolution. The presence of strong complexing agents for aluminium is also known to assist this process (and to prevent reprecipitation) [Watteau and Berthelin, 1994]. (2) A second source of aluminium is that which is bound to solid phase organic materials. It has been shown that aluminium may be mobilised from this pool more rapidly than its dissolution from mineral phases. This allows that, under certain conditions, organic material may control the solubility of aluminium even though it is a smaller pool than mineralised aluminium in most environments [Cronan *et al.*, 1986, Dahlgreen and Walker, 1993]. (3)

[1] Note all references are to tri-valent aluminium, Al(III). Metallic aluminium is not observed naturally.

The most rapidly mobilised source of aluminium is that which may be released from charged surfaces by ion exchange. These surfaces range from mineral phases to suspensions of colloidal matter [Zelazny and Jardine, 1989].

In Fig. 1.1 a pathway is given for the up-take of aluminium into living organisms. Although aluminium is not considered a trace element it is known that some organisms, especially some plants, will take it up from their environment.

In solution aluminium is mobile and may be transported by water movement within the environment. Later it may be removed from solution by precipitation into a mineral phase. This may settle as a sediment or remain suspended in solution as a colloid.

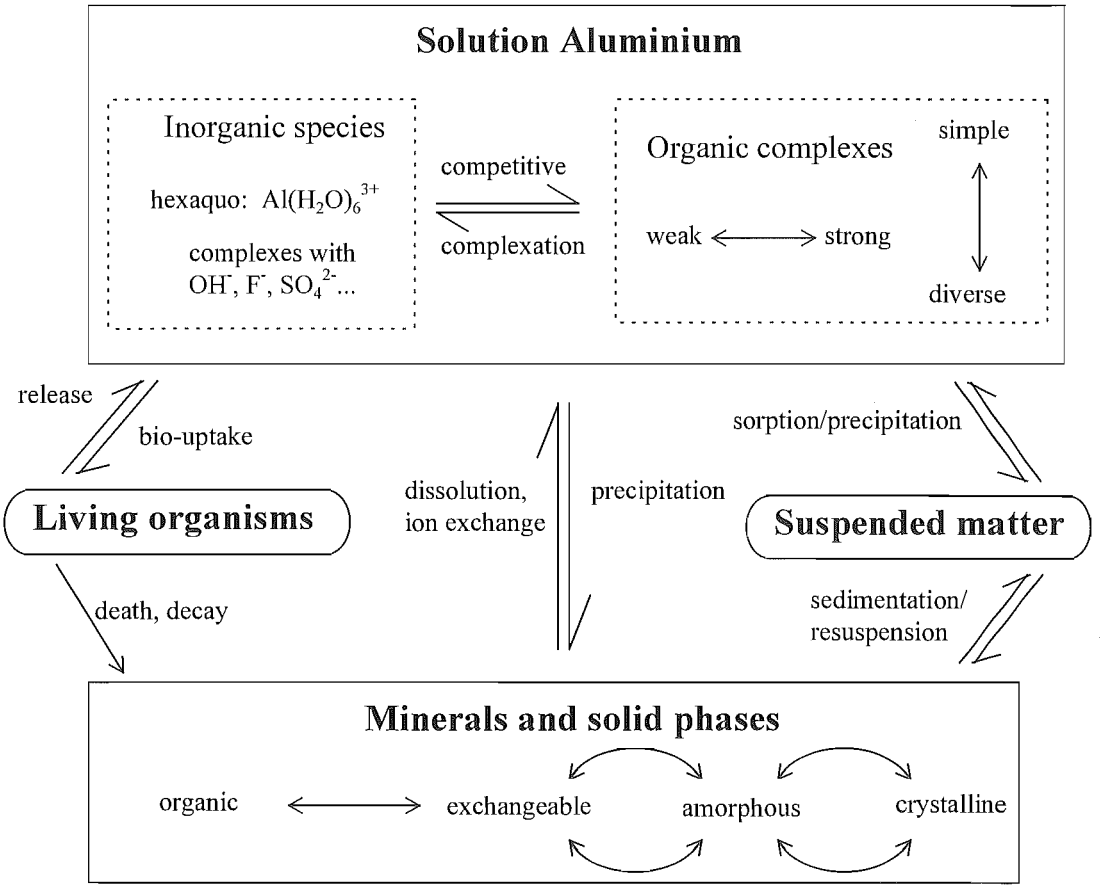

Figure 1.1 The aluminium cycle.

Solution aluminium is the most chemically and biologically available form, although this pool represents an extremely small fraction of the total aluminium in the environment. Aluminium is a strongly hydrolysing metal and the ion is relatively insoluble in the neutral pH range (6.0 to 8.0). Under more acidic or alkaline conditions, and/or in the presence of complexing ligands, the solubility of aluminium is increased. The ligands which complex aluminium in the environment may be classed either as inorganic or as organic.

The most significant inorganic ligands for aluminium are water (H_2O), OH^-, F^- and to a lesser extent SO_4^{2-} [Nordstrom and May, 1989]. Complexation with hydroxide gives, in the first instance, monomeric species such as $[AlOH]^{2+}$ and $Al[(OH)_2]^+$. In solutions that have pH values in the range 5.0 - 6.5 polymeric hydroxy species form. The identity of these species is not known definitively and has been the subject of much discussion in the scientific literature. The species for which there is the greatest amount of evidence are the dimer, $[Al_2(OH)_2]^{4+}$, and the 'Al_{13}' species, $[AlO_4Al_{12}(OH)_{24}(H_2O)_{12}]^{7+}$. These species coalesce to form aluminium hydroxide, $Al(OH)_{3(s)}$ which has minimum solubility at pH 6.5. Above pH 7.0 the aluminate complex, $[Al(OH)_4]^-$, forms and is the dominant form of aluminium in alkaline solutions (in the absence of stronger ligands) [Bertsch, 1989].

The organic compounds that form stable complexes with aluminium are far more diverse and can be placed into two groupings: (1) well-defined biochemical compounds synthesised by living organisms, such as simple aliphatic acids, phenols and phenolic acids, hydroxamate siderophores and sugar acids, and (2) a series of acidic, yellow to black coloured substances formed by secondary synthesis reactions (eg. decay) and referred to as humic and fulvic acids [Schnitzer and Khan, 1972]. The relative importance of the two types of compound is difficult to evaluate and will vary with soil and environmental conditions. Biochemical compounds may be expected to play a dominant role where microbial activity is intense. Humic substances may be of great importance in reducing the toxicity of aluminium in acid soils, mediating the interaction of aluminium at reactive surfaces (eg oxides), and binding aluminium in most natural waters (rivers and lakes).

The distribution of aluminium between the various pools illustrated in Fig. 1.1 may be predicted using thermodynamic equilibrium relationships. Thus the dissolution of minerals may be described by solubility products and the complexes formed by aluminium in solution and at surfaces can be described by complex formation constants. Computational models have been developed for the calculation of aluminium species concentrations from given inputs of pH, total or monomeric aluminium and ligand concentrations. [LaZerte, 1984; Gherini *et al.*, 1985; Backes and Tipping, 1987; Driscoll and Schecher, 1990].

In practice most environmental systems are extremely diverse and are not accurately described by such models. They often contain diverse, poorly characterised materials such as amorphous mineral phases and humic and fulvic substances. Also precipitation and dissolution reactions rarely achieve thermodynamic equilibrium. Instead metastable species of aluminium may be formed and persist for months or years [Wright *et al.*, 1988; Furrer *et al.*, 1992].

Rather than relying on geochemical thermodynamic models a preferable approach is to directly determine the concentration of aluminium species by an analytical technique. Much research activity has been directed towards the development of methods which are sensitive to a particular fraction of aqueous aluminium species.

1.2 TOXICITY OF ALUMINIUM.

It is not known if aluminium is a necessary trace element for the support of life. The conventional approach to determining the role of aluminium is to withhold it from an organism and observe the effects of 'aluminium deficiency'. However the ubiquitous nature of aluminium makes it extremely difficult to exclude all traces of this element. The most confident statement that can be made is that there is no known biochemical pathway for which aluminium is essential.

Conversely toxic impacts of aluminium to a range of organisms have been documented, notably to plants, fish, birds and humans.

1.2.1 ALUMINIUM TOXICITY TO PLANTS.

Aluminium toxicity to plants growing in acidic soils has been identified as a problem for 80 years [Hartwell and Pember, 1918]. Soil acidification may develop naturally when basic cations are leached from soils and it can be accelerated by some farming practices such as the application of fertilisers. 'Acid rain', produced by fossil fuel powered industry in some parts of northern Europe and north-eastern America, may have an average pH as low as 4 [Cronan and Schofield, 1979] and also contributes to acidification of the environment.

The most easily recognised symptom of aluminium toxicity in plants is the inhibition of root growth, and this has become a widely accepted measure of aluminium stress. Other symptoms are root thickening, roots becoming brittle and root tip dieback.

With prolonged exposure secondary effects to the plant tops may occur, indicated by decreased vigour and stunted growth [Mookherji and Floyd, 1991; Delhaize and Ryan, 1995].

Delhaize and Ryan (1995) have reviewed the physiological aspects of aluminium toxicity to plants. It is suggested that aluminium may bind to the pectic residues or proteins of the root cell walls, displacing other ions and inhibiting normal nutrient transport and disrupting cell metabolism. An alternative possibility is that aluminium may penetrate the cell wall, entering the cytoplasm. Once inside the cell there are several ligands which may bind aluminium and whose metabolic functions may become impaired, e.g. enzymes, calmodulin, tubulin, ATP, ADP, DNA.

The susceptibility to aluminium toxicity varies with different plant species and even with different cultivars of the same species [Shann and Bertsch, 1993; Mookherji and Floyd, 1991]. The primary mechanism for ameliorating aluminium appears to the excretion of organic acids which complex free aluminium in the soil solution [Delhaize and Ryan, 1995, Miyasaka *et al.* 1991].

Some farm management practices may overcome the effects of aluminium toxicity in acidified agricultural soils. These include the application of lime to raise soil pH and of calcium salts and increasing the level of organic material in the soils. It is likely that these strategies act to reduce the level of free inorganic aluminium activity at the root surface either by precipitating it (raised pH), displacing it by ion exchange (calcium) or by complexing it (organic material).

Considerable research has been directed by agronomists towards determining the particular species of aluminium which are toxic to plants. This has proved problematic for several reasons. Several species of aluminium coexist in solution so that individual species cannot be investigated in isolation. This is especially true of the hydrolytic species of aluminium which are all formed over a narrow pH range (pH 5-7). The activities of individual species must be calculated from equilibrium data that may be uncertain. The unexpected or undetected appearance of the 'Al_{13}' species ($[AlO_4Al_{12}(OH)_{24}(H_2O)_{12}]^{7+}$) may cause toxicity to be mistakenly attributed to other species. However the picture is becoming more clear and Kinraide (1991) has hypothesised that it is the polyvalent cationic (charge >2) species of aluminium which are toxic as are the polyvalent cations of some other elements (e.g. Ga, In, La and Sc).

Thus the hexaquo ion, $Al(H_2O)_6^{3+}$ and the Al_{13}^{7+} species are considered toxic. This has been demonstrated experimentally by Parker *et al.* (1988, 1989) for wheat and soybean plants. Complexes formed with fluoride, sulfate and organic ligands are all classed as non-toxic (charge $\leq +2$). This has also been demonstrated experimentally by several workers [see Kinraide, 1991, and references therein].

This hypothesis classifies the mononuclear hydroxy species ($AlOH^{2+}$, $Al(OH)_2^+$) as non-toxic, despite the claims of some authors to the contrary. Investigations of the toxicities of these species are plagued with difficulties. As argued by Kinraide (1991), it seems likely that researchers have often not considered the formation of the polynuclear 'Al_{13}' species in their nutrient solutions and wrongly attributed its toxicity to the mononuclear species.

1.2.2 ALUMINIUM TOXICITY TO FISH.

Elevated levels of aluminium in freshwaters (rivers and lakes) have been connected with toxic impacts on both fish and invertebrate organisms (molluscs, insects *etc.*). The impacts on fish have been the most thoroughly studied.

For example McCahon *et al.* (1989) studied the effects of acid, aluminium and lime additions on a number of fish species in an acidic Welsh stream. Aluminium dosing was found to greatly increase fish mortalities, with 100% of salmon dead within 24 hours in the streams dosed solely with aluminium or with aluminium plus acid. Addition of lime decreased the rate of fish mortalities.

Typically fish show damage to gill structures and lose the ability to maintain osmotic balance [Kramer *et al.*, 1986; Playle and Wood, 1990; Rosselund *et al.*, 1992]. The binding and accumulation of aluminium to fish gills has been proposed as the cause of respiratory and/or ionoregulatory disturbances [Booth *et al.*, 1988; Playle and Wood, 1989; Waring and Brown, 1995]. Fish gills may act as nucleating surfaces upon which aluminium can precipitate since the mucus layer of the gills carries a negative charge [Wood *et al.*, 1995]. Fish respond to aluminium binding by excreting increased mucus. This discharge coats the gills, resulting in increased diffusion distances and less efficient exchange of gaseous and ionic species between the fish's blood and the surrounding waters.

Early studies established a strong connection between aluminium toxicity and high levels of labile inorganic aluminium in acidified lakes and streams [Driscoll *et al.*, 1980]. This suggests that the hexaquo ion, $Al(H_2O)_6^{3+}$ should be considered toxic to fish. In a more recent study Rosselund *et al.* (1992) also found inorganic aluminium to be toxic to Atlantic salmon and sea-run trout in an acidified river. Interestingly they found an even greater toxicity in the mixing zone where this river merged with a limed (higher pH) river. In this zone the pH increased from 4.8 to 6.5 and inorganic monomeric aluminium (Al_i) decreased from 8.7 μM to 1.8 μM. The decrease in Al_i reflects its polymerisation into colloidal species. Evidently these polymeric species, especially in the early stages of their formation, are particularly toxic to fish. This suggests that the Al_{13} species should also be considered to be toxic.

1.2.3 ALUMINIUM TOXICITY TO HUMANS.

Aluminium has been suggested to be associated with various neurological disorders, including dialysis dementia, Alzheimers disease, Parkinsonism dementia and a form of amyotrophic lateral sclerosis.

Dialysis dementia was first reported by Alfrey *et al.* (1972 and 1976). They described a serious neurological syndrome in patients on prolonged haemodialysis [i.e. those undergoing kidney treatment]. Its symptoms included progressive dementia, speech difficulties, facial grimacing, motor abnormalities and electroencephalographic changes. In the majority of patients the onset was insidious and therefore often overlooked. Death followed diagnosis in 1-15 years. The syndrome was often accompanied by a form of bone disease with symptoms of bone pain, fractures and deformity. Also patients often suffered from an iron resistant form of anaemia.

The causative agent was eventually traced to elevated levels of aluminium in dialysate, often resulting from the use of alum-treated tap water. This allowed direct passage of aluminium species into the blood serum of patients. Purification of the dialysate, either by distillation or reverse osmosis, gave an immediate improvement. Epidemics were halted and the progression of patients already diagnosed with dialysis dementia was slowed [Parkinson *et al.*, 1981]. Dialysis dementia is the only clear case of a disorder in humans which may be directly attributed to intoxication by aluminium. Modern dialysis treatment practices have eliminated its occurrence.

Alzheimers disease is characterised by a progressive impairment of learning and memory, usually leading within 8 years to severe impairment of judgement, language and motor function. *Post-mortem* examinations reveal brain lesions which contain neurofibrillary tangles and plaques. The connection with aluminium was made when these lesions where found to contain aluminium [Perl and Brody, 1980]. It is unclear whether aluminium acts as a nucleating centre for these lesions. They may be formed by other processes and attract aluminium afterwards. In some families there is a high incidence of the disease, indicating genetic factors play a role.

There is some epidemiological evidence that suggests that Alzheimers disease may be more common in regions where there is a higher concentration of aluminium in drinking water [Martyn *et al.*, 1989, Craun, 1990, Flaten, 1990]. However the correlations are relatively poor and the findings are not conclusive.

Very high incidences (up to 50 times the world-wide rate) of Parkinsonism dementia and a form of amyotrophic lateral sclerosis have been observed in certain native populations of western New Guinea (Iryan Jaya), southern Guam and the Kii peninsula of Japan. In these diseases brain neurofibrillary tangles containing deposits of aluminium have been observed although, unlike Alzheimers disease, plaques are not observed [Garruto, 1991]. Each of the regions in the western Pacific is subject to high rainfall and the local soils contain high levels of exchangeable aluminium and low levels of magnesium and calcium.

Fortunately the incidence of these diseases has declined in the last 40 years, presumably as a result of changes in diet and lifestyle as the regions are influenced by foreign cultures. This decline suggests that environmental factors have contributed to the high incidences of the diseases.

From the foregoing discussion it appears that aluminium may be involved in a range of serious and debilitating diseases. It is only in the case of dialysis dementia however that a causal relationship and the form of exposure has been clearly established.

1.2.4 THE TOXIC FRACTION OF AQUEOUS ALUMINIUM.

Aluminium toxicity varies with its chemical form. For both plants and fish the most toxic forms are the free hexaquo aluminium ion, Al^{3+}, and the hydroxy-polymeric species (probably the 'Al_{13}' ion).

In the development of an analytical methodology for aluminium it is an advantage if a particular species, or class of species, may be selected for measurement, i.e. the aluminium present within a sample is separated into different fractions. Ideally for the estimation of aluminium toxicity this means isolation of a fraction containing both the Al^{3+} ion and the hydroxy-polymeric species. This is rarely achieved because the free aluminium ion and the hydroxy-polymeric species differ in molecular size, charge and reactivity.

Instead aluminium toxicity is estimated by determining 'reactive' aluminium. This contains the most rapidly reacting species, primarily the Al^{3+} ion, monomeric hydroxy complexes, $AlOH^{2+}$ and $Al(OH)_2^+$, and possibly other inorganic monomeric species.

A limitation of this approach is that the hydroxy polymeric species are not included in the reactive fraction. These species are not readily amenable to measurement. The only selective and direct technique available for the measurement of 'Al_{13}' in solution is ^{27}Al NMR. Less symmetric hydroxy-polymeric species are not measured by this technique.

1.3 FRACTIONATION OF ALUMINIUM SPECIES.

A number of authors have presented various analytical methods for the fractionation of aluminium species in water solutions. A general problem in this field is the operational definition of almost all proposed methods. This makes it difficult to compare results from different speciation protocols although several authors have attempted this [LaZerte, 1984; Seip *et al.*, 1984; Lalande and Hendershot, 1986; Hodges, 1987; Backes and Tipping, 1987; LaZerte *et al.*, 1988; Berggren, 1989]. A very important task when developing a new method is to verify the results by, for example, equilibrium calculations [Clarke *et al.* 1992].

Note that the fractionation of aluminium species is a separate issue from their analysis. It involves the separation of the different classes of aluminium species that are present within a sample. In some cases this may occur concurrently with the detection step while in others an independent means of detection is required.

1.3.1 LITERATURE METHODS FOR THE FRACTIONATION OF ALUMINIUM SPECIES.

The following principles have been used for species discrimination in the methods for aluminium fractionation:

1. The *rapid and limited reaction* of Al^{3+} with a complexing agent, commonly oxine[2], pyrocatechol violet[3] or ferron[4].
2. The removal of charged species by their sorption on *cation-exchange resins*.
3. A *kinetic analysis* of the rate of reaction of aluminium species.
4. Separation of various aluminium species by *ion chromatography*.
5. *Size exclusion* of large complexes, e.g. by filtration or dialysis.
6. Reduction of $[F^-]$ through complex formation with Al^{3+}, giving an indirect measurement of aluminium by the *fluoride ion selective* electrode.

Use of a rapid and limited reaction with a complexing agent is the preferred method for the fractionation of aluminium species for the following reasons: the contact time is brief and equilibrium shock is minimised so that there is little re-distribution of aluminium between different species. The fraction which is measured is usually described as 'reactive' or 'inorganic monomeric aluminium' and this equates closely to toxic aluminium (as discussed in the previous section, section 1.2.4).

The 'CAS 7 seconds' technique [Hawke *et al.* 1996] is an example of this strategy. Samples are mixed online in a flow injection analysis (FIA) manifold with a complexing agent, chrome azurol S (CAS). This complexing agent undergoes a colour change upon coordination with aluminium and this change is measured immediately (within 7 seconds). Within such a brief reaction time it is only the most labile aluminium species that are able to react. Analyses may be performed very quickly, in less than one minute.

There are many other examples in the literature of the use of a rapid and limited reaction for the fractionation of aluminium species [see Clarke *et al.*, 1992 and the references therein].

[2] see Goto *et al.*, 1958; Okura *et al.*, 1962; Turner, 1969; Barnes, 1975; Bloom *et al.* 1978; May *et al.*., 1979; Lalande and Hendershot, 1986, Hodges, 1987.
[3] see Seip *et al.*, 1984; LaZerte *et al.*, 1988; Rogeborg and Henriksen, 1985.
[4] see Driscoll *et al.*, 1980; Smith, 1971.

Driscoll (1984) has introduced a fractionation method which uses a cation exchange column. The novel step consists of passing a sample across a cation exchange column before analysis. Inorganic species of aluminium are assumed to be cationic, labile and retained by the column. Organically complexed aluminium is assumed to be anionic, non-labile, and hence to pass the column.

The sample is analysed before and after application to the column. Analysis is performed with a technique similar to the rapid and limited reaction techniques described above. However a relatively long contact time (30 seconds) is used so that both inorganic and organic species of aluminium are included in the analysis. This gives two measurements of 'monomeric' aluminium. The measurement of the sample before application to the column gives 'total reactive aluminium' and measurement afterwards gives 'organic reactive aluminium. The difference between the two measurements is assumed to give 'inorganic monomeric aluminium'.

Although the method of Driscoll (1984) has been widely used for field work [Vogt *et al.*, 1990; Berggren *et al.*, 1990; Christophersen *et al.*, 1990; Rosselund *et al.*, 1992] there are some draw-backs to the method. The fractionation procedure depends on the clean separation of aluminium species as they pass the cation exchange column. In practise Driscoll (1984) found that some of the aluminium bound in organic complexes was taken up, the relative amount being strongly dependent on sample flow rate. Cation exchange may cause considerable changes to the pH and the ionic strength of samples which will change the distribution of aluminium between different species. Determination of inorganic monomeric aluminium is uncertain since it requires the subtraction of two values which are operationally defined. The analysis method chosen by Driscoll (1984) requires impractically large sample volumes (~ 500 mL); this may be overcome by use of an alternative analysis method.

Some workers have developed a kinetic analysis for the reaction of aluminium species. Jardine and Zelazny (1986) studied the reaction of the colorimetric reagent ferron with partially neutralised aluminium solutions. They found that colour formation could be described by three parallel pseudo first-order reactions with each reaction corresponding to a particular fraction of aluminium species. An advantage of this approach is that arbitrary reaction times are avoided. Disadvantages are that a relatively long reaction time of 4 minutes is required, the technique is not readily adapted to a flow application and

heterogenous and/or natural samples may not be well described by only three parallel reactions.

Size exclusion techniques (equilibrium dialysis, filtration) have been used to distinguish between aluminium species on the basis of their molecular size [LaZerte *et al.*, 1988; Lalande and Hendershot, 1986; Backes and Tipping, 1987; Berggren, 1989; Benes and Steinnes, 1974]. The larger aluminium species are inorganic precipitates and colloids and the complexes formed with polymeric organic materials, i.e. humic substances. The fraction of aluminium which passes dialysis and filter membranes is a mixture of inorganic complexes and complexes formed with low molecular weight organic acids (e.g. citrate, oxalate etc.) and the lower molecular weight components of the fulvic acid fraction.

Weaknesses of size exclusion techniques are that the technique does not distinguish between weakly and strongly complexed aluminium or between aquo/hydroxo and fluoro complexed aluminium. Thus the results are of little use in the estimation of 'toxic' or reactive aluminium. The dialysis technique requires long (24 hour) equilibration times. In this time there may be considerable redistribution of aluminium between different species, changing the results. Problems with adsorption onto filter surfaces has been encountered with the use of Ultra-filtration apparatus [LaZerte, 1984].

The fluoride ion selective electrode may be used to determine the activity of free aluminium ion, $\{Al^{3+}\}$. A knowledge of the ionic strength, pH, total and free activity of fluoride and the total concentration of aluminium is required. Thermodynamic calculations are used to determine $\{Al^{3+}\}$ [Driscoll, 1984; Hodges, 1987]. An advantage of this technique is that it causes little or no change to the equilibrium state of the sample.

Disadvantages of this technique are that the ion selective electrode requires a long time to reach a stable potential. The method assumes thermodynamic equilibrium has been reached in the sample which may not be the case. The greatest accuracy is achieved when a large proportion of the fluoride within a sample is present as aluminate complexes, limiting the pH of the samples which may be examined to being less than 5.5. Above this pH fluoride does not compete with hydroxide for aluminium. Many natural samples will have insufficient fluoride to give a measurable response. Determination of $\{Al^{3+}\}$ requires measurement of the 5 parameters mentioned above plus a thermodynamic calculation, making the technique complex and time consuming.

1.3.2 THE FRACTIONATION METHOD USED IN THIS WORK.

The method used in this work for the fractionation of aluminium follows one recently proposed by Simpson *et al.* (1997). This combines the strategies of species sorption onto a resin with the use of a rapid reaction with a complexing agent. Samples are loaded within a FIA manifold onto a column of an oxine-derivatised gel. Within the brief contact time of 1.3 seconds aluminium is taken up from the most reactive species in the sample. An injection of alkali is then made which elutes the aluminium (as the aluminate ion, $Al(OH)_4^-$) as it passes through the column. Other species retained by the column, e.g. Fe^{3+}, are not eluted. The carrier stream containing the aluminium eluted from the column is merged with an appropriate reagent and measured spectrophotometrically.

In this technique the column-bound aluminium is measured directly, in contrast to the cation exchange technique [Driscoll, 1984] where the column-bound aluminium is inferred from the difference between two measurements. A further advantage is that the fractionation is based on the reactivity of species rather than their charge or size. This is likely to give a better measure of aluminium toxicity. There should be little equilibrium shock to samples since they are applied to the column without prior adjustment to their pH, and the contact time is brief (1.3 seconds). Chemical interferences in the down-line analysis of aluminium are overcome since the aluminium within a sample is completely removed from the sample matrix.

1.4 MEASUREMENT OF ALUMINIUM

1.4.1 STANDARD METHODS.

There are a wide range of techniques available for the measurement of aluminium. Each has its own qualities which makes it appropriate for a particular application. Some are more accurate than others or measure to a lower limit, some require large expensive instruments while others are relatively simple and portable, some give precise speciation information while others are more suited to the determination of 'total' aluminium.

The classical method for the measurement of aluminium is gravimetric analysis. A precipitate is quantitatively formed between aluminium and an anionic chelate (often oxine) and weighed [Vogel, 1961]. The procedure is not easily automated and requires some competence on the part of the analyst. However it does remain the method

of choice where very accurate measurements of total aluminium are required with the minimum of equipment.

Atomic absorption (AA) spectrometry is probably the most routinely used instrumental technique for aluminium. It involves the direct spectrometric determination of aluminium, i.e. the measurement of light absorbed by aluminium atoms at characteristic wavelengths. Aluminium is vaporised and atomised by either a flame or a furnace. The method is only appropriate for determinations of total aluminium as speciation information is destroyed in the atomisation process. The instrument is not portable and is not suitable for 'in-field' determinations.

Flame AA is not a very sensitive technique for aluminium, with a detection limit of ~40 μM [Slavin, 1978]. Sensitivity can be increased by preconcentration and extraction into a non-aqueous solvent. Barnes (1975) used oxine to complex and extract aluminium into the solvent MIBK. A similar method is recommended by 'Standard Methods for the Examination of Water and Wastewater' for samples low in aluminium.

Furnace AA is more sensitive for aluminium, with a detection limit of 0.04 μM. $Mg(NO_3)_2$ has been recommended as a matrix modifier [Slavin, 1982a,b] and an Ar atmosphere is required.

Inductively coupled plasma (ICP) techniques using either optical emission spectrometry or mass spectrometry (OES or MS) are suitable for the determination of total aluminium. They have the advantage of being multi-element techniques with high sensitivities. Unfortunately the instruments are expensive and their use is confined to laboratories.

Neutron activation analysis is another very sensitive multi-element technique. It is the most reliable means of measuring the total aluminium within a sample. The technique is based upon quantitation of the gamma rays emitted by Al nuclei that have become radioactive through irradiation with neutrons. Its advantages are a low detection limit (10^{-6} to 10^{-9} g), accuracy and precision, lack of chemical interferences and the lack of the need for sample pretreatment. Salbu *et al.* (1975) demonstrated that 0.007 μM of aluminium can be detected in water and that 30 elements can be determined simultaneously. The major disadvantage is that its use is limited to those investigators who have access to a nuclear reactor. Also the technique requires attention to detail that can only be given by a well trained analyst.

Spectrophotometry is perhaps the simplest of methods for the measurement of aluminium and yet may be very sensitive. The sample is reacted with an organic reagent and the light absorbed by the aluminium-reagent complex is measured. A large number of reagents have been used. Tikhonov (1973) describes several of these.

Spectrophotometers are relatively inexpensive instruments, the analysis is easily automated and may be made portable (with reduced precision). An important issue is that for aluminium spectrophotometry is an *indirect* means of analysis. It is a property of the complexing reagent (its colour) which is measured. The aluminium is not directly measured.

1.4.2 INDIRECT ANALYSIS.

Complexing agents are required for the indirect analysis of aluminium. They are utilised in combination with either spectrophotometric or electrochemical detection. A few considerations are common to both cases.

The extent and stoichiometry of complex formation is pH dependent. Analytical solutions are generally buffered to some optimal value.

Complex formation is a competitive process. The rate at which aluminium is taken up from a sample will depend on its initial coordination environment. For natural samples there will always some aluminium which is so strongly bound or mineralised that it will not be complexed by the analytical reagent. For this reason the use of chelating ligands is not suitable for quantitative determination of total aluminium unless samples are appropriately pretreated (e.g. by acidification).

This property can be turned to advantage if speciation information is desired. As described in the earlier section the rate of reaction with a complexing reagent can be used to discriminate between different fractions of aluminium species. A problem which arises is that the fraction of aluminium species which is measured is operationally defined. It will change with differences in the choice of ligand, contact time, pH etc.

There may also be competition from other cations for the analytical reagent. The most important competitor with aluminium is ferric iron, Fe(III). Its reactions are more rapid and its complexes more stable with most ligands. For most analyses it must either be masked or removed in some way.

1.4.3 ELECTROANALYSIS OF ALUMINIUM.

Electroanalysis is a technique which offers promising sensitivity for aluminium (to sub micro-molar levels) with the use of simple and inexpensive equipment. Disadvantages of its use are poor selectivity, that it requires trained operators and the results are often of a lower precision.

The development of direct electrochemical methods for the analysis of aluminium is limited by the very large and negative reduction potential for trivalent aluminium ($E^{\circ}_{Al^{3+}+3e^{-}\Leftrightarrow Al_{(s)}}$ = -1.706 V *vs.* NHE) [Bard and Faulkner, 1980]. For aqueous systems application of the very negative potentials required for the reduction of aluminium results in the evolution of hydrogen [i.e. $H_2O + e^{-} \rightleftharpoons OH^{-} + {}^{1}/_{2}H_{2\,(g)}$]. Nonetheless some polarographic methods have been developed for the direct determination of aluminium [Gull, 1937]. Most commonly however aluminium is measured indirectly, that is after it has been complexed by some electroactive organic ligand.

1.4.4 INDIRECT ELECTROANALYSIS OF ALUMINIUM.

A ligand which is suitable for the indirect electroanalysis of aluminium will form a strong complex with that metal, and preferably not with others. After coordination there should be some change in the redox potential for the ligand. This forms the basis for the measurement. In Fig. 1.2 the voltammetry of oxine and its aluminium complex is illustrated. The peak at +0.905 V corresponds to oxidation of the aluminium complex and has been used for the quantitation of aluminium [Cai and Khoo, 1993].

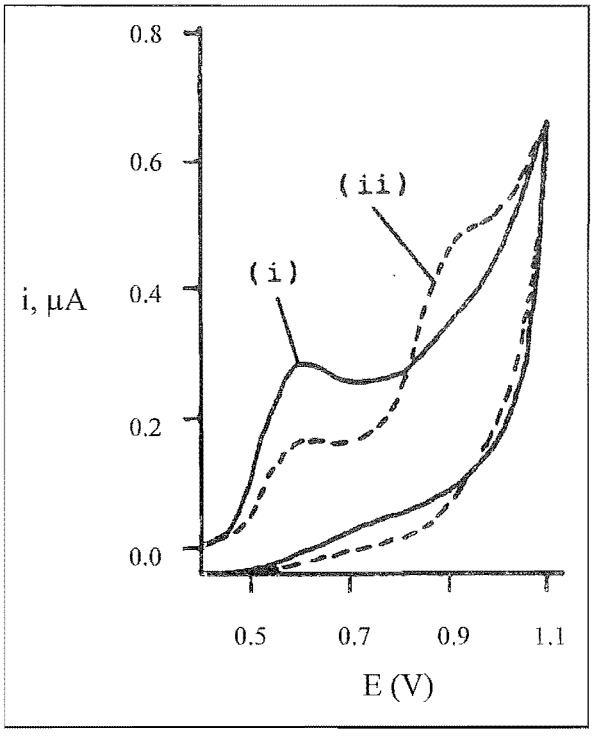

Figure 1.2. Cyclic voltammograms (ν = 100 mV/s) of oxine and its aluminium complex, reproduced from Cai and Khoo (1993). (**i**) 1 x10^{-4} oxine, (**ii**) 1 x10^{-4} oxine and 2 x10^{-5} aluminium. Both scans in 0.024 M NH_4OAc, pH 6.8

Table 1.1 summarises many of the ligands which have been used for the indirect electroanalysis of aluminium and the changes in their redox potentials. The peak potentials quoted are for the experimental conditions (pH, metal and ligand concentrations, voltammetric waveform, scan rate etc.) described in the cited articles.

Recent work in the development of electroanalytical applications has been focused along two lines: adsorptive stripping voltammetry (AdSV) of aluminium chelates which show strong adsorption on mercury electrodes (e.g. SVRS, PCV and DASA) and voltammetry of aluminium-ligand complexes which exhibit oxidation processes which are accessible at solid electrodes (e.g. alizarin, DASA, oxine, tiron).

Changes in redox potential after complexation is a well known phenomenon. Indeed one of the classical applications of polarography is to use shifts in redox potentials to determine complex formation constants. The systems studied by polarography differ from those summarised in Table 1.1 in that it has generally been the metal centre which is redox active and not the ligand. For example Koryta (1962) has studied the effect of CN^- on the reduction wave of Cd^{2+} and Killa *et al.* (1984) have determined formation constants for the systems Cu^{2+}-oxalate and Cd^{2+}-propylenediamine.

Table 1.1 Ligands used for the indirect electroanalysis of aluminium.

Name	Redox potential	References.
Solochrome violet RS (SVRS) 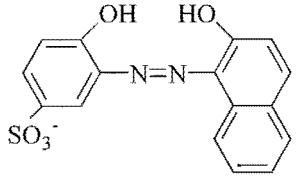	AdSV (reducing) $E_{p\ (ligand)}$ = -0.4 V $E_{p\ (complex)}$ = -0.76 V Voltammetric (oxidising) $E_{p\ (ligand)}$ = +0.53 V $E_{p\ (complex)}$ = +0.85 V	Willard and Dean (1950) Wang *et al.* (1985) Downard *et al.* (1992)b Florence *et al.* (1966)
Calmagite 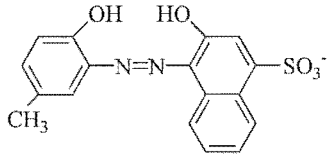	AdSV (reducing) $E_{p\ (complex)}$ = -0.4 V	Karpiuk *et al.* (1995)
Pyrocatechol violet (PCV) 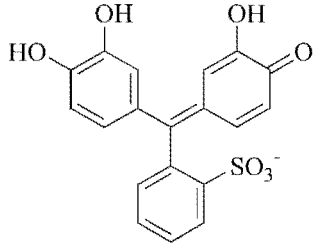	AdSV (reducing) $E_{p\ (ligand)}$ = -0.7 V $E_{p\ (complex)}$ = -0.9 V	Vukomanovic *et al.* (1991)
Tiron 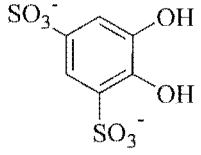	Voltammetric (oxidising) $E_{p\ (ligand)}$ = 0.7 V $E_{p\ (complex)}$ = 0.8 V	Wang and Liu (1991)
Dihydroxyanthraquinone-3-sulfonic acid (DASA) 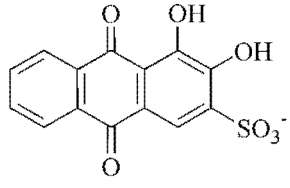	AdSV (reducing) $E_{p\ (ligand)}$ = -0.9 V $E_{p\ (complex)}$ = -1.2 V Amperometric (oxidising) $E_{p\ (ligand)}$ = 0.4 V $E_{p\ (complex)}$ = 0.8 V	van den Berg *et al.* (1986) Hernandez-Brito *et al.* (1994) Downard *et al.* (1992)a Downard *et al.* (1997)b
Alizarin 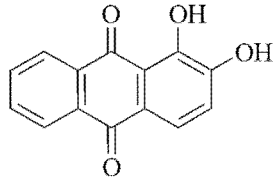	Voltammetric (oxidising) $E_{p\ (ligand)}$ = +0.4 V $E_{p\ (complex)}$ = +0.6 V	Downard *et al.* (1991)
Oxine 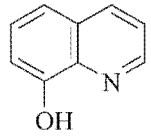	Voltammetric (oxidising) $E_{p\ (ligand)}$ = +0.620 V $E_{p\ (complex)}$ = +0.905 V	Cai and Khoo (1993)

Theoretical models have been developed for ligand-centred redox systems. Florence and Belew (1969) have studied the shifts in the reduction wave of the ligand Solochrome violet RS after complexation with some 23 different metal ions. They used a Nernstian model to relate each system's complex formation constant to the shift in reduction potential. Equations were developed for two distinct cases, one in which the complex dissociates after the ligand is reduced and one where the complex remains intact, but with a different formation constant.

The treatment of Florence and Belew (1969) has been fully generalised by Shiu and Harrison (1989). Allowance is made for any number of complexation reactions occurring with both the reduced and oxidised forms of the ligand. Eqn. 1.1 gives the shift in the redox potential of a ligand relative to its uncomplexed form ($\Delta E_{1/2}$). It is the ratio of the formation constants, i.e. $\beta_{(ox.)}$:$\beta_{(red.)}$, which determines the shift in redox potential.

$$\Delta E_{1/2} = \frac{-RT}{nF}\left\{\ln\frac{\beta_{(ox)}\alpha^{(ox)}}{\beta_{(red)}\alpha^{(red)}} + (j-p)\ln[M]\right\} \qquad (1.1)$$

Equation 1.1 is a simplified version given by Shiu and Harrison (1989) of the expression for the shift in redox potential of a ligand which participates in coordination reactions. It assumes that only one complex stoichiometry is important for each oxidation state of the ligand, that the terms in [M] are large compared to unit, activity coefficients are unity and that the ratio of Ilkovic constants is one. E, R, T, n, and F have their usual electrochemical meanings. β values give complex formation constants, α values give the activity of a particular protonated form of the ligand, M indicates the metal and (j-p) gives the change in coordination number.

The model of Shiu and Harrison (1989) is illustrated in Fig. 1.2. The participation of the complexes in the redox reaction is passive. Their only involvement is to control the concentration of the free ligand. The model makes no allowance for the separate electrode reactions of the complexes themselves. This model may be appropriate for highly labile systems in which the rate of ligand exchange about the metal centre is rapid compared to the timescale of the electrochemical experiment. Conversely for inert systems (e.g. aluminium) it may be that the model of Shiu and Harrison (1989) is not appropriate and the direct electrode reaction of metal-bound ligand must be considered.

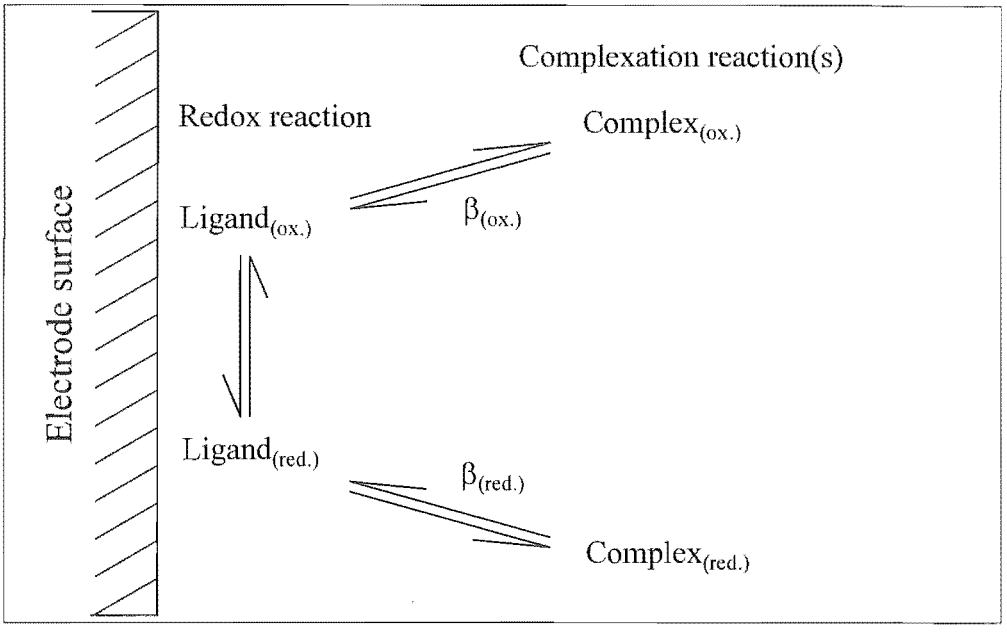

Figure 1.2. The theoretical model developed by Shiu and Harrison (1989) for the shift in a ligand's redox potential after complexation with a metal.

1.5 THE SCOPE OF THIS WORK

The aim of this project is the development of new electroanalytical methods for aluminium. Indirect methods were used and initial studies were directed towards various fundamental aspects of these. An essential step of these methods is the formation of a chelate between aluminium and an electroactive ligand. For this reason the complexation chemistry of aluminium was studied, using the techniques of solution thermodynamics. The voltammetric behaviour of selected aluminium-ligand systems was also studied with respect to (i) the effect of variation in complex stoichiometry and (ii) the origin of the shifts in ligand redox potential which occur with complex formation.

The experience gained in these studies was used in the development of a flow injection analysis (FIA)-based method for the electrochemical determination of reactive aluminium in environmental freshwaters. Fractionation of aluminium species was achieved using the column of oxine-derivatised gel described in Section 1.3.2.

Some difficulty was encountered with electrode instability in the FIA system. This was attributed to electrode fouling by the ligand and was overcome by incorporating a correction for the amperometric background into each measurement. Some novel FIA strategies were also developed to address this problem. These functioned by removing the

electrochemical response of free ligand so that only that due to aluminium-bound ligand was measured, greatly reducing the amount of oxidative electrolysis in the system.

Electrochemical methods are simple, rapid and require inexpensive equipment. They may be made portable and give a response which is easily interfaced with modern data-logging equipment (e.g a laptop computer). These advantages make electrochemical methods natural candidates for the development of portable methods, i.e. for performing analyses in the field, outside of the laboratory.

'In-field' analysis of aluminium would be of advantage in the determination of reactive (toxic) aluminium in natural freshwaters (soil solutions, rivers and lakes). In most conventional methods the distribution of aluminium between reactive and nonreactive forms will change with sample storage, making analyses performed in a remote laboratory inaccurate, hence the advantage of an 'in-field' method. It would be of particular value in dynamic systems (e.g. following the mixing of acidic and limed streams) in which the metastable 'Al_{13}' species plays an important role in aluminium toxicity.

Field sensors for aluminium were fabricated with screen printing technology. Use of this technology allows chemical modification of the electrode surface to be performed during manufacture, reducing the amount of chemical manipulation required in the field. A further advantage of screen printing manufacture is that electrodes may be mass produced precisely and at low cost. Thus the sensors may be treated as disposable (one measurement only) and reagents with irreversible redox chemistry may be used.

Again the column of oxine-derivatised gel was used for the fractionation of aluminium species so that reactive aluminium could be targeted. This required the development of a new protocol whereby the column could be used in a 'batch' mode rather than the FIA mode as previously.

Chapter 2

EXPERIMENTAL METHODS AND MATERIALS.

Information is given in this chapter concerning experimental methods, equipment and reagents which are used in common throughout this work. Details which are relevant to only a particular section are given in the appropriate chapter.

2.1 BUFFER SOLUTIONS.

Where necessary the pH of solutions was controlled by the addition of a buffer reagent. This was taken in its acid form (generally to a concentration of 0.05 M) and pH adjustment was made with an appropriately-sized addition of standardised potassium hydroxide as determined by the buffer equation, eqn. 2.1. The ionic strength of all solutions was adjusted to 0.1 M by the addition of KCl unless explicitly stated otherwise.

Buffer equation:

$$pH = pK_a + \log\frac{[A^-]}{[HA]} \qquad (2.1)$$

pK_a = negative logarithm of the acid dissociation constant.
HA = acid form, A^- = conjugate base.

Table 2.1 Buffers used for the control of pH.

pK_a	Name	grade/source
3.6	Formic acid	reagent /Hopkins and Williams
4.7	Acetic acid	(glacial) analytical reagent / BDH
6.1	MES [2-[N-morpholino]ethane-sulfonic acid]	reagent / Sigma
7.5	HEPES [N-[2-hydroxyethyl]piperazine-N'-[2-ethane-sulfonic acid]]	reagent / Sigma
9.2	Ammonium chloride	analytical reagent / BDH
9.3	CHES [2-[N-cyclohexylamino]-ethane-sulfonic acid]	reagent / Sigma

After preparation the pH was checked with an Ionode glass electrode and a laboratory-built meter. This equipment was calibrated against NBS buffers [Vogel, 1961].

Note this section does not apply to the work on solution equilibria (Chapter 3) where the pH was more carefully controlled and measured.

2.2 LIGANDS.

The following ligands were used in connection with the electroanalysis of Al: 9,10-dioxo-1,2-dihydroxy-anthracene (**alizarin**), 9,10-dioxo-1,2-dihydroxy-2-anthracene-3-sulfonic acid monosodium salt (**DASA, or alizarin red S**) and 1,2-dihydroxyanthraquinon-3-yl-methylamine-N,N-diacetic acid (**alizarin complexone, ACN**), 3,4-dihydroxy-benzylamine.HBr (**DHB**), 4-nitro-1,2-benzenediol (**4-nitrocatechol, 4-ncat**), 1,2-benzenediol (**catechol**).

Alizarin complexone, DASA and alizarin (all reagent grade) were obtained from Sigma. DHB (98%) and 4-ncat (97%) were obtained from Aldrich. Catechol (reagent grade) was obtained from BDH.

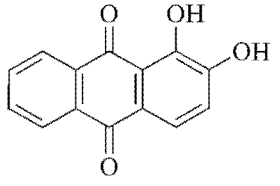

alizarin

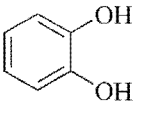

catechol

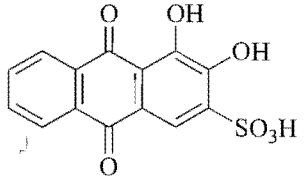

DASA

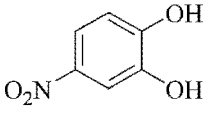

4-nitrocatechol

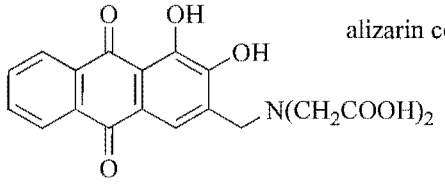

alizarin complexone

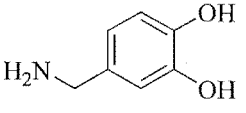

DHB

2.3 SPECIATION CALCULATIONS.

Solution compositions were modelled (where possible) using complex formation constants and the program SOLGASWATER [Eriksson, 1979].

2.4 ELECTROCHEMISTRY.

An electrolyte of 0.1 M KCl was used in all electrochemical experiments unless stated otherwise.

Instruments for performing electrochemical experiments were selected on the basis of their availability and their suitability for a particular experiment. The following were used:

Potentiostats and data recorders:

PAR 273a in combination with EG&G m270 software.
PAR 173/ 276 interface / 175 universal programmer/ graphtec WX 1200 x-y recorder.
PAR 362/ graphtec WX 1200 x-y recorder.
PAR 174a/ graphtec WX 1200 x-y recorder.
PAR 384b (internal data recorder)

Rotating disk electrodes:

Metrohm 628-10

PAR 616

For three electrode cell measurements the cell comprised a glassy carbon disk working electrode (area=0.07 cm^2), a platinum wire auxiliary and a saturated calomel (SCE) reference electrode. The glassy carbon working electrodes used for hydrodynamic voltammetry were supplied by the manufacturers of the rotating disk electrodes; for other experiments the working electrode was fabricated from Atomergic Chemetals, VC-10 glassy carbon. Before use both types of working electrode were polished with 1 μm diamond paste and ultrasonically cleaned for 15 s in acetone followed by triply distilled water.

Electrochemical measurements were made at 22±2°C. Solutions containing aluminium were equilibrated for at least 15 minutes prior to measurement.

2.4.1 ELECTROCHEMICAL PRETREATMENTS OF THE GLASSY CARBON ELECTRODE.

In the first instance electrodes were always polished using the procedure outlined in the previous section, (2.4).

In the voltammetric studies of Chapter 4 electrochemical pretreatments were used. For pretreatment in acid, the general method of Cabaniss *et al.* (1985) was followed; the polished electrode was repetitively scanned (nine cycles) in 1 M H_2SO_4 between 0 and 2.15 V vs SCE with ν=200 mV s^{-1}. Base pretreatment was carried out at an applied potential of 1.2 V vs SCE in 1 M NaOH for 5 min., as described by Anjo *et al.* (1989). All pretreatment solutions were air-saturated. The pretreated electrodes were rinsed with triply distilled water before use.

2.5 AMPEROMETRIC FLOW INJECTION ANALYSIS (FIA).

2.5.1 FIA EQUIPMENT.

A selection of the equipment used in the construction of flow manifolds is illustrated in Fig. 2.1. Solutions were pumped into the FIA manifolds with either a 4 channel Alitea (C4-XV) or a 10 channel Ismatec peristaltic pump. Tygon pump tubing in a range of sizes was used. Manifolds were constructed from microline tubing (Cole-Parmer 0.51 mm i.d.). Short (2 cm) lengths of silicon tubing (Pharmacia LKB, 1.3 mm i.d., 3.3 mm o.d.) were used to connect the microline tubing to other components of the manifolds. Occasionally noise dampeners were fitted immediately after the pump to reduce peristaltic pressure pulsations. These consisted of glass T-pieces, the vertical side arm of which was sealed off to trap a large volume of air. Two types of injection valve were used, either a commercially supplied six port valve (Rheodyne) or a home built double injection valve (double sided - 8 port) constructed from delrin. Solutions were mixed at confluence points using a 30°-30° tee mixer [following Clarke *et al.*, 1989]. In one case a co-axial jet mixer was used. This was constructed from glass by artisans employed within the Chemistry Department, University of Canterbury. Its design was based on that presented by Scampavia *et al.* (1995) and recommended for rapid on-line mixing.

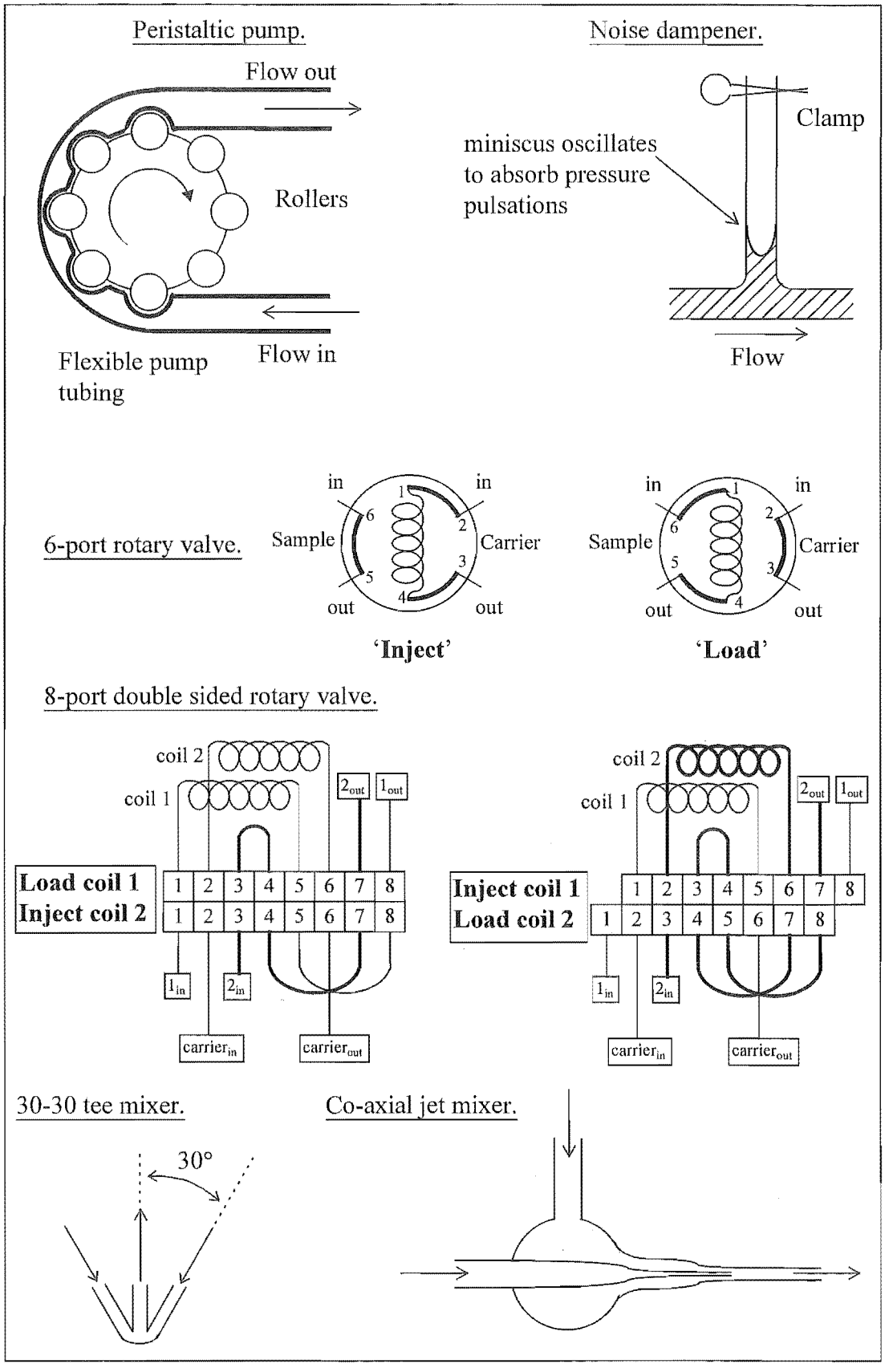

Figure 2.1. A selection of the components used to make FIA manifolds.

2.5.2 THE AMPEROMETRIC FLOW CELL.

Amperometric FIA measurements were made with a large volume wall-jet cell, based on a design described by Wang and Freiha (1985). The cell comprised a GC working electrode (area = 0.07 cm^2), Pt auxiliary and SCE reference electrode. When required the GC electrode was polished, using the procedure described in section 2.4.1

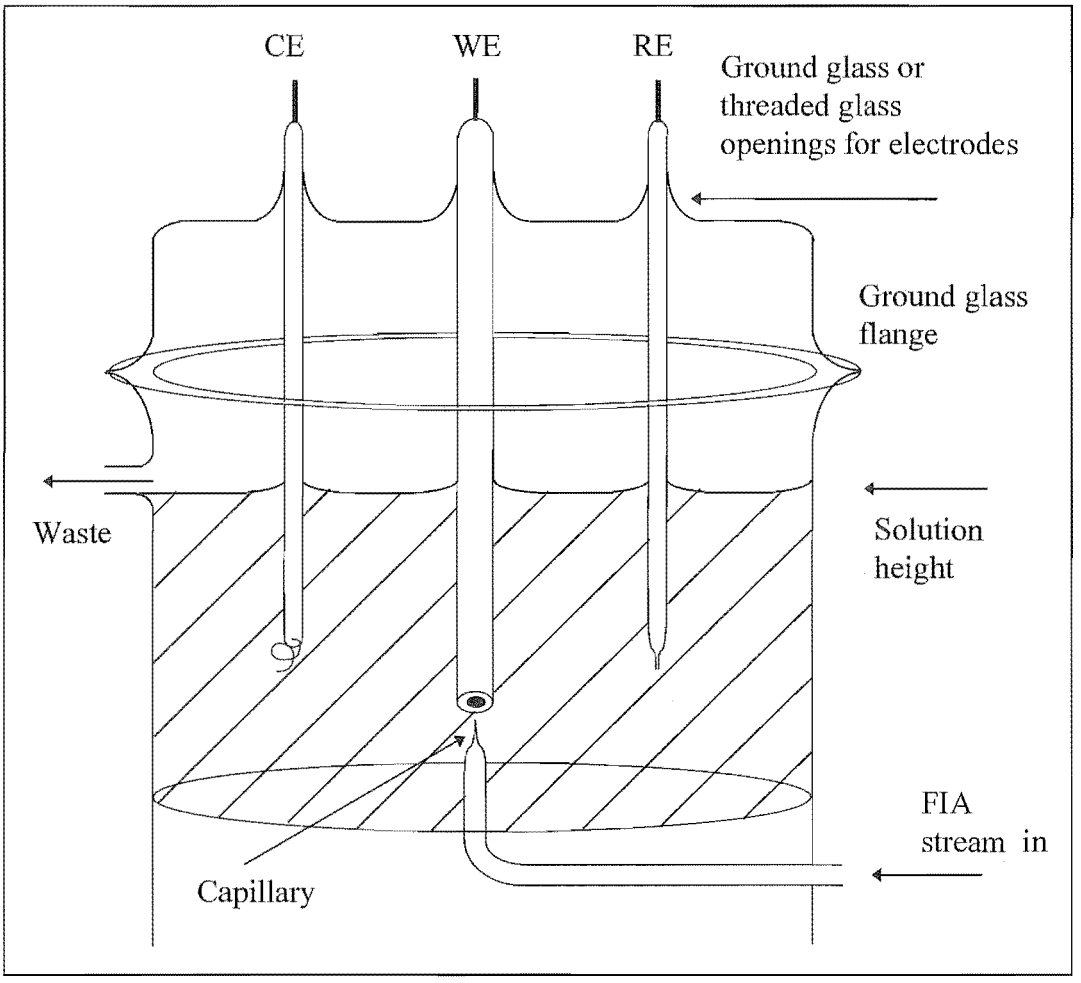

Figure 2.2 Schematic of the amperometric detector, built from glass for amperometric analysis of the flow injection analysis stream.

2.5.3 THE OXINE MICROCOLUMN.

The oxine microcolumn was constructed using the method of Simpson *et al.* (1997). Derivatisation of the gel was performed by S.L. Simpson and sufficient material for this project was kindly supplied by him.

Two sizes of column were used, with an internal volume of 22 μL for FIA work and 74 μL for use in the batch mode. Their construction is briefly described. A cavity in a home-built polycarbonate block was filled with beads of oxine-derivatised gel and sealed at each end with a small circular disk of fine nylon mesh. Lengths of microline tubing terminated each end of the column. This tubing was attached by threaded Teflon-tube end fittings and grippers (Omnifit).

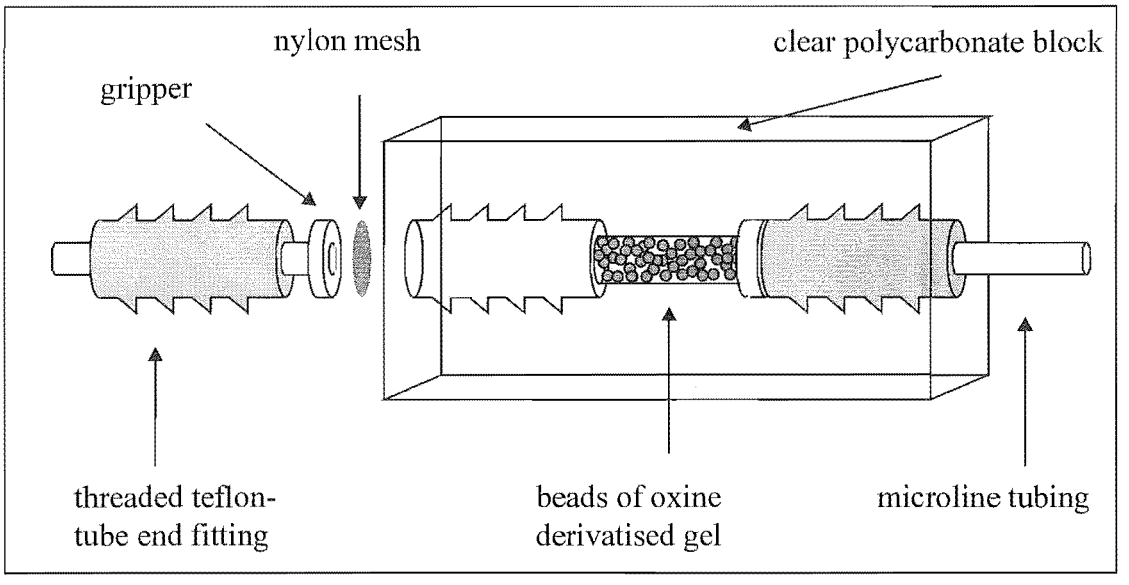

Figure 2.3. The oxine microcolumn. Note the left hand connection is given in an expanded view.

Chapter 3

SOLUTION EQUILIBRIUM STUDIES

3.1 INTRODUCTION

3.1.1 On the Relevance of Solution Thermodynamics to Indirect Electrochemical Analysis.

Indirect electrochemical analysis involves the treatment of samples with an appropriate ligand. Complex formation between this ligand and the analyte (in this work Al) changes the electrochemical properties of the ligand. This change may be measured so as to indirectly quantify the analyte. In the selection of ligands for new analytical methods it is helpful to be able to predict the extent of complex formation between potential ligands and the analyte.

Complex formation is one competing reaction amongst many others in solution and it occurs simultaneously with a range of hydrolytic and protonation reactions. Examples of these are solvolysis, ligand (de-)protonation reactions, metal ion hydrolysis and the hydrolysis of complex species to produce ternary M(OH)L species. Solution thermodynamics may be used to examine these complicated processes.

In work described in Chapters 4 and 5 solution thermodynamics are used to rationalise the electrochemical response for each of the ligands catechol, DASA and 4-ncat in the presence of Al.

3.1.2 Solution Thermodynamics.

Thermodynamics, in general, is the study of the transfer of energy in chemical and physical systems. Solution thermodynamics refers to the branch of this subject which describes the properties of solvent phases (normally water). Processes such as ion hydration, electrolyte dissociation, temperature effects and complex formation may be studied. The latter, the formation of complex species between metal ions and ligands, is the concern of this work.

Complex formation may be generalised by the reaction in eqn. 3.1. According to this reaction an equilibrium constant, K, may be defined, (eqn. 3.2). This is given in terms of the activities of the reacting species, at equilibrium, by the 'law of mass action'. The constant is a quotient with a product of the activities of the adduct species divided by a product of the activities of the reactant species. The activities of all species are raised to the power of their stoichiometric coefficients.

$$aA + bB \rightleftharpoons cC + dD \qquad (3.1)$$

$$K = \frac{\{C\}^c \{D\}^d}{\{A\}^a \{B\}^b} \qquad (3.2)$$

The equilibrium constant, K, may be related to the change in chemical energy in the course of the reaction. This is defined as the Gibbs function, ΔG, eqn 3.3 [Atkins (1987) eqn 10.1.14].

$$\Delta G = -RT \ln K \qquad (3.3)$$

R = gas constant

T = temperature.

From these definitions it follows that measurements of the activities of species in solution gives equilibrium information which in turn describes the energy change associated with a chemical reaction.

In practice species' concentrations are more often used than their activities in the calculation of equilibrium constants. A species' concentration is related to its activity by its activity coefficient, γ, (eqn. 3.4, [ ] brackets denote concentrations and { } brackets activities).

$$\{A\} = \gamma_a [A] \qquad (3.4)$$

γ_a = activity coefficient of species A

Activity coefficients are not easily determined although several equations have been put forward as approximate solutions [e.g. Debye and Hückel, 1923]. Determination of activity coefficients may be avoided by replacing activity terms by concentration values, i.e. by rewriting the equilibrium constant as K_c as in eqn. 3.5. This requires that the activity coefficient quotient, Q_γ, remains constant for all solution compositions. Since activity coefficients are a function of the ionic strength this parameter must remain constant also.

$$K = \frac{[C]^c[D]^d}{[A]^a[B]^b}\frac{\gamma_c\gamma_d}{\gamma_a\gamma_b} = K_cQ_\gamma$$

$$K_c = \frac{[C]^c[D]^d}{[A]^a[B]^b} \quad (3.5)$$

A constant ionic strength is commonly achieved by the addition of a high concentration of some inert electrolyte. If this is present at a concentration at least 100x greater than that of the reacting species then the disappearance of the various reactants and the appearance of new differently charged species has no significant effect on the ionic strength. Also this electrolyte must have negligible interactions with the species in the reaction of interest. If these conditions are met then concentration terms may be used in equilibrium calculations (ie. eqn. 3.5)

The resulting concentration-based equilibrium constants are unique to the choice of electrolyte since the value of Q_γ is a function of this electrolyte. Thus the nature and concentration of the inert electrolyte must be reported along with any concentration quotient equilibrium constants. This contrasts with activity-based equilibrium constants which are independent of ionic strength.

Equilibrium constants on the standard activity scale may be obtained by determining K_c at different ionic strengths and extrapolating to infinite dilution (i.e. zero ionic strength where activities and concentrations become equal).

For this work a cumulative formation constant, β_{pqr}, for the complexation reaction between a metal, M, and a ligand, L, and involving the exchange of protons, H, is generalised according to equations 3.6 and 3.7. Note this is a K_c type equilibrium constant.

$$pH^+ + qM^{n+} + rL^{x-} \rightleftharpoons [H_pM_qL_r]^{(p+qn-rx)+} \quad (3.6)$$

$$\beta_{pqr} = \frac{[H_pM_qL_r]}{[H]^p[M]^q[L]^r} \quad (3.7)$$

This formulism can be used to represent not only complex formation but also the hydrolytic equations listed at the end of section 3.1.1, ie solvolysis (q = r = 0), ligand (de-)protonation reactions (q = 0), metal ion hydrolysis (r = 0) and the formation of ternary species (p may be negative).

3.1.3 DETERMINATION OF SOLUTION EQUILIBRIUM CONSTANTS

The determination of solution equilibrium constants has been practised at least since the late 1920s [see references to work by Bjerrum, J., 1931, 1932, 1934 cited in Beck, 1970]. Since this time there has been a great proliferation in experimental techniques and in the number of researchers active in the field. Developments prior to 1970 have been described by Beck (1970) and Rossotti and Rossotti (1961). The greater part of the techniques described in these sources are graphical methods of calculating equilibrium constants. Since that time the advent of computers has allowed the development of numerical methods of calculation, [Leggett, 1985]. Both of these approaches, graphical and numerical, are used here.

With such a great number of active researchers and range of experimental strategies available it has inevitably occurred that different laboratories have published conflicting results for identical chemical systems. For some of the more thoroughly studied systems the International Union of Pure and Applied Chemistry (IUPAC) has published critical reviews. These present a benchmark. Independent and/or new researchers may examine one of the critically reviewed systems in order to test the validity of their own experimental strategy. In this project the system H^+/Cu^{2+}/L-histidine has been investigated and the results compared with the appropriate critical review [Pettit, 1984].

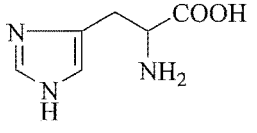

histidine

3.1.3-A SPECTROPHOTOMETRIC DETERMINATION. Solution equilibria may be monitored spectrophotometrically where one or more of the reacting species produces a differently coloured species during the course of the reaction. A simple example of this is the deprotonation reaction where the ligand HL loses a proton to form the differently coloured species L^-, eqn. (3.8). This system is described by equations (3.9) - (3.11). The Beer-Lambert law is the classical expression for describing the absorbance (A) of a coloured solution [Atkins, 1987, eqn. 19.1.4].

Reaction	HL	$\rightleftharpoons$	L^-	+	H^+	**(3.8)**
Mass balance	T_L	=	$[HL]$	+	$[L^-]$	**(3.9)**
Equilibrium constant	K	=	$\frac{[H^+][L^-]}{[HL]}$			**(3.10)**
Beer-Lambert Law	A	=	$\varepsilon_{HL}[HL]$	+	$\varepsilon_{L^-}[L^-]$	**(3.11)**

Path length, l, taken as unity.
ε_x = molar absorptivity of species x.

Equations (3.9) - (3.11) may be combined to give equation (3.12). This is a linear relationship of the form $y = mx + c$, as indicated. Thus by constructing a plot of the appropriate variables a value for the molar absorptivity of one form of the ligand (ε_{L^-}) is taken from the intercept, c, and using this a value for the equilibrium constant may be derived from the slope, m. An advantage of this technique is that it may be used where only one of the molar absorptivities is known (the equations may be rewritten for whichever ε_x is known).

$$\frac{T_L}{A} = \frac{1}{K\varepsilon_{L^-}}\left([H]\frac{A-\varepsilon_{HL}T_L}{A}\right) + \frac{1}{\varepsilon_{L^-}} \qquad \textbf{(3.12)}$$

$$y = m\,x + c$$

This is an example of a graphical approach to the determination of equilibrium constants. It was introduced by Agren (1955) who used the formulation to derive the acidity constants of various phenols. Havel and Meloun (1985) have reviewed a series of equivalent transformations, the earliest of which appeared in 1935.

This strategy is extended here to allow its application to complexation equilibria. Formation of a 1:1 complex between a metal, Al, and a protonated ligand, LH_x, may be written as eqn. (3.13). Note that this reaction is similar to reaction (3.8) because the ligand becomes deprotonated. In this case there may be more than one proton which is

lost (n = the number of protons displaced) and the reaction also involves the metal, Al.

Equations analogous to (3.9) - (3.11) may be written, (eqn.s (3.14) - (3.16)). Effectively the ligand, HL, has been replaced by the multi-protic ligand, H_xL, and the deprotonated form of the ligand, L^-, has been replaced by the complex, $Al(H_{x-n}L)$.

Reaction $$Al + H_xL \rightleftharpoons Al(H_{x-n}L) + nH^+ \quad (3.13)$$

Mass balance $$T_L = [H_xL] + [Al(H_{x-n}L)] \quad (3.14)$$

Equilibrium constant $$K = \frac{\beta_{(x-n)11}}{\beta_{x01}} = \frac{[Al(H_{x-n}L)][H^+]^n}{[Al][H_xL]} \quad (3.15)$$

Beer-Lambert Law $$A = \varepsilon_{H_xL}[H_xL] + \varepsilon_{H_{x-n}AlL}[Al(H_{x-n}L)] \quad (3.16)$$

Path length, *l*, not considered.
ε_x = molar absorptivity of species x.

Again equations (3.14) - (3.16) may be combined to give a linear transformation, eqn. (3.17). This is identical to eqn. (3.12) except that the proton concentration, $[H^+]$, is raised to the power of n and there is now a term for the metal concentration, [Al]. This equation may be rewritten for whichever ε_x value is known. Trial values of n may be used to find the value which gives a linear plot (simultaneously giving the number of protons displaced in the complexation reaction, eqn. (3.13)). The molar absorptivity for the complexed form of the ligand is taken from the intercept, (c). This together with the slope, (m), gives the value of the equilibrium constant.

$$\frac{T_L}{A} = \frac{1}{K\varepsilon_{Al(H_{x-n}L)}} \underbrace{\left([H]^n \frac{A - \varepsilon_{H_xL}T_L}{A[Al]}\right)} + \frac{1}{\varepsilon_{Al(H_{x-n}L)}} \quad (3.17)$$

$$y = m \quad x \quad + \quad c$$

Eqn. (3.14) assumes only two forms for the ligand, free LH_x and complexed $AlLH_{x-n}$. Thus there must be no significant side equilibria with differently protonated forms of the ligand. Similarly there must be no significant hydrolysis of the metal ion.

In eqn. (3.17) the term for the ordinate variable, x, contains the concentration of free metal, [Al]. This can only be accurately calculated with a prior knowledge of the equilibrium constant, K. However if a large excess of metal over ligand is used then the change in free metal throughout the course of the reaction is negligible. The concentration of free metal may be approximated by the total concentration of metal.

Thus for certain systems where these conditions are met the formulism of Agren may be used to calculate complex formation constants from spectrophotometric data. In this work it is applied to the system H^+/Al^{3+}/DASA.

3.1.3-B CONTINUOUS VARIATION PLOTS. The principle of continuous variation has been applied from as early as 1911 [Ostromisslensky, 1911; Denison, 1912]. It is frequently associated with the name of Job (1928) who applied it to complex systems.

For a given metal - ligand system a series of solutions are prepared in which the sum of the total concentration of metal plus ligand is held constant but their proportions are continuously varied. Each solution has a unique ligand to metal ratio ranging from 0 (100% metal, 0% ligand) to infinity (0% metal, 100% ligand).

The concentration of any complex formed between the metal and ligand will reach a maximum when the continuous variation ratio matches the stoichiometry of the complex. At this point any solution property which varies linearly with the concentration of the complex will also reach a maximum. A plot of this property against the ratio will show either a maximum or an inflection.

The method of continuous variation has been most commonly applied in the evaluation of spectrophotometric data but in principle it can be applied in connection with polarimetry, NMR, magnetic susceptibility measurements, etc. In this work it is used to interpret spectrophotometric data. This gives a means of independently verifying potentiometric results.

3.1.3-C POTENTIOMETRIC DETERMINATION. Potentiometry refers to the use of electrode potential data to determine equilibrium constants. The most commonly used type of electrode, and that which is used in this work, is the glass bulb electrode which is sensitive to the hydrogen ion. Other electrode materials such as metals, amalgams and ion sensitive membranes have been used to monitor a range of species such as free cations and anions.

Glass bulb electrodes give a linear response to hydrogen ion activity. If the activity coefficient of the hydrogen ion remains constant (by the use of a constant and high ionic strength) then this response is also linearly related to the hydrogen ion concentration.

The hydrogen ion concentration may be determined by two independent means. Firstly it may be calculated from electrode potential data. Secondly it may be calculated from the solution stoichiometry and the β_{pqr} values since the latter contain a term for the hydrogen ion concentration, $[H^+]$ (see equation 3.7). The two values may be compared.

This principle is used by the computer program SUPERQUAD [Gans *et al.*, 1985], employed in this work for the numerical calculation of β_{pqr} values. Estimates of β_{pqr} values are refined by the Gauss-Newton least-squares method so as to minimise the sum U, eqn. 3.18. U is the sum over all data points of the squared residuals between the observed and calculated hydrogen ion concentrations.

$$U = \sum w\left([H^+]^{obs} - [H^+]^{Calc}\right)^2 \qquad \textbf{(3.18)}$$

w = weighting factor.

It follows directly that this strategy requires measurements of $[H^+]$ of the greatest possible precision and accuracy. For experiments employing the glass bulb electrode, as in this work, this effectively limits the range of solution pH that may be investigated to pH 2.5 to 10.5 [Henry *et al.*, 1971]. Above pH 10.5 the very low concentration of free hydrogen ion makes the electrode susceptible to interference from alkali cations (e.g. Na^+ or K^+), especially when these are present at a high concentration as the electrolyte. This produces curvature in the electrode response. Below pH 2.5 the concentration of free hydrogen ion is very high ($[H^+]$ = 0.01 M at pH 2). The large concentration gradient across the junction between the filling solution of the reference electrode and the test solution causes a liquid junction potential. This also produces a curvature in the electrode response.

3.1.4 3,4-DIHYDROXYBENZYLAMINE (DHB).

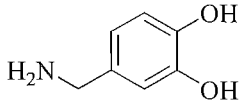

3,4 Dihydroxybenzylamine, DHB

DHB is an example of a catecholamine, that is it has the basic structure of catechol modified with an aliphatic amine substituent. Examples of naturally occurring catecholamines are the neurotransmitters (nor-)epinephrine, L-DOPA, serotonin and dopamine. The solution equilibria between these and Al have been comprehensively described by Kiss *et al.* (1989).

Coordination of Al to DHB is expected to occur at the catecholate (1,2-dihydroxy) moiety since Al is known to prefer 'hard' oxygen donor atoms in preference to coordination to primary amines. This same functional group is expected to be redox active. By analogy with other catechol derivatives it is predicted to show a 2 electron oxidation to an *ortho*-quinone [Ryan *et al.*, 1980]. Thus DHB was selected as a candidate ligand for the indirect electrochemical analysis of Al and investigations of the system's solution equilibria were made.

3.1.5 ALIZARIN COMPLEXONE (ACN).

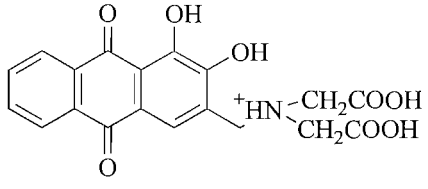

Alizarin Complexone, (ACN)

Alizarin complexone is also known as Alizarin fluorine blue. This name derives from its introduction in 1958 by Belcher *et al.* as an analytical reagent for the photometric determination of fluoride. Formation of a ternary complex between the ligand, lanthanum (or cerium) and the fluoride ion, F^-, gives a strong blue colour [Deane and Leonard, 1977; Leonard and West, 1960].

Zhang *et al.* (1993, 1994) have produced graphite electrodes chemically modified with ACN. Coordination of Fe(III) to the adsorbed ligand gave an electrode that was able to catalytically reduce O_2, H_2O_2, nitrite (NO_2^-) and nitric oxide (NO). The catalytic behaviour was also observed for a range of ligands all of which contained the common structural feature of a methyl-iminodiacetate group in an *ortho* position to a phenol group. This clearly suggests that Fe(III) coordinates within the pocket formed by these two functional groups in the ACN structure.

These observations show that ACN will readily form complexes with 'hard' trivalent cations, i.e. La^{3+} and Fe^{3+}. The anthraquinone structure of the ligand is known to exhibit reductive and oxidative reactions [Zhang and Anson, 1993]. Thus ACN was selected as a candidate for the indirect electrochemical analysis of Al. Investigations into the solution equilibria formed in the system H^+/Al^{3+}/ACN were made.

3.1.6 1,2-DIHYDROXYANTHRAQUINONE-3-SULFONIC ACID (DASA).

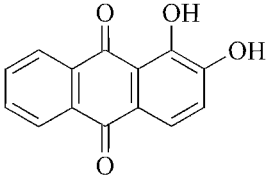

Alizarin

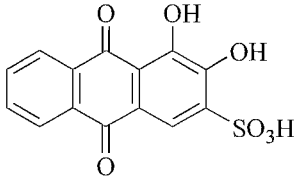

DASA

DASA is the sulfonic acid derivate of alizarin. This modification confers greater solubility to the ligand and its complexes.

Alizarin is a natural dye found in the madder plant (*Rubia tinctorum*). It has been used for centuries in the textile industries of the Middle East and Europe. Interestingly in the mordant dying process aluminium salts are added. Formation of a complex between aluminium and alizarin gives a different colour. Also linkage via aluminium to oxygen donor groups within textile fibres gives improved fastness of the dye.

Alizarin has been recommended as a colorimetric reagent for Al from as early as 1915 [Atack, 1915]. DASA has been applied in a number of electrochemical methods for the analysis of Al. Van den Berg *et al.* (1986) have used DASA for the adsorptive cathodic stripping voltammetric analysis of Al (their method has been subsequently modified by Hernandez-Brito *et al.* (1994)). DASA has been applied within flow injection analysis manifolds for the amperometric analysis of total Al at pH 9 at a gold electrode [Downard *et al.*, 1992a] and of reactive Al at pH 5 at a glassy carbon electrode [Downard *et al.*, 1997b].

The solution equilibria between DASA and Al have been investigated spectrophotometrically by Couturier (1987, 1989) with graphical methods of data analysis. This chemical system has been re-investigated here using (where possible) potentiometric techniques and numerical methods of data analysis. It is hoped that this may give a more accurate description of the system.

Coordination of Al to DASA may occur at one of two sites, either at the 1,9 keto-α-hydroxy position, giving a 6-membered ring, or at the 1,2-*ortho*-dihydroxy

position, giving a 5 membered ring. Evidence may be drawn from the literature showing coordination of a range of cations at both of these sites.

In 1947 Liebhafsky and Winslow reported their spectrophotometric study of complex formation between hafnium and alizarin. They found that hafnium formed a strong chelate ring with alizarin at the 1,2 position while ferric ion, and most other cations, would form a weaker 'inner complex' at the 1,9 position. Zittel and Florence (1967) have presented voltammetric and spectrophotometric evidence showing that zirconium, Zr^{4+}, binds at the 1,2 position with DASA. Bakola-Christianopoulou (1984) has reported a study of the alizarin chelates of the transition metals Ni^{2+}, Pd^{2+}, Cu^{2+}, Zn^{2+} and Mn^{2+}. She observed, by infrared spectroscopy, chelation of the metals at the carbonyl group suggesting binding at the 1,9 position. Larsen and Zink, 1990, have studied the absorption and emission spectra of the alizarin salts of Al^{3+}, Zn^{2+}, K^{+}, Co^{2+}, Ni^{2+} and Cu^{2+}. They observed fluorescence from the Al, K and Zn alizarinates while in the Co, Ni and Cu salts the fluorescence was quenched by the presence of *d-d* bands.

It appears that binding at the 1,2 position is favoured by 'hard' cations such as Zr^{4+} and Hf^{4+}. For other cations binding at the 1,9 position is favoured. This seems to be especially true for transition metals with vacant *d* orbitals that may favourably interact with the quinoid oxygen at the 9 position.

Al(III) would fit best in the former category, the 'hard' cations. It is investigated here if indeed Al does bind at the 1,2 position of DASA.

3.2 EXPERIMENTAL.

3.2.1-A PURITY OF LIGANDS.

(S)-α-amino-1H-imidazole-4-propionic acid (L-histidine) was obtained from Sigma.

The purity of DHB was analysed potentiometrically by titration against standard $AgNO_3$ using a Ag,AgBr electrode and a $Zn^{2+}/Zn_{(s)}$ counter cell connected by a salt bridge. This gave a 97.7±0.7 % purity by bromide content in agreement with the suppliers specifications (Aldrich, 98%).

Table 3.1 gives microanalysis results for each ligand, performed by the Chemistry Department, University of Otago. For L-histidine and DHB the agreement was satisfactory. Calculated values for ACN were obtained assuming the material contained one water of crystallisation. DASA showed slightly elevated levels of hydrogen and

diminished carbon and sulfur suggesting the presence of some inorganic impurity. This was determined (see below) to be a mixture of sodium and potassium chlorides and one water of crystallisation.

Table 3.1 Microanalysis results. Calculated values are for the formulae $C_6H_9O_2N_3$ (L-histidine), $C_7H_{10}O_2NBr$ (DHB), $C_{14}H_7O_7NaS$ (DASA) and $C_{19}H_{15}NO_9$ (ACN).

Ligand	%carbon		%hydrogen		%nitrogen		%sulfur	
	obs.	calc.	obs.	calc.	obs.	calc.	obs.	calc.
L-histidine	46.42	46.4	5.95	5.8	27.36	27.1		
DHB	37.98	38.2	4.71	4.6	6.24	6.4		
DASA	42.62	49.1	2.31	2.1			8.22	9.4
ACN	56.62	56.6	4.09	4.2	3.36	3.47		

^{13}C NMR analysis of DASA showed only 14 non-equivalent carbon resonances, consistent with there being no organic impurity. Acid/base titration against standard KOH established a molecular mass of 405 ± 5 grams per DASA equivalent. Elemental analysis by ICP-OES (performed by the Chemistry Department, University of New South Wales) indicated elevated levels of sodium and potassium. Potentiometric titration against standard $AgNO_3$ (as for DHB above) indicated a chloride content of 6.4%. This potentiometric method is able to measure the halides Cl^-, Br^- and I^- separately.

These analyses (summarised in Table 3.2) are consistent with the impurities present within the DASA (as supplied by Sigma) being (Na/K)Cl and H_2O in the proportions $(C_{14}H_7O_7NaS)(H_2O)(NaCl)_{0.6}(KCl)_{0.14}$ giving a molar mass of 406 grams per DASA equivalent. These impurities were considered inert.

On the basis of these analyses all of the ligands were used as supplied, without purification.

Table 3.2. Analysis of the DASA sample as supplied by Sigma. Figures give percentage by weight. Elements not registering above their detection limits (ICP-OES) are not reported. DASA formula for calculation: $(C_{14}H_7O_7NaS)(H_2O)(NaCl)_{0.6}(KCl)_{0.14}$

Element	Micro-analysis (±SD)	ICP-OES	X^-/AgX,Ag titration.	Calculated
C	42.62±1.6			41.4
H	2.31±0.1			2.2
S	8.22	7.2		7.9
Na		9.0		9.1
Cl			6.4	6.5
K		2.9		1.4
Al		<0.0003		
Fe		0.004		
Ca		0.04		
Cu		0.002		
Fe		0.004		
Mg		0.005		
Zn		0.001		
P		0.3		

3.2.2 METAL SOLUTIONS.

A Cu(II) stock solution (approx 0.1 M) was prepared in 1 mM HCl (BDH, 0.2 N, convol) from $Cu(NO_3)_2.3H_2O$ (BDH, Analar) and TDW. It was standardised gravimetrically as the benzoin-α-oximate (cupron) according to Vogel (1961).

Stock solutions of Al (approx 0.025 M) were prepared from milli-Q water (>18 MΩ resistance) and $AlCl_3.6H_2O$ (99.9995% purity, ALFA) and sufficient HCl (BDH, 0.2 N, convol) to give 0.01 M free acid. Standardisation was gravimetrically as the oxinate as described by Vogel (1961) except that addition of ammonium acetate before heating the sample to boiling was found to give a precipitate with a coarser grain size.

KCl (BDH, AR grade) (oven dried overnight at 105°C) was added directly to solutions as required.

3.2.3 CO_2 FREE ALKALI.

Alkali was prepared from Analar grade (BDH) KOH pellets. CO_2-free water was prepared by heating milli-Q water to boiling and cooling under nitrogen in an ice-bath. This was used to clean the carbonate coatings from the surface of the KOH pellets. The first two rinsings were discarded (a 2.5-fold excess of KOH pellet was initially taken) and the remainder were collected and made to volume. Alkali was stored in plastic under nitrogen.

Alkali was standardised by acid/base titration in the potentiometric cell (see

Fig. 3.1) against weighed amounts of the primary standard tris[hydroxymethyl]-aminomethane hydrochloride (Trizma hydrochloride, SigmaUltra >99%, Sigma). Solutions were periodically checked for evidence of CO_2 contamination by restandardisation; no evidence of contamination was found in the course of this work. Approximately two months after preparation alkali was discarded and a fresh solution prepared.

3.2.4 TITRATION APPARATUS.

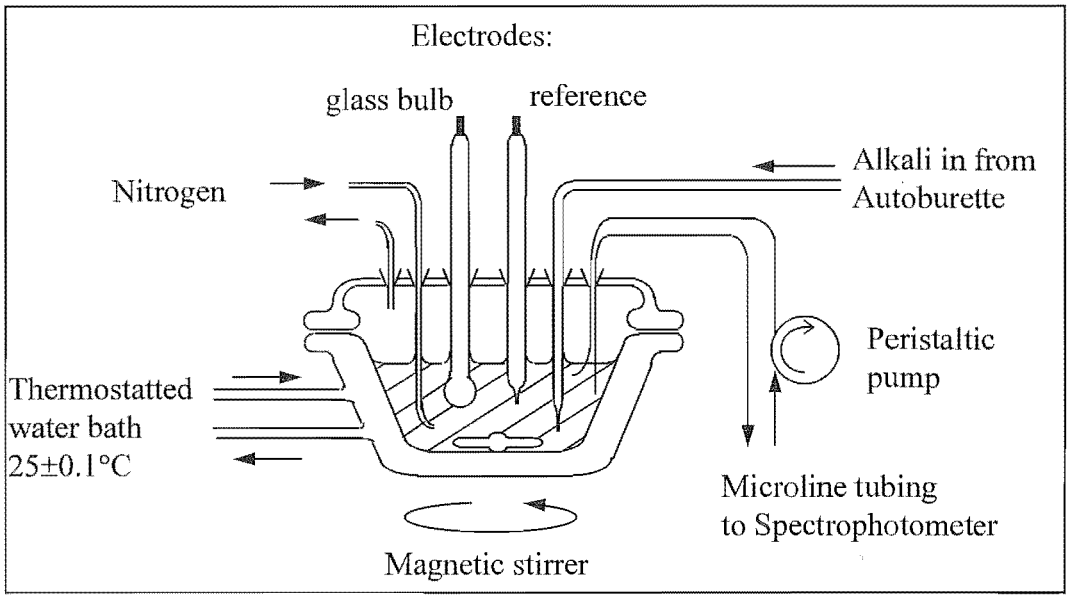

Figure 3.1 Titration Apparatus. Note: the spectrophotometer was present for spectrophotometric experiments only.

Fig. 3.1 illustrates the apparatus used for the acquisition of potentiometric and spectrophotometric equilibrium data. The entire apparatus was located within a temperature controlled room (25±2 °C). The glass titration cell had a volume of 100 mL and contained a water jacket for stricter temperature control. All connections to the cell were formed by ground glass joints.

Nitrogen gas was supplied from a commercial cylinder of oxygen-free nitrogen and was passed through a Zn/Hg-V^{2+} oxygen scrubber [as described by Russell, 1977, (p78)] (for DHB titrations only) and through a gas scrubber containing 0.1 M KCl to adjust humidity (for all titrations). The gas supply line was fitted with a three way tap allowing nitrogen to be delivered under or over the surface of the test solution.

An ABU80 autoburette and a PHM64 pH meter were both supplied by Radiometer, Copenhagen. These were controlled by a personal computer (PC, 08086),

using 'in house' software, to make additions of alkali, enforce appropriate equilibration times and monitor the pH. The electrodes used were a Russell SWR757 glass bulb electrode in combination with a Russell CR5 saturated calomel reference (SCE) electrode except for titrations with DASA where a home built SCE was used. This contained an outer sleeve filled with 0.1 M KCl so that the test solution containing DASA did not come into contact with the inner filling solution of saturated KCl.

A Hewlett-Packard HP8452a diode array spectrophotometer was used for the acquisition of spectral data. For these experiments the autoburette was controlled manually.

3.2.5 ELECTRODE CALIBRATION.

Calibration was performed by titration of strong acid (HCl) against standardised strong base (KOH, CO_2 free). The endpoint was determined by the method of Gran (1952). This allowed the concentration of hydrogen ion, $[H^+]$, to be calculated for each point in the titration and the 'slope' and 'intercept' of the electrode response to be determined by linear regression. Typically 30 data points spread over the pH ranges 2.9-3.6 and 9.9-10.6 were included in the regression, giving r^2 values of 0.99999 or greater.

The system was calibrated before and after each titration. A linear shift between the two calibrations throughout the course of the titration was assumed.

It should be stressed that the form of calibration used here implies that all references to pH in this work actually mean $p[H^+]$, ie the negative logarithm of the hydrogen ion *concentration* (as opposed to activity).

3.2.6 ELECTROLYTE.

All titration solutions (electrode calibrant and the test solutions) were prepared to have an ionic strength of 0.1 M by the addition of KCl.

3.2.7 EQUILIBRATION.

After each addition of alkali into the titration cell the system was left to equilibrate. For titrations not involving Al a short period (1 minute) was used while the system was left to equilibrate for 20 minutes after titre increments in the presence of Al. After this time the pH was measured (see below). After 10 seconds (or 5 minutes in the

presence of Al) the pH was measured again. If the readings did not agree to within 0.003 pH units then 'drift' was considered to be present and the datum point excluded from equilibrium constant calculations.

The pH was measured by the computer by taking 20 successive readings 1 second apart. If the readings did not agree to within 0.002 pH then 'noise' was considered to be present and again the datum point was discarded.

3.2.8 Al Hydrolysis Constants.

Below pH 4.0 the dominant form of Al in aqueous solution is the hexaquo ion, $Al(H_2O)_6^{3+}$. Above this pH a complicated series of hydrolytic reactions occur with rearrangement of the coordination sphere so that the tetra-coordinate aluminate ion, $Al(OH)_4^-$, becomes the dominant solution species above pH 7 [Baes and Mesmer, 1976].

These reactions have been investigated by Brown *et al.* (1985). A background electrolyte of 0.1 M $NaNO_3$ was used. Hydrolysis constants, β_{pq} values, were determined by numerical refinement of potentiometric data using the program MINIQUAD. The values determined by Brown *et al.* (1985) are reported in Table 3.3. These present a 'hydrolytic background' for the determination of solution equilibria involving Al. They have been included in all numerical calculations of Al speciation performed in this work.

Brown *et al.* (1985) gave several stoichiometries and β_{pq} values for the polymeric species corresponding to the Al_{13} polymer. For this work the value for the coefficients p =24 and q=10 was chosen since this had a log β value less than 100. Values greater than this could not be accepted by the program SUPERQUAD.

The formation constant for log β_{-41} was calculated by the method of Millero and Schreiber (1982) from the thermodynamic constants of Palmer and Wesolowski (1992) (assuming $\gamma\ [Al(OH)_4^-] = \gamma\ OH^-$).

Table 3.3 Hydrolytic constants of Al used in this work. β_{pq} values are defined according to the reaction:

$$pH^+ + qAl^{3+} \rightleftharpoons [(OH)_{-p}Al_q]^{(-p+3q)+}$$

p	q	log β_{pq}	Proposed formula
-1	1	-5.33	$[OHAl]^{2+}$
-2	1	-10.91	$[(OH)_2Al]^+$
-4	3	-13.13	$[(OH)_4Al_3]^{5+}$
-10	24	-81.18	$[(OH)_{32}Al_{13}]^{7+}$
-4	1	-23.3	$[(OH)_4Al]^-$

3.3 RESULTS.

3.3.1 POTENTIOMETRY OF THE H^+/Cu^{2+}/L-HISTIDINE SYSTEM.

The protonation constants of L-histidine were determined from two titrations giving 138 data points. The concentration of the ligand was varied over the range 2.0 - 2.5 mM. Complex formation with Cu^{2+} was investigated by performing two titrations in which the concentration of L-histidine was 2.5 mM and that of Cu^{2+} was 1.25 mM, giving 110 datum points.

These data were analysed with the program SUPERQUAD to give refined values of the cumulative formation constants, β_{pqr}, as reported in Table 3.4. Also reported are the values recommended by the IUPAC critical review [Pettit, 1984].

It is considered that the agreement is satisfactory. Increasing the size of the data set and varying the ligand and metal concentrations would undoubtedly have improved the match but this was considered unnecessary for the purposes of verifying the experimental strategy used here.

Thus it is considered that the solution equilibria of systems of more immediate interest may be studied, i.e. those involving Al and ligands suitable for the development of electroanalytical applications.

Table 3.4 Formation constants determined for the system H^+/Cu^{2+}/L-histidine. β_{pqr} values are defined according to the equation:

$$pH^+ + qCu^{2+} + rL^{2-} \rightleftharpoons H_pCu_qL_r^{(p+2q-2r)+}$$

p q r	log β_{pqr} (σ)				Proposed product
	this work		(IUPAC) recommended		
3 0 1	16.83	(0.01)	16.88	(0.1)	H_3L^+
2 0 1	15.159	(0.002)	15.16	(0.03)	H_2L
1 0 1	9.126	(0.001)	9.11	(0.02)	HL^-
1 1 1	14.07	(0.026)	14.11	(0.02)	HCuL
0 1 1	10.12	(0.01)	10.16	(0.03)	CuL
1 2 2	27.2	(fixed)	27.2	(0.1)	H_2CuL_2
1 1 2	23.81	(0.033)	23.81	(0.07)	$HCuL_2$
2 1 0	18.07	(0.041)	18.11	(0.09)	CuL_2
-1 1 1	not determined		2.0	(0.2)	(OH)CuL
-2 2 2	not determined		7.9	(0.1)	$(OH)_2Cu_2L_2$

3.3.2 POTENTIOMETRY OF THE H^+/Al^{3+}/DHB SYSTEM.

The protonation reactions of DHB were investigated by performing 6 titrations with the concentration of DHB varied over the range (4.0 - 0.87) $x10^{-3}$ M and yielding 300 datum points. Complex formation with Al was investigated by performing 10 titrations (674 datum points) with the concentration of DHB varied over the range (1.46 - 3.65) $x10^{-3}$ M and the concentration of Al varied over the range (1.17 - 0.56) $x10^{-3}$ M. The ratio of DHB to Al was varied between1.33:1 and 5.9:1.

Complex formation constants (β_{pqr} values) were refined numerically from these data with the program SUPERQUAD and are reported in Table 3.5. σ gives the standard deviation for each constant.

Table 3.5 Formation constants determined for the system H^+/Al^{3+}/DHB. β_{pqr} values are defined according to the equation:

$$pH^+ + qAl^{3+} + r(H_3L^+) \rightleftharpoons H_pAl_q(H_3L)_r^{(p+3q+r)+}$$

p q r	log β_{pqr}	(σ)	Proposed formula
0 0 1	0		H_3L^+
-1 0 1	-8.577	(0.002)	H_2L^0
-2 0 1	-18.901	(0.006)	HL^-
-3 0 1	-32.0	estimated	L^{2-}
-2 1 1	-5.58	(0.006)	$AlHL^{2+}$
-4 1 2	-13.74	(0.013)	$Al(HL)_2^+$
-6 1 3	-25.51	(0.023)	$Al(HL)_3^0$
-7 1 3	-35.55	(0.055)	$AlL(HL)_2^-$
-8 1 3	-46.39	(0.098)	AlL_2HL^{2-}
-9 1 3	-56.79	(0.072)	AlL_3^{3-}
-6 2 2	-19.58	(0.041)	$(OH)_2Al_2(HL)_2^{2+}$

A selection of the titration data is plotted in Fig. 3.2. The function Z_c gives the average number of protons bound per DHB ligand. Plotting of titration data as this function gives a graphical curve that may be intuitively understood. Thus in Fig. 3.2 each titration curve starts with a Z_c value of 3 (corresponding to H_3L^+) which decreases as the pH increases and de-protonation and complexation reactions occur.

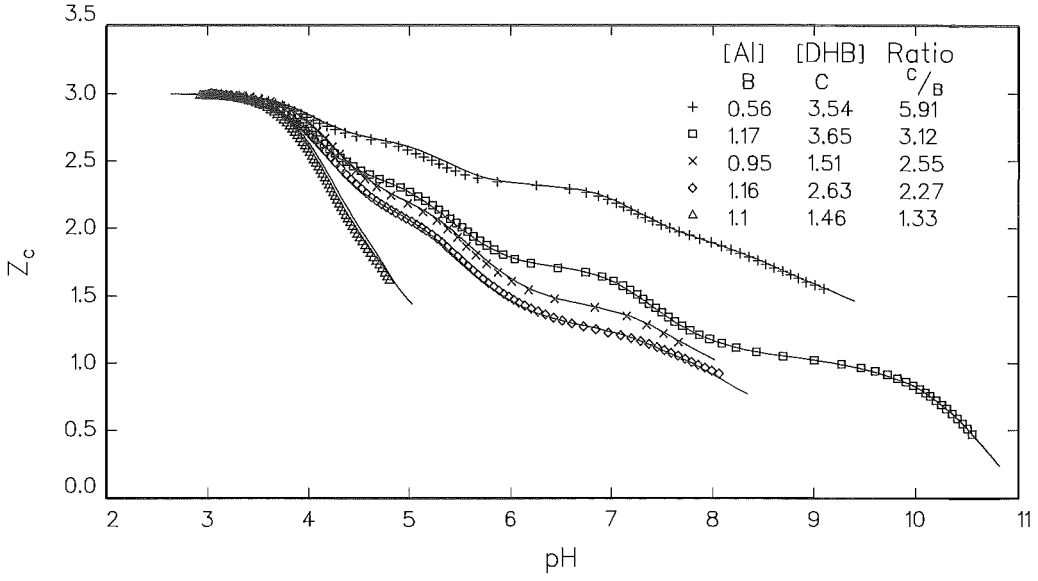

Figure 3.2 Z_C curves for the system H^+/Al^{3+}/DHB. Symbols give Z_C values calculated from titration data using eqn. (3.19). Solid lines were calculated using the constants given in Table 3.5.

Z_c may be calculated according to the definition of eqn. (3.19). This gives a value derived from the experimental variables of pH, volume of alkali added and the total ligand concentration and is plotted as the symbols in Fig. 3.2. Z_c may also be calculated from the derived complex formation constants with the assistance of the computer program SOLGASWATER [Eriksson, 1979]. Thus the formation constants of Table 3.5 were used to calculate the solid lines in Fig 3.2 and the 'goodness of fit' may be inspected visually.

$$Z_c = \frac{H - h + K_w h^{-1}}{L_T} \qquad \textbf{(3.19)}$$

H	=	total acidity	mol L^{-1}
h	=	free acidity, $[H^+]$	mol L^{-1}
K_w	=	water hydrolysis constant	mol^2 L^{-2}
L_T	=	total ligand concentration	mol L^{-1}

3.3.3 POTENTIOMETRY OF THE H^+/Al^{3+}/ALIZARIN COMPLEXONE (ACN) SYSTEM.

The protonation reactions of ACN were investigated by performing 9 titrations with the concentration of ACN varied over the range (4.0 - 0.87) $x10^{-3}$ M and yielding 428 datum points.

Cumulative protonation constants (β_{pr} values) were refined numerically from these data with the program SUPERQUAD and are reported in Table 3.6. Satisfactory agreement with literature values is observed. The study of Ingman (1973) was more comprehensive than that presented here in that values were obtained for β_{-11} and β_{41}. Determination of β_{-11} is beyond the scope of potentiometry as it corresponds to proton loss from a very weakly acidic phenolic functional group. It was studied by Ingman spectrophotometrically. The value of β_{41} is just within the bounds of that which may be determined potentiometrically ($\log\beta_{41}$ - $\log\beta_{31}$ = 2.4). However insufficient data were collected below pH 4.0 to allow its determination in this study.

Table 3.6 Protonation constants determined for the system H^+/ACN.
β_{pr} values are defined according to the equation:

$$pH^+ + r(HL^{3-}) \rightleftharpoons H_p(HL)_r^{(p-3r)+}$$

p r	log β_{pr}	(σ)	Lit. value[a]	Proposed formula
-1 1	not determined		-11.98	L^{4-}
0 1	0		0	HL^{3-}
1 1	10.229	(0.006)	10.07	H_2L^{2-}
2 1	15.80	(0.01)	15.61	H_3L^-
3 2	29.03	(0.03)	27.88	$H_5L_2^{3-}$
4 1	not determined		18.01	H_4L^0

[a]Ingman (1973)

Complex formation with Al was investigated. At millimolar concentrations ACN formed an orange coloured precipitate with Al from pH 3.0 and above. The very low solubility of this complex prevented the potentiometric determination of solution equilibrium constants. From the literature discussed in the introduction it is likely that Al occupies a cage-like coordination pocket formed by the imino-diacetate group and the phenolate group at the *ortho* position on the anthraquinone ring. This gives a complex of neutral charge and hence low solubility. A molecular structure is suggested:

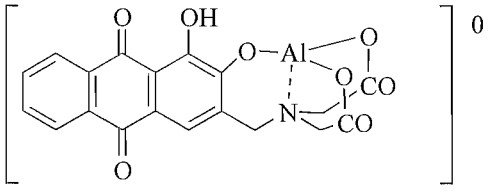

Al-ACN complex

3.3.4 POTENTIOMETRY OF THE H^+/Al^{3+}/DASA SYSTEM.

The protonation reactions of DASA were investigated by performing 10 titrations in which the concentration of DASA was varied over the range 1.2 - 3.3 mM giving 685 datum points. Complexation reactions with Al were investigated by performing 9 titrations (453 datum points) in which the concentrations were varied over the ranges 0.71 - 2.0 mM for DASA and 0.25 - 0.5 mM for Al. The ratio of ligand to metal was varied over the range 2.4 - 4.0. These data were analysed numerically with the program SUPERQUAD, giving the formation constants in Table 3.7. σ gives the standard deviation for each constant.

Table 3.7 Equilibrium constants determined for the system H^+/Al^{3+}/DASA. β_{pqr} values are defined according to the equation:

$$pH^+ + qAl^{3+} + r(L^{3-}) \rightleftharpoons H_pAl_qL_r^{(p+3q-3r)+}$$

p q r	Method	log β_{pqr}[a]	(σ)	Lit. value	Proposed formula
1 0 1	pot.	10.942 (0.003)		10.91[c]	$[HL]^{2-}$
1 0 1	sp.	10.95 (0.03)		10.96[b]	$[HL]^{2-}$
2 0 1	pot.	16.740 (0.004)		16.7[c]	$[H_2L]^-$
3 0 2	pot.	29.909 (0.02)			$[H_3L_2]^{3-}$
0 1 1	sp.	14.19 (0.04)		14.11[b]	$[AlL]^0$
0 1 2	pot.	28.244 (0.009)		26.93[b]	$[AlL_2]^{3-}$
-1 1 2	sp.			34.1[b]	$[(OH)AlL_2]^{4-}$
-2 2 4	pot.	44.19 (0.03)			$[(OH)_2Al_2L_4]^{8-}$

pot.- potentiometry, sp.- spectrophotometry
[a] this work
[b] Couturier (1987) (0.1 M $NaClO_4$),
[c] Forsling and Wu (1992) (0.1 M KCl).

A selection of titration curves which covers the widest range of metal to ligand ratios examined is presented in Fig. 3.3. The curves are plotted as the Z_c function (eqn. 3.19) which gives the average number of protons bound per DASA equivalent. Solid lines give the value of Z_c calculated with the computer program SOLGASWATER from the constants presented in Table 3.7.

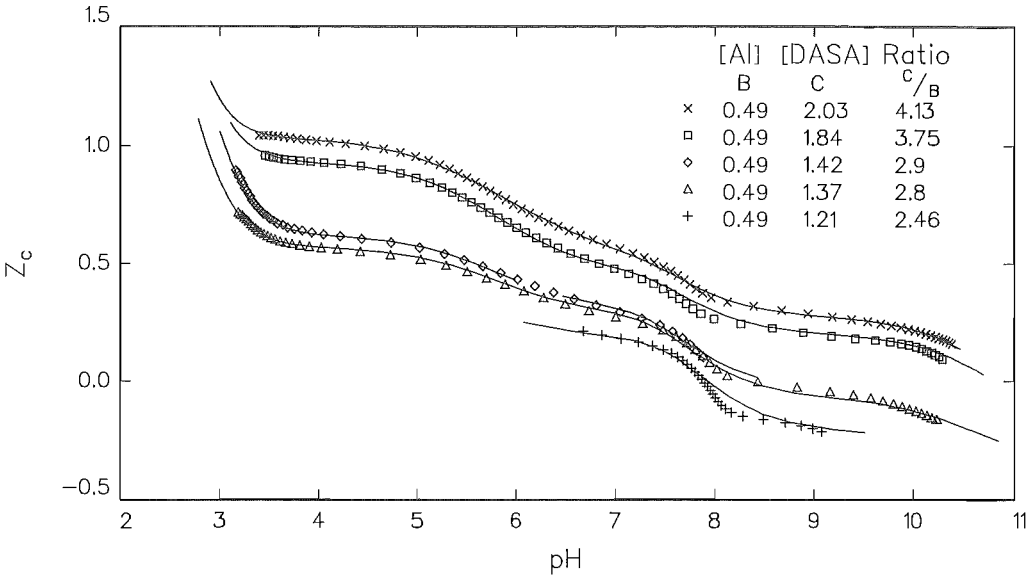

Figure 3.3 Z_C curves for the system H^+/Al^{3+}/DASA. Symbols give Z_C values calculated from titration data using eqn. (3.19). Solid lines were calculated using the constants given in Table 3.7.

3.3.5 SPECTROPHOTOMETRY OF THE H^+/Al^{3+}/DASA SYSTEM.

3.3.5-A DETERMINATION OF β_{101}. The protonation constant for the most strongly basic functional group of DASA was determined by potentiometry as 10.942 (log β_{101}), Table 3.6). At pH 10.6 (the limit for pH measurement by the glass bulb electrode) this functional group will be only 30% ionised. Thus the value of β_{101} determined by potentiometry was viewed with suspicion and it was redetermined spectrophotometrically using the method of Agren (1955), eqn.s 3.8 - 3.12.

A solution containing 48.0 μM DASA was titrated with standard alkali. 19 spectra were collected over the pH range 9.5 - 11.6. Since the concentration of ligand was low and the pH moderately high, the pH was determined by calculation (rather than by potentiometric measurement). This was performed using the hydrolysis constant of water ($10^{-13.79}$ for 0.1 M KCl) and by calculation of the concentration of hydroxide ion arising from the additions of standard CO_2 free alkali. This allowed the pH to be determined to a higher value than that possible by potentiometric measurement with a glass bulb electrode. Also the resulting calculation of β_{011} is truly independent of the value determined potentiometrically.

Graphical plots (equation 3.12) were formed using data taken from 10 wavelengths over the ranges 326-336 and 560 - 600 nm. These are the wavelengths where the difference in absorbance for free and protonated ligand is the greatest (see Fig. 3.4,

compare curves B and C). A typical plot is given in Fig. 3.5.

The average value determined spectrophotometrically for β_{101} is given in Table 3.7. This shows excellent agreement with values taken from the literature and with that determined potentiometrically.

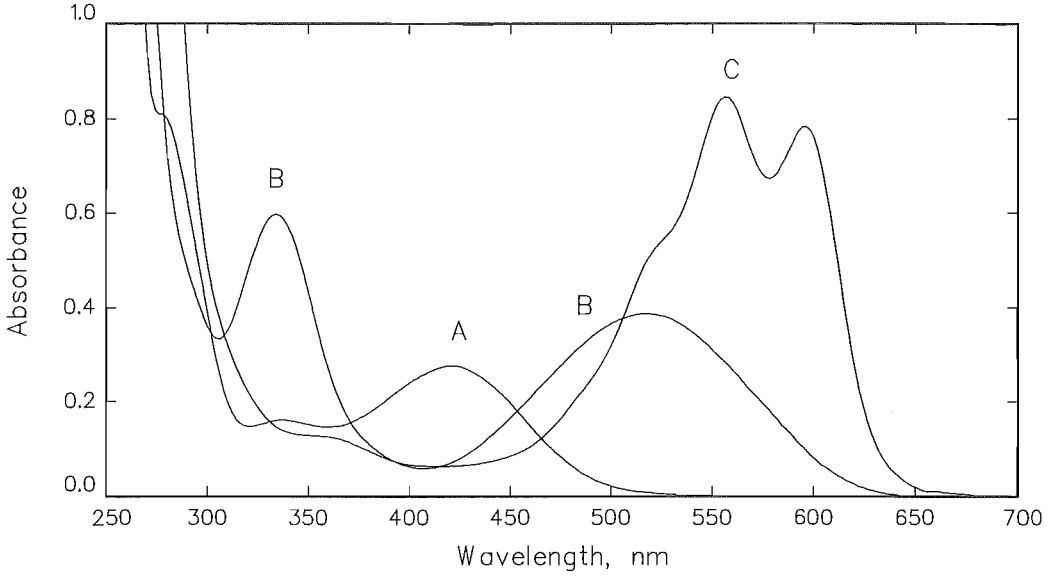

Figure 3.4 Absorbance spectra for DASA showing the effect of ligand de-protonation. [DASA] = 48.0 μM. Ionic strength adjusted to 0.1 M (KCl)
A) H_2DASA^- in 0.01 M HCl, pH 2
B) $HDASA^{2-}$ in 0.05 M NH_4Cl buffer, pH 8.4
C) $DASA^{3-}$ in 0.15 M KOH, pH 13.0.

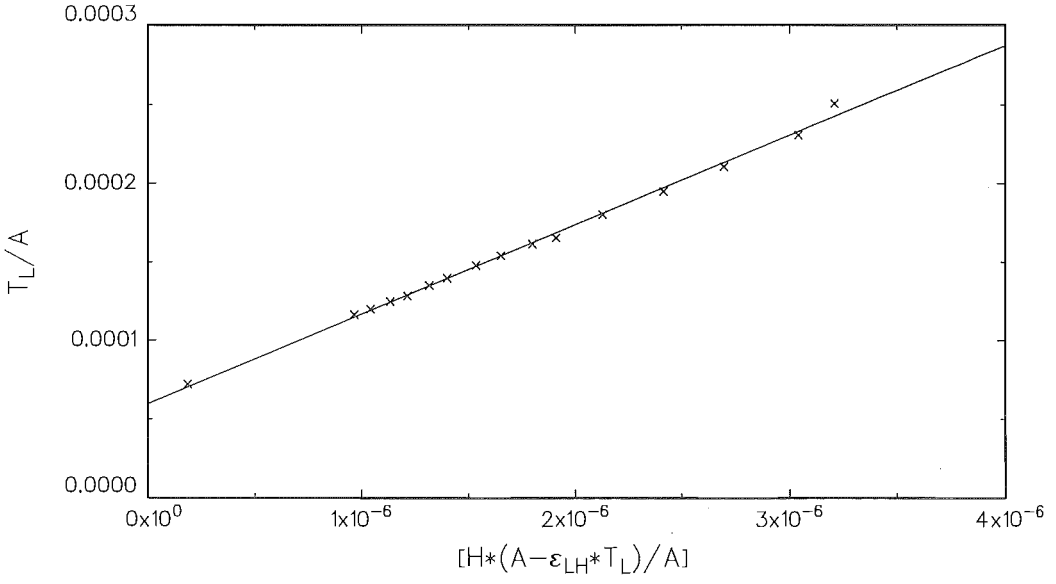

Figure 3.5 'Agren' plot for the calculation of β_{101} (see eqn.s 3.8 - 3.12). Absorbance values were collected at 590 nm.

3.3.5-B DETERMINATION OF β_{011}. The 1:1 complex formed between Al and DASA was observed to have a low solubility of approximately $1x10^{-4}$ M in 0.1 M KCl. At the pH where this species is formed (pH 2.6 - 3.5) the concentration of free protons is up to 20 fold greater. Thus the changes in free proton concentration that are produced by formation of the complex are relatively insignificant and a value for the complex formation constant (β_{011}) cannot be accurately determined by potentiometry.

Instead the value of β_{011} was determined spectrophotometrically using the adaptation of Agren's (1955) method described in section 3.1.3-A, (eqn.s (3.13) - (3.17)). The necessary conditions required for the application of Agren's method to complexation equilibria were met by using a large excess of Al over DASA and by holding the experimental conditions to pH values of 3.5 or less.

Over this pH range the dominant protonated form of DASA is H_2DASA^-. The deprotonation reaction to form the species $HDASA^{2-}$ has a pK_a value of 5.80 so only 0.5% of the total free ligand is in this form at pH 3.5 and even less at lower pH values. Thus it may be assumed that there is only a single protonation state of the ligand. The hydrolysis of Al may be neglected for pH values less than 4.0.

Two titrations were performed with the concentration of DASA being 48 μM in both and the concentration of Al being 1.33 and 2.26 mM. This gave 28 and 47 fold excesses of Al over DASA respectively. The pH was varied over the range 2.5 - 3.5 and measured potentiometrically. 10 spectra were collected in the 28 fold excess titration and 16 in the 47 fold excess titration.

Agren plots (eqn. 3.17) were formed using data taken from 7 wavelengths over the ranges 320-326, 400-404 and 480-500 nm. These are the wavelengths where the difference in absorbance for free and complexed ligand is the greatest (see Fig. 3.6, compare curves A and B). Calculations were performed in both 'directions', ie using known values of the molar absorptivity, ε_x, for both the free and complexed forms of DASA. This gave 14 measurements of β_{110} from each titration. One of these plots is given in Fig. 3.7.

Fig. 3.7 also shows the effect of varying the parameter n, the number of protons displaced by Al from DASA. Clearly n has a value of 2.

The average value determined for β_{011} is given in Table 3.7. This shows excellent agreement with a value taken from the literature.

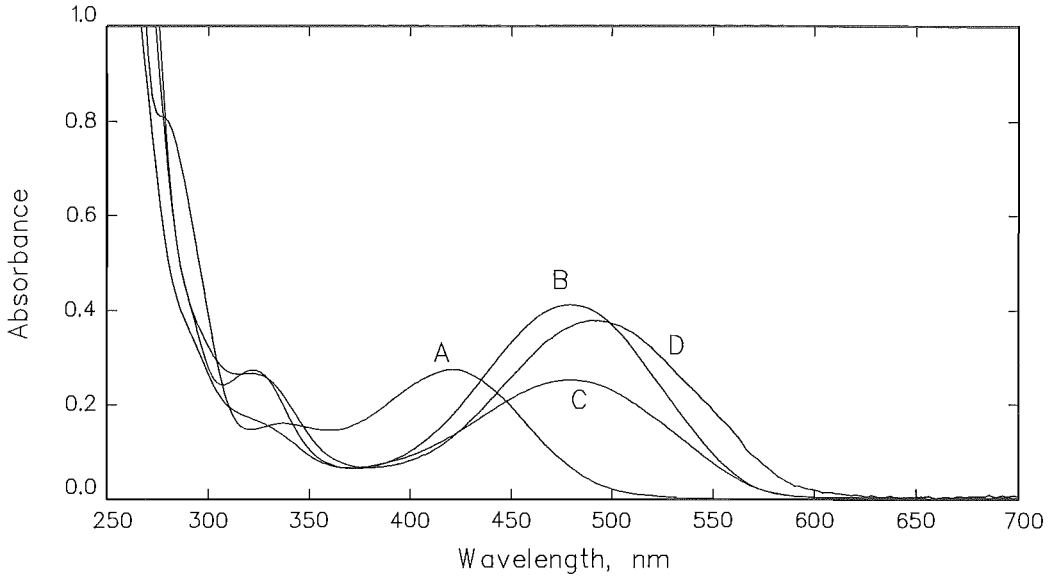

Figure 3.6 Absorbance spectra for DASA showing the effect of complexation. In each case [DASA] = 48.0 μM and the ionic strength is adjusted to 0.1 M with KCl.

A)	H_2DASA^-	[Al] = 0	0.01 M HCl, pH 2.
B)	$[AlDASA]^0$	[Al] = 2.7 mM,	0.05 M acetate buffer, pH 3.7.
C)	$[Al(DASA)_2]^{3-}$	[Al] = 25 μM,	0.05 M acetate buffer, pH 5.4.
D)	$[Al_2(DASA)_4(OH)_2]^{8-}$	[Al] = 24 μM,	0.05 M NH_4Cl buffer, pH 9.2.

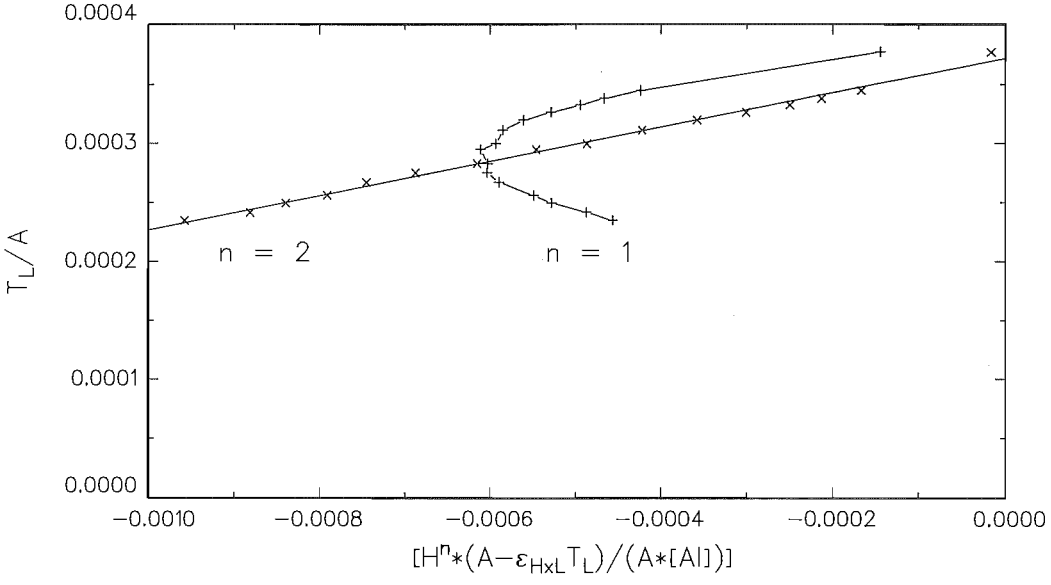

Figure 3.7 'Agren' plot for the calculation of β_{011} (see eqn.s (3.13) - (3.17)). n gives the number of protons displaced by Al from H_2DASA^- (eqn. (3.13)). The horizontal axis is labelled for n=2 data only. Absorbance values were collected at 404 nm. [DASA] = 48 μM, [Al] = 2.26 mM.

3.3.5-C CONTINUOUS VARIATION DIAGRAM. The stoichiometry of the complex formed between Al and DASA at pH 9.2 was investigated by constructing a continuous variation plot. This assisted in establishing the end member of the equilibrium model.

Fifteen solutions were prepared in which the sum of the concentrations of Al and DASA was held constant at 10 μM. The pH was buffered to pH 9.2 (0.05 M NH_4Cl/NH_4OH) and the ionic strength adjusted to 0.1 M with KCl. After 20 minutes equilibration the absorbance spectrum of each solution was measured. The absorbance at 332 nm is plotted in Figure 3.8.

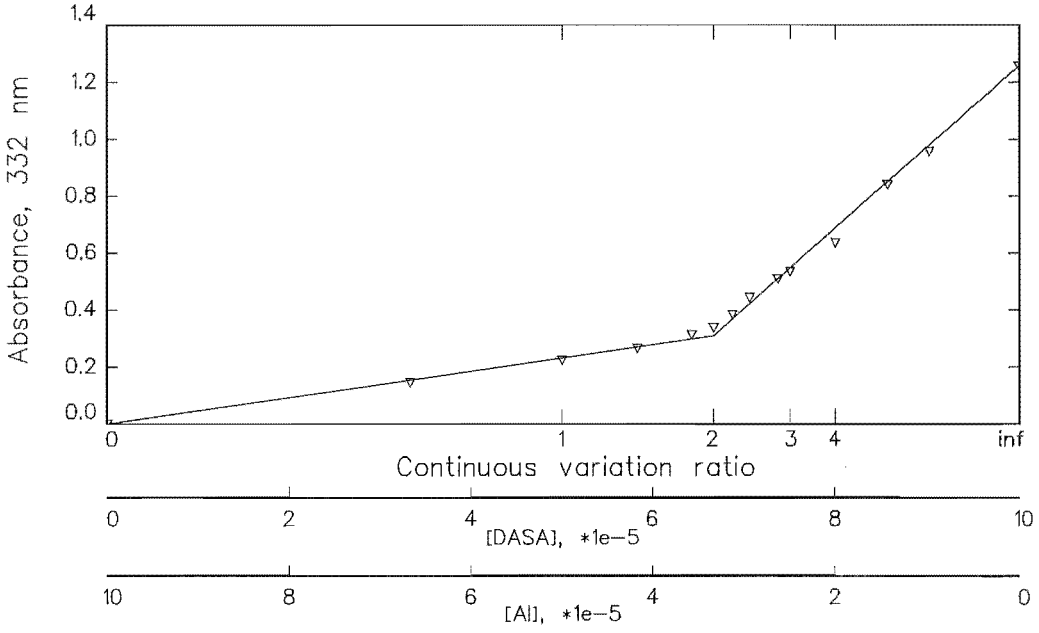

Figure 3.8. Continuous variation plot for the system Al/DASA at pH 9.2.

At the extreme ends of the ratio axis the absorbance is equivalent to that for either 10 μM $Al(OH)_4^-$ or $HDASA^{2-}$. An inflection is observed at a ratio *ca.* 2.0. This indicates that Al and DASA combine to form a complex of stoichiometry Al:DASA = 1:2 at pH 9.2.

3.4 DISCUSSION.

3.4.1 SOLUTION EQUILIBRIA BETWEEN Al AND A CATECHOL DERIVATIVE, (DHB).

The model of the solution equilibrium constants determined for the system H^+/Al^{3+}/DHB, Table 3.5, may be illustrated by a species distribution diagram as shown in Fig. 3.9. This gives the distribution of Al over the species which are formed as a function of pH.

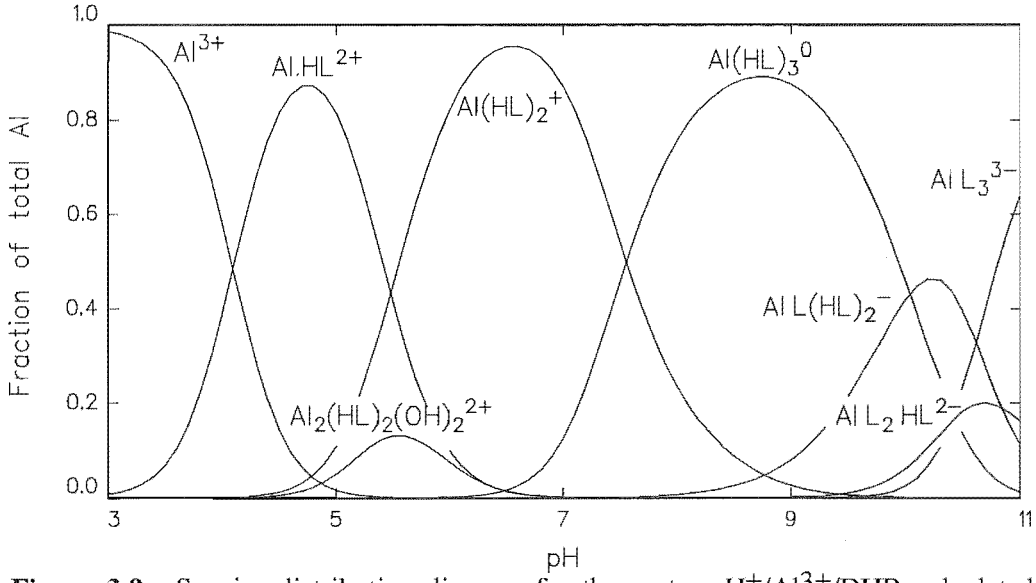

Figure 3.9. Species distribution diagram for the system H^+/Al^{3+}/DHB calculated with the program SOLGASWATER using the equilibrium constants of Table 3.5. [DHB] = 3 mM, [Al] = 1mM.

Below pH 3.0 Al is not bound by DHB. Above this pH DHB binds to Al via its catecholate moiety with 1, 2 and 3 ligands successively adding to the metal centre. This results in Al being surrounded by up to 6 phenoxy donors in an octahedral environment, giving the species $[AlL_3]^{3-}$ with pqr coefficients (-6 1 3). This is consistent with the coordination chemistry observed for Al and other catechol derivatives [Kiss *et al.*, 1989].

The complexes bear an ammonium functional group on their exterior from each catecholamine ligand. Successive deprotonation of these three groups in the tris species (pqr = -6 1 3) gives rise to the species with pqr coefficients (-7 1 3), (-8 1 3) and (-9 1 3). The average (log) spacing between these constants is 10.43 which compares closely to the corresponding pK_a for the free ligand, 10.32. Thus the acidity of the amine group remains relatively unaffected by coordination of the ligand to aluminium, as expected.

In the course of numerical modelling of the potentiometric data substantial improvements to the fitting were obtained by inclusion of a dimer species into the model,

$[Al_2(DHB)_2(OH)_2]^{2+}$. This is consistent with the model developed by Kiss *et al.* (1989) for coordination of Al by other catecholamines.

Other species whose presence might be anticipated from studies published in the literature for analogous ligands are $[OHAlHL]^{+}$, $[OHAl(HL)_2]^{0}$, $[HAl(HL)_2]^{2+}$, $[HAl(HL)_3]^{1+}$ and $[Al_2(HL)_2(OH)_2H_{-1}]^{+}$ [Motekaitis and Martell, 1984; Kennedy and Powell, 1985; Kiss *et al.*, 1989]. None of these species was determined to be present within the solutions examined in this study since their inclusion did not improve the goodness of fit.

The strength of the binding of Al by DHB cannot be directly compared with that by other catechol derivatives using the cumulative equilibrium constants reported in Table 3.5. This is because the cumulative constants contain deprotonation terms as well as complex formation terms. The deprotonation terms may be subtracted out if the protonation reactions are fully characterised.

Unfortunately the deprotonation constant for the most strongly basic functional group in DHB (β_{-301}) could not be determined. Comparison with catechol and with other catecholamines [Kennedy and Powell, 1985; Kiss *et al.*, 1989] suggests that this reaction corresponds to deprotonation of the second phenol group (to give a di-*ortho* anion) and that it should occur above pH 12.5. This is beyond the range of potentiometry but may be studied spectrophotometrically. This was attempted (unsuccessfully) in this study on at least two separate occasions.

Deprotonation of catechol derivatives makes them highly susceptible to oxidation and subsequent polymerisation reactions [Ryan *et al.*, 1980]. This gives DHB solutions a brown discolouration and the corresponding spectra are broad and featureless. Precautions were taken to exclude oxygen. These precautions were to maintain the titration cell in a positive atmosphere of oxygen-free nitrogen. The nitrogen supply was commercially supplied as O_2-free and was also bubbled through a Zn/Hg-V^{2+} oxygen scrubber as an extra precaution. Despite these precautions polymerisation of DHB could not be prevented in this study once the pH rose above 11.0. It may be that there was a fault in the experimental set-up allowing inclusion of O_2 (e.g. with alkali additions) or it may be that the amine substituent in DHB makes it highly susceptible to polymerisation reactions. A value of β_{-301} was estimated (-32.0) from inspection of the spectra.

The coordination of Al by DHB may be compared with other catechol

derivatives by the calculation of pM values, i.e. the negative logarithm of the free metal ion concentration. This was calculated for DHB and a range of catechol derivatives using the program SOLGASWATER and is shown in Fig. 3.10 as a function of pH. For DHB the equilibrium constants of Table 3.5 were used, for the other ligands equilibrium constants were taken from the literature [epinephrine: Kiss *et al.*, 1989; 4-ncat: Downard *et al.*, 1997a; catechol: Kennedy and Powell, 1985; tiron: Havelkova and Bartusek, 1969].

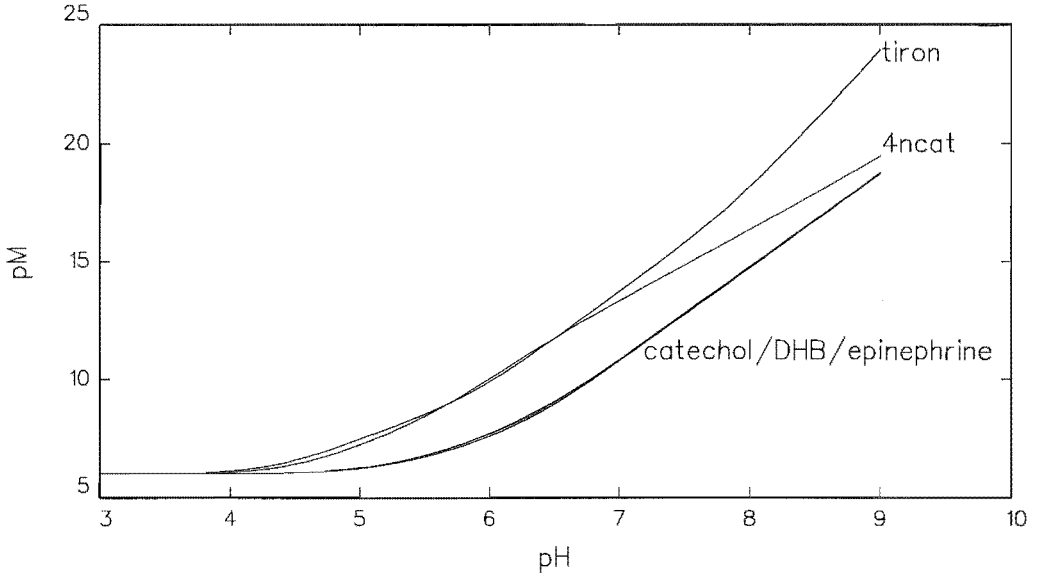

Figure 3.10. pM values for Al and a range of catechol derivatives. For each curve the total concentrations are [Al] = 1 μM and [ligand] = 10 μM.

A large pM value indicates a low concentration of free metal and a very stable complex. In Fig. 3.10 each curve starts at a pM value of 6 below pH 4. This is the value expected for 100% free Al at 1 μM total metal concentration. Above pH 4.0 the curves rise to higher pM values as Al becomes complexed. Tiron gives the highest pM values and forms the strongest complexes with Al. DHB and epinephrine are both examples of catecholamines and their pM curves overlie the curve for catechol. Evidently the *para*-amino substituent in the catecholamines makes little difference to the strength of each ligand's coordination to Al. The ligand 4-ncat shows a pM curve which is intermediate between that for tiron and those for catechol and the catecholamines.

3.4.2 A REDETERMINATION OF THE SOLUTION EQUILIBRIA PRESENT IN THE H^+/Al^{3+}/DASA SYSTEM.

The model of the solution equilibrium constants determined for the system H^+/Al^{3+}/DASA, Table 3.7, may be illustrated by a species distribution diagram as shown in Fig. 3.11. This gives the distribution of Al over the species which are formed as a function of pH.

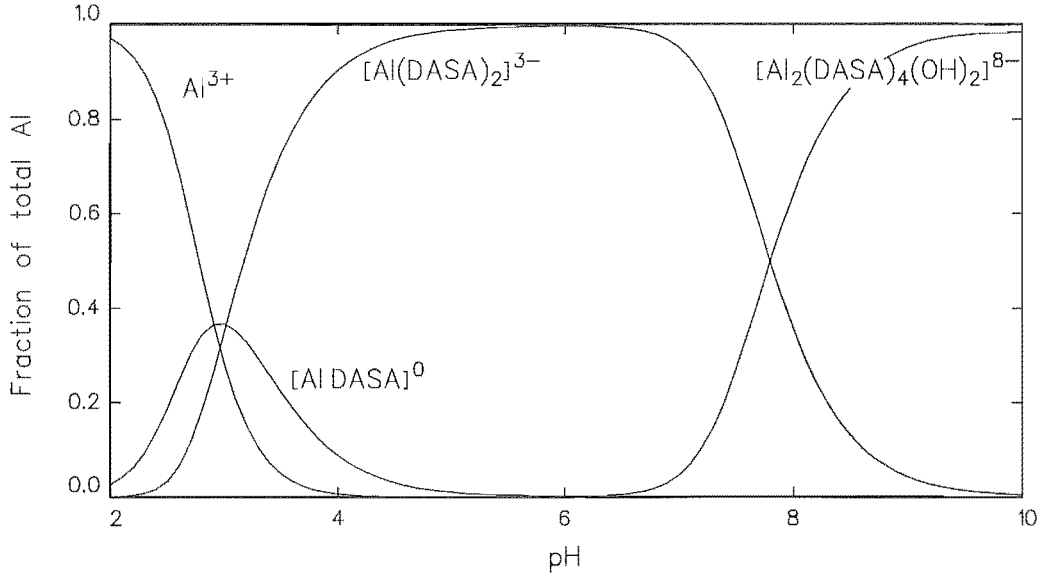

Figure 3.11. Species distribution diagram for the system H^+/Al^{3+}/DASA calculated with the program SOLGASWATER with the equilibrium constants of Table 3.7. [DASA] = 1 mM, [Al] = 0.5 mM.

The protonation constants determined for DASA agree with those reported by other workers except that a new dimer species of the formula $[H_3(DASA)_2]^{3-}$ was observed. This reaches a maximum concentration at pH 5.8 when there is an equal concentration of the species $[HDASA]^{2-}$ and $[H_2DASA]^-$. Its presence is inferred from an improved numerical fit to the potentiometric data. ACN, which shares the di-hydroxyanthraquinone structure of DASA, showed a similar species. Dimerisation of ACN has also been observed potentiometrically by Ingman (1973).

The formation constant determined spectrophotometrically for the 1:1 complex, β_{011}, corresponds closely to the value determined previously by a similar technique by Couturier (1987, 1989).

The number of protons displaced by Al from DASA in the course of forming the 1:1 complex was determined (spectrophotometrically) to be 2. This was also observed by Couturier (1987) and suggests that Al coordinates at the 1,2-*ortho*-diphenolate site of DASA rather than at the 1,9-quinoid-phenolate site. Also displacement of two protons

allows the complex formula to be written as $[AlDASA]^0$. This explains the low solubility of the 1:1 complex since it has zero charge.

The value determined (potentiometrically) for β_{012} was a little higher than that determined by Couturier (1987) (spectrophotometrically). This may be a result of the different experimental method employed.

The data determined here indicates that the stepwise constants K_1 ($=\beta_{011}$) and K_2 ($= \beta_{012}/\beta_{011}$) are approximately equal. This indicates that, in the solutions studied, the 1:2 complex formed almost concurrently with the 1:1 complex.

In potentiometric studies conducted above pH 7.0 a buffer region was observed in which one equivalent of alkali was consumed per Al ion. At this pH the ligand DASA is singly protonated and it was initially thought that this buffer region corresponded to uptake of one ligand per $[Al(DASA)_2]^{3-}$ complex to give the species $[Al(DASA)_3]^{6-}$. The buffer region was not diminished, however, in titrations where less than a three fold excess of DASA over Al was used. A 3:1 complex was finally discounted by constructing a continuous variation diagram. This showed that, at pH 9.2, the stoichiometry of the complex was 1:2, Al:DASA.

The study of Couturier (1987) suggested that the species $[Al(DASA)_2OH]^{4-}$ may be forming. Inclusion of this species into the model did not give a good fit to the data. The abrupt flatness of the buffer region indicated that a polymerisation reaction was occurring. The conclusion of Couturier was reinterpreted as suggesting a species of the formula $[(Al(DASA)_2OH)_x]^{4x-}$ where x gives the extent of polymerisation. Values of x other than one would not have been observed by Couturier who used spectrophotometric/graphical methods of investigation.

Wunderlich and Bergerhoff (1994) have published a crystallographic investigation of the structure of aluminium calcium alizarinate. Figure 3.12 reproduces their illustration of a structure with the formula $[(Al(alizarin)_2OHCa)_2]$. The two Al ions are bridged by two hydroxide ions. The coordination sphere of each Al ion is completed by two alizarin ligands with coordination occurring at the 1,2 -*ortho*-di-phenolate sites. Two calcium ions join the structure by filling the vacant 1,9-quinoid-phenolate coordination sites. This structure offers strong supportive evidence for a value of 2 for x in the formula above. Inclusion of a species of the formula $[Al_2(DASA)_4(OH)_2]^{8-}$, β_{-224}, in the numerical calculations gave an acceptable fit to the potentiometric data.

It has been noted in some of the analytical applications which use DASA for the AdSV measurement of Al that addition of calcium gives improved sensitivity [Hernandez-Brito *et al.* (1994); Carrera *et al.*, 1993]. This further supports the suggestion that a structure resembling that illustrated in Fig. 3.12 is formed in solution.

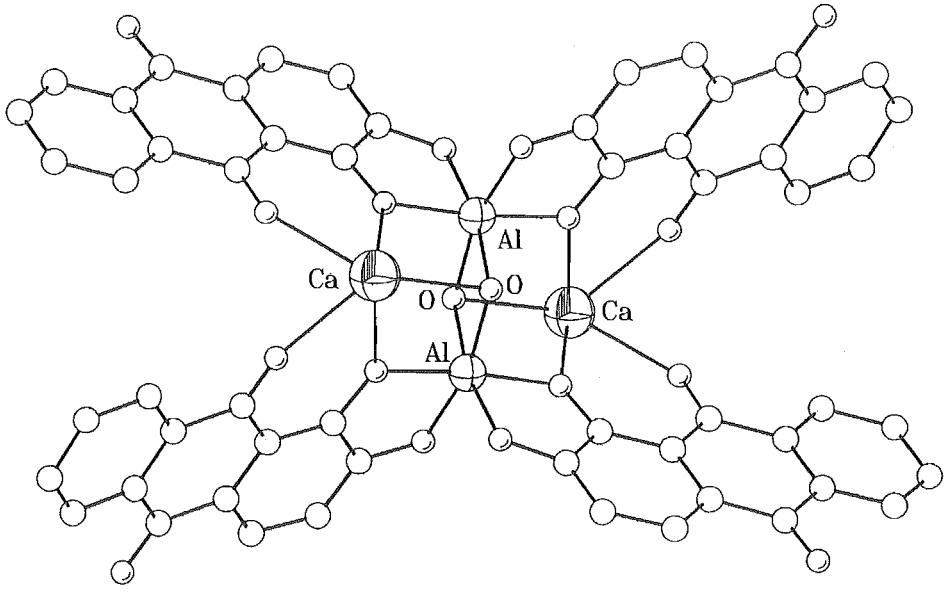

Figure 3.12 Crystal structure of aluminium calcium alizarinate reproduced from Wunderlich and Bergerhoff (1994).

The qualifying statement should be made that the equilibrium model reported for the system H^+/Al^{3+}/DASA should not be applied to conditions that are widely divergent from those used in the model's determination. These conditions are micromolar concentrations of DASA with a large excess of Al below pH 3.5 and millimolar concentrations of DASA with an excess of ligand above pH 4. For solutions having an excess of Al and pH greater than 4.0 it is expected that hydrolysis of the excess metal will occur. Thus for analytical applications a 2-fold excess of DASA over Al should be maintained.

3.5 CONCLUSION

The techniques of solution thermodynamics have proven to be a useful, if somewhat painstaking, tool for the investigation of the complex formation reactions of Al.

The interaction of DHB with Al conforms to the pattern observed for other catecholamines. The strength of the coordination of DHB to Al is lower than that for some other catechol derivatives (e.g. 4-ncat and tiron). Also DHB was found to be highly susceptible to oxidation/polymerisation reactions in alkaline solutions. These properties make it unlikely that DHB will be further developed as an analytical reagent for Al.

Determination of the deprotonation constant for the most strongly basic functional group of DHB would complete the characterisation of the system H^+/Al^{3+}/DHB.

The solution chemistry in the system H^+/Al^{3+}/DASA has been examined and found to conform in many respects to the observations of Couturier (1987, 1989). Use of potentiometric/numerical techniques has revealed the presence of two new dimer species.

The species $[H_3(DASA)_2]^{3-}$ is comparable to a species observed in the protonation reactions of ACN.

A species written by Couturier as $[Al(DASA)_2(OH)]^{4-}$ was determined in this study to be present as the dimer $[Al_2(DASA)_4(OH)_2]^{8-}$. Independent spectrophotometric and crystallographic evidence for this structure has been presented. This is an important observation. In many of the electroanalytical protocols that have been developed for Al using DASA it is likely that this species is the analytical complex formed since an excess of DASA and an alkaline pH is often used [e.g. van den Berg *et al.*, 1986; Hernandez-Brito *et al.*, 1994; Carrera *et al.*, 1993; Downard *et al.*, 1992a]

The formulism of Agren (1955) has been successfully modified to allow (under certain conditions) the spectrophotometric examination of complex formation equilibria.

Chapter 4

VOLTAMMETRY OF SOME ALUMINIUM COMPLEXES.

4.1 INTRODUCTION.

In this chapter voltammetry is used to examine the shifts in ligand redox potential which are the basis of the indirect electroanalysis of Al.

The results described here have been published [Downard *et al.*, 1996].

4.1.1 INDIRECT VOLTAMMETRIC ANALYSIS.

The basis of the indirect voltammetric analysis of a metal is the appearance of a separate electrochemical response for metal-bound ligand. Compared with the corresponding redox process for the metal-free ligand, this response generally appears at more negative potentials for reduction and more positive potentials for oxidation.

This strategy has been exploited in the analysis of Al and its use is discussed in the introductory chapter, section 1.4.4.

Although the utilisation of these Al-ligand signals is well established, the electrochemistry of the systems has not been studied in detail. Two aspects of the systems are of particular interest. First, treatment of shifts in metal or ligand redox processes after complexation have usually assumed that the complexes are labile on the timescale of the measurement and that dissociation of ligand occurs prior to electron transfer [Florence and Belew, 1969 and Shiu and Harrison, 1989]. This model is not likely to be appropriate for complexes of Al, a relatively inert ion, [see Fig. 6.13, section 6.4.1] for which direct oxidation and/or reduction of coordinated ligand is expected.

Also the electrochemical responses of Al complexes with different stoichiometries do not appear to have been previously examined. As the excess of ligand used in a metal determination varies, complex stoichiometry may change and hence it is of interest to observe the effect of such change.

4.1.2 THE OXIDATIVE ELECTROCHEMISTRY OF Al-CATECHOL AND Al-DASA.

Reported here is an investigation of the oxidative electrochemistry of the Al-catechol and Al-DASA systems at glassy carbon (GC) electrodes. Although complexes formed between catechol and Al are not sufficiently stable to be widely applied in analysis of Al, study of their electrochemistry provides generally useful results. DASA was chosen because of its relatively clean electrochemical behaviour and usefulness as an electroactive ligand for Al determination [van den Berg *et al.*, 1986; Hernandez-Brito *et al.*, 1994; and Downard *et al.*, 1992a and 1997b]. Most importantly, the stability constants for both systems are available [Al-catechol; Kennedy and Powell, 1985; Al-DASA; see Chapter 3]. This enables interpretation of the electrochemistry to be based on calculated solution compositions.

Oxidative electrochemistry has been used since this removes the need for removing di-oxygen (O_2). The reduction of oxygen to hydrogen peroxide often interferes in electrochemical measurements where reducing (negative) potentials are applied. O_2 is removed by solution purging with an inert gas. A long-term goal of this project is the development of measurement systems suitable for 'in-field' use. For such systems gas purging is not practical and is assumed here to be not available.

A complication arises for alkaline solutions containing catechol. These were observed to undergo oxidation reactions in the presence of di-oxygen, turning brown and depleting the concentration of ligand. For these solutions gas purging was used in order to remove O_2 but it was still the oxidative chemistry of the ligand that was examined. Purging was achieved with dinitrogen.

Glassy carbon (GC) has been chosen as the working electrode material because of its widespread availability and cheapness, its relatively wide potential (electromotive force) window and since carbon is a safe material for 'in-field' applications, (i.e. compared with Hg.)

The electrode kinetics of catechol at a polished GC electrode are slow over the pH range of interest to this study (pH 5-10). Improvements in electrode kinetics following a variety of electrode activation protocols have been reported for catechol and its derivatives [for some examples see Stutts *et al.*, 1983; Wang and Hutchins, 1985; Cabaniss *et al.*, 1985; Deakin *et al.*, 1986; Poon and McCreery, 1986; Rice *et al.*, 1990; and Anjo *et al.*, 1989]. Hence in initial experiments the effects of electrochemical pretreatments in acidic and basic media were examined.

Experimental details concerning equipment and electrode pretreatments are given in section 2.4 of Chapter 2.

4.2 RESULTS.

4.2.1 PRETREATMENT OF THE GC WORKING ELECTRODE.

ΔE_p, the potential separation between the anodic and cathodic peaks in a cyclic voltammogram is given as $59/n$ mV (n = number of electrons transferred) [see Bard and Faulkner, 1980, section 6.5.1, Nernstian behaviour is assumed]. Values greater than this indicate some kinetic limitation on the reaction of the redox species at the electrode surface [McCreery, 1991; Cabaniss *et al.*, 1985]. In this section surface pretreatments for GC are developed to give the optimum rate of electron transfer for species of catechol and DASA.

Figure 4.1a shows cyclic voltammograms (ν=100 mV s^{-1}) for 1 mM catechol in acetate buffer, pH 5.1, at polished, base- and acid-pretreated electrodes. Clearly both pretreatments dramatically increase the apparent rate of electron transfer with ΔE_p (= E_{pa} - E_{pc}) decreasing from *ca.* 400 mV at the polished electrode to 94 and 60 mV at base- and acid-pretreated electrodes respectively.

At pH 8.1 (HEPES buffer) in a solution of 1 mM catechol and 0.3 mM Al, where significant formation of Al-catechol complexes occurs, responses at the three electrodes are dramatically different (Figure 4.1b). At the polished electrode one broad response is observed whereas for the base pretreated electrode there are two well-separated peaks corresponding to oxidation of free and complexed ligand at E_{pa} = 0.13 and 0.27 V respectively. In contrast, at the acid pretreated electrode the oxidation of free catechol gives a well-defined signal but there is no response due to oxidation of complexed ligand.

Clearly the base pretreated surface combines the advantages of a kinetically fast surface with one where catechol species may freely access the redox active surface.

A possible complication is that the high activity of catechol at the base pretreated surface may arise from adsorption of species. However both oxidation processes for free and Al bound catechol exhibit a linear relationship between anodic peak current (i_{pa}) and the square root of the scan rate, $\nu^{1/2}$, for $20 < \nu < 330$ mV s^{-1} at the base pretreated surface indicating diffusion control of the response [Bard and Faulkner, 1980, see their eqn. 6.3.8]. Hence accumulation of catechol species at the base pretreated surface may be considered insignificant.

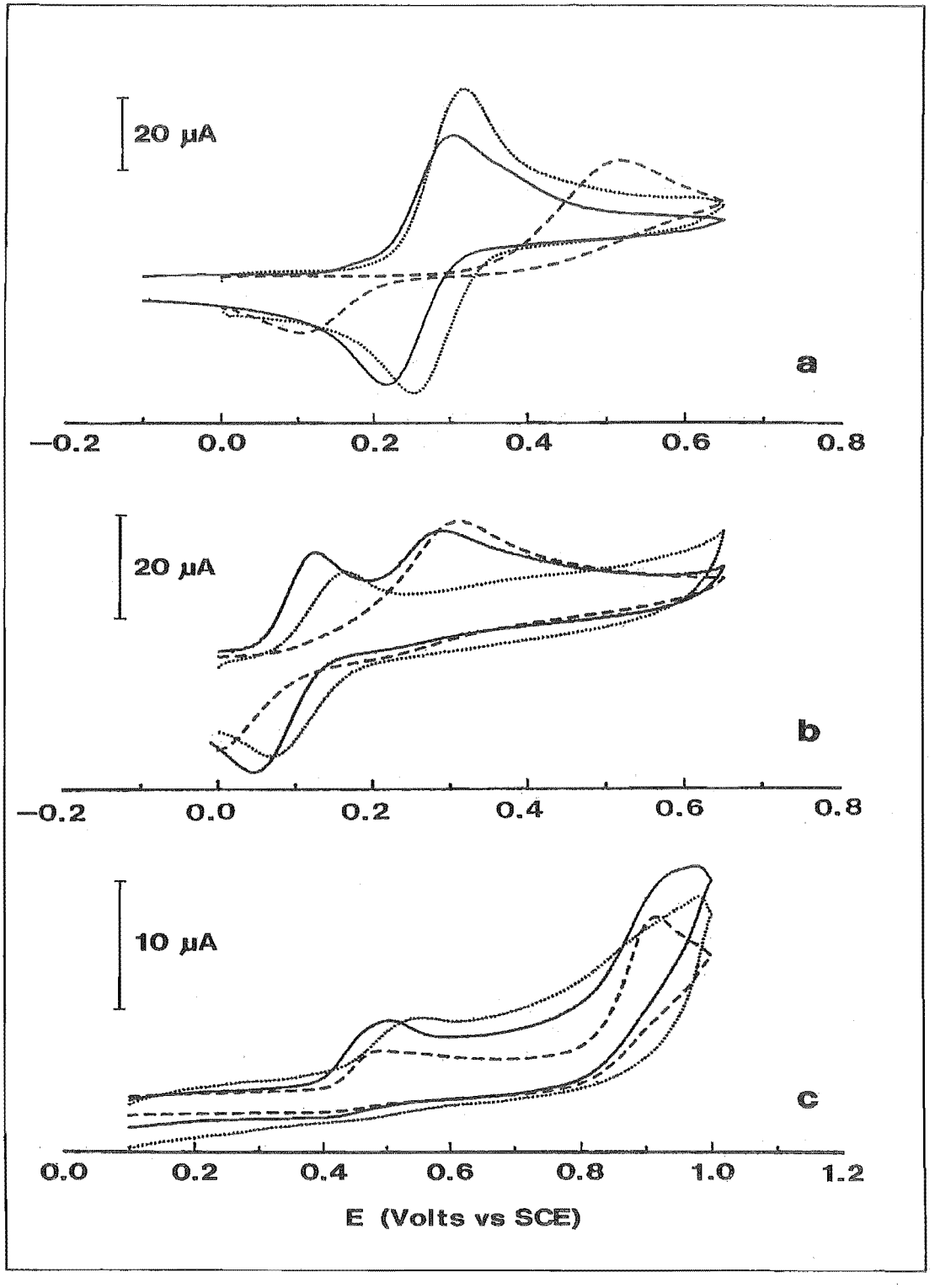

Figure 4.1 Cyclic voltammograms recorded at polished (- - -), acid pretreated (.....) and base pretreated (—) GC electrodes of:
a) 1.0 mM catechol in acetate buffer, pH 5.1, ν=100 mV s^{-1}
b) 1.0 mM catechol and 0.30 mM Al in HEPES buffer, pH 8.1, ν=100 mV s^{-1}
c) 0.85 mM DASA and 0.33 mM Al in acetate buffer, pH 5.5, ν=50 mV s^{-1}.

The results shown in Fig. 4.1b indicate that catechol species may readily access the base pretreated electrode surface while complexed ligand is excluded from the acid pretreated surface. However the base pretreated surface was found to exhibit selective sensitivity to DASA and its Al complexes. Thus the oxidations of the free ligand and the complex $[AlDASA]^0$ [see section 4.2.5, for Al-DASA species distribution diagram] were observed with high sensitivity at the base pretreated electrode (not shown) but, as is apparent in Figure 4.1c, the response of the complex $[Al(DASA)_2]^{3-}$ at $E_{pa} = 0.92$ V (acetate buffer, pH 5.5) is broad and merges with the large background current. Clearly the response at polished GC is better-defined. As expected, a response due to the complex is not detected at the acid pretreated electrode.

Therefore all voltammetry of catechol and its Al complexes was recorded at base pretreated electrodes and that of the DASA-Al system at polished GC electrodes.

4.2.2 ELECTROCHEMISTRY OF CATECHOL.

The electrochemistry of catechol has been thoroughly studied over a wide pH range [Ryan *et al.*, 1980; and Proudfoot and Ritchie, 1983]. Figs. 4.2a-e, solid lines, show cyclic voltammograms of 1 mM catechol at a range of pH values.

A two-electron oxidation to the quinone form occurs at all pH values; the potential of the process and the stability of the quinone (and hence chemical reversibility of the electrode process) are pH-dependent. At lower solution pH where there is significant stability of the quinone, the redox processes are quasireversible with ΔE_p values of 74, 70 and 60 mV ($\nu = 100$ mVs^{-1}) at pH 8.1, 7.2 and 4.8 respectively. At pH 4.8 there are small shoulders at the foot of the oxidation peak and following the peak; both features are absent at polished GC electrodes and hence are assumed to arise from a small amount of adsorbed catechol at the pretreated surface.

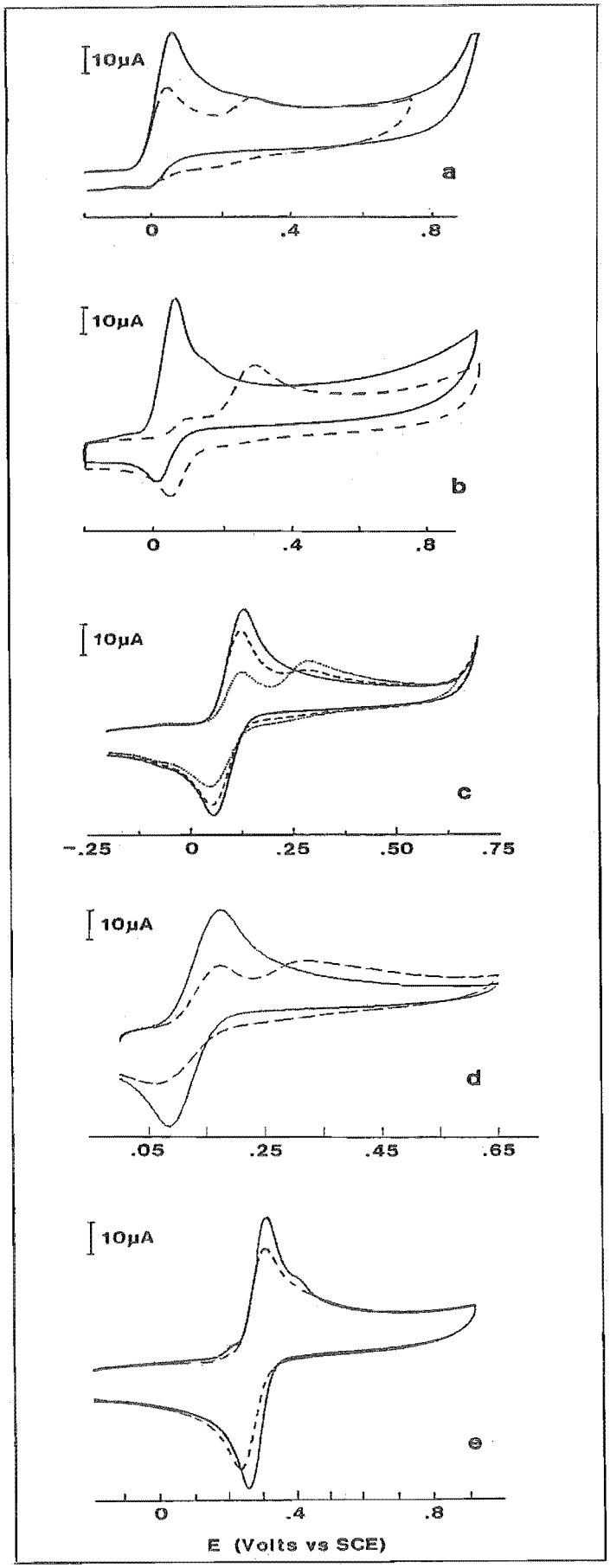

Figure 4.2
Cyclic voltammograms recorded using a base pretreated GC electrode at ν=100 mV s^{-1} of 1 mM catechol in the absence (——) and presence (- - -) of;

a) 0.17 mM Al, CHES buffer, pH 9.9;

b) 1.0 mM Al, NH_3/NH_4Cl buffer, pH 8.8;

c) 0.1 (- - -) and 0.30 mM (·····) Al, HEPES buffer, pH 8.1;

d) 0.50 mM Al, HEPES buffer, pH 7.2

e) 0.33 mM Al, acetate buffer, pH 4.8.

4.2.3 ELECTROCHEMISTRY OF Al-CATECHOL COMPLEXES.

The stability constants reported by Kennedy and Powell (1985) for the Al-catechol system were used to generate the species distribution diagram shown in Fig. 4.3 for total catechol and Al concentrations of 1.0 and 0.2 mM respectively. Such diagrams identify conditions under which a complex of a particular stoichiometry is dominant in solution. Table 4.1 lists the pH and total concentrations of catechol and Al used in each electrochemical experiment, the calculated concentrations of each species present, and the measured concentrations of free and complexed catechol. Measured concentrations were obtained from cyclic voltammetric peak currents assuming one catechol per complex is electroactive (see below).

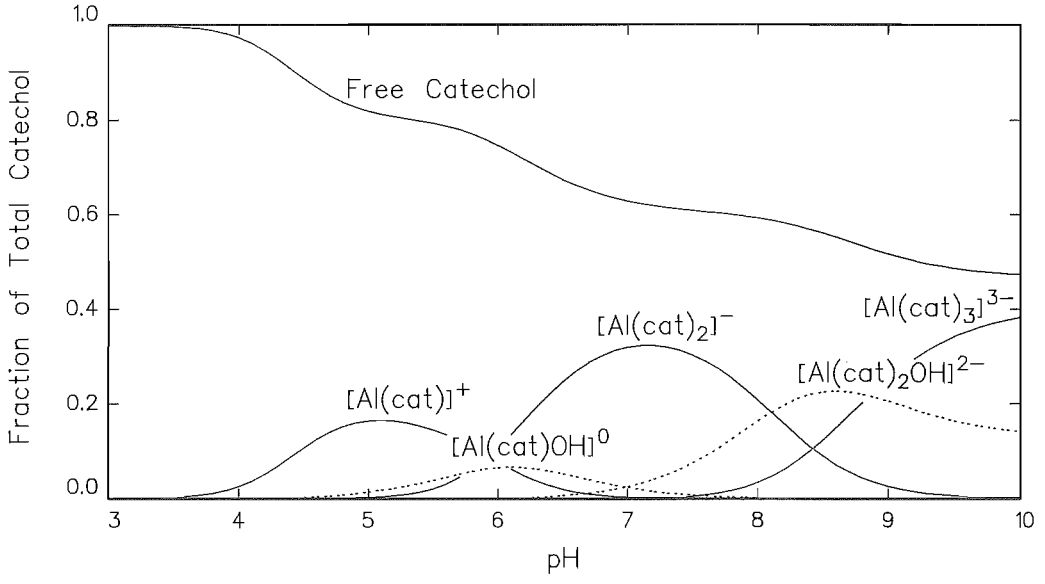

Figure 4.3 Species distribution diagram for the system H^+/Al^{3+}/catechol showing the fraction of total catechol present as each species when the total catechol and Al concentrations are 1.0 and 0.2 mM respectively.

Figure 4.2a shows cyclic voltammograms recorded in CHES buffer solutions containing 1 mM catechol and 1 mM catechol plus 0.17 mM Al at pH 9.9. On addition of Al, i_{pa} for the irreversible oxidation of free catechol at E_{pa} = 0.04 V decreases to *ca.* 55 % of its initial value and a second irreversible oxidation peak appears at E_{pa} = 0.27 V with i_{pa} *ca.* 12 % of the current of the original free ligand peak. From the results of species distribution calculations for pH 9.9 given in Table 1, the concentrations of free ligand and $[Al(cat)_3]^{3-}$ are predicted to be 0.55 and 0.11 mM respectively. Thus the redox process at E_{pa} = 0.27 V can be assigned to $[Al(cat)_3]^{3-}$ with a two-electron oxidation of only one ligand. Oxidation of $[Al(cat)_2OH]^{2-}$ also occurs at this potential, making a small contribution to the current (see below).

Table 4.1 Calculated solution compositions for the catechol-Al system and measured concentrations of free catechol and complexed catechol.[a]

Solution pH	Total Concentration (mM) Total catechol	Total Al	Free catechol	Calculated Concentration (mM) $[Al(cat)]^+$	$[Al(cat)OH]^0$	$[Al(cat)_2]^-$	$[Al(cat)_2OH]^{2-}$	$[Al(cat)_3]^{3-}$	Measured Concentration (mM) Free catechol	Complexed catechol
9.9	1.0	0.17	0.55	-	-	-	0.06	0.11	0.55	0.12
8.8	1.0	1.0	0.03	-	-	0.08	0.39	0.01	0.07	0.40
8.1	1.0	0.10	0.79	-	-	0.05	0.04	0.01	0.81	0.06
8.1	1.0	0.30	0.39	-	-	0.14	0.14	0.01	0.45	0.23
7.2	1.0	0.50	0.18	0.01	0.10	0.32	0.04	-	0.48	0.13
4.8	1.0	0.33	0.74	0.25	0.01	-	-	-	0.80	-

[a] Calculated concentrations were obtained using SOLGASWATER [Eriksson, 1979] and stability constants from Kennedy and Powell (1985). Measured concentrations are from cyclic voltammetric peak heights, ν = 100 mV s^{-1}, using a base-pretreated GC electrode. Measured concentrations of complexes assume that one catechol ligand per complex is electroactive.

The electrochemistry of $[Al(cat)_2OH]^{2-}$ was examined at pH 8.8 (NH_3/NH_4Cl buffer) in a solution containing 1 mM of both catechol and Al, giving calculated concentrations of 0.39, 0.08 and 0.01 mM for $[Al(cat)_2OH]^{2-}$, $[Al(cat)_2]^-$ and $[Al(cat)_3]^{3-}$ respectively. Figure 4.2b shows, in addition to the response due to uncomplexed catechol, a peak with E_{pa} = 0.27 V and i_{pa} *ca.* 40 % that of the original free ligand peak. The new peak is assigned to oxidation of both $[Al(cat)_2OH]^{2-}$ and $[Al(cat)_3]^{3-}$ with only one ligand in each complex electroactive. Oxidation of $[Al(cat)_2]^-$ may also contribute to the current, as discussed below.

Speciation calculations indicate that pH~7 is most suitable for the study of the complex $[Al(cat)_2]^-$. However, at neutral pH hydrolysis of Al is difficult to control at the Al concentrations required for voltammetric measurements. Figure 4.2d shows cyclic voltammograms of a 1 mM solution of catechol at pH 7.2 (HEPES buffer) with and without 0.5 mM Al. The free ligand peak decreases on addition of Al but the decrease is considerably smaller than that predicted from speciation calculations. A new oxidation peak appears at E_{pa} = 0.27 V but i_{pa} is smaller than expected for oxidation of one ligand per complex (based on calculated complex concentrations). These results are consistent with extensive hydrolysis of Al.

At pH 4.8 in a solution containing 1 mM catechol and 0.33 mM Al, $[Al(cat)]^+$ is calculated to be the dominant complex. As shown in Fig. 4.2e (acetate buffer, pH 4.8), the free ligand peak decreases by the expected *ca.* 20 % on addition of Al, but no new oxidation peaks appear within the solvent limit implying that $[Al(cat)]^+$ is not electroactive over this potential range.

In order to investigate the system more fully, measurements were made at pH 8.1 where the catechol redox couple exhibits significant chemical reversibility and the concentrations of both $[Al(cat)_2OH]^{2-}$ and $[Al(cat)_2]^-$ are sufficiently high to be observed. Figure 4.2c shows cyclic voltammograms of a solution containing 1 mM catechol in the absence and presence of 0.1 mM and 0.3 mM Al in HEPES buffer, pH 8.1. On addition of Al, i_{pa} for the free ligand (E_{pa} = 0.12 V) decreases and the expected peak for oxidation of the complexes appears at E_{pa} = 0.27 V. The corresponding entries in Table 4.1 show the observed increase in i_{pa} for complexed ligand is consistent with one ligand from both $[Al(cat)_2OH]^{2-}$ and $[Al(cat)_2]^-$ being oxidised.

It is noteworthy that oxidation of coordinated ligand is irreversible and after scanning through the complex oxidation peak, i_{pc} (the cathodic peak current) for free ligand is greater than i_{pa} for free ligand on the forward scan in Fig. 4.2c. These observations are consistent with rapid dissociation of oxidised ligand from the metal followed by reduction of the *o*-quinone at E_{pc} = 0.05 V. Indeed, the observed changes in i_{pa} and i_{pc} for free ligand and i_{pa} for the complex peak show satisfactory agreement with those calculated from speciation data, assuming that only one ligand in each of the complexes $[Al(cat)_2OH]^{2-}$, $[Al(cat)_2]^-$ and $[Al(cat)_3]^{3-}$ is oxidised at E_{pa} = 0.27 V and reduced at the potential of the free ligand. Dissociation of the metal-bound *o*-quinone is to be expected considering the preference of Al for hard bases, and the lack of complex formation in the Al-1,2-naphthoquinone system [Ohman *et al.*, 1983].

Table 4.2 summarises cyclic voltammetric data for Al-catechol complexes, obtained at ν=100 mV s^{-1}.

Table 4.2 Cyclic voltammetric data for Al-catechol complexes obtained using a base-pretreated electrode and $\nu = 100$ mV s^{-1}.

Complex	Solution pH	Buffer	E_{pa} (V)
$[Al(cat)_3]^{3-}$	9.9	CHES	0.27
$[Al(cat)_2OH]^{2-}$	8.8	NH_3/NH_4Cl	0.27
$[Al(cat)_2]^-$	8.1, 7.2	HEPES	0.27

4.2.4 ELECTROCHEMISTRY OF DASA.

The electrochemistry of DASA has been examined previously [see Zittel and Florence, 1967; Ohsaka *et al.* 1988; and Ohsaka *et al.* 1989] and is characterised by a two electron oxidation and a two electron reduction process described by eqn.s (4.1) and (4.2) (for pH 3.0).

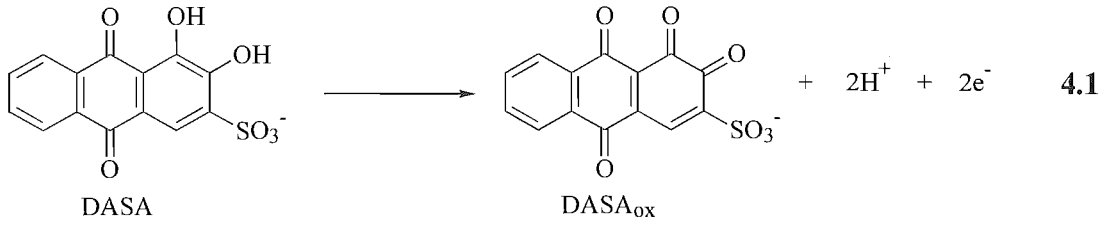

Fig. 4.4a shows two cyclic voltammograms recorded at a polished GC electrode with ν=50 mV s^{-1} for a solution of 0.85 mM DASA in formate buffer, pH 3.0. These correspond to the two reactions given in eqn.s (4.1) and (4.2). The oxidation step (+ive potentials, Fig. 4.4a) is chemically irreversible over the pH range of interest to this study (pH 3 - 9) at scan rates up to 500 mV s^{-1} whereas the chemical and electrochemical reversibility of the reduction process (-ive potentials, Fig. 4.4a) depends on pH and scan rate.

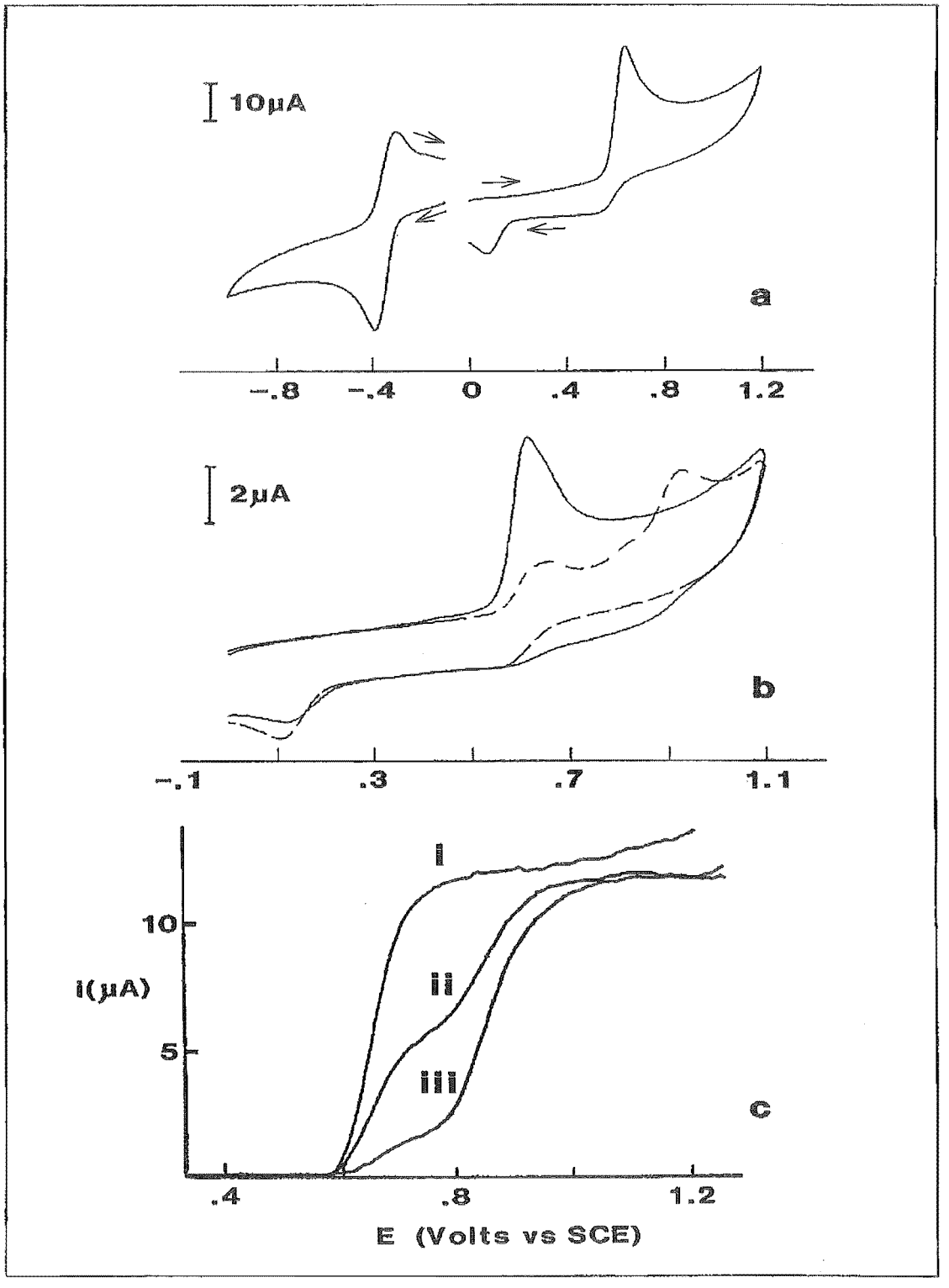

Figure 4.4 Voltammetry of DASA and $[AlDASA]^0$ in formate buffer using a polished GC electrode.

a) Cyclic voltammograms (ν=50 mV s^{-1}) of 0.85 mM DASA, pH 3.0.

b) Cyclic voltammograms (ν=50 mVs^{-1}) of 0.17 mM DASA in the absence (—) and presence (- - -) of 4.0 mM Al, pH 3.0.

c) Steady state voltammograms at the RDE (ν=10 mV s^{-1}, ω =209.4 s^{-1}) of 0.17 mM DASA, pH 3.1, in the presence of (i) 0; (ii) 0.4 mM and (iii) 4 mM Al.

4.2.5 ELECTROCHEMISTRY OF Al-DASA COMPLEXES.

Stability constants for the Al-DASA system have been determined and are reported in Chapter 3. These were used to generate the species distribution diagram in Figure 4.5. Consideration of the diagram led to the choice of conditions listed in Table 4.3 for study of the system. This table gives calculated concentrations of each species in solution and measured concentrations of free and complexed DASA obtained from limiting currents at the rotating disk electrode (RDE) under steady state conditions (assuming one DASA ligand per complex is electroactive).

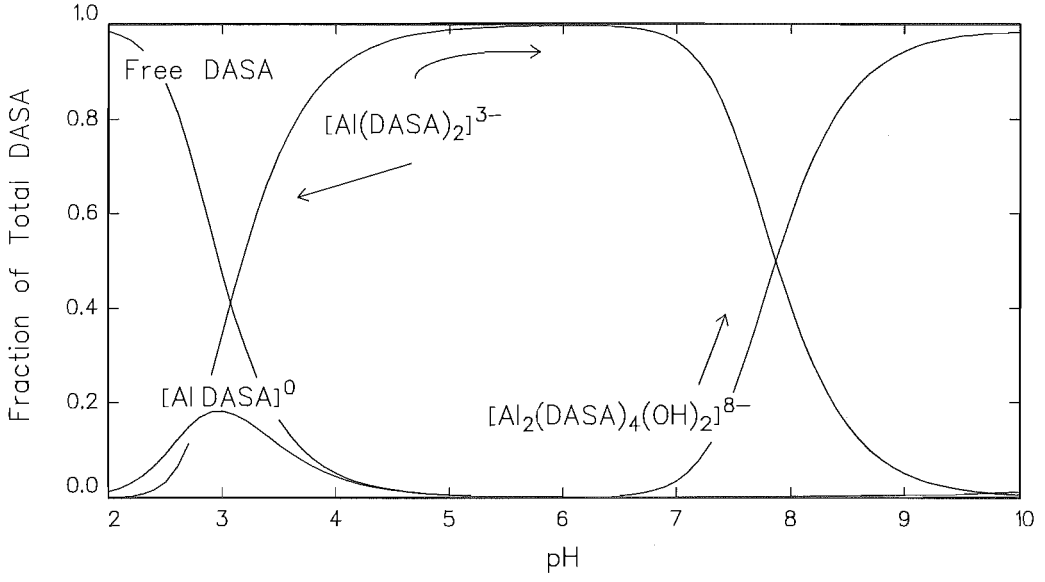

Figure 4.5 Species distribution diagram for the system H^+/Al^{3+}/DASA showing the fraction of total DASA present as each species when the total DASA and Al concentrations are 1.0 and 0.5 mM respectively.

4.2.5-A ELECTROCHEMISTRY OF [AlDASA]^0. The electrochemical behaviour of the complex $[AlDASA]^0$ was examined by cyclic voltammetry and hydrodynamic voltammetry at an RDE; the results are shown in Figure 4.4b,c. The maximum solubility of $[AlDASA]^0$ was found to be *ca.* 0.25 mM in formate buffer, pH 3.1, and hence cyclic voltammetry was performed using a DASA concentration of 0.17 mM. In the presence of 4.0 mM Al, the free ligand peak at E_{pa}=0.62 V decreases and a new peak assigned to oxidation of $[AlDASA]^0$ appears at E_{pa}=0.93 V (Figure 4.4b). Due to the low concentrations of ligand and complex, meaningful measurements of cyclic voltammetric peak heights could not be made. Quantitative investigations therefore used hydrodynamic voltammetry at the RDE. Figure 4.4c shows background-subtracted steady-state voltammograms (ν = 10 mVs^{-1}, ω =

209.4 s^{-1}) recorded in a formate buffer solution containing 0.17 mM DASA plus 0, 0.4 or 4 mM Al at pH 3.1. For these latter conditions speciation calculations indicate that 47 and 88 % of the ligand respectively is bound to Al as $[AlDASA]^0$. The total limiting current shows a small decrease as the concentration of $[AlDASA]^0$ increases suggesting that in each solution (i) all DASA is electroactive and undergoing a two-electron oxidation, and (ii) the diffusion coefficient of $[AlDASA]^0$ is *ca.* 95 % that of free DASA. The changes in limiting current for the free ligand ($E_{1/2}$ = 0.63 V) and complexed ligand ($E_{1/2}$ = 0.86 V) are consistent with the calculated concentrations of DASA and $[AlDASA]^0$.

Table 4.3 Calculated solution compositions for the DASA-Al system and measured concentrations of free DASA and complexed DASA.[a]

Total Concentration (mM)			Calculated Concentration (mM)				Measured Concentration (mM)	
pH	DASA	Al	Free DASA	$[AlDASA]^0$	$[Al_2(DASA)_4(OH)_2]^{8-}$	$[Al(DASA)_2]^{3-}$	DASA Free	DASA Complexed
3.1	0.17	0.40	0.06	0.08	0.02	0.0	0.07	0.10
3.1	0.17	4.0	0.01	0.15	0.00	0.0	0.02	0.15
5.65	0.10	0.05	0.00	0.00	0.05	0.0	0	0.06
8.9	0.85	0.33	0.2	0.00	0.02	0.30	0	b

[a] Calculated concentrations were obtained using SOLGASWATER [Eriksson, 1979] and stability constants from Chapter 3. Measured concentrations are from RDE steady-state limiting currents making the simplifying assumptions of equal diffusion coefficients for free ligand and complexes and that one DASA ligand per complex is electroactive. Voltammograms were recorded using a polished GC electrode, ω = 209.4 s^{-1} and ν = 10 mV s^{-1} .

[b] not measurable.

4.2.5-B ELECTROCHEMISTRY OF $[Al(DASA)_2]^{3-}$. For pH between 4 and 7 the complex $[Al(DASA)_2]^{3-}$ dominates speciation. Its oxidative electrochemistry was examined by cyclic voltammetry (Fig. 4.6a) in acetate buffer solutions, pH 5.5, containing 0.85 mM DASA and 0 or 0.5 mM Al. A new oxidation process with E_{pa} = 0.92 V (ν=50 mV s^{-1}) is observed and the loss of the free ligand peak current is in agreement with speciation calculations (Table 4.3).

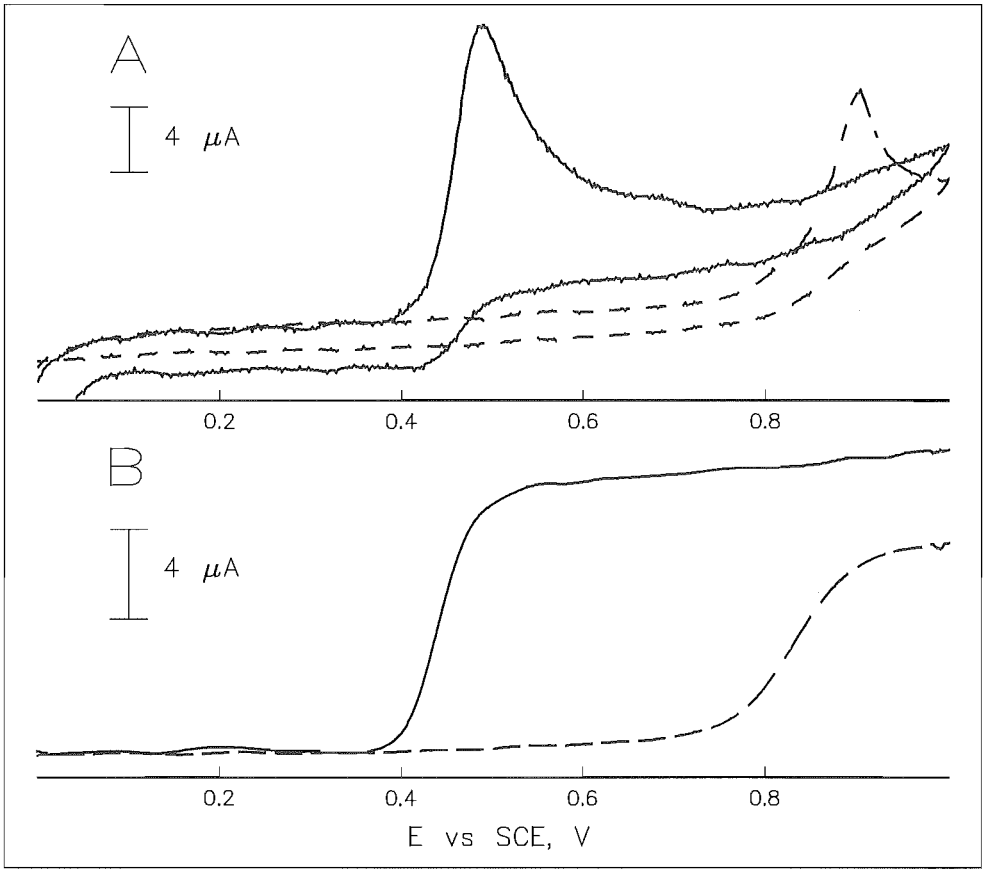

Figure 4.6 Voltammetry of $[Al(DASA)_2]^{3-}$ in acetate buffer, using a polished GC electrode. **A)** pH 5.5, Cyclic voltammograms (ν=50 mVs^{-1}) of 0.85 mM DASA in the absence (——) and presence (- - -) of 0.5 mM Al; **B)** pH 5.65, steady state voltammograms at the RDE (ν=10 mV s^{-1}, ω=209.4 s^{-1}) of 0.10 mM DASA in the absence (——) and presence (- - -) of 0.05 mM Al

To establish the relative currents due to oxidation of free ligand and complex, hydrodynamic voltammograms were recorded at the RDE (Fig. 4.6b) with 0.1 mM DASA at pH 5.65 in the presence and absence of 0.05 mM Al. Formation of $[Al(DASA)_2]^{3-}$ gives the new electrochemical process with $E_{1/2}$ = 0.83 V (ν = 10 mVs^{-1}, ω = 209.4 s^{-1}). The plateau current of this process is half (*ca.* 60%) that for the free ligand indicating that one ligand per complex is oxidised. This fraction remained constant (50 ± 10 %) with varied electrode rotation rates over the range 26.2 s^{-1} to 314 s^{-1} indicating no further reaction of the remaining coordinated ligand within the timescale of the experiment.

4.2.5-C ELECTROCHEMISTRY OF $[Al_2(DASA)_4(OH)_2]^{8-}$. As illustrated in Figure 4.5 the complex $[Al_2(DASA)_4(OH)_2]^{8-}$ is formed above pH 7. This is a dinuclear chelate and as such is structurally distinct from the other DASA and catechol chelates considered.

Figure 4.7a illustrates voltammograms of DASA at pH 8.9 before and after addition of Al. Formation of $[Al_2(DASA)_4(OH)_2]^{8-}$ decreases the wave for oxidation of free DASA and gives a new wave with $E_{1/2}$ = 0.8 V (vs. SCE, ω = 209.4 s^{-1}, ν = 10 mV s^{-1}). This new wave is very broad as indicated by the greater $E_{3/4}$-$E_{1/4}$ value in Table 4.4, suggesting a complex electrochemical mechanism. It cannot be assumed, as earlier, that only one ligand per complex is oxidised. Thus the concentration of the complex present cannot be estimated from the voltammograms. Also the broadness of the complex wave makes it very difficult to estimate the plateau current. However it does appear that the current is larger than 1/4 of the decrease of the free ligand oxidation current. Thus it may be concluded that the initial ligand oxidation step is followed by further electrochemical reaction(s) and by a chemical reaction step (involving ligand dissociation and/or chelate rearrangement).

Cyclic voltammetric experiments also indicate the formation of an $[Al_2(DASA)_4(OH)_2]^{8-}$ species. Fig. 4.7b shows that when 0.2 mM Al is added to 0.85 mM DASA, the free ligand current drops to *ca.* 30 % of its initial value and a new peak appears with E_{pa}=0.80 V (ν = 50 mV s^{-1}).

Table 4.4 summarises electrochemical data obtained for Al-DASA complexes.

Table 4.4 Electrochemical data for Al-DASA complexes obtained using a polished GC electrode.

Complex	Solution pH	Buffer	E^a_p (V) [i]	$E_{1/2}$ (V) [ii]	$E_{3/4}$-$E_{1/4}$ (mV) [ii]
$[AlDASA]^0$	3.1	formate	0.93	0.86	85
$[Al(DASA)_2]^{3-}$	5.65	acetate	0.92	0.83	85
$[Al_2(DASA)_4(OH)_2]^{8-}$	8.9	NH_3/NH_4Cl	0.80	0.80	175

i Cyclic voltammetry, ν = 50 mV s^{-1}

ii RDE, ω = 209.4 s^{-1}, ν = 10 mV s^{-1}

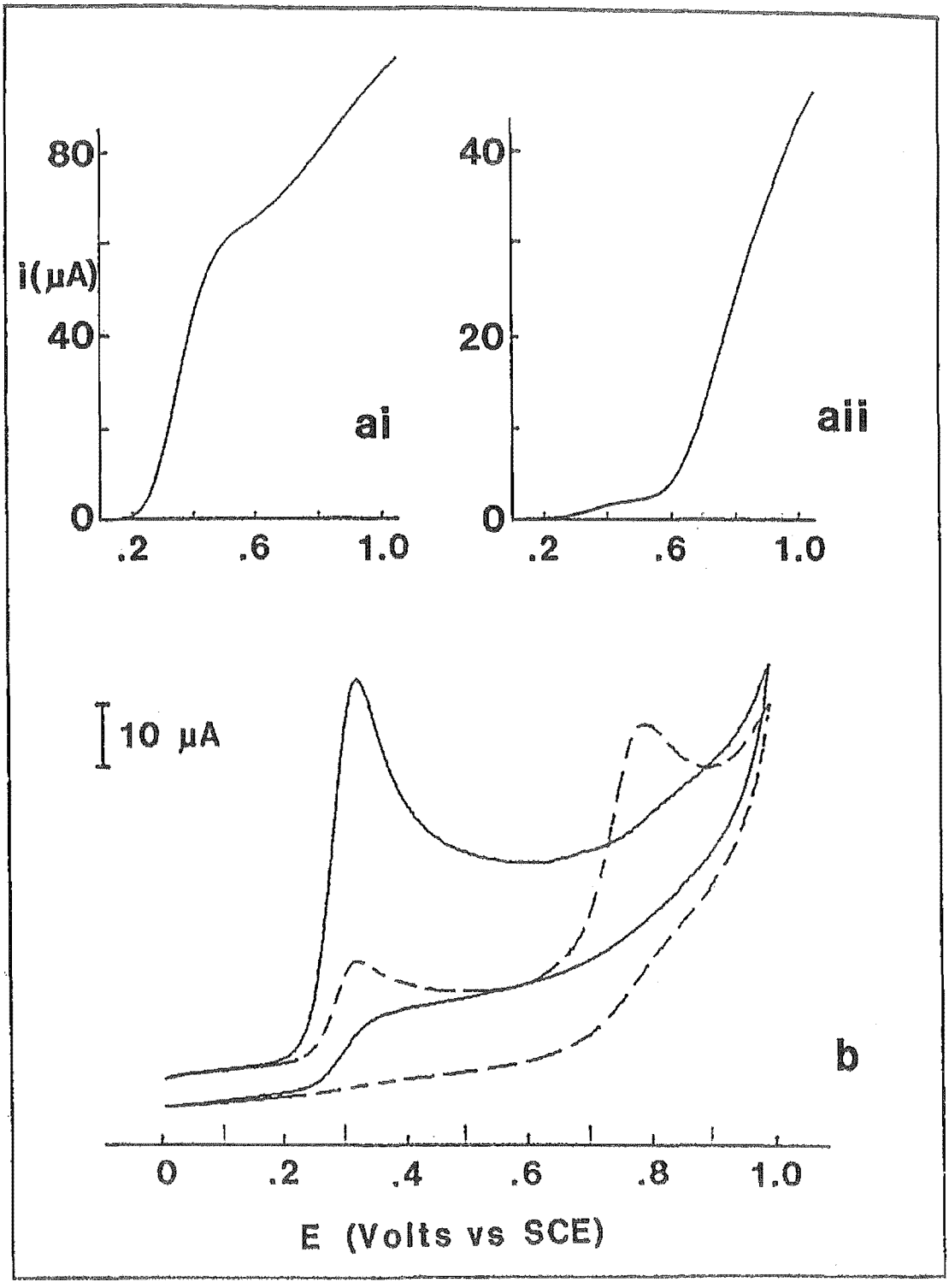

Figure 4.7 Voltammetry of $[Al_2(DASA)_4(OH)_2]^{8-}$ in NH_3/NH_4Cl buffer using a polished GC electrode.

a) Steady state voltammograms at the RDE (ν=10 mV s^{-1}, ω=209.4 s^{-1}) of 0.85 mM DASA, pH 8.9, in the presence of (ai) 0 and (aii) 0.33 mM Al.

b) Cyclic voltammograms (ν=50 mVs^{-1}) of 0.85 mM DASA, pH 8.9, in the absence (—) and presence (- - -) of 0.2 mM Al.

4.2.6 THE ORIGIN OF POTENTIAL SHIFTS ON COMPLEXATION.

The above description of the electrochemistry of Al-ligand complexes is based on the assumption that complexes formed between Al and the initial (reduced) forms of the ligands are inert. This assumption was tested by electrochemical studies which examined the influence of Al concentration on $E_{1/2}$ for oxidation of coordinated ligand. For labile systems with the metal in excess, the effect of complex formation on $E_{1/2}$ values of redox active ligands has been treated in detail by Shiu and Harrison (1989). Under conditions relevant to the complex $[AlDASA]^0$ (ie. the coordination number of the ligand decreases by one on oxidation and only one complex stoichiometry is important for each ligand oxidation state) the shift in oxidation potential for a labile complex, $\Delta E_{1/2}$ (= $E_{1/2}$(complex) - $E_{1/2}$(ligand)), depends on metal concentration according to equation 4.3. Thus, at constant pH, a shift of 29 mV per unit change in ln[M] is predicted.

$$\Delta E_{1/2} = \frac{RT}{2F}\ln\left(\frac{\beta}{K_1K_2}\right) + \frac{RT}{2F}\ln[H^+] + \frac{RT}{2F}\ln[M] \qquad \textbf{(4.3)}$$

where

$$\beta = \frac{[ML]}{[M][L]}$$

$$K_1 = \frac{[HL]}{[L][H^+]}$$

$$K_2 = \frac{[H_2L]}{[HL][H^+]}$$

The dependence of $E_{1/2}$ for oxidation of $[AlDASA]^0$ on Al concentration was examined by hydrodynamic voltammetry at the RDE. In a formate buffer solution, pH 3.4, containing 0.085 mM DASA and Al concentrations ranging from 0.5 - 10 mM (ie ln[Al] changes by 3 $\log_e$ units), the $E_{1/2}$ values were found to be independent of Al concentration, showing a random variation of ± 5 mV attributed to experimental uncertainty.

For an irreversible ligand oxidation process, equation 4.3 must be regarded as an approximate relationship. Nevertheless, the observed independence of $E_{1/2}$ on Al concentration for $[AlDASA]^0$ (compared to the predicted 29 mV per unit change in ln[Al]) strongly suggests that equation 4.3 is not appropriate. Hence $[AlDASA]^0$ is not labile on the experimental timescale and the separate oxidation process arises from direct oxidation of coordinated ligand. Furthermore it is reasonable to generalise this result to all Al complexes in the study.

4.3 DISCUSSION.

4.3.1 GLASSY CARBON PRETREATMENTS.

The effects of the various electrode pretreatments have been discussed by McCreery (1991). Electrode polishing scores the surface. This reveals the underlying active carbon as well as depositing polishing debris (polishing oils, abrasive particles and fractured electrode material). The sonication in acetone step employed here is intended to continue this fracturing process as well as cleaning off much of the polishing debris. Electrochemical pretreatment in acidic solution is known to generate a porous surface layer of graphite oxide which exhibits selective uptake of solution species. Electrochemical pretreatments in strong base dissolve the layers of graphite oxide as they form. This is presumed to arise from deprotonation reactions of phenol-like functional groups and the subsequent build up of anionic charge, giving the graphite oxide greater solubility. The resulting electrode has a freshly revealed carbon surface carrying little more than a monolayer of phenol and quinone -like functional groups.

It appears that the graphite oxide layer formed by the electrochemical pretreatment in acid is impermeable to Al-catechol complexes which are thus prevented from reaching, and undergoing electron transfer at, the underlying active electrode surface. Both size and charge may be responsible for the different permeabilities of catechol and its complexes. On the other hand both free catechol and the larger Al-catechol complexes may more readily access the surface produced by electrochemical pretreatment in strong base.

The Al-DASA complexes were also excluded by the surface layers produced by electrochemical pretreatment in acid. Unlike catechol the electrode kinetics of DASA were not improved by base pretreatment. Thus for DASA the best pretreatment was electrode polishing. It may be that the large hydrophobic π-structure of the anthracene ring of DASA is responsible for this behaviour. This may have an unfavourable interaction with the hydrophilic phenolic and quinone-like groups found at the base pretreated surface. Conversely it may have a favourable π-π interaction with the bare carbon surfaces revealed at the polished surface.

4.3.2 Al-CATECHOL ELECTROCHEMISTRY.

The electrochemistry of the Al complexes of catechol has been interpreted under the assumption that only one ligand from each complex is electroactive. Dissociation of one ligand (after oxidisation) from the initial complexes $[Al(cat)_2OH]^{2-}$, $[Al(cat)_2]^-$ and $[Al(cat)_3]^{3-}$ gives the products $[Al(cat)OH]^0$, $[Al(cat)]^+$ and $[Al(cat)_2]^-$ respectively. Further oxidation of these complexes at the same potential (E_{pa} = 0.27 V) would give an ECE mechanism (ie electrochemical step followed by a chemical step (ligand dissociation) followed by an electrochemical step) [see chapter 11 of Bard and Faulkner, 1980]. This would lead to currents greater than those expected for a two-electron oxidation of one ligand. However, the good agreement between calculated solution compositions and measured concentrations of complexes from cyclic voltammetric peak currents (Table 4.1) suggests that at ν=100 mV s^{-1} any influence of an ECE process is small. Hence under these conditions the response is best described as a quasireversible electrochemical step (ligand oxidation) followed by an irreversible chemical step (ligand - metal dissociation) ie. an $E_{qr}C_i$ reaction scheme.

In summary, over the range pH 9.9 - 4.8, formation of Al-catechol complexes leads to a decrease in i_{pa} for the free ligand that is consistent (except near pH 7) with calculated values of ligand concentration. The complexes $[Al(cat)_3]^{3-}$, $[Al(cat)_2]^-$ and $[Al(cat)_2OH]^{2-}$ are electroactive with E_{pa} = 0.27 V. Peak currents indicate a two-electron oxidation of only one coordinated ligand. Dissociation of oxidised ligand is clearly established by comparisons of i_{pa} and i_{pc} for the free ligand redox processes at pH 8.1 (Figure 4.2c). Further oxidation of the resultant complexes (of lower stoichiometry) was not detected. The complex $[Al(cat)]^+$ is not electroactive within the solvent limit at pH 4.8 and the electroactivity of $[Al(cat)OH]^0$ could not be established due to its low concentration under all solution conditions. The redox processes for Al-catechol complexes are thus represented by equations 4.4-4.6.

$$[Al(cat)_3]^{3-} \rightarrow [Al(cat)_2]^- + cat_{ox} + 2e^- \quad (4.4)$$

$$[Al(cat)_2OH]^{2-} \rightarrow [Al(cat)OH]^0 + cat_{ox} + 2e^- \quad (4.5)$$

$$[Al(cat)_2]^- \rightarrow [Al(cat)]^+ + cat_{ox} + 2e^- \quad (4.6)$$

4.3.3 Al-DASA ELECTROCHEMISTRY.

The primary anodic process for the complexes $[AlDASA]^0$ and $[Al(DASA)_2]^{3-}$ is summarised as an irreversible two-electron oxidation of one coordinated ligand occurring at a cyclic voltammetric peak potential of 0.93 and 0.92 V respectively (ν=50 mV s^{-1}). The voltammetry is described by eqn.s 4.7-4.8.

The $[Al_2(DASA)_4(OH)_2]^{8-}$ complex is significantly easier to oxidise (E_p less positive at 0.80 V) and gives rise to a very broad wave (large $E_{3/4}$-$E_{1/4}$, Table 4.4). The broad ill-defined response suggests that more than one ligand per complex is oxidised and the oxidations occur at different but similar potentials. The sequence of oxidative steps will depend on the extent to which ligands on different Al centres interact with each other. The details of this were not investigated. The complex mechanism for $[Al_2(DASA)_4(OH)_2]^{8-}$ oxidation is unique amongst the Al-chelates investigated. This is not surprising considering the di-nuclear structure of the chelate and is supportive of the solution thermodynamics study which established its structure (Chapter 3).

$$[AlDASA]^0 \rightarrow Al^{3+} + DASA_{ox} + 2e^- \quad (4.7)$$

$$[Al(DASA)_2]^{3-} \rightarrow [AlDASA]^0 + DASA_{ox} + 2e^- \quad (4.8)$$

4.3.4 THE ORIGIN OF POTENTIAL SHIFTS ON COMPLEXATION.

The model of Shiu and Harrison (1989) describes the shifts in ligand centred redox potentials that occur with complex formation. It has been shown to not be appropriate for coordination systems involving Al since the predicted dependence of potential shifts on Al concentration was not observed. For these systems the shifts are not produced through Al simply limiting the concentration of free ligand which is available at the electrode surface for reaction. Instead the shifts indicate the presence of a distinct redox active species, the aluminium-ligand complex. Structural features within the complex control the magnitude of the shift and its variation with complex stoichiometry.

Coordination of catechol and DASA to Al is expected to stabilise the ligands to oxidation via an essentially electrostatic interaction between the catecholate moiety and the hard metal centre. Steric interactions with further ligands (if present) will have a destabilising effect, encouraging dissociation. The observed E_{pa} values for the complexes $[Al(cat)_3]^{3-}$, $[Al(cat)_2]^-$ and $[Al(cat)_2OH]^{2-}$ which undergo an E_iC_i or $E_{qr}C_i$ mechanism, will depend on both the formal potential (E°) for the oxidation process (in the absence of ligand dissociation) and the rate of ligand dissociation after oxidation [Bard and Faulkner, 1980]. From the concurrence of E_{pa} values it is reasonable to assume that $[Al(cat)_3]^{3-}$, $[Al(cat)_2]^-$ and $[Al(cat)_2OH]^{2-}$ have similar formal potentials and ligand dissociation rates. However the apparent difficulty of oxidation of $[Al(cat)]^+$ (electroinactive to 0.9 V) must arise from either a very positive value for E° or a very sluggish ligand dissociation rate, suggesting a much lesser degree of steric interaction for this 1:1 complex.

Similarly for the DASA series the $[Al_2(DASA)_4(OH)_2]^{8-}$ species stands out as being relatively easy to oxidise (Table 4.4). Compared to the complex $[Al(DASA)_2]^{3-}$ the coordinated hydroxide ions in the dinuclear complex may reduce the effective charge of Al upon the DASA ligands, making them easier to oxidise. Also shifts in E_{pa} and $E_{1/2}$ to less positive values as the number of coordinated ligands increases are consistent with increased steric interactions between ligands giving lower complex stability and/or an increased rate of dissociation of oxidised ligand.

4.4 CONCLUSION

In the first step electrochemical pretreatments of the glassy carbon electrode surface were developed to give the optimal rate of electron transfer for each Al-ligand system. The effects of each pretreatment could be rationalised in terms of the known chemistry of glassy carbon. The acid pretreatment gave rise to a layer of graphite oxide at the electrode surface which excluded the Al complexes of both catechol and DASA. The base pretreatment gave a surface at which catechol was highly active while the electrochemistry of DASA was best investigated at the polished surface.

The oxidative electrochemistry of the mononuclear complexes was interpreted under the assumption that only one ligand from each complex is electroactive (the dinuclear complex, $[Al_2(DASA)_4(OH)_2]^{8-}$, was the exception with oxidation of more than one ligand per complex). After oxidation an ortho-quinone was formed from the catecholate moiety of the ligands and this dissociated from the metal centre. This is consistent with the lack of complex formation in the Al-1,2-naphthoquinone system [Ohman *et al.*, 1983].

The theoretical model developed by Shiu and Harrison (1989) was shown to be inappropriate for complexes formed with Al. This model assumes that metal-ligand complexes are labile on the electrochemical timescale and that the only interaction of the metal is to limit the concentration of the free ligand. Here it is proposed that coordination systems involving Al are too inert to be described by this model. The shifts in redox potentials which are observed in the presence of the metal are produced by the direct electrode reaction of metal bound ligand. It follows that the magnitude of these shifts is controlled by structural and electronic factors within the complexes.

This is observed for the catechol series in which the complex of lowest stoichiometry, $[Al(cat)]^+$, shows greater stabilisation by Al than the complexes of higher stoichiometry and was not electroactive within the solvent limit. For the DASA series the complex $[Al_2(DASA)_4(OH)_2]^{8-}$ stands out as being relatively easy to oxidise. It may be summarised that the oxidation potentials of the DASA complexes decrease with increasing complex stoichiometry (i.e. increasing number of ligands about the metal centre(s)).

This may result from decreasing stabilisation of the ligands as the metal's charge is countered by a greater number of ligands. Also it may be that steric factors lead to a greater rate of ligand dissociation in the complexes of higher stoichiometry.

Chapter 5

APPLICATION OF 4-NITROCATECHOL TO ALUMINIUM ANALYSIS

5.1 INTRODUCTION

5.1.1 SELECTION OF 4-NITROCATECHOL (4-NCAT).

Al is readily detected by voltammetric techniques after coordination to an electroactive ligand. The method is based on the different potential for reduction and/or oxidation of the ligand after coordination. The voltammetric behaviour of the ligands 1,2-dihydroxyanthraquinone-3-sulfonic acid (DASA), catechol (1,2-benzenediol) and their Al complexes is described in chapter 4. However a third ligand, 4-ncat, has been used in this chapter in the development of an analytical method for Al.

An electrochemical method of analysis for Al using DASA has been described [Downard *et al.*, 1992a]. DASA was monitored amperometrically (after complexation with Al) by oxidation at a gold electrode within a Flow Injection Analysis (FIA) manifold. Unfortunately the system was prone to electrode fouling by the oxidation products of DASA. To counter this a complicated double pump FIA manifold was combined with an electrochemical cleaning step. A further problem was that interference by Fe(III) could not be removed

Although the electrochemistry of the Al-catechol system is suitable for Al detection, the complexes are not sufficiently stable for quantitation of Al at environmental concentrations. Stability constants are expected to increase on addition of an electron-withdrawing substituent to the catechol ring and published data for the Al-4-ncat system confirm this [Simpson, 1996; Downard *et al.*, 1997a]. Thus it is anticipated that 4-ncat and its Al complexes should exhibit suitable electrochemistry and complex stability for Al determination at micromolar levels.

5.1.2 Al FRACTIONATION.

As discussed in section 1.1, aluminium is present in natural waters and soils as a range of chemical species. Knowledge of the nature and concentrations of these species is useful for understanding the chemistry of the natural system and anthropogenic effects on the soil or water. Rather than simply measuring total Al, quantitation of reactive Al allows an estimation of Al toxicity. The species which are most likely to contribute to reactive (i.e. toxic) Al are discussed in section 1.2.4.

Recently, a microcolumn of oxine-derivatised gel has been developed for the kinetic discrimination of reactive Al species and for the elimination of Fe(III) interference in a flow injection analysis (FIA) system [Simpson *et al.*, 1997].

The aluminium within samples is captured on the column and subsequently eluted with base. An important advantage of the method is that the detection step is decoupled from the separation step and hence any suitably sensitive detection method can be used. Simpson *et al.* (1997) detected the eluted Al spectrophotometrically. In this work electrochemical detection is used.

The work of Simpson *et al.* (1997) in characterisation of the oxine column has been extended. The effect of a wide range of cations as potential interferents has been examined. This has been undertaken, in part, because of the large number of cations that are known to complex 4-ncat (see section 5.4.2-B,) and are therefore potential interferents in its amperometric analysis.

5.1.3 IN THIS CHAPTER.

In the work described in this chapter the voltammetric responses of 4-ncat and its Al complexes have been characterised by employing a similar strategy to that described in chapter 4. Optimised conditions for the amperometric detection of Al in an FIA system are established. Coupling the amperometric detection method to the oxine microcolumn fractionation protocol allowed determination of reactive Al in soil solutions and the Al complexing capacity of a soil-derived fulvic acid. These analyses of natural samples have been independently verified using an FIA-based spectrophotometric method.

The greater part of this work has been published [Downard *et al.* 1997a].

5.2 EXPERIMENTAL

Electrochemical procedures and equipment were as described in Chapter 2, section 2.4.

5.2.1 REAGENTS.

All chemicals were used as received and with the following exceptions were of analytical reagent grade or better: 4-nitrocatechol (Aldrich, 97%); $CrCl_3$, $CoCl_2$ and $CuCl_2$ (all BDH laboratory reagent grade).

Solutions for flow injection analysis were prepared with triply distilled water. Al standards were diluted from the standard solution used for potentiometry (chapter 3, section 3.2.2) and acidified to 0.1 mM HCl. Cation solutions for interference studies were prepared from $MgSO_4$, $CaCO_3$, $CrCl_3$, $CoCl_2$, $CuCl_2$, $ZnCl_2$ and $Pb(NO_3)_2$ and were acidified as for the Al standards. Fe(III)-tartrate solutions were prepared by dilution of an acidified (pH 2, HCl) stock solution of $Fe(NO_3)_3$ with a two-fold excess of tartaric acid and buffered to pH 5 with acetate buffer

Soil fulvic acid was extracted from the International Humic Substances Society (IHSS) Reference Peat by the acid pyrophosphate-XAD-7 method [Gregor and Powell, 1986; Gregor, 1987]. Extraction was performed by J.E. Gregor, sample code: FAG-4c.

Soil solutions were extracted from Southland, New Zealand, soils. Each sample comprised 20 combined cores (0-10 cm) taken at native forest and pasture sites. The soils are described as Edendale silt loams (yellow brown earths; firm brown soil). Solutions were extracted by centrifuging the soils at 3000 rpm for 30 min. and filtered (0.025 μm) before analysis.

5.2.1 FLOW INJECTION ANALYSIS.

The manifold shown in Figure 5.1 was used for the standard analytical procedure (see below). A two sided, 8 port, double sample loop injection valve was used. Injection loops were 700 μL and 200 μL for sample and alkali eluent, respectively. Sample injections were dispersed by a factor of 2.0 before reaching the detector, while eluent injections were dispersed by a factor 4.0. Noise dampeners were fitted to each line, positioned immediately after the pump. The oxine microcolumn was as described in section 2.5.3, Chapter 2. The amperometric flow cell, as illustrated in section 2.5.2 was

used as the detector, **D**. The GC electrode of the detector was polished daily. A PAR model 174A potentiostat in combination with a Graphtec WX 1200 recorder was used to control the cell potential and to record amperometric measurements.

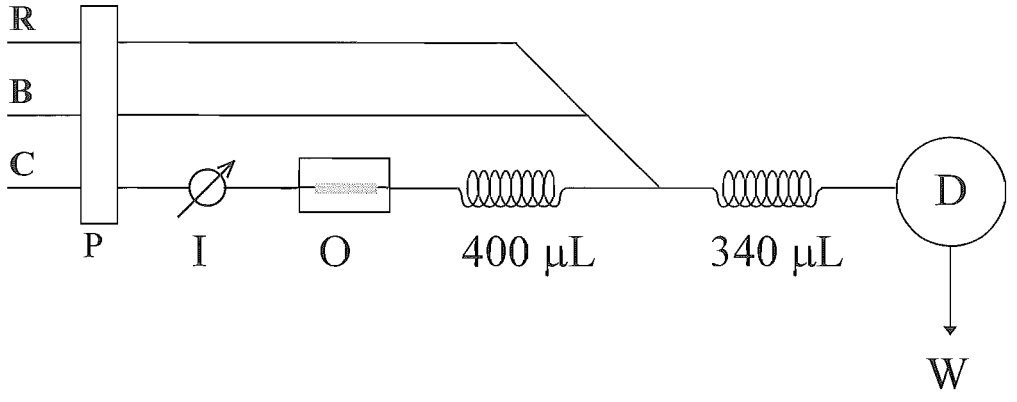

Figure 5.1 Schematic diagram for the FIA manifold.; **P** = pump; **I** = double injection port; **O** = oxine microcolumn; **D** = amperometric detector and **W** = waste.

C = carrier; pH 5.0 acetate buffer (0.05 M CH_3COOH, 0.035 M KOH, 0.065 M KCl).
Flow rate 0.98 mL min^{-1}, ene 16 tubing, 1.42 mm i.d.
B = buffer; pH 8.9 ammonium buffer (2.0 M NH_4Cl, 0.5 M KOH, 2M KCl).
Flow rate 0.36 mL min^{-1}, ene8 tubing, 0.76 mm i.d.
R = reagent; 1.6 mM 4-ncat
Flow rate 0.03 mL min^{-1}, ene1 tubing, 0.19 mm i.d.

5.2.1-A THE STANDARD ANALYTICAL PROCEDURE. Prior to sample introduction the oxine column was buffered (by the carrier stream) to pH 5.0. Samples were introduced into the manifold as 700 µL injections without prior adjustment of pH or ionic strength. Al sequestered by the oxine column was subsequently eluted by a 200 µL injection of eluent (0.02 M KOH in 0.08 M KCl), yielding an elution zone of $[Al(OH)_4]^-$ in which Al has been concentrated by the retention/elution steps. This elution zone merged with 4-ncat and buffer and the associated response at the detector (Fig. 5.2) was measured. The peak size (background-subtracted) was expressed as a percentage decrease in the baseline current (see below, section 5.3.4-A and equation 5.3) and is proportional to reactive Al in the sample. A further four injections of alkali were made after each measurement to clean the column before further analysis. Successively smaller signals were recorded after each injection of alkali with no detectable signal for the fourth injection. The signals arising from these four elutions were not used in the analysis.

5.3 RESULTS.

5.3.1 SOLUTION EQUILIBRIA OF Al AND 4-NCAT.

The species distribution diagram shown in Figure 5.2 demonstrates the suitability of 4-ncat for the analysis of Al in environmental samples. At micromolar concentrations of Al there is essentially quantitative formation of binary Al-4-ncat complexes up to pH 10. At higher pH, competition with hydroxide ion to form the aluminate ion, $[Al(OH)_4]^-$, is observed. The ternary complex, $[Al(4\text{-ncat})_2OH]^{2-}$, remains a minor species when a greater than 3-fold excess of 4-ncat over Al is maintained.

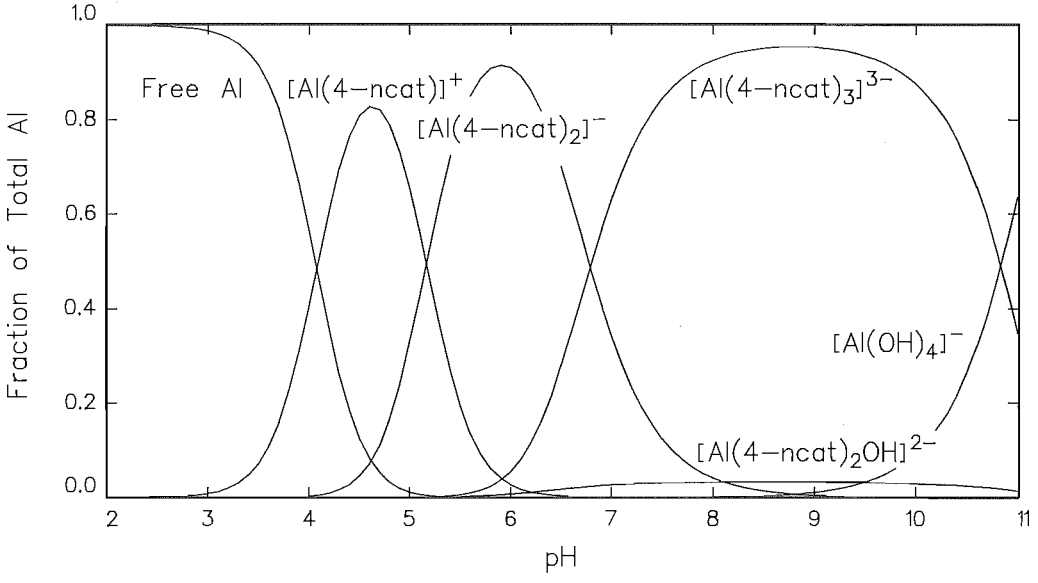

Figure 5.2 Species distribution diagram for the system 50 μM 4-ncat and 10 μM Al. Calculations were performed using the program SOLGASWATER [Eriksson, 1979] and complex formation constants were taken from Simpson (1996) [also published by Downard *et al.*, 1997a].

5.3.2 OXIDATIVE ELECTROCHEMISTRY OF 4-NCAT.

Figure 5.3 shows cyclic voltammograms of 1.0 mM 4-ncat in ammonium buffer, pH 9.4. At a scan rate (ν) of 100 mV s^{-1} the major feature for free ligand (curve a) is an irreversible oxidation process with a peak potential (E_{pa}) of 0.25 V *vs* SCE. By analogy with the electrochemistry of other catechol derivatives, [Ryan *et al.*, 1980; Proudfoot and Ritchie, 1983], the major redox process at pH 9.4 is assigned to the reaction shown in equation 5.1 (4-ncat has pK_a values of 6.67 and 10.88 and thus its structure is written as a monoanion for pH 9.4). The oxidation wave was found to be irreversible at all pH studied (pH 3-11).

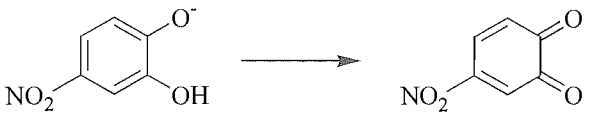

(5.1)

5.3.3 OXIDATIVE CHEMISTRY OF THE Al-4-NCAT COMPLEXES.

Curve b, Figure 5.3 shows the voltammogram for 1.0 mM 4-ncat after addition and equilibration of 0.33 mM Al (giving a calculated solution composition of 0.02 mM free ligand and 0.32 mM $[Al(4\text{-ncat})_3]^{3-}$). The voltammogram shows the free ligand peak decreases to *ca.* 2% of its initial height and a new irreversible oxidation peak appears at E_{pa} = 0.54 V *vs* SCE. This peak is assigned to the oxidation of complexed ligand.

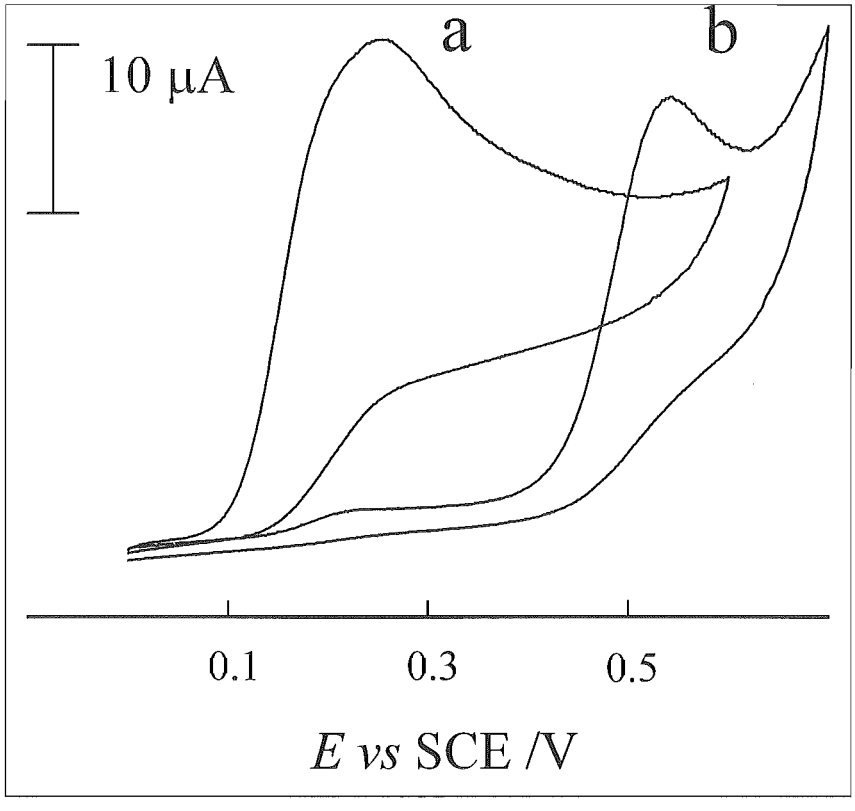

Figure 5.3 Cyclic voltammograms recorded at ν = 100 mV s^{-1} for 1 mM 4-ncat in the absence (a) and presence (b) of 0.33 mM Al, ammonium buffer, pH 9.4.

The potential for oxidation of free ligand is expected to be pH-dependent below pH ~10.9 because the redox reaction involves both proton(s) and electrons (pK_{a2} = 10.88). In contrast, oxidation of complexed ligand does not involve a change in proton content and hence the potential should be independent of pH. However, complexes of different stoichiometries dominate in different pH ranges (see Figure 5.2) and may oxidise at different potentials. In order to investigate the responses of the ligand at different pH and of the complexes $[Al(4\text{-ncat})_3]^{3-}$, $[Al(4\text{-ncat})_2]^{-}$ and $[Al(4\text{-ncat})]^{+}$, steady-state

voltammograms of ligand and complexes were recorded at the rotating disk electrode (RDE). Figure 5.4 shows voltammograms obtained at an angular velocity (ω) of 314 s^{-1} and ν=10 mV s^{-1}. Electrochemical data are given in Table 5.1.

Table 5.1 Electrochemical data for 4-ncat and Al-4-ncat complexes obtained at an RDE using ω = 314.4 s^{-1} and ν = 10 mV s^{-1}.

	$E_{1/2}$ (*vs* SCE, V)[a]			
pH	4-ncat	$[Al(4\text{-ncat})]^+$	$[Al(4\text{-ncat})_2]^-$	$[Al(4\text{-ncat})_3]^{3-}$
4.3	0.46 (35)	0.81 (85)		
6.0	0.36 (39)		0.65 (63)	
9.4	0.21 (67)			0.50 (53)

[a] $E_{3/4}$ - $E_{1/4}$ values (mV) given in parentheses

The responses recorded at pH 4.3 for 100 μM 4-ncat and 100 μM 4-ncat plus 1.0 mM Al (giving a calculated solution composition of 2 μM 4-ncat and 98 μM $[Al(4\text{-ncat})]^+$) are shown in Fig. 5.4a. The half wave potential ($E_{1/2}$) for free ligand is 0.46 V *vs* SCE and for complexed ligand $E_{1/2}$=0.81 V. The limiting current for oxidation of the complex is approximately equal to that in the absence of Al, suggesting complete oxidation of the metal bound ligand in the 1:1 complex.

Fig. 5.4b shows voltammograms obtained at pH 6.0, of 100 μM 4-ncat and 100 μM 4-ncat plus 50 μM Al (giving a calculated solution composition of 6.8 μM free ligand, 6.8 μM $[Al(4\text{-ncat})]^+$ and 42.3 μM $[Al(4\text{-ncat})_2]^-$). At this pH oxidation of free ligand has $E_{1/2}$=0.36 V and for $[Al(4\text{-ncat})_2]^-$, $E_{1/2}$=0.65 V *vs* SCE. The wave for oxidation of the small amount of $[Al(4\text{-ncat})]^+$ present presumably occurs at potentials beyond the positive limit of the scan (i.e. at potentials not accessible with pH 6.0 MES buffer). The magnitude of the limiting current for oxidation of $[Al(4\text{-ncat})_2]^-$ implies that on the timescale of the measurement, both (or close to both) of the ligands in the $[Al(4\text{-ncat})_2]^-$ complex are oxidised and that diffusion coefficients are approximately equal for free ligand and complex.

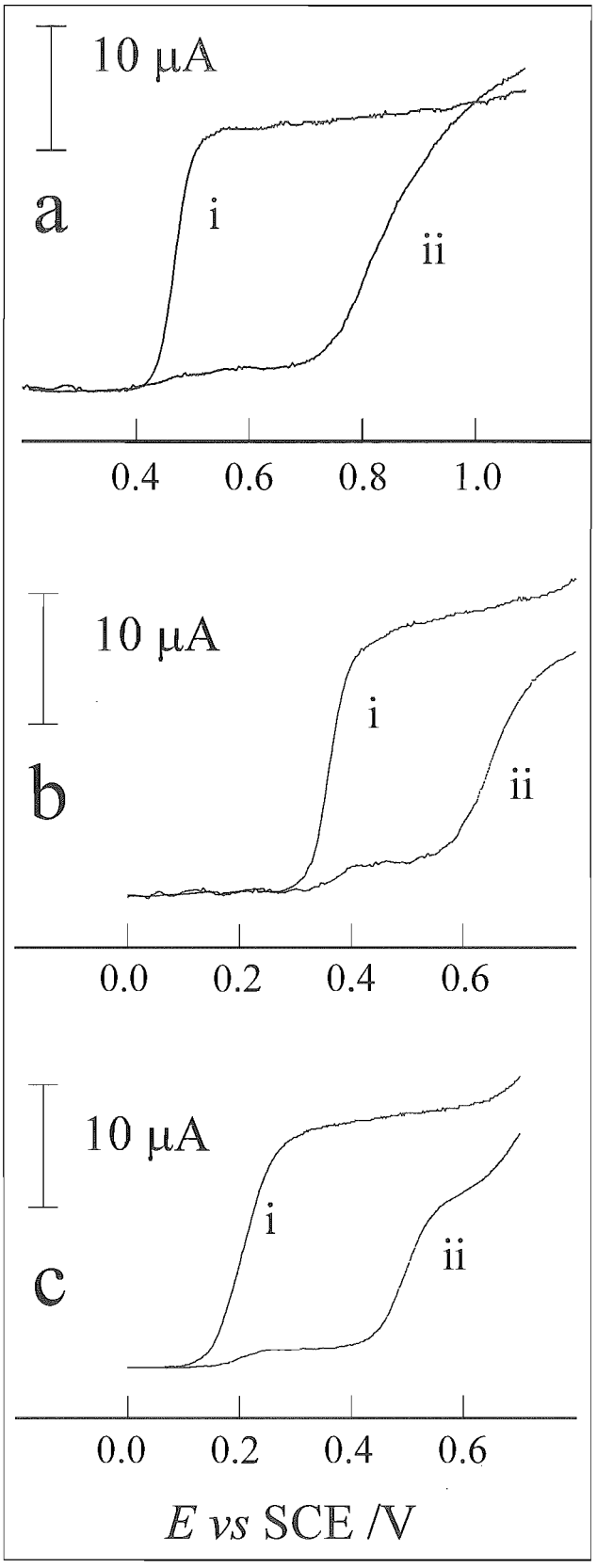

Figure 5.4 Steady-state voltammograms recorded at the RDE using ω = 314.4 s^{-1} and ν = 10 mV s^{-1} for 0.1 mM 4-ncat in the absence (i) and presence (ii) of
(**a**) 1.0 mM Al; acetate buffer, pH 4.3.
(**b**) 50 μM Al; MES buffer, pH 6.0.
(**c**) 33 μM Al; ammonium buffer, pH 9.4.

At higher solution pH, the complex $[Al(4\text{-ncat})_3]^{3-}$ is dominant. At pH 9.4, the calculated concentrations are 4-ncat = 12 μM and $[Al(4\text{-ncat})_3]^{3-}$ = 28 μM for total concentrations 100 μM 4-ncat plus 33 μM Al. The oxidation wave for 4-ncat has $E_{1/2}$ = 0.21 V *vs* SCE and oxidation of $[Al(4\text{-ncat})_3]^{3-}$ occurs at $E_{1/2}$ = 0.50 V (Fig. 5.4c).

Although *ca.* 96% of the 4-ncat is present as either free ligand or $[Al(4\text{-ncat})_3]^{3-}$ the total limiting current for oxidation of these two forms (curve ii) is significantly less than that for oxidation of 4-ncat in the absence of Al (curve i).

The behaviour at this higher pH was further investigated by varying the RDE rotation rate (ω) over the range 104 - 733 s^{-1} (1000-7000 rpm). Figure 5.5 illustrates the limiting currents observed for free 4-ncat and the complex, $[Al(4\text{-ncat})_3]^{3-}$, plotted against $\omega^{1/2}$.

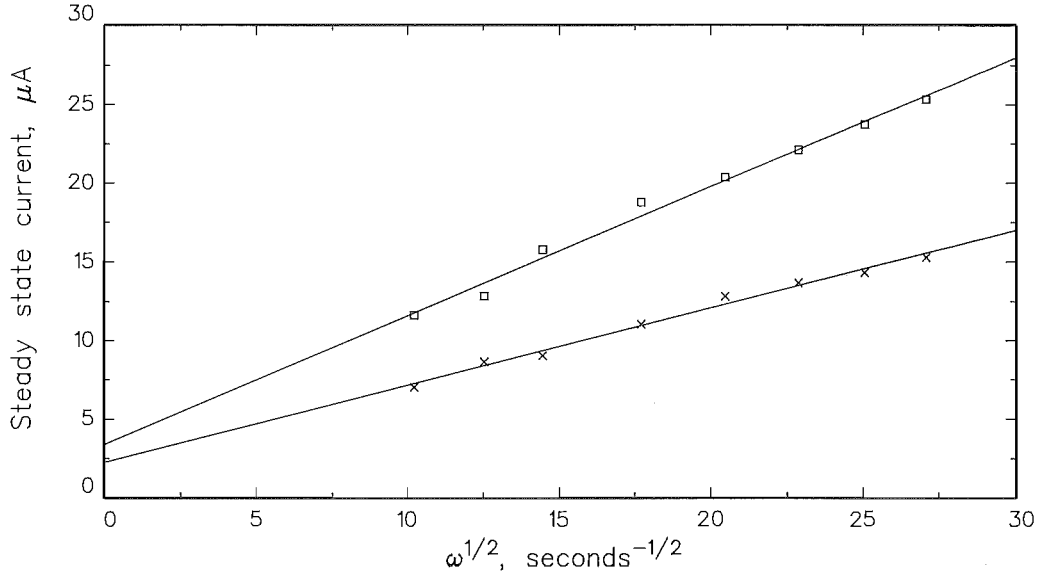

Figure 5.5 RDE limiting currents. (□) 100 μM 4-ncat and (X) 100 μM 4-ncat plus 33 μM Al. ν = 10 mVs^{-1}, pH 9.4, ammonium buffer. ω is the electrode rotation rate (radians per second).

The Levich equation, equation. 5.2 [Bard and Faulkner, 1980, their eqn. 8.3.22], gives the relationship between the limiting (or steady state) current and ω.

The Levich equation: $$I_l = \omega^{1/2}(0.62\, n\, F\, A\, D_0^{2/3}\, \upsilon^{-1/6}\, C_0^*) \qquad (5.2)$$

(I_l = limiting current, ω = electrode rotation rate, n = number of electrons transferred, F = Faraday's constant, A = electrode area, D_0 = diffusion coefficient, C_0^* = concentration in the bulk solution, υ = kinematic viscosity of water.)

The Levich relationship is clearly held by both free 4-ncat and the $[Al(4\text{-ncat})_3]^{3-}$ species. Furthermore the limiting current for oxidation of $[Al(4\text{-ncat})_3]^{3-}$ is consistently two thirds (0.66±0.03) that of free 4-ncat over all rotation rates studied.

It is noteworthy that the limiting current for oxidation of free 4-ncat (in the presence of complexed 4-ncat) was also found to vary linearly with $\omega^{1/2}$ (data not shown). This is consistent with the expected inertness of the (initial) complexes on the electrochemical timescale since the complexed 4-ncat is not able to dissociate and increase the observed concentration of free 4-ncat at the longer timescales (slower rotation rates).

5.3.4 FLOW INJECTION ANALYSIS OF Al.

Amperometric determination of Al was achieved by monitoring the decrease in current for oxidation of 4-ncat after its reaction with Al. The detection potential is chosen so that oxidation of coordinated ligand does not contribute to the measured current.

The species distribution diagram (Fig. 5.2) for the 4-ncat-Al system suggests that pH~9 is most appropriate for amperometric determination of Al using 4-ncat. At this pH, in the presence of sufficient excess of ligand, the reaction is quantitative and a single 4-ncat-Al complex is formed. The coordination of three ligands per Al gives the maximum change in concentration of free ligand as compared to formation of a bis or mono complex. This gives the maximum signal size per Al ion since it is the change in free ligand concentration which is actually monitored.

Figure 5.6 shows hydrodynamic voltammograms of 4-ncat and $[Al(4\text{-ncat})_3]^{3-}$ obtained using the FIA system. 100 μL samples of ligand or complex were injected into ammonium buffer, pH 9.5, in a one-line manifold. As expected, there is close correspondence with the voltammograms recorded at the RDE, Fig. 5.4c. Based on these voltammograms an applied potential of 0.3 V *vs* SCE was selected for the amperometric determination of Al. Clearly, oxidation of free, but not coordinated, 4-ncat occurs at this potential.

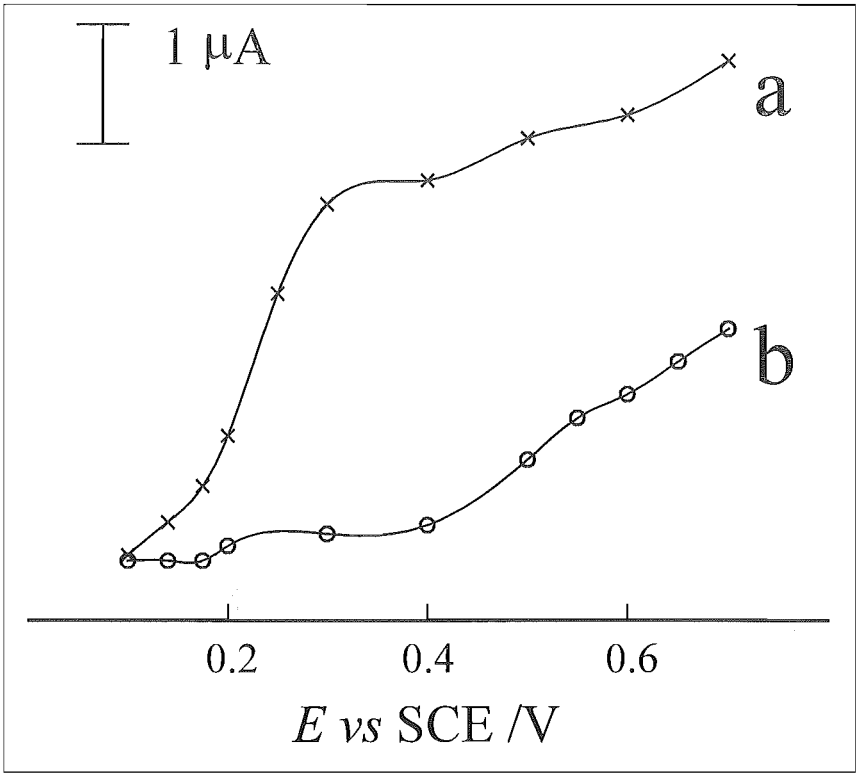

Figure 5.6 Hydrodynamic voltammograms obtained in the FIA system with a one-line manifold (carrier = ammonium buffer, pH 9.5) for injected 100 μL samples of ammonium buffer, pH 9.5 plus (a) 100 μM 4-ncat and (b) 100 μM 4-ncat plus 33 μM Al (calculated composition = 28 μM $[Al(4\text{-ncat})_3]^{3-}$ and 12 μM free 4-ncat).

Typical signals for 6.0, 4.0, 2.0, 1.0 and 0 μM Al generated in the flow system operating in the amperometric detection mode (manifold shown in Fig. 5.1) are shown in Fig. 5.7. The signal used for quantitation of Al is labelled I in Fig. 5.7b and the baseline for signal measurement is also indicated (arrow IV) (see equation 5.3). The broad dip and sharp peak (labelled II) which precede the Al-dependent peak are due to non-uniform dilution of 4-ncat at the merging zones. This is caused by pressure fluctuations within the manifold arising from switching the injection valve and by pH-shock swelling of the gel in the microcolumn. A 400 μL coil was placed immediately down-line of the microcolumn to resolve the Al-dependent peak from the pressure-related peaks. Peak III (Fig. 5.7b) arises from species which are not retained on the column and is the sum of two components: a "positive" peak due to direct oxidation of components of the sample matrix (for example natural organic matter) and a "negative" peak arising from species which pass the microcolumn and react with 4-ncat (for example organically complexed Al and Fe(III)).

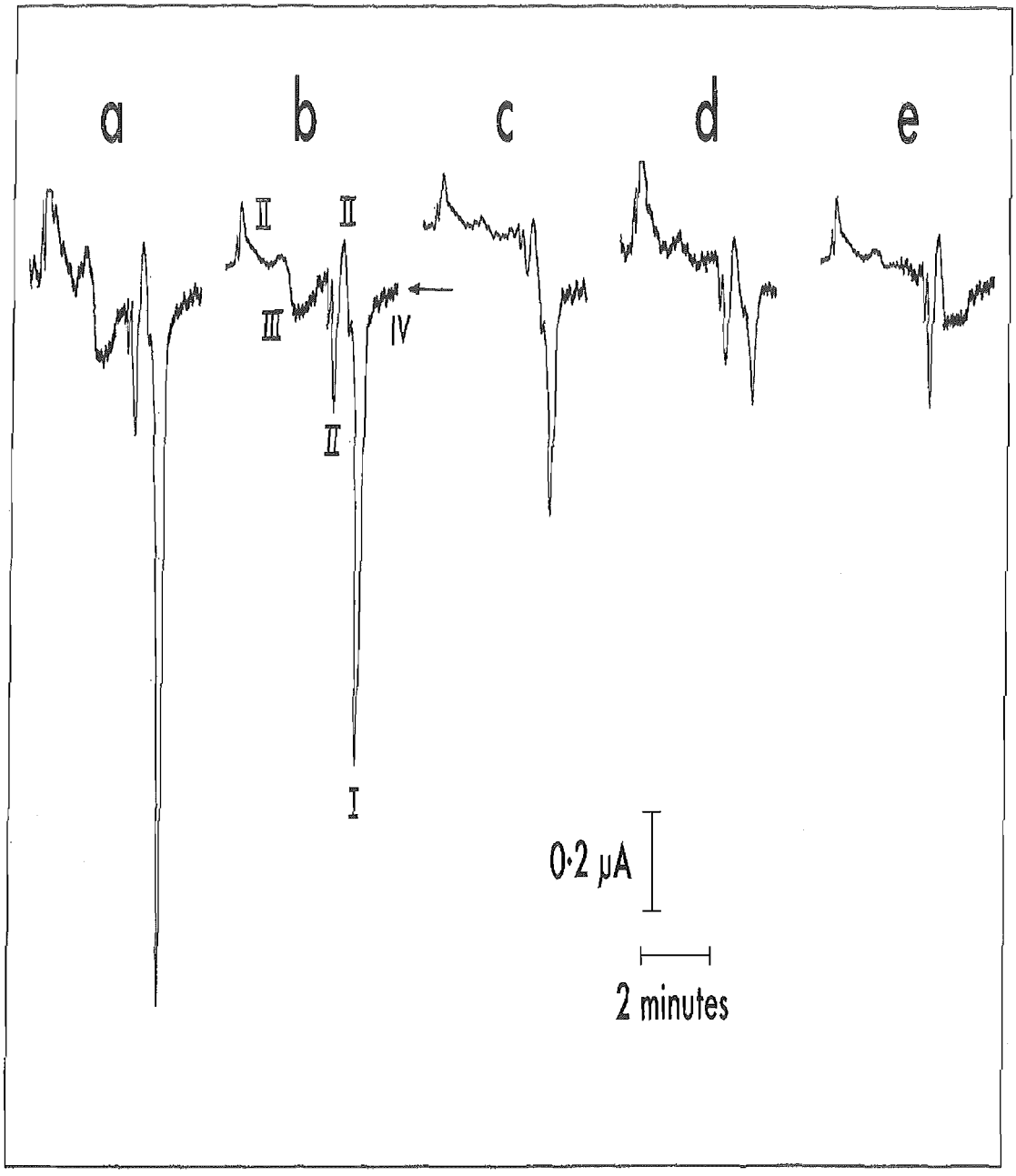

Figure 5.7 The response of the FIA system to injections of (a) 6.0; (b) 4.0; (c) 2.0; (d) 1.0 and (e) 0 μM Al standards. I = signal used for quantitation of Al; II = 'pressure' peaks; III = peak arising from species not retained by the oxine microcolumn. The baseline used for measurement of peak I is indicated by arrow IV.

5.3.4-A ANALYTICAL PERFORMANCE. The procedure described gave a detection limit (DL) of 0.12 μM Al (3σ for a 1 μM Al^{3+} standard) and the bottom of the linear working range as 0.4 μM (10σ). The linear working range was 0.4 to 8 μM Al. The equation of the regression line is given by equation 5.3.

Note the value $(i_p/_{ib})*100$ is the percentage decrease in baseline current caused by an Al sample. Reporting the system response in this manner gave an experimental value which was corrected for the degree of electrode deactivation (Fig. 5.8, □ data). Absolute current values, i_p, could not be used since these showed an exponential decrease with time (Fig. 5.8, Δ data).

$$\frac{i_p}{i_b} * 100 = 7.37 * [Al] + 1.64 \qquad \textbf{(5.3)}$$

r^2 = 0.998, (n = 7)
i_p = peak current (μA)
i_b = background current (μA)
[Al] concentration in μM

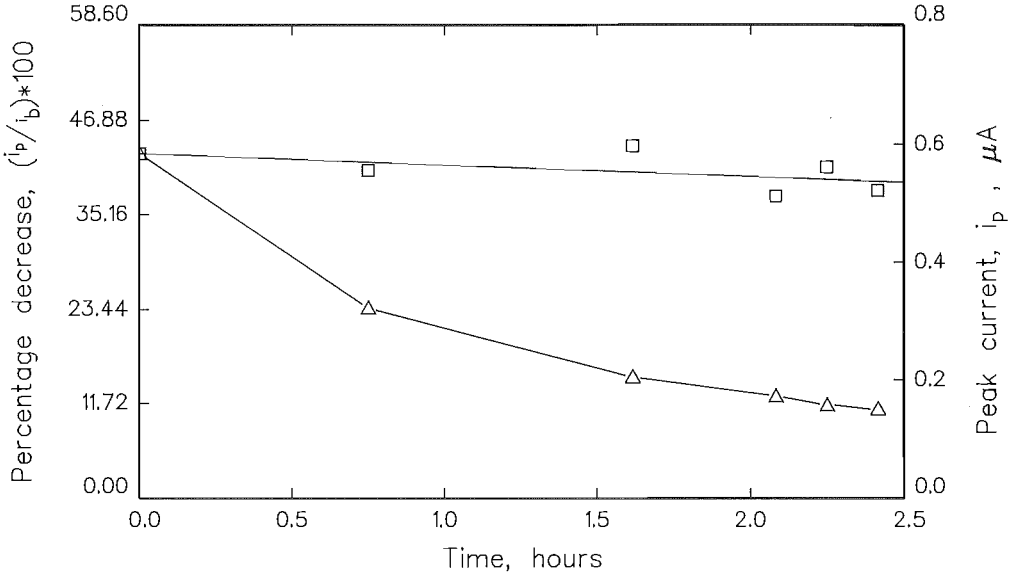

Figure 5.8 Signal stability. The response for repeat injections into the FIA manifold of an Al standard is plotted. Data is plotted either as peak current values, i_p (Δ) or as the percentage decrease in the baseline current, $(i_p/_{ib})*100$ (□).

Relative standard deviations were 3.5% and 0.3% at 1 and 10 μM Al, respectively (n = 6). The linear working range can be shifted by varying either the volume of sample injected or the concentration of 4-ncat pumped in the manifold. Increasing each of these quantities will move the linear working range to lower and higher values, respectively.

5.3.5 INTERFERENCES

Cations were screened for their ability to cause interference by injecting solutions of them into the manifold with the oxine column both absent and present. Table 5.2 shows that in the absence of the column, Pb(II) and organically complexed Fe(III) were strong interferents. Incorporation of the column into the manifold reduced these interferences below the detection limit. Evidently both metal ions are retained on the oxine column but neither cation is liberated by the weak alkali used for column elution. Thus when operating with the column no cations, at environmentally significant levels, were found to interfere in the electrochemical analysis of reactive Al.

Table 5.2 Concentrations of interferents giving a response equal to 1 μM Al in the absence and presence of the oxine microcolumn.

	Concentration (μM)	
Interferent	Oxine microcolumn	
	absent	present
Mg^{2+}	100	*a*
Ca^{2+}	*a*	*a*
Cr^{3+}	*a*	*a*
Fe^{3+}*b*	1	>100
Co^{2+}	75	>100
Cu^{2+}	70	>100
Zn^{2+}	*a*	*a*
Pb^{2+}	5	>100

a No interference; *b* Fe-tartrate complex.

5.3.6 DETERMINATION OF REACTIVE Al IN SOIL SOLUTIONS AND A FULVIC ACID COMPLEXATION CAPACITY

Reactive Al in four soil solutions was determined by two techniques, the 4-ncat/oxine method proposed here and the CAS 7s spectrophotometric method [Hawke and Powell, 1995]. The results are shown in Table 5.3. Similar amounts of Al were detected by both methods, with the 4-ncat/oxine method giving a slightly lower estimate.

Table 5.3 Reactive Al in soil solutions and Al- kinetic complexation capacity (Al–CC_k) of a soil derived fulvic acid, determined using the oxine column/4-ncat amperometric method and 7-second CAS spectrophotometric method.

	Reactive Al (μM)				
	soil sample[a]				Al–CC_k (μM)
Method	KF	KP	MF	MP	for a soil derived fulvic acid
oxine/4-ncat	<0.4	<0.4	2.9	3.0	10.1
7s CAS	<0.2	<0.2	4.4	4.0	9.6

[a] KF = Kamahi Rd forest; KP = Kamahi Rd pasture; MF = Matai Rd forest; MP = Matai Rd pasture (refer section 5.2.1). Al-CC_k was determined for a fulvic acid (FAG-4c) concentration of 17 mgL^{-1}. Determination of Al-CC_k by the 7s CAS technique was performed by Hawke *et al.* (1996).

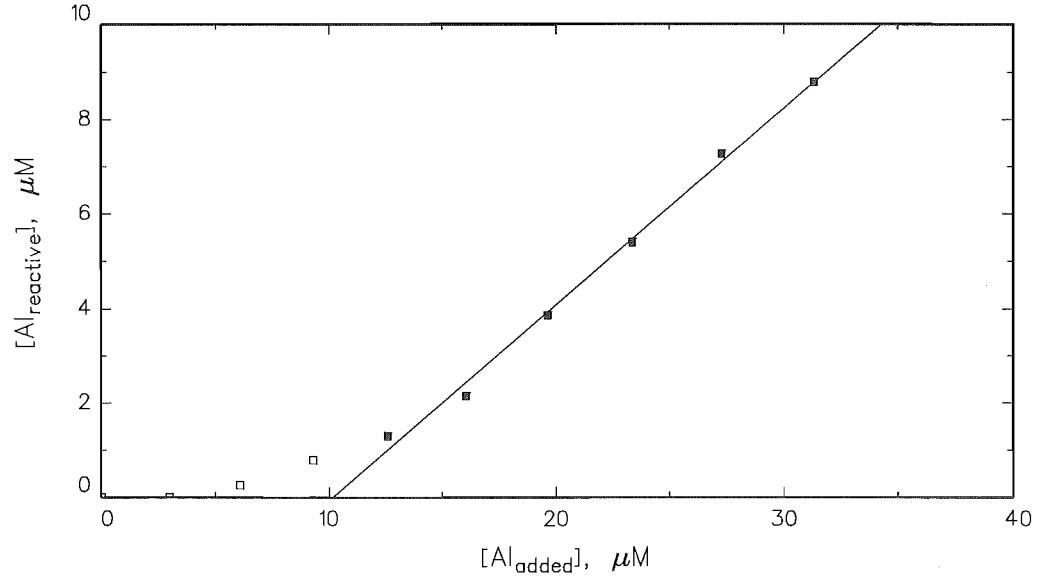

Figure 5.10 Kinetic complexation capacity, (Al-CC_k), of a soil-derived fulvic acid determined by the oxine/4-ncat amperometric method. Filled symbols (■) indicate data included in the linear regression.

The kinetic complexation capacity (Al-CC_k) of a soil-derived fulvic acid was also determined using the approach of Hawke *et al.* (1996). For this measurement a solution of the fulvic acid was prepared. Al was titrated into this solution at constant pH (4.7, 0.005 M acetate buffer). After each addition a sample was withdrawn for later

analysis of reactive Al. Data treatment involved plotting [$Al_{reactive}$] *vs* [Al_{added}] and extrapolating the linear portion of the graph to the *x* intercept (Figure 5.9). Table 5.3 illustrates the close correspondence in results when the samples are analysed by the 7s CAS technique and the oxine/4-ncat method.

5.4 DISCUSSION

5.4.1 ELECTROCHEMISTRY OF 4-NCAT AND ITS Al-COMPLEXES.

The electrochemistry of 4-ncat is comparable to that of catechol and other derivatives of catechol [Ryan *et al.*, 1980; Proudfoot and Ritchie, 1983]. It shows a two electron oxidation, the potential of which is pH dependent for solution conditions where the phenolic groups are protonated (ie below pH 11). The irreversibility of the oxidative electrochemistry of 4-ncat indicates that the *ortho*- quinone product is unstable on the timescale of the measurement. This is consistent with the reactivity of quinones with electron-withdrawing substituents [Proudfoot and Ritchie, 1983].

Coordination by Al shifts the oxidation potential of 4-ncat to higher (more positive potentials). As in Chapter 4 the shift in oxidation potential on complexation is assumed to arise from stabilisation of the ligand to oxidation, via an essentially electrostatic interaction with the hard metal centre. At the three solution pH values examined in Fig. 5.4, there is a *ca.* 300 mV separation between the oxidation waves for free ligand and the dominant Al-4-ncat complex.

The oxidation potential for Al complexed 4-ncat shifts to lower potentials as the complex stoichiometry increases (Table 5.1), i.e. as n increases from 1 to 3 for $[Al(4\text{-}ncat)_n]^{(3-2n)+}$. This is consistent with the decreasing "hardness" of the Al centre as subsequent ligands transfer electron density to the Al centre and with the destabilising effects of steric interactions between coordinated ligands as observed for the DASA series (Chap. 4).

For the complexes $[Al(4\text{-}ncat)]^{+}$ and $[Al(4\text{-}ncat)_2]^{-}$ complete oxidation of coordinated ligand was observed. However for $[Al(4\text{-}ncat)_3]^{3-}$ the RDE limiting currents for complex oxidation were significantly less than for the same concentration of 4-ncat in the absence of Al.

A possible explanation is that not all three ligands in the $[Al(4\text{-}ncat)_3]^{3-}$ species are oxidised. Thus it might be expected that the limiting currents in the presence of Al are

kinetically controlled, i.e. that there is some process limiting the amount of electroactive ligand (eg ligand dissociation). This may be probed by varying the timescale of the electrochemical experiment as in figure 5.5. At longer timescales (slower rotation rates) the extent of oxidation of coordinated ligand might increase. The ratio of limiting currents for reaction of 4-ncat in the absence and presence of Al would approach equality. Conversely at shorter timescales (faster rotation rates) the extent of oxidation of coordinated ligand should decrease and the difference in total limiting currents would become greater.

Such a kinetic process would produce non-Levich behaviour (eqn. 5.2). Figure 5.5 shows that the limiting currents for oxidation of $[Al(4\text{-ncat})_3]^{3-}$ do hold the Levich relationship, neither curving up to higher currents at lower rotation rates nor down to lower currents for higher rotation rates. Notably the current due to oxidation of $[Al(4\text{-ncat})_3]^{3-}$ was consistently 2/3 the limiting current for oxidation of 4-ncat in the absence of Al for all rotation rates studied.

This indicates that limiting currents are not kinetically-controlled and it may be assumed that two ligands per complex are oxidised at all rotation rates.

An alternative explanation is that all three coordinated ligands are oxidised but that the diffusion coefficient for the complex is less than half that of the free ligand (from the Levich equation current depends on (diffusion coefficient)$^{2/3}$ for hydrodynamic voltammetry at the RDE). These possibilities were not investigated further but the former explanation is more consistent with the behaviour of the Al-DASA and Al-catechol systems reported in the previous chapter. Thus diffusion coefficients are assumed to be very similar for the complex and for the free ligand.

Because the oxidation wave of free 4-ncat (in the presence of Al complexed 4-ncat) was observed to hold to the Levich relationship (data not shown) the initial (reduced) Al-4-ncat complexes are considered inert on the experimental timescale (as found for the Al-DASA complexes in section 4.2.6). Oxidised ligand is expected to rapidly dissociate from the Al centre and further oxidation of coordinated ligand may take place, up to a maximum of two ligands per complex.

5.4.2 FLOW INJECTION ANALYSIS.

The use of solution equilibrium calculations has established pH~9 as the optimum pH for the amperometric analysis of Al. Hydrodynamic voltammetry at this pH (Figure 5.6) established the optimum applied potential as 0.3 V *vs* SCE. These parameters were incorporated into the Flow Injection Analysis (FIA) manifold of Figure 5.1.

Section 5.3.4-A reports the analytical performance of this system. A linear working range of 0.4 - 8 μM reactive Al was observed. The levels of reactive Al expected for natural waters are 0.1 -30 μM Al [Driscoll and Schecher, 1990].

5.4.2-A ELECTRODE FOULING. In the course of operating the FIA manifold significant electrode deactivation was encountered This is assumed to originate from deposition of oxidation products on the electrode surface, resulting in a decreased active electrode area and/or a decreased rate of electron transfer at the electrode. The effect of this electrode fouling was to halve the current response approximately every half hour.

Al was measured by the decrease in the free 4-ncat oxidation which it causes. This response was expressed as a percentage decrease in the baseline current (eqn. 5.3). The response recorded in this way was less sensitive to the condition of the electrode (see Fig. 5.8) than simply recording the absolute current (i_p in eqn. 5.3). The ratios of signal size:background current, and signal size:noise, remained constant regardless of the degree of electrode deactivation.

A drawback of this approach is that the baseline current must be measured immediately after every injection.

5.4.2-B INTERFERENCES. Only metal ions which accompany Al through each step in the analytical protocol (i.e. retention on the oxine microcolumn, elution with base and complexation by 4-ncat) will interfere with its determination. Interaction with the microcolumn and reaction with 4-ncat are not expected to afford significant separation of Al from interfering cations. It is the use of a weakly basic eluent which is designed to achieve selectivity for Al.

Oxine is a non-specific chelator forming complexes with over 40 cations [Tikhonov, 1973]. Thus the oxine column will capture many metal ions in addition to Al, although some which form less stable complexes may not bind at the weakly acidic pH to which the column is buffered. Similarly, 4-ncat forms complexes with many cations and

equilibrium constants have been determined for Cd^{2+}, Be^{2+}, Mg^{2+}, Ca^{2+}, Sr^{2+}, Ba^{2+}, Cu^{2+}, Zn^{2+}, Mn^{2+}, Co^{2+}, Ni^{2+}, Fe^{3+} [Hakkinen, 1984a, 1984b, 1984c and 1985] and Ga^{3+} [Pichet and Benoit, 1967]. Metal ions which are eluted from the column will reduce the concentration of free 4-ncat at the detector if their complexes are formed in significant amounts at micromolar concentrations. However, few metal ions form hydroxy anions in the dilute alkali used for column elution.

Thus, as observed in section 5.3.5, potentially interfering metal ions remain on the column while the aluminate ion, $[Al(OH)_4]^-$, is eluted.

5.4.2-C FRACTIONATION OF REACTIVE Al. In order to demonstrate the selective determination of reactive Al species, the present protocol was tested against the "7-second CAS" method developed by Hawke and Powell (1995). In this method measurement of reactive species of Al is achieved by a strategy different from that of the oxine column. Thus it offers a means of independently checking the selectivity of the 4-ncat/oxine method towards reactive Al.

In techniques using the oxine column selection of reactive Al species is achieved by virtue of a brief contact time with the immobilised ligand oxine. This ligand is held by a diazonium coupling to the solid support material of the fractogel beads within the column. In the 7-second CAS technique Al samples are combined on line with the ligand CAS which is in solution. CAS is also a chromophore and undergoes a colour change upon coordination to Al. A short (7 s) reaction time is used (within a FIA manifold) to selectively measure only the most reactive and labile species of Al.

The agreement between the two techniques is indicated in Table 5.3. Very similar results are observed for the determination of an Al kinetic complexation capacity, Al-CC_k. In the determination of reactive Al in soil solutions the 4-ncat/oxine method gives slightly lower results. This is expected from the longer fractionation time in the 7-seocnd method. It is consistent with published work where the oxine column method coupled to spectrophotometric detection was found to determine *ca.* 20 % less Al than the 7-second CAS method [Simpson *et al.*, 1997]. These results indicate the importance of minimising the contact time between the sample and the competitive ligand (oxine or CAS) when targeting the reactive Al fraction.

5.5 CONCLUSIONS

Solution equilibrium calculations have demonstrated the formation of suitably stable complexes between Al and 4-ncat for the development of an analytical application.

The voltammetric studies have extended the observations of Chapter 4 to a further Al/ligand system. As in that chapter the complexes formed with Al were found to be inert on the electrochemical timescale and distinctly different potentials exist for oxidation of free and Al complexed ligand. The redox potential of the complexes depends on complex stoichiometry. The wave for oxidation moves to lower (less positive) potentials as the number of coordinated ligands is increased.

This information has been valuable for optimising conditions (pH, ligand concentration and voltammetric potential) for amperometric detection. A FIA manifold has been developed for the analysis of Al at micromolar levels. Electrode deactivation has been overcome by incorporating a correction for the changing condition of the electrode into the analytical response.

By including a microcolumn of oxine-derivatised gel into the FIA manifold interferences are eliminated and reactive Al species may be selectively measured at levels relevant to environmental waters.

A drawback to the method proposed here is the necessity to correct for electrode deactivation. This derives from the strategy of amperometric monitoring of free ligand, i.e. Al is measured by the decrease it causes in the oxidation current of free 4-ncat. This means that for the greater part of the time there is a constant current passed from oxidation of free 4-ncat. The reaction products of this oxidation cause electrode fouling and require a separate measurement of the background current to be included in every measurement.

Novel FIA strategies to overcome this problem are presented in chapter 6.

Chapter 6

NOVEL FIA STRATEGIES FOR THE AMPEROMETRIC ANALYSIS OF ALUMINIUM

6.1 INTRODUCTION.

6.1.1 THE PROBLEM DEFINED.

This chapter presents novel FIA strategies for the indirect amperometric analysis of Al. It is intended that these will overcome the difficulties with electrode instability encountered with the FIA system described in Chapter 5. For that system electrode instability resulted from the necessity to constantly oxidise the ligand (4-ncat). Reaction products of this oxidation cause electrode fouling and produce an exponential decrease in the amperometric background and signal.

Continuous ligand oxidation is necessary because the analytical complex may only be detected indirectly, by observing a decrease in the concentration of free reagent. This is because the analytical complex is electroactive only at a higher potential than the free reagent. At lower potentials the free ligand may be selectively oxidised but at higher potentials both free and metal bound ligand are oxidised. Thus a potential cannot be chosen where only metal-bound ligand may be monitored.

This relationship between electrode potentials for free ligand and complex is found for a range of metals and ligands. There are numerous examples available in the scientific literature of the use of electroactive ligands for indirect electroanalysis. In Table 6.1 the electrochemical parameters are summarised for a selection of these. In each case the analytical complex is redox active at a higher potential (more negative for reductive processes, more positive for oxidative processes) than the free ligand. The case of Al^{3+} and SVRS is a good example, showing both an oxidative and a reductive wave.

It seems likely that this shift in potentials will always be the case for electrochemical systems where a stable complex is formed. The chemical energy released by complex formation must be compensated for in the electrochemical process. Thus an

extra electromotive force must be supplied in the redox reaction of the complex (relative to the free ligand) and the complex is electroactive only at a higher potential.

Table 6.1 Electrochemical parameters for various analytical applications.

RED/OX	Metal	Ligand	E_p(V) ligand	E_p(V) complex	reference
Reducing, (AdSV)					
	Al^{3+}	SVRS	-0.6	-0.72	Downard *et al.*, 1992b
	Al^{3+}	DASA	-0.7	-1.2	van den Berg, 1986
	Y^{3+}	SVRS	-0.82	-1.24	Lanza, 1997
	Yb^{3+}	MR19	-0.71	-0.79	Lee *et al.*, 1997
	Fe^{3+}	1N-2N	-0.45	-0.67	Gelado-Caballero *et al.*, 1996
	Cu^{2+}	DPT	-0.26	-0.38	Mlakar, 1997
Oxidising					
	Al^{3+}	SVRS	0.53	0.88	Florence *et al.*, 1966
	Al^{3+}	4ncat	0.21	0.50	Downard *et al.*, 1997a
	Al^{3+}	DASA	0.3	0.8	Downard *et al.*, 1992a
	Al^{3+}	oxine	0.53	0.88	Cai and Khoo, 1993
	Co^{2+}	oxine	0.53	0.80	Cai and Khoo, 1993
	Mn^{2+}	oxine	0.53	0.95	Cai and Khoo, 1993
	Fe^{3+}	oxine	0.53	0.82	Cai and Khoo, 1993
	Ni^{2+}	oxine	0.53	0.77	Cai and Khoo, 1993
	Cu^{2+}	oxine	0.53	0.78	Cai and Khoo, 1993

It would be interesting to identify a ligand for which changing the oxidation state would increase the stability of the complex with a particular metal ion. This extra stability would enhance the driving force towards the different oxidation state of the ligand and the initial complex would be electroactive at a lower potential than the free ligand. An analytical potential could be chosen for such a system where only the metal-bound ligand would be electroactive.

Unfortunately no such system is known for Al. The ligands used in this work show no coordination to Al after a change in their oxidation state. These ligands all have catecholate centres for coordination to Al. Upon oxidation these give *ortho*-quinones which do not chelate Al [Ohman *et al.* 1983]. Thus oxidation will destroy the complex. Since the complex has been destroyed an extra electromotive force must be supplied to compensate for the lost stabilisation of the ligand by Al and the complexes are always electroactive at higher potentials than the free ligand. For these systems it is not possible to amperometrically monitor Al-bound ligand without interference from free ligand unless the free ligand is either removed or made electroinactive.

Van den Berg *et al.* (1986) have achieved this in their development of an adsorptive stripping voltammetry (AdSV) technique for the measurement of Al in fresh and sea water using the ligand DASA. They observed that reduction of the free ligand occurred at potentials more negative than -0.7 V (*vs.* Ag,AgCl/sat. KCl) and for Al bound ligand at potentials more negative than -1.2 V. By using an accumulation potential of -0.9 V they were able to reduce all free ligand within the vicinity of the mercury drop electrode while Al-bound ligand was not reduced and could be accumulated for subsequent stripping measurement.

In this chapter FIA strategies are presented for eliminating the response for free ligand, thus allowing the selective amperometric analysis of Al-bound ligand. A desired result is the improved electrode stability that should arise from the greatly reduced oxidative electrolysis at the working electrode. This is illustrated in Fig. 6.1. A FIA trace is given for an amperometric system in which the free ligand is monitored and also for one in which only metal-bound ligand gives a response. The shading indicates the large amount of charge which is passed for the former system. In the second system there is only a very small time when significant currents are passed and thus less opportunity for electrode fouling.

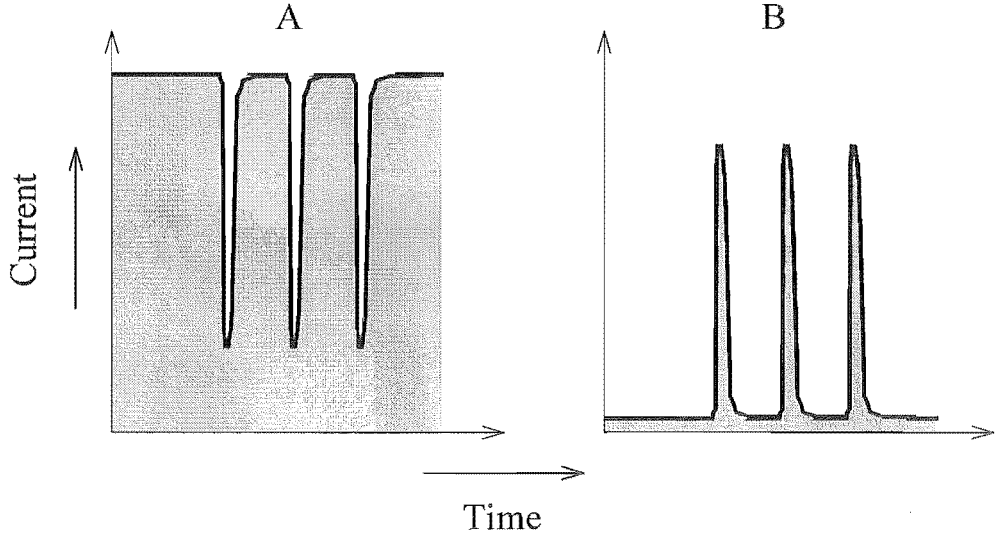

Figure 6.1 Schematic FIA amperograms. Each shows three replicate injections of the analyte.
A) Conventional system where free ligand oxidation is monitored (as in Chapter 5).
B) Modified system where the electrochemistry of the analyte/reagent complex is monitored.

6.1.2 FIA TECHNIQUES.

Two distinct strategies have been used in this work to remove the response of free ligand at an amperometric detector.

Firstly a guard reagent has been used to complex free ligand. The complex formed with the guard reagent is redox active at an even higher potential than the complex formed with the analyte, Al. This allows an analytical potential to be selected at the detector where only Al-bound ligand is electroactive.

In the second approach on-line solvent extraction has been used to extract free ligand, leaving only Al-bound ligand to pass on to the electrochemical detector.

6.1.2-A USE OF BORONIC ACID AND A DERIVATIVE AS GUARD REAGENTS. Trivalent boron is in the same group as Al within the periodic table and shows a similar affinity for bonding with oxygen donors. It differs from Al in that its bonding is primarily covalent rather than being essentially electrostatic [Cotton and Wilkinson, 1988].

Observations may be drawn from the literature to show that boron compounds will readily form complexes with catechol and catechol derivatives. Griffith *et al.* (1996) have published a crystal structure of Meulenhoff's salt. This was originally synthesised in 1925 [Meulenhoff, 1925]. The structure contains a boron atom bonded in a tetrahedral environment by the oxygen atoms of two catechol molecules. Boronic acid derivatives have been applied as pairing agents for catecholamines and other catechol derivatives in High Pressure Liquid Chromatography (HPLC) [Joseph, 1985].

The catechol moiety is present in many of the ligands which are suitable for the indirect electrochemical analysis of Al. Thus boronic acid and a derivative, phenyl boronic acid, were selected as potential guard reagents to bond to excess free ligand during indirect amperometric analysis of Al.

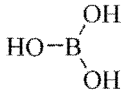

boronic acid

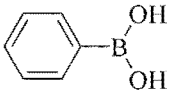

phenyl-boronic acid

6.1.2-B SOLVENT EXTRACTION. Solvent extraction in a FIA system has been used since 1978 [Karlberg and Thelander, 1978]. Use of FIA gives an automatic, precise and reproducible extraction.

A typical system will include three essential components: the solvent segmentor, the extraction coil, and the phase separator. The solvent segmentor, where the organic and the aqueous phases converge, functions to provide alternate segments of both phases. These segments enter the extraction coil. This is a length of an inert tubing, often Teflon or glass. Lucy and Yeung (1994) have shown that a wetting film of the extracting organic solvent forms on the walls of this tubing and the extractable component is taken up by this film.

Down-line from the extraction coil is the phase separator which divides the incoming flow into two streams, each containing one of the phases. There are two basic types of phase separator, T-shaped and membrane separators [Valcarcel and Gallego (1989)]. T-shaped separators consist simply of a T-shaped junction where the segments separate. The side arm of the T leads vertically down to allow the most dense phase to separate. Often separation is promoted by placing a string of Teflon in the junction. This guides the organic solvent stream away.

Membrane separators are more common. The membrane is usually made of micropore Teflon (pore size = 0.5 -1.0 μm) which allows selective passage of the organic (non-aqueous) phase. The membrane is often sandwiched between two blocks of Teflon or Perspex. The segmented flow passes through a channel in one block and runs across the surface of the membrane. The organic phase passes the membrane and exits via a channel in the opposite block.

Valcarcel and Gallego (1989) have reviewed the use of on-line solvent extraction for sample pretreatment prior to analysis by atomic absorption spectrometry (AAS). In this context it improves sensitivity by a preconcentration effect and improved flame atomisation. Also it allows separation of the analyte from problematic matrices.

Clarke *et al.* (1992) have presented a flow system for the spectrophotometric analysis of Al as the oxinate. By use of solvent extraction of the analytical complex after a very brief reaction time (2.3 seconds) they were able to target only 'quickly reacting Al' in their analysis. ('quickly reacting Al' was found to approximate to Al^{3+}, $AlOH^{2+}$, probably

$Al(OH)_2^+$, Al sulfato complexes and some of the weaker organic complexes.) Detection was by spectrophotometry.

In this work on-line solvent extraction within a FIA manifold was selected as a means of physical removal of free ligand from that bound to Al. At pH 5.0 the free ligand selected for this application is nonionic while it's Al complex is charged. After phase separation the metal-bound ligand may be measured in isolation by amperometry.

6.2 EXPERIMENTAL.

For details describing reagents, FIA equipment and manifold construction, electrochemical equipment etc. see Chapter 2.

The pH of all buffer solutions was adjusted by the addition of KOH. Solutions containing alizarin were prepared by first combining alizarin and KOH and sonicating before addition of ammonium acetate. This procedure eliminated problems with alizarin solubility.

For Manifolds 6.2 and 6.3 Al standards were prepared in of $1x10^{-4}$ M HCl. For Manifold 6.1 Al standards were prepared in a matrix of $1x10^{-4}$ M 4-ncat and 2.0 M NH_4Cl / NH_4OH, pH 8.6.

6.2.1 FIA MANIFOLDS

In each diagram p indicates a peristaltic pump, injection valves are given by an arrow passing through a circle, D indicates the amperometric detector (as illustrated in Fig. 2.2) and W indicates discarding the stream to waste. Internal diameters for the various sizes of pump tubing used were; ene 1, 0.19 mm; ene 8, 0.79 mm; ene 9, 0.89 mm.

MANIFOLD 6.1 Boronic guard reagent. Preformed metal-ligand solutions were injected into a carrier stream. After mixing on-line with a boron reagent the analysis stream passed quickly through a series of mixing tanks and on to the amperometric detector.

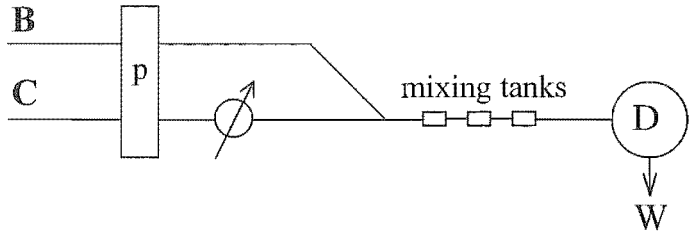

C - Carrier line, $1x10^{-4}$ M 4-ncat, 2.0 M NH_4Cl/NH_4OH, pH 8.6. Flow rate = 0.79 mL/min., ene 8 tubing.

B - Boron reagent line, either 0.1 M phenyl-boronic acid ($C_6H_7O_2B$, Aldrich, 97%) or a saturated solution of boronic acid (H_3BO_3, approx. 0.05 M, Hopkins and Williams, AR). Flow rate = 0.79 mL/min., ene 8 tubing.

Samples contained 5-33 μM Al, 100 μM 4-ncat and 2.0 M NH_4Cl/NH_4OH, pH 8.6. An Alitea 4-channel peristaltic pump was used (setting 40.0). The mixing tanks were a series of alternating 1 cm lengths of silicon and microline tubing as described by Hawke *et al.* (1996).

MANIFOLD 6.2 Conventional Amperometry. Samples containing Al were injected into a carrier stream and mixed on-line with a buffered solution of the reagent. The flowing stream passed through a reaction coil to allow complexation reactions to occur before reaching the amperometric detector.

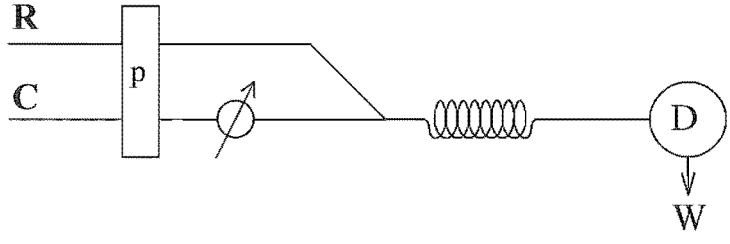

C - Carrier line, $1x10^{-4}$ M HCl. Flow rate = 0.30 mL/min., ene 8 tubing.

R - Reagent line, $1x10^{-4}$ M alizarin in 0.05 M NH_4acetate, pH 8.9. Flow rate = 0.30 mL/min, ene 8 tubing.

An Ismatec 10-channel peristaltic pump was used (setting 50). The injection valve had a 140 μL sample loop. The reaction coil consisted of 150 cm of coiled microline tubing.

MANIFOLD 6.3 Solvent extraction. In reaction coil R1 a complex was formed between Al and the ligand alizarin. Excess ligand was removed by solvent extraction in coil R2. In coil R3 alizarin was liberated from the Al complex before measurement at the detector, D.

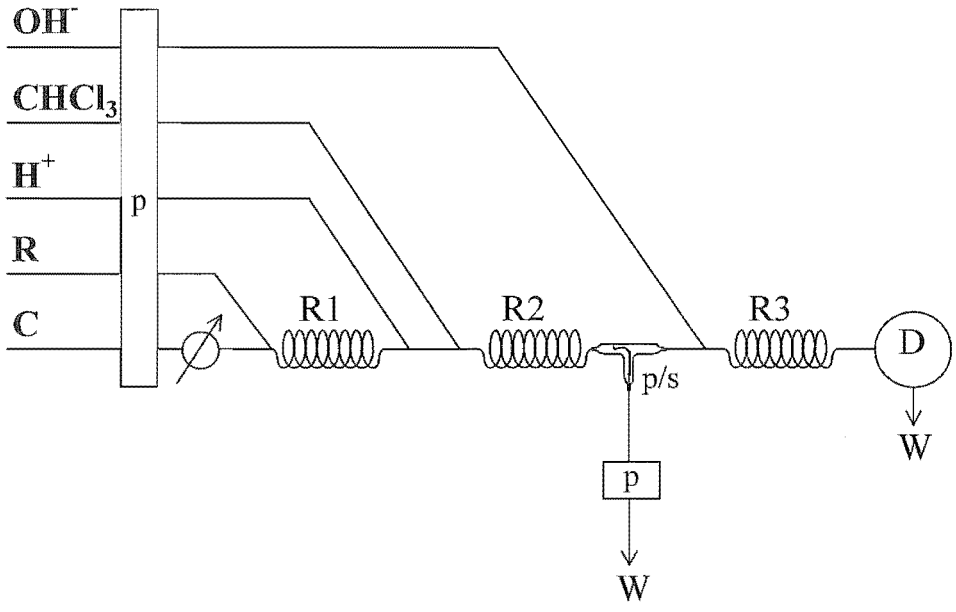

OH⁻ - Alkali line, 1.0 M KOH. Flow rate = 0.038 mL/min., ene 1 tubing.

C - Carrier line, $1x10^{-4}$ M HCl. Flow rate = 0.30 mL/min., ene 8 tubing.

R - Reagent line, $1x10^{-4}$ M alizarin in 0.05 M NH_4acetate, pH 8.9. Flow rate = 0.30 mL/min, ene 8 tubing.

H^+ - Acid line, 0.22 M HCl, 1.7 M KCl. Flow rate = 0.038 mL/min., ene 1 tubing.

$CHCl_3$ - Solvent line. Flow rate = 0.383 mL/min., ene 9 tubing, viton rubber.

p/s - Phase separator.

The main pump was an Ismatec 10-channel peristaltic pump (setting 50). An Alitea 4-channel belt peristaltic pump was used for achieving balanced solvent withdrawal from the phase separator. The injection valve had a 140 µL sample loop. A T-shaped phase separator with a Teflon string was used. The reaction coils were coiled lengths of micro-line tubing; R1=150 cm, R2=100 cm, R3=100 cm. The extraction coil, R2, was seasoned by running the system continuously for 8 hours.

For this manifold the glassy carbon working electrode of the amperometric detector was electrochemically cleaned by sweeping the potential at 100 mV s^{-1} from the detection potential (+0.15 or +0.3 V) to +1.5 V and holding for 10 seconds. The potential was then switched back to the detection potential. Once the system had stabilised

(typically within 1 minute) a sample could be injected into the manifold. When electrochemical cleaning was used the protocol was applied before each analysis.

6.3 RESULTS.

6.3.1 BORONIC GUARD REAGENT.

The voltammetric behaviour of 4-ncat and the complexes formed with Al and phenyl boronic acid was examined by linear sweep voltammetry at a rotating disk electrode (RDE). The voltammograms in Fig. 6.2 show that oxidation of free 4-ncat gives a wave with an $E_{1/2}$ value of 0.21 V at pH 8.7. Coordination to Al and phenyl-boronic acid gives complexes with $E_{1/2}$ values shifted to 0.50 and 0.87 V respectively. Thus on the basis of the observed potentials phenyl-boronic acid is a suitable guard reagent for 4-ncat. It stabilises the ligand towards oxidation. Its oxidation potential is 370 mV more positive than the oxidation potential for Al-bound 4-ncat.

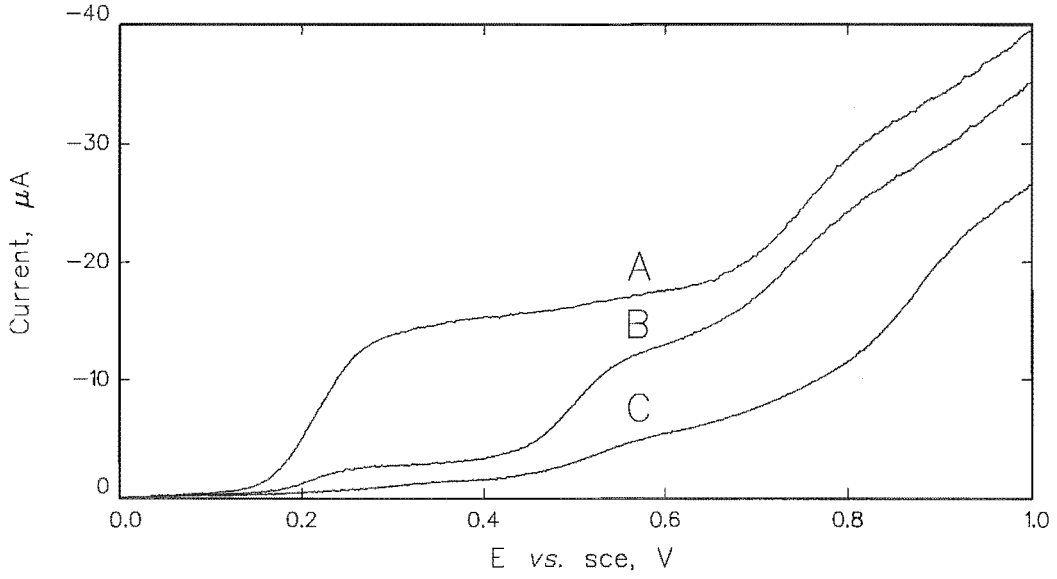

Figure 6.2, Linear sweep voltammograms (ν = 100 mV s^{-1}) collected at an RDE, ω = 50 s^{-1}, for 4-ncat ($5x10^{-5}$ M) in the presence of
A) electrolyte only (pH 8.7, 0.05 M NH_4Cl/NH_4OH)
B) electrolyte and $1.3x10^{-5}$ M Al
C) electrolyte and $1.3x10^{-5}$ M Al and $5x10^{-3}$ M phenyl boronic acid.

To function satisfactorily the guard reagent must react quantitatively with free ligand. In order for all free ligand to be scavenged by phenyl-boronic acid a considerable excess must be used. At this concentration of guard reagent the ligand is also taken up from the complex formed with Al. This is reflected in Fig. 6.2, curve C, where both Al and

phenyl-boronic acid are present. Compared with curve B only a small step remains at the potential where Al-bound 4-ncat is oxidised (0.50 V). Virtually all of the ligand has been complexed by phenyl-boronic acid because this is present at a much greater concentration.

Although the guard reagent is able to complex both free and Al-bound ligand there is a kinetic discrimination between the two processes which may be exploited. The chronoamperograms in Fig. 6.3 were formed by holding an RDE at a fixed potential, 0.6 V, such that the free ligand and that bound to Al were both oxidised but that bound to the guard reagent was not (refer Fig. 6.2). Each curve in Fig. 6.3 starts with a plateau current from the steady state oxidation of either free (A) or Al-bound (B) ligand. Phenyl-boronic acid was not initially present but an aliquot was added at time = 0.

The guard reagent quickly coordinates to all free 4-ncat present with a rapid decrease in oxidation current (curve A).

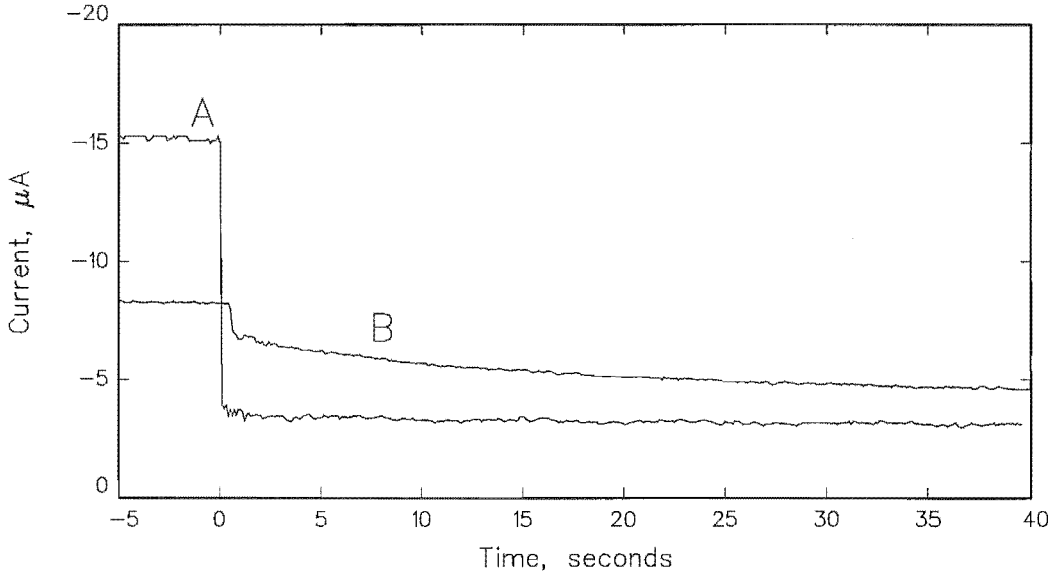

Figure 6.3. Chronoamperograms recorded at an RDE (ω = 50 s^{-1}, E = 0.6 V *vs.* SCE). pH = 8.7, 0.05 M NH_4Cl/NH_4OH. At time = 0 an aliquot of phenyl-boronic acid solution was added to the electrochemical cell to give a final concentration of $5x10^{-3}$ M. The RDE provided rapid mixing.
A) 4-ncat = $5x10^{-5}$ M.
B) 4-ncat = $5x10^{-5}$ M and Al = $1.8x10^{-5}$ M.

In the presence of Al (curve B) there is an initial sharp decrease in current associated with the residue of free ligand which is present. Then there is a gradual decrease in current as the guard reagent takes up the 4-ncat from the Al complexes, with the current still decreasing after 40 seconds. A significant length of time is required for the complete dissociation of the Al-4-ncat complexes. This time presents a window within which Al-bound ligand may be measured electrochemically (e.g. at 0.6V) while all free

ligand has been scavenged by phenyl-boronic acid and made electroinactive (at potentials up to 0.87 V).

Manifold 6.1 was constructed to make use of this strategy. Coordination of the ligand (4ncat) to the analyte (Al) was effected off-line by combining appropriate solutions. This allowed the manifold to be greatly simplified so that the performance of the boronic guard reagent could be studied in isolation.

The concentrations of ligand and buffer/electrolyte in the samples was matched with the carrier stream so that the preformed samples could be injected directly into the carrier stream. After mixing on-line with a boron reagent the analysis stream passed quickly through a series of mixing tanks and on to the amperometric detector.

Figure 6.4 presents a series of current-time traces recorded with this manifold.

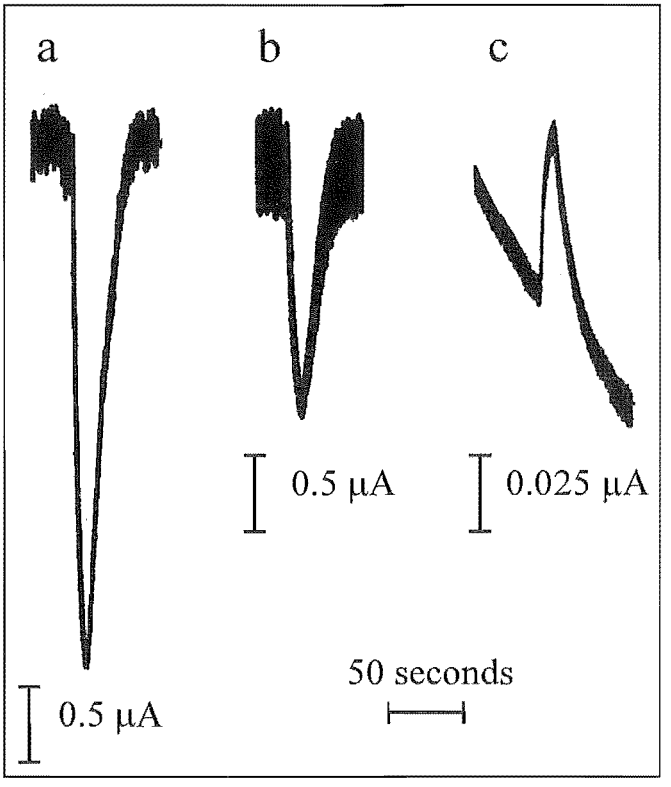

Figure 6.4. FIA traces generated with Manifold 6.1 flowing various solutions into the guard reagent line. Concentration of Al injected = 33 μM.
Guard reagent line =
a) triply distilled water, $E_{applied}$ = 0.3 V (*vs.* SCE).
b) triply distilled water, $E_{applied}$ = 0.6 V (*vs.* SCE).
c) 0.1 M phenyl-boronic acid, $E_{applied}$ = 0.6 V (*vs.* SCE).

In trace A of Fig. 6.4 the detector was poised at a potential of 0.3 V and triply distilled water was substituted for the guard reagent. At this potential free 4-ncat may be oxidised but Al-bound 4-ncat may not. Injection of a solution containing Al complexed 4-ncat gave the large downward peak in the cathodic direction (less oxidation). This corresponds to the analytical response used in Chapter 5.

Raising the potential of the detector to 0.6 V gave trace B. At this potential both free and Al complexed 4-ncat are electroactive. At the pH used in Manifold 6.1 (pH 8.6) the dominant complex formed between Al and 4-ncat is $[Al(4\text{-ncat})_3]^{3-}$ [see Fig 5.2, section 5.3.1]. In Chapter 5 it was observed that this complex gives rise to a smaller oxidation current than the equivalent concentration of free 4-ncat. Hence trace B shows a downward peak which corresponds to this difference in currents.

In the next step phenyl-boronic acid was pumped in the guard reagent line. This lead to a large decrease in the baseline current as the 4-ncat was rendered electro-inactive (up to potentials of 0.87 V). Injection of Al-complexed 4-ncat gave the anodic peak in trace C (increasing oxidation). The guard reagent is successfully scavenging the free ligand while some fraction of the Al-bound ligand remains electroactive. This fraction must be small since the peak current is very low.

Attempts were made to increase the signal by reducing the distance between the confluence with phenyl-boronic acid and the detector, thus reducing the contact time between the sample and the guard reagent. This also decreased the mixing efficiency, resulting in an erratically pulsating baseline current which was unusable. Scampavia *et al.* (1995) have promoted the use of a co-axial jet mixer for the complete mixing of FIA streams within 55 milliseconds. A similar mixer was constructed 'in-house' for use in this project. Unfortunately it did not give significantly improved mixing over the glass mixing tees used normally.

The baseline current in trace C slopes strongly downwards. This demonstrates the loss in electrode sensitivity caused by the guard reagent, phenyl-boronic acid. After approx. 20 minutes of operation there was no response to injections of Al-bound 4-ncat and the detector electrode had to be withdrawn and repolished.

This deactivation was attributed to adsorption at the electrode surface by the phenyl ring of phenyl-boronic acid. No deactivation was observed from the use of boronic acid (H_3BO_3) and this was examined as a substitute guard reagent.

Boronic acid showed similar voltammetric and kinetic properties to the phenyl derivative as illustrated in Figs 6.2 and 6.3. A difficulty encountered was that quantitative reaction between 4-ncat and boronic acid could not be forced, even with a 2000-fold excess of boronic acid. Greater excesses could not be used because of the limited solubility of boronic acid (estimated as 0.05 M at 20 °C). When boronic acid was pumped into the manifold there was no signal for injections of Al-bound 4-ncat.

Thus it appears that boronic acid reagents do not function adequately as guard reagents. This work was not pursued further.

6.3.2 ON-LINE SOLVENT EXTRACTION.

Initial experiments were aimed at finding a suitable ligand and solvent for the solvent extraction system. The extraction of the ligands 4-ncat and alizarin from aqueous solution at pH 5.0 (where both ligands are non-ionised) into the solvents chloroform, dichloromethane, carbon tetrachloride, pentane, petroleum ether, ethyl acetate and hexane was examined. 4-ncat was not extracted by any of these solvents and only the chlorinated solvents were effective for the extraction of alizarin. Chloroform was selected because of its common use as an extraction solvent.

Manifold 6.3 was constructed for on-line solvent extraction. Samples were injected into the carrier line and mixed on-line with the reagent. Complexation of the analyte, Al, occurred at pH 8.9 in reaction coil R1. The flowing stream was mixed with an acid line to lower the pH to 5.0 and then with the solvent, chloroform. Extraction of free alizarin into the solvent occurred in reaction coil R2. After phase separation (p/s) the organic solvent was directed to waste and the aqueous stream was mixed with strong alkali to solubilise and dissociate the Al-bound alizarin in reaction coil R3. The liberated ligand was then measured amperometrically.

It was necessary to establish optimum conditions for complex formation between Al and alizarin (reaction coil R1), quantitative extraction of excess alizarin into chloroform (reaction coil R2) and decomposition of the complex to give free ligand and $Al(OH)_4^-$ (reaction coil R3). Each of these processes was optimised separately.

6.3.2-A OPTIMISATION OF COIL R1. In this reaction coil Al is complexed by alizarin at pH 8.9. The kinetics of this complexation reaction were examined using Manifold 6.2. This manifold is essentially a simplification of Manifold 6.3 with R1 being directly plumbed into the amperometric detector.

The residence time within R1 was varied by using a slower pumping rate (to give longer residence times) and by decreasing the length of tubing (to give shorter residence times). The amperometric detector was held at a potential of 0.3 V. At this potential only free alizarin gives an oxidation current. The extent of complexation was measured by making injections of Al into the manifold and observing the decrease in current. The decrease was calculated as the percentage decrease in the baseline current, as described in section 5.3.4-A. This method of calculation largely overcame any variation due to electrode fouling.

As shown in Fig. 6.5 the reaction is largely complete after 20 seconds. This time reflects the effects of both physical (mixing) and chemical processes. A residence time of 30 seconds was adopted as standard in Manifold 6.3

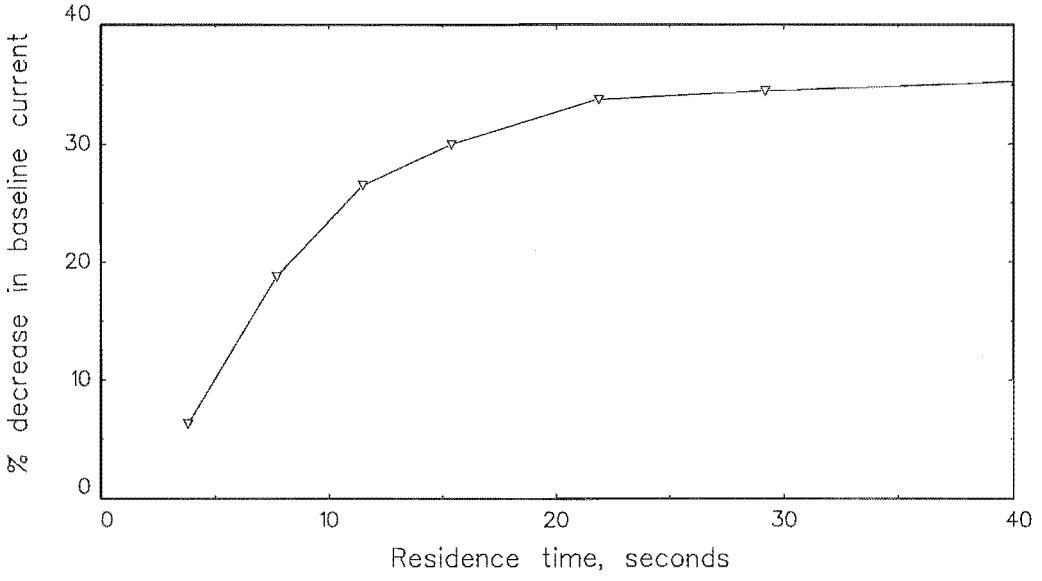

Figure 6.5. Extent of reaction between Al and alizarin. The residence time gives the time for any fluid element to pass through reaction coil R1. Manifold 6.3 was used with E_{app} = 0.3 V (*vs.* SCE). 30 μM Al injections were made.

6.3.2-B OPTIMISATION OF COIL R2. In this reaction coil free alizarin is extracted by the solvent chloroform while Al-bound alizarin remains in the aqueous phase. The experimental parameters were optimised towards extraction of free alizarin. The effect on Al-bound alizarin was not considered. Should a fraction of the Al-bound alizarin be extracted then this is preferable to allowing some of the free alizarin to escape extraction and remain in the aqueous phase.

The optimal pH for extraction of alizarin was established by preparing solutions of alizarin at various pH and adding an aliquot of chloroform. After prolonged shaking the residual alizarin remaining in the aqueous layer was measured spectrophotometrically. As shown in Fig 6.6 the extraction decreased with increasing pH. A pH of 5.0 was used in coil R2 of Manifold 6.3.

It should be emphasised the each datum point in Fig. 6.6 represents the partition of alizarin across a single phase boundary. This differs from the flow environment where extraction occurs at multiple points within the extraction coil and is likely to achieve a much greater efficiency. The trend in behaviour with pH should remain however.

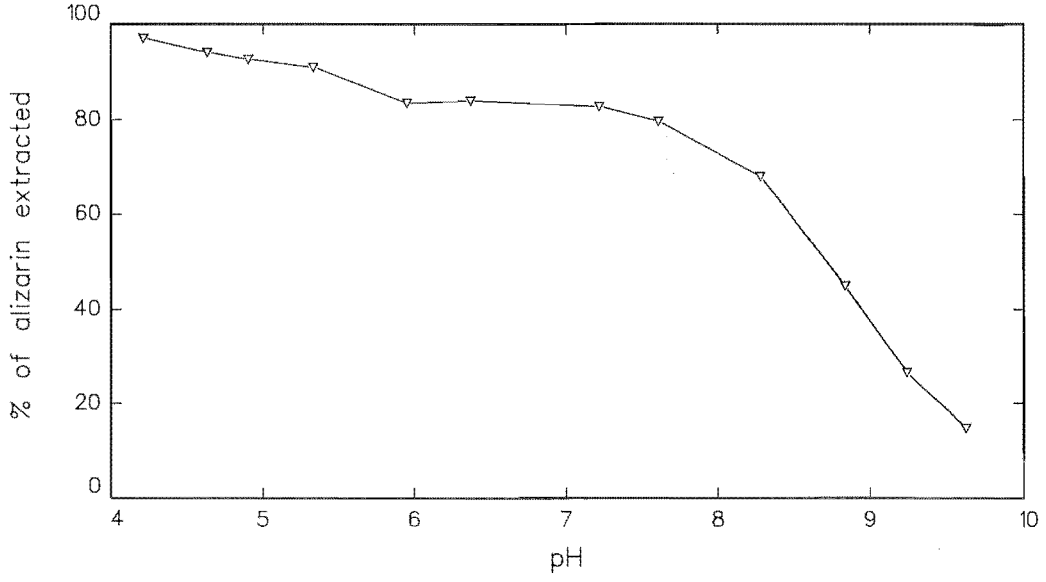

Figure 6.6. Variation in extraction efficiency with pH. 10 mL solutions were prepared with 100 μM alizarin and 0.005 M of one of the buffers NH_4Cl/NH_4OH, acetic acid/acetate, HEPPSO or MES. pH adjustment was made with KOH. 1.0 mL of chloroform was added to each solution and the absorbance at the isosbestic point (506 nm) of the aqueous phase measured after vigorous shaking. The percentage of alizarin extracted was determined by comparison with a control in which no solvent was added.

The effect of ionic strength on the extraction was examined in a similar manner. A range of samples were prepared, all containing alizarin and variable amounts of KCl. As shown in Fig. 6.7 extraction was assisted by the presence of salt and a standard concentration of 0.1 M KCl in reactor R2 was used.

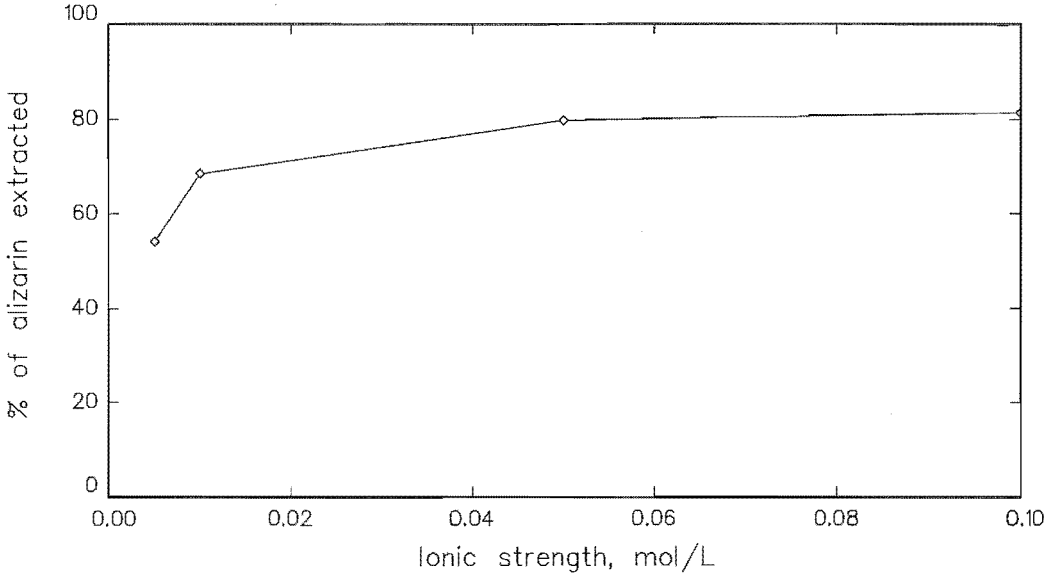

Figure 6.7. Variation in extraction efficiency with ionic strength. 10 mL solutions were prepared with 100 μM alizarin, 0.005 M acetic acid and variable amounts of KCl. The pH was adjusted to 5.5 with KOH. 1.0 mL of chloroform was added to each solution and the absorbance of the aqueous phase was measured at the absorbance maximum of alizarin at pH 5.5 (434 nm) after vigorous shaking. The percentage extraction was determined by comparison with a control in which no solvent was added.

The length of tubing in reactor R2 was varied in order to determine the amount required for complete extraction of alizarin. Again the manifold was diverted at the point where the tubing enters the detector and samples were collected for various tubing lengths. As shown in Fig. 6.8 100 cm of tubing gave 95% extraction of alizarin. This length was adopted in the standard procedure.

The effect of the solvent flow rate on the extraction efficiency was examined. The manifold was diverted at the point where the tubing enters the detector (the end of reaction coil R3) and samples were collected for different solvent flow rates. The residue of alizarin present in these samples was measured spectrophotometrically. No significant variation in the efficiency of extraction was observed (data not shown) for all flow rates examined (0.1 to 0.8 mL per minute).

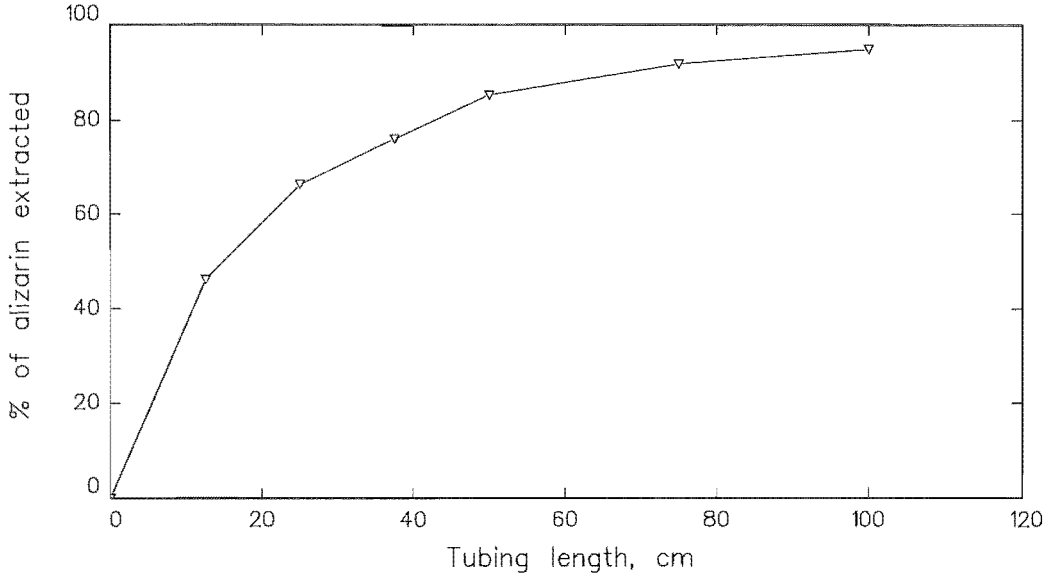

Figure 6.8. Variation in extraction efficiency with tubing length in reactor R2. Samples were obtained from Manifold 6.3 at the point where the manifold enters the detector and the residual alizarin measured spectrophotometrically.

From these observations it appears that alizarin is not significantly extracted into the segments of solvent that flow through the extraction coil. Instead it is predicted that the bulk of the extraction occurs into the film of the solvent which coats the walls of the tubing (as observed by Lucy and Yeung (1994)), hence the dependence of the extraction efficiency on the tubing length illustrated in Fig. 6.8.

6.3.2-C OPTIMISATION OF COIL R3. In this reaction coil an adjustment is made to the pH of the aqueous stream exiting the phase separator before it reaches the detector. This is necessary because the Al-bound alizarin is in a colloidal form at pH 5 and not electroactive. This reaction coil was optimised with respect to the final pH attained at the detector.

The pH at the detector was varied by flowing different concentrations of KOH in the alkali line of the manifold. Figure 6.9 shows hydrodynamic voltammograms generated with Manifold 6.3 at pH 9.1 and 12.6 (pH was measured at the detector).

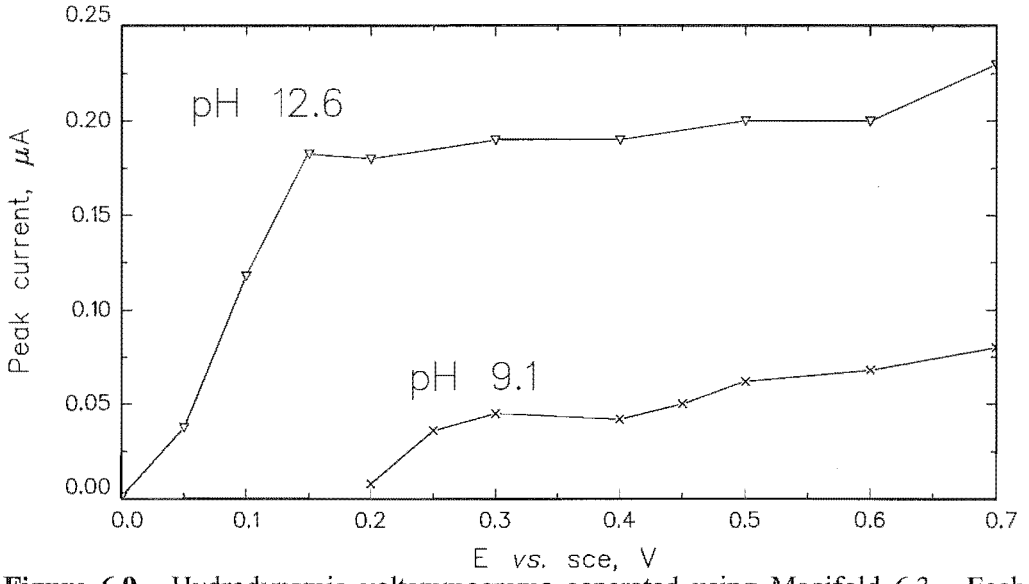

Figure 6.9. Hydrodynamic voltammograms generated using Manifold 6.3. Each point gives the peak current arising from an injection of 30 μM Al.
(X) pH 9.1 (at the detector) (▽) pH 12.6 (at the detector)

The potential for oxidation of free alizarin moves to lower potentials with increasing pH, with the $E_{1/2}$ value moving from 0.23 V at pH 9.1 to 0.10 V at pH 12.6.

At the lower pH the currents for oxidation of free alizarin are smaller. It may be expected that a significant proportion of the alizarin remains coordinated to Al at pH 9.1 and is electroinactive. Assuming similar oxidative behaviour to DASA (Chapter 4, section 4.2.5) alizarin complexes of Al would not be oxidised at potentials below *ca.* 0.8 V.

At pH 12.6 all alizarin should be dissociated from Al and be electroactive at the lower potentials characteristic of free ligand oxidation. At this pH all Al will form the aluminate ion, $Al(OH)_4^-$. A pH of 12.6 at the detector was adopted in the standard procedure as the greater currents gave improved sensitivity and lower potentials could be applied.

6.3.2-D ANALYTICAL PERFORMANCE OF SOLVENT EXTRACTION (MANIFOLD 6.3).

Fig. 6.10 compares the response obtained for identical injections of Al into Manifold 6.3 (solvent extraction) (trace B) with that obtained with Manifold 6.2 (no solvent extraction) (trace A).

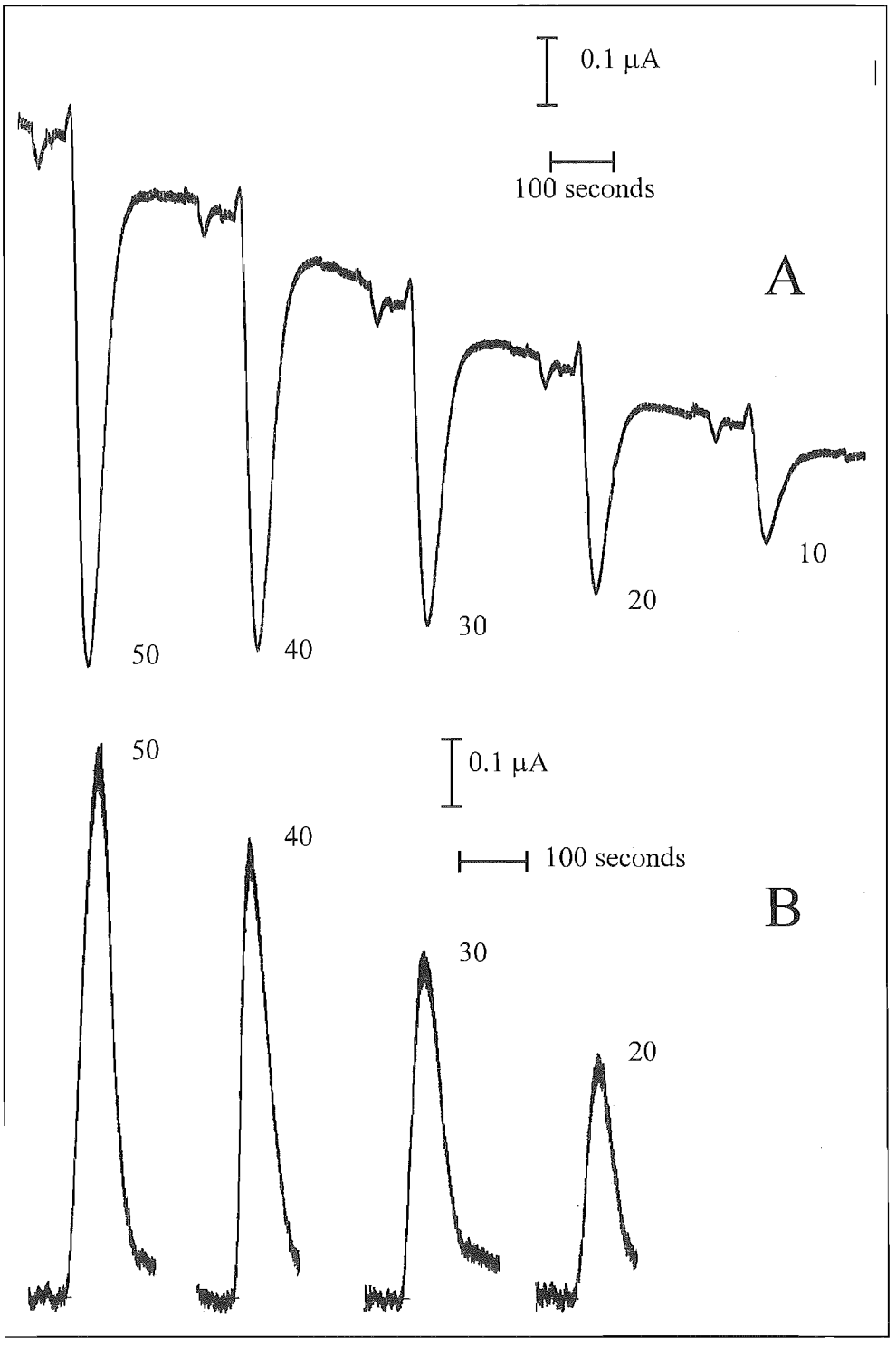

Figure 6.10. Comparison of FIA traces for A) Manifold 6.2 and B) Manifold 6.3. Figures give the concentrations (μM) of Al injected. Monitoring potential = 0.3 V in both cases.

The most obvious difference is that with solvent extraction the signals appear as positive anodic peaks of increasing oxidation current while without solvent extraction the peaks are in the cathodic direction, indicating a decrease in oxidation current. This is as expected because the solvent is physically removing all free alizarin from the analysis stream, leaving only Al-bound alizarin to be detected (after decomposition of the complex). In the absence of solvent extraction it is the free alizarin which is being continuously monitored. The decrease in current reflects a decrease in the concentration of free ligand as it becomes bound to Al.

The susceptibility of the system to electrode fouling was tested by making repeat injections of a 30 μM Al standard over the course of several hours. In Fig. 6.11 a comparison of the performance of Manifolds 6.2 and 6.3 is illustrated. The detection potential for Manifold 6.2 is 0.3 V and for Manifold 6.3 is 0.15 V. This reflects the shift in ligand oxidation potential with the increase in pH (from 8.9 to 12.6).

Manifold 6.2 (Fig. 6.11, × data) shows a rapid decrease in response, typical of a system which is highly susceptible to electrode fouling. With the removal of free ligand by solvent extraction (Fig. 6.11 □ data) there is a considerable improvement in the stability of the response, with an approximately constant and gradual decay with time.

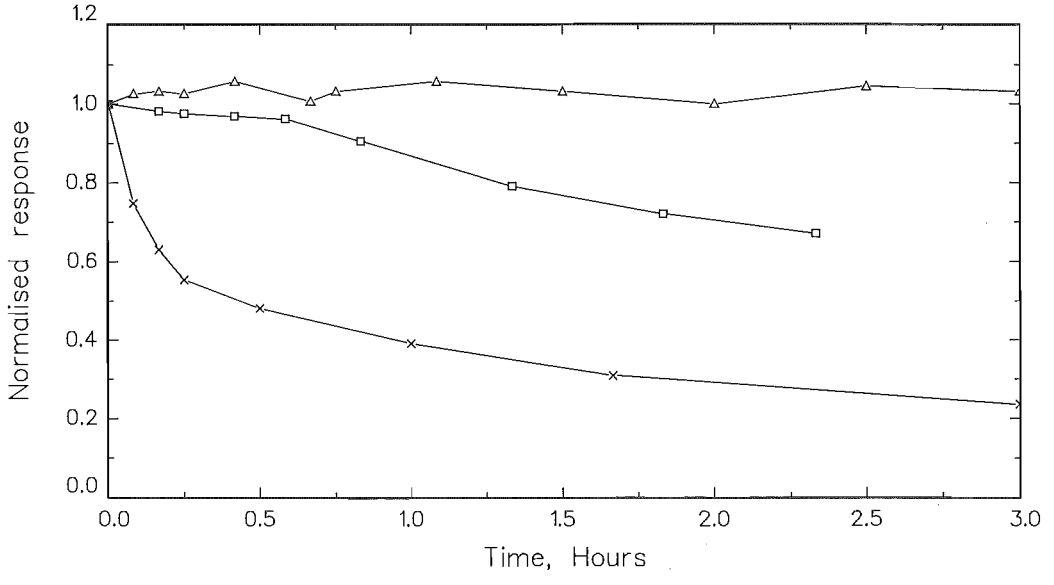

Figure 6.11. Response - time curves for Manifolds 6.2 and 6.3. Each curve was normalised to the value at the start of the experiment. Repeat injections of 30μM Al were made.
(×) Manifold 6.2 (no solvent extraction), working electrode potential = 0.3 V.
(□) Manifold 6.3 (solvent extraction), working electrode potential = 0.15 V.
(△) Manifold 6.3 (solvent extraction), working electrode potential = 0.15 V, electrochemical cleaning before each injection.

The most stable response was observed when solvent extraction was combined with electrochemical cleaning of the electrode surface (Fig. 6.11, Δ data). The response was stable for a period of at least three hours, showing only the random variability that is typical of the 3-5% RSD observed for the technique (see below).

With use of electrochemical cleaning before each analysis the analysis time was extended to approx. 4 minutes per sample, allowing a sampling frequency of 15 analyses per hour.

Repeat injections (n = 7) of a 10 μM Al standard into the solvent extraction system gave an RSD of 5.0%, a limit of detection (2σ) of 1.0 μM Al and the bottom of the linear working range (10σ) as 5 μM Al. At the top of the linear working range, 50 μM Al, the RSD value was 3.5% (n = 7). A calibration graph is illustrated in Fig. 6.12.

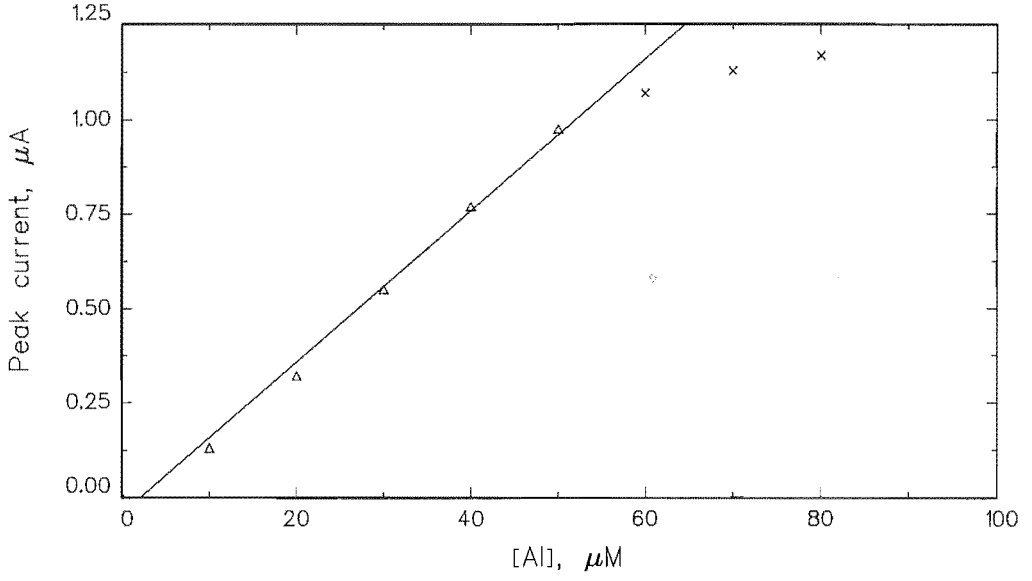

Figure 6.12. Calibration graph for Manifold 6.2.

The calibration graph deviates from linearity above 50 μM Al. This concentration is half that of the ligand as it is pumped into reaction coil R1 (100 μM). On the basis of speciation data for Al-DASA complexes (Chapter 3) a 1:2 Al:alizarin complex is predicted. Hence quantitative formation of the complex cannot occur when the Al concentration rises above 50 μM.

6.4 DISCUSSION.

6.4.1 USE OF PHENYL-BORONIC ACID AS A GUARD REAGENT.

Coordination of 4-ncat by phenyl-boronic acid greatly stabilises the ligand towards oxidation. This is indicative of the strong covalent bonds which are likely to be formed by boron with the catecholate oxygens of 4-ncat.

For the proper function of a guard reagent the reaction with the ligand, 4-ncat, must proceed quantitatively, i.e. there must be no free 4-ncat available for oxidation at the electrode surface. This means that a considerable excess of the guard reagent must be used. It was found that such an excess leads to the stripping of ligand out of the analytical complex formed with Al.

Al is a moderately inert metal ion. Its rate of inner sphere water exchange places it in the middle of the diagram reproduced in Fig. 6.13. This makes it more inert than Fe^{3+} or Cu^{2+} but still labile when compared with Cr^{3+} or Ru^{3+} for example.

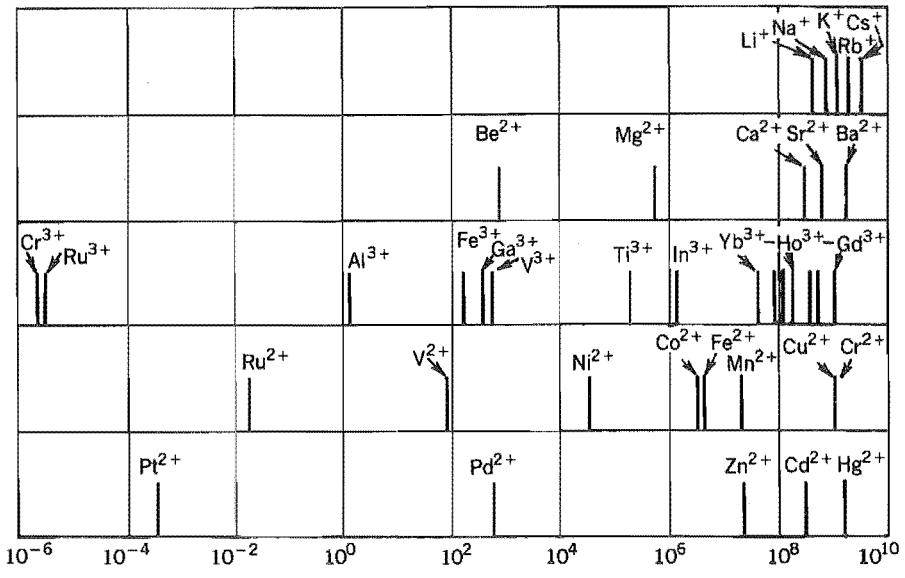

Figure 6.13. Characteristic rate constants (s^{-1}) for substitution of inner-sphere water molecules on various metal ions, reproduced from Cotton and Wilkinson (1989).

The system constructed for Manifold 6.1 exploits this relative inertness. A stream containing a mixture of both free and Al-bound 4-ncat is combined with phenyl-boronic acid. Amperometric measurement is performed within the minimum possible time after the confluence so that Al-bound 4-ncat may be directly analysed while free 4-ncat has been rendered electroinactive by the guard reagent. While minimising the contact time, sufficient time must be allowed for efficient mixing of the carrier and guard reagent

streams. Efficient mixing is especially important for systems with electrochemical detection since even a variation in ionic strength may give a response. Also the amperometric detector is sensitive to a very small volume of the analysis stream as it ejects from a capillary and strikes the working electrode surface. There is less averaging of heterogeneous regions than there is in, for example, spectrophotometric flow cells where the detector contains a relatively large volume of the analysis stream.

So a reasonably long mixing time is required and yet the mixing time is too long in the system developed here. It allows the guard reagent to strip a large part of the ligand which is bound to Al. Further development of this system would require the introduction of a new mixing system which gives complete and rapid mixing. Use of a co-axial jet-mixer (after Scampavia *et al.* (1995)) gave no improvement. This may be because the literature design incorporated extremely fine fused silica capillaries which were not available for the mixer used here.

A second problem encountered with the use of phenyl-boronic acid was severe electrode fouling, causing complete electrode deactivation within half an hour of operation. This was clearly a case of the cure being worse than the complaint. It is likely that this undesirable property derives from the phenyl group as this may be expected to adsorb strongly at the glassy carbon surface of the working electrode. Boronic acid, which lacks the phenyl functional group, did not show any electrode fouling behaviour but did not show promising behaviour as a guard reagent when incorporated into the manifold.

Nonetheless phenyl-boronic acid does illustrate the useful coordination and voltammetric properties of boronic compounds. It is possible that a different derivative may retain these properties while not showing any propensity for electrode fouling.

6.4.2 SOLVENT EXTRACTION.

The ligand alizarin is subject to a range of chemical and physical processes in each of the reactor coils of Manifold 6.2. Table 6.1 predicts the species of both free and Al-bound alizarin that are likely to be formed in each coil. These predictions are made by comparison with the solution chemistry of DASA (sulfonated alizarin) which has been investigated in Chapter 3.

Table 6.1 Predicted species of alizarin in the various reaction coils of Manifold 6.2. L^{2-} represents the deprotonated ligand, alizarin^{2-}.

	R1	R2	R3
pH	8.9	5.0	12.6
Free alizarin	$[HL]^-$	$[H_2L]^0$	$[L]^{2-}$
Al complex	$[Al_2L_4(OH)_2]^{4-}$	$[AlL_2]^-$	none formed

At pH 8.9, in coil R1, alizarin is deprotonated and therefore soluble and yet the pH is not so high as to prevent coordination of Al to the ligand. A drop in pH to 5.0 in coil R2 protonates the free ligand so that it becomes nonionic, precipitates from the aqueous phase, and is readily removed by solvent extraction.

Interestingly, solutions containing Al-bound alizarin at pH 8.9 also formed precipitates when the pH was lowered to 5.0. These precipitates were distinguishable from the precipitates of alizarin formed in the absence of Al in that they were orange not yellow and were not soluble in chloroform. It is likely that precipitation of the analytical complex in the extraction coil (R2) may assist in preventing its re-equilibration and dissociation when free ligand is removed by solvent extraction.

In the final reaction coil a highly alkaline pH is used. This ensures that all alizarin species are made soluble. Also all Al-bound alizarin is dissociated so that it may be analysed amperometrically at the lower applied potential at which the free ligand is electroactive.

Use of on-line solvent extraction has allowed the separate amperometric analysis of Al-bound alizarin although, ironically, the ligand is no longer bound to Al by the time it reaches the detector. This has considerably reduced the amount of oxidative electrolysis at the amperometric detector, with the expected improvement in detector stability. Complete detector stability was only achieved when the solvent extraction manifold was combined with electrochemical cleaning of the electrode surface.

The electrochemical cleaning protocol was based on that described by Anjo *et al.* (1989). It involves holding the working electrode at a large positive potential while immersed in a strongly alkaline solution. As discussed in Chapter 4, section 4.3.1, this form of electrochemical treatment will produce a fresh carbon surface carrying little more than a monolayer of phenol and quinone -like functional groups. Many of the phenolic groups will be deprotonated and anionic. Evidently alizarin and/or its oxidation products do not readily adsorb at this surface. The ability to perform the electrochemical cleaning step is an advantage of the use of a highly alkaline pH in reaction coil R3.

A limitation of the method is the short linear working range (5-50 μM Al) and the high detection limit (5 μM Al). It would be most useful if this range could be extended to lower concentrations. This would involve reducing the baseline noise which appears to come from the particular peristaltic pump used. This pump was the most suitable of those available for use with the five line manifold.

The contact time between the injected sample and the reagent stream is 30 seconds at pH 8.9. The system would be unsuitable for the direct measurement of reactive (toxic) Al in natural samples since there would be considerable 'speciation shock' to samples within that 30 seconds. During this time an unpredictable proportion of the organically-complexed species of Al would dissociate and become included in the analysis. Inclusion of an oxine column in the manifold as described in Chapter 5 would give a predictable fractionation of Al species and eliminate any potential interferrents. It would also allow modification of the linear working range of the method by simply changing the volume of sample injected.

6.5 CONCLUSION.

The FIA manifolds developed in this chapter attempt to address the problem of electrode fouling which is a feature of conventional amperometric analysis of Al.

When free ligand may be eliminated, either by making it electroinactive or by physical removal then metal-bound ligand may be directly measured, significantly reducing the total amount of anodic current to be passed.

This is shown most clearly by the phenyl-boronic guard reagent system. After scavenging of the free ligand by the guard reagent an oxidation peak appears which may be assigned to the direct oxidation of the Al-4-ncat complex.

Some problems remain unresolved in the guard reagent system. A chemical derivate of phenyl-boronic acid which retains its useful properties yet does not cause electrode fouling is required. Also a more rapid on-line mixer is needed.

The solvent extraction system was the most successful in eliminating electrode fouling. By only measuring that ligand which is associated with the analyte the oxidative electrolysis load at the detector was substantially reduced with a consequent improvement in the stability of the electrode response. This supports the initial conjecture that it is the practise of constantly oxidising the ligand (which is in excess of the analyte in conventional amperometric analysis) which leads to problems with electrode fouling.

The solvent extraction system gives a stable electrode response over a period of several hours and might therefore be suitable for automation or on-line process monitoring. Inclusion of the oxine column as in Chapter 5 would allow measurement of reactive Al and give the technique a more flexible linear working range.

Problems with the solvent extraction system are that it is complex by comparison with conventional amperometric analysis (ie compare Manifold 6.3 with Manifold 6.2), and uses a toxic organo-chlorine solvent, chloroform. Complete stability of the system was only achieved by the use of electrochemical cleaning of the amperometric detector. This has the disadvantage of reducing sample throughput.

Chapter 7

SCREEN PRINTED ELECTRODES FOR ALUMINIUM ANALYSIS

7.1 INTRODUCTION.

7.1.1 Chemically Modified Electrodes.

Chemically modified electrodes (CMEs) are electrodes which have been deliberately treated with some reagent, having desirable properties, so as to take on the properties of the reagent. Conventionally the electrode materials used in electrochemistry have been limited to carbon, mercury and various noble metals. These materials are conductive and provide a useful potential window for analysis. Unfortunately there is a relatively small range of analytes that may be measured directly at such materials. Chemical modification of electrodes allows measurement of a much wider range of analytes. Sensitivity and selectivity may be enhanced.

Chemical modification has been achieved in a number of ways, such as inclusion of a modifier into the electrode material, covalent attachment to the electrode surface and entrapment within polymeric coatings. This is a very active area of research. Three examples are given here. Baldwin *et al.* (1986) have incorporated the ligand dimethylglyoxime into a carbon paste electrode, producing an electrode sensitive to Ni^{2+}. The ligand preconcentrates nickel before its voltammetric measurement. Downard *et al.* (1995) attached *p*-phenylacetate groups by a diazonium salt coupling procedure to glassy carbon electrodes conferring resistance to fouling and interference by ascorbic acid and enhancing the sensitivity to dopamine. Cha *et al.* (1993) have used ion exchange to incorporate nicotinic acid into a polycationic film of electropolymerised $[Ru(bpy)_3]^{2+}$. The resulting electrodes were used for the voltammetric determination of mercury.

7.1.2 Screen Printed Electrodes.

Screen printing of thick-film circuits is a well established technology, developed by the electronics industry for the mass production of miniaturised electrical

circuits. In recent years electroanalytical chemists have taken up this technology to produce electrochemical sensors [reviewed by Galan-Vidal *et al.*, 1995; Hart and Wring, 1994]. Use of this technology allows sensors to be produced in high volume at low cost, with high reproducibility and in miniaturised form.

Undoubtedly the most successful example is the development and commercialisation of the ExacTech disposable glucose sensor, [Green and Hilditch, 1991a & 1991b], for the personal monitoring of whole blood glucose concentrations in diabetics [Mathews *et al.*, 1987]. Screen printing technology is used to deposit electrode substrates and enzyme reagents onto an inert poly(vinyl chloride) (PVC) support material. Individual electrode strips are inserted into a small measuring device that provides the applied potential and converts current response information to a digital glucose concentration value.

7.1.3 SCREEN PRINTED ELECTRODES FOR METAL ANALYSIS.

One of the first approaches used in developing screen-printed metal sensors was to apply the well known technique of anodic stripping voltammetry, (ASV) [see Wang and Tian 1992; Wang and Tian, 1993, Wang *et al.*, 1993, Wang, 1994; Seddon *et al.*, 1994; Brainina and Bond, 1995]. In an early example Wang and Tian (1992) showed that stripping analysis may be performed at mercury-coated screen printed carbon electrodes. Conventional ASV and the more novel potentiometric stripping analysis (PSA) was used to measure lead down to 30 ppt (parts per trillion). A number of advantages have been identified which would make the electrodes suitable for decentralised (clinical, industrial or environmental) testing. In particular deoxygenation and stirring of samples was not necessary reducing the amount of equipment that must be carried into the field. The low cost of the electrodes permitted their disposal after a single use.

Unfortunately there is only a limited number of elements that may be analysed by ASV. Another disadvantage is the safety considerations necessary when taking mercury containing devices out of the laboratory. Fortunately other strategies have been developed for the sensitive electroanalysis of metals. They have been accumulated at sensors by ion exchange and by association with coordinating ligands.

Neuhold *et al.* (1995b) employed a screen printed electrode (SPE) modified with the cation-exchange resin Dowex 50W-X8. The electrode material was prepared by adding finely ground resin to a commercial carbon ink prior to printing. Copper was preconcentrated, at open circuit, prior to reduction and measurement by stripping analysis over the range 0.5 to 110 ppb. The same research group has also successfully incorporated an anion exchange material into SPEs for the measurement of nitrite [Neuhold *et al.*, 1995a].

Recently metal sensors have been presented which utilise coordinating ligands incorporated into SPEs. Somasundrum and Bannister (1993) produced graphite SPEs containing the ligand bis-cyclohexanone oxaldihydrazone. An oxidation wave at +0.235 V (*vs.* SCE), assigned to reaction of the copper-ligand complex, was used to amperometrically measure copper over the range 1.9 to 19 ppm.

Wang *et al.* (1996) have described a screen printed sensor using the ligand dimethylglyoxime to preconcentrate nickel. The ligand was incorporated by simply mixing it into the ink before printing. After accumulation nickel was measured by differential pulse voltammetry giving a peak at -1.1 V (vs Ag/AgCl). A working range of 5 to 320 ppb was reported and the electrodes could be re-used after a cleaning step in 0.1 M HCl.

These last two examples illustrate the potential of using coordination chemistry in the development of metal sensors. Chelating ligands present the possibility that new patterns of reactivity may be exploited for the accumulation of metal ions as well as the possibility that ligand-based redox processes may be used for analysis.

7.1.4 Al MEASUREMENTS IN THE FIELD.

The greater number of techniques for the quantitation of Al are reliant on large delicate instruments which are confined to laboratories (eg spectrophotometry, AAS, ICP-OES/MS). For environmental samples this enforces a separation in time and location between sampling and measurement. There are established procedures for sampling and storage of natural waters containing Al prior to analysis. These have been reviewed by Bloom and Erich (1989). However these authors comment that preventing the introduction of artefacts into samples is not simple and involves consideration of many factors. At the low levels of Al characteristic of most natural waters, sample contamination is a major analytical problem. Changes in pH value, because of microbial activity or loss of dissolved

CO_2, can cause significant changes in Al chemistry. The presence (or absence after filtration) of suspended solids and/or colloidal material may lead to adsorption or release of Al and change its fractionation between different chemical species during storage. The development of a field-applicable method for Al would therefore be a considerable advantage.

Electrochemical methods are suitable candidates for field measurements, being simple, rapid, portable and providing a response easily converted into digital data for information handling and storage.

7.1.5 TWO *VERSUS* THREE ELECTRODE CELLS FOR A FIELD SENSOR.

Figure 7.1 illustrates a 2 and a 3 electrode electrochemical cell. The 2 electrode cell lacks a reference electrode. In Bond's (1980) seminal book on polarographic analysis the author strongly recommends the use of 3 electrode cells [see pp.47-53 and pp.67] since they allow greater flexibility in the location of the counter/reference electrode relative to the working electrode and they minimise the effect of 'IR drop'.

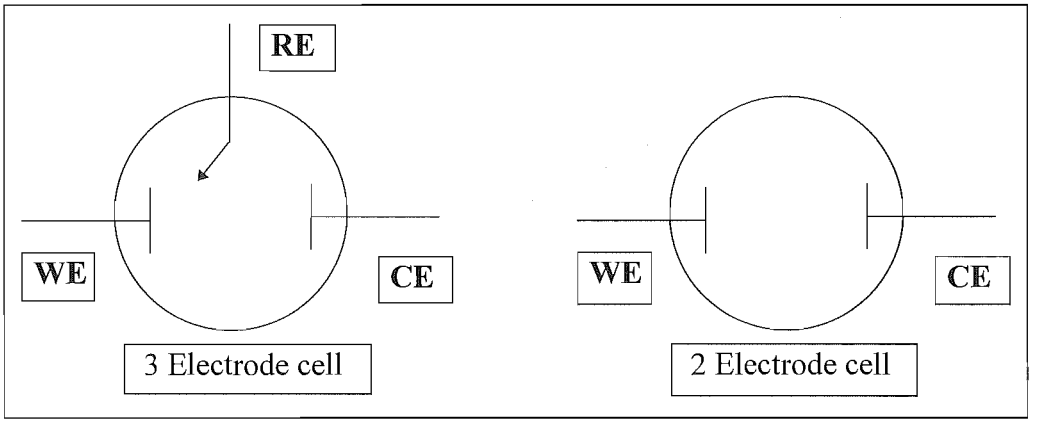

Figure 7.1 2 and 3 electrode cells. **WE** = working electrode, **CE** = counter electrode, **RE** = reference electrode.

IR drop arises where the combination of the current in an electrochemical cell (I) and the cell resistance (R) combine by Ohm's law, eqn 7.1 (overleaf), to form a significant potential drop. This 'potential drop' lowers the potential applied to the working electrode, causing significant errors in electrochemical experiments (producing for example non-linear potential sweeps).

Ohm's Law: $V = I * R$ (7.1)

V = potential, (Volts)
I = current, (Amperes)
R = resistance, (Ohms)

In the 3 electrode case having a separate reference electrode overcomes this problem since virtually no current passes between this electrode and the working electrode. The bulk of the current passes between the counter (or auxiliary) electrode and the working electrode.

In a 2 electrode system where there is just the counter electrode in addition to the working electrode the current and potential cannot be separated, causing an IR drop. This can often be ignored however in applications where the currents are low (eg below 1μA) and where the cell resistance is negligible.

Operation of a 3 electrode cell requires the advanced electronics of a potentiostat. Although these are produced commercially for use in the field the resulting instruments are heavy, cumbersome and relatively expensive. For example Chemtronics Lt. offer an instrument which weighs 9 kg and measures 27x37x32 cm.

Operation of a 2 electrode cell simply requires a variable voltage source and measurement of currents in the nA-μA range. Use of a potentiostat may be replaced with simpler electronics and the cell may be analysed directly from a laptop computer.

In this work the initial development of SPEs was conducted using 3 electrode electrochemical cells. Then, as the SPEs were modified towards being sensors suitable for field use, 2 electrode cells were used. This required that the factors contributing to IR drop were minimised.

7.1.6 FRACTIONATION OF Al.

As in Chapter 5 the oxine column has been used for the fractionation of Al species. In this section it is used in a batch mode, i.e. samples are manually injected across the column and the column eluent is collected into a flask for later analysis. This differs from the original development of the oxine column by Simpson *et al.* (1997) where it was mounted in a FIA manifold. Samples were injected into the carrier stream which carried them to the column. The elution stream from the column was merged on-line with a chromophore to allow spectrophotometric detection.

Using the column in batch mode may change the contact time between the sample and the chelating gel, possibly altering the 'aggressiveness' of the column and changing the fraction of Al species retained by the column. This was investigated.

7.1.7 THE ALIZARIN CME.

Downard *et al.* (1991) have reported the development of a chemically modified electrode (CME) for the detection of Al. By dip-coating a high-density graphite electrode with alizarin they were able to measure Al in the range $1.5x10^{-7}$ M to $1.0\ x10^{-5}$ M by differential pulse voltammetry (DPV). This measurement utilised a ligand-based oxidation wave. Use of positive oxidising potentials meant that de-oxygenation was not required.

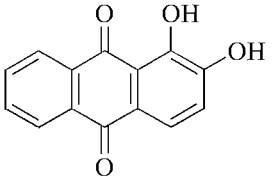

Alizarin

Unfortunately the oxidation of alizarin is irreversible. Thus each modified surface was single use, requiring manual regeneration before performing a measurement. This ligand appears promising for incorporation into a screen printed electrode since modification may be affected during manufacture and the resulting electrodes may be thrown away after use.

This chapter describes the fabrication of alizarin modified SPEs. The performance of the SPEs is characterised and compared to the CME. Further development is undertaken towards use of the SPEs in the field as sensors for reactive (toxic) Al. This includes a pretreatment protocol with the oxine column and modifications to the electrodes to allow them to be scanned in the two electrode mode.

7.2 EXPERIMENTAL

7.2.1 SCREEN PRINTING.

The screen printing process has been described by Galan-Vidal *et al.*, (1995). The company Du Pont de Nemours (E.I. & Co.) Inc. [see references, (1970)] have produced a technical overview describing the process and containing a trouble shooting guide for overcoming the practical problems that may arise. Figure 7.2 illustrates the main steps in screen printing.

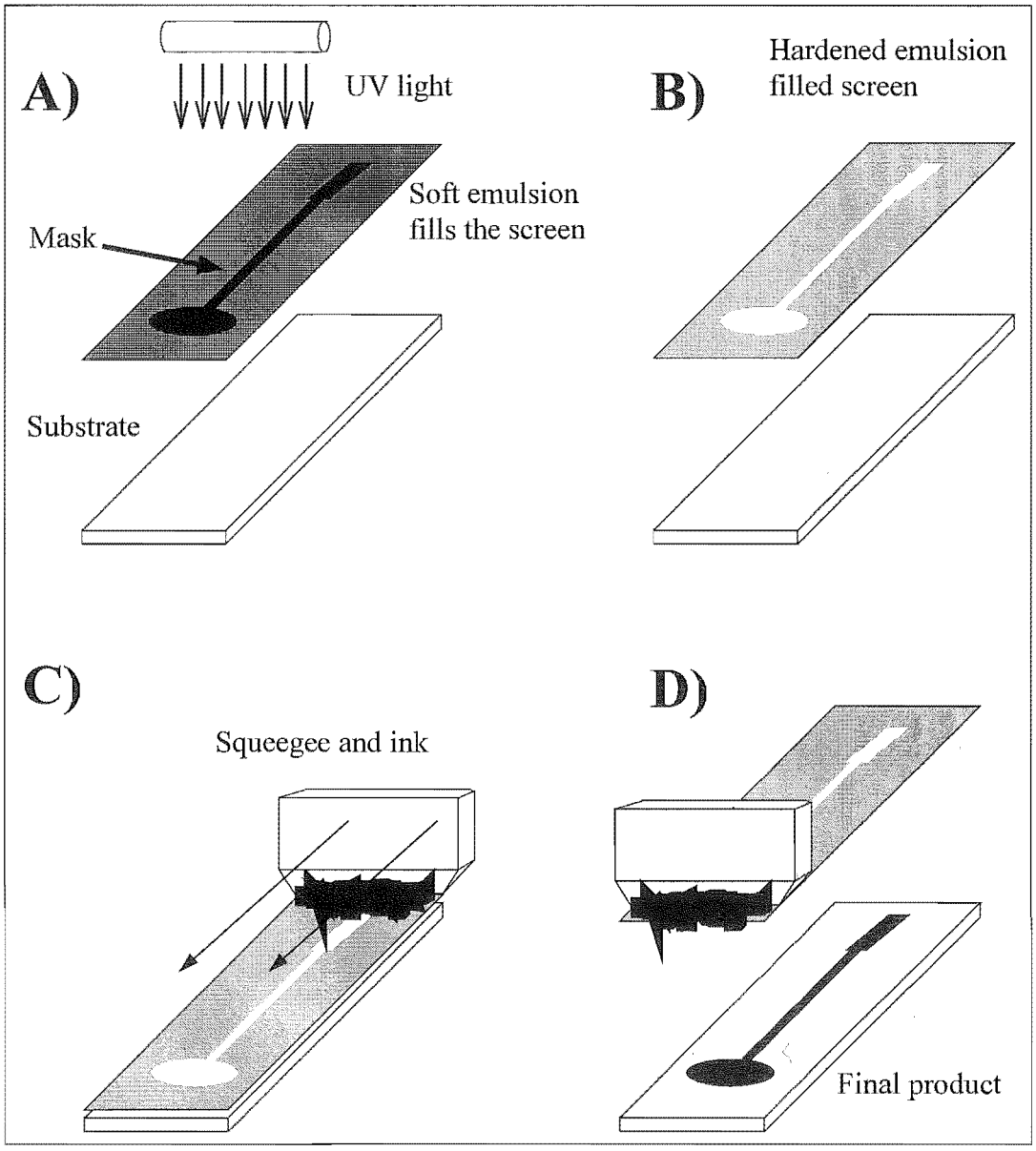

Figure 7.2 Screen printing. **A)** The desired image is photocopied onto transparent mylar and laid onto a sheet of light sensitive emulsion. This in turn is laid onto the screen and exposed. **B)** After exposure the emulsion hardens, filling up the screen pores and leaving gaps where the mask prevented exposure. **C)** A rubber squeegee is drawn across the screen, forcing ink through the gaps. **D)** The screen is lifted vertically from the substrate to reveal the desired pattern.

Clear PVC sheet (approx 0.5 mm thickness) was used as the printing substrate, cut into 100x50 mm rectangular pieces. In each print run 50 to 150 pieces of PVC substrate were printed. Each piece was printed with a pattern giving between 10 and 20 electrodes. Individual electrodes were cut free by hand with scissors immediately before use.

Screen printing was conducted using equipment in the Microelectronics laboratory of the Electrical and Electronic Engineering Department of the University of Canterbury.

A DEK model - 65 screen printer modified with a home-built compressed air ram for squeegee control was used. The printing inks used are described in Table 7.1. Alizarin was supplied by Sigma. Screens were nylon mesh, 196 counts/inch. All inks were dried at room temperature except the silver inks which were cured at 55°C for 2 hours. Cappilex 25 photocure emulsion was used (cured under a UV lamp). This was removed when necessary by soaking in bleach (5 % aqueous NaOCl). Blank areas around the edges of the screens were filled in with Ulano no. 60 screen filler as this material is less expensive than the cappilex emulsion.

Table 7.1 Inks utilised in the printing of SPEs. All abbreviations are manufacturers codes except EGME - Ethylene Glycol Monobutyl Ether, CAS no. [111-76-2].

Ink	Manufacturer	Code	Thinner	Clean up
Graphite	Acheson	E423-SS	EGME	EGME
Silver [a]	Electro-science Laboratories	ESL 1109-S or ESL 1112-S	ESL 402	EGME
Di-electric	Coates Lorilleux	Signwriting white DC7900	Retarder YK46-02	Ecowash YK26-00

[a] ESL 1112-S was the preferred ink and was used when available.

In the course of developing the alizarin modified SPE three distinct designs were used. These are referred to as the different marks, ie as mark (I), (II) and (III). The design of each of these is illustrated in Fig. 7.3. Table 7.2 describes the layers of each design. The mk. I SPEs are graphite SPEs modified with a pad of graphite/Alizarin printed over the working surface. The mk. II SPEs added to this design with an unmodified graphite strip as counter electrode and a silver strip as reference electrode, giving a printed 3 electrode electrochemical cell. In the mk. III design 2 electrode electrochemical cells

were produced by dispensing with the graphite counter electrode and the geometries of the remaining graphite/alizarin and silver electrodes were changed. The resistance of the working electrode was reduced by printing a strip of silver under the electrode.

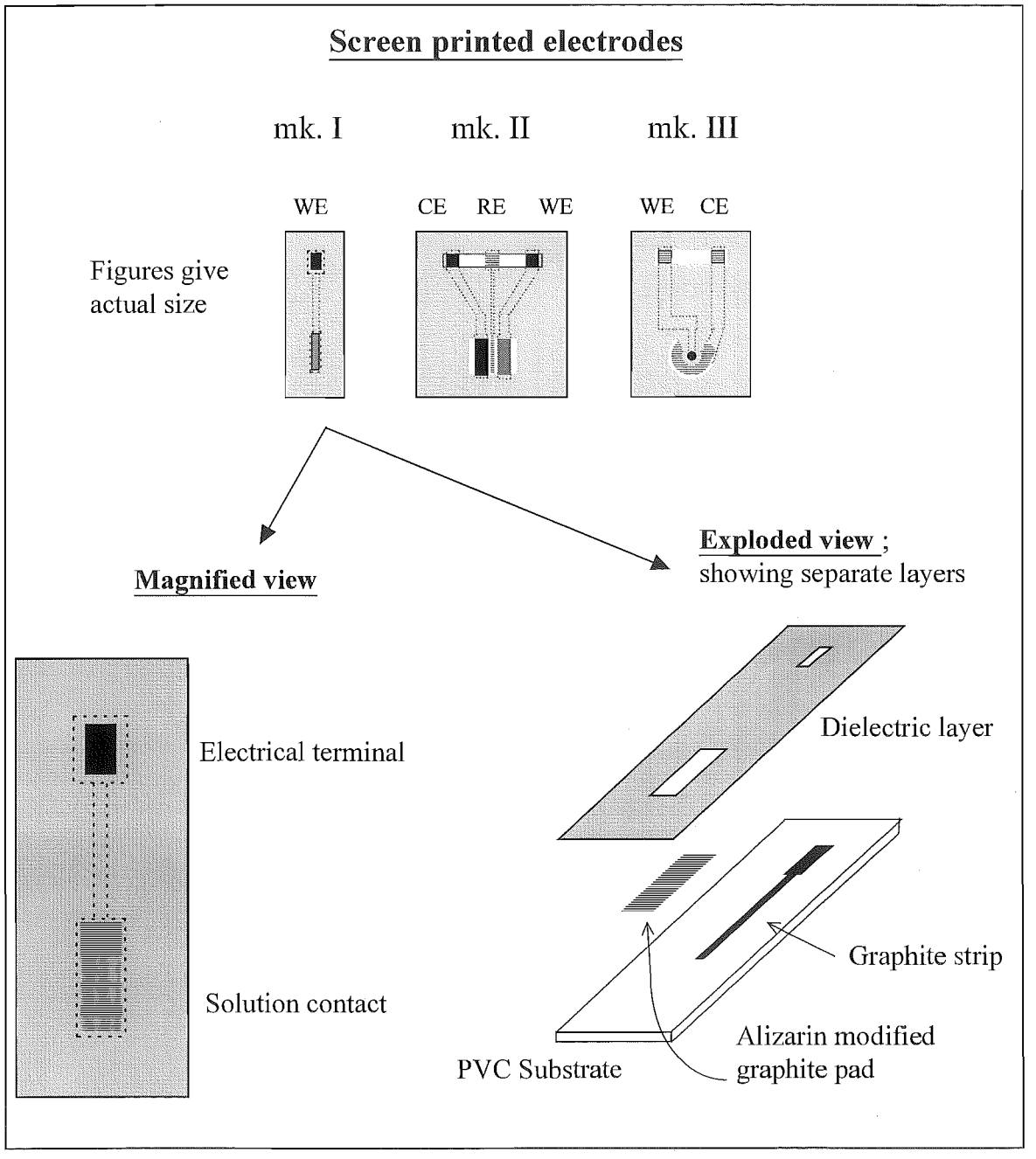

Figure 7.3 Standard and exploded views of the screen printed electrodes. 'Solution contact' indicates the end dipped into aqueous solution. An alligator clip made contact with the electrical terminal. The exploded view indicates the layered nature of screen printed electrodes.

Table 7.2 Function and ink composition of each layer of the various SPE designs.

SPE layer	function	layer	ink
MK I			
Layer 1	WE	graphite strip	20g E423SS + 2 mL EGME
Layer 2	WE modifier	alizarin modified graphite pad	50g E423SS + 5 mL EGME + 2.5g alizarin
Layer 3	insulating layer	vinyl shroud	30g DC7900 + 3 mL retarder
MK II			
Layer 1	WE + CE	2 graphite strips	20g E423SS + 2 mL EGME
Layer 2	RE	silver strip	11.6g ESL 1109-S + 0.7 mL EGME
Layer 3	WE modifier	alizarin modified graphite pad	10g E423SS+ 1.0 mL EGME + 0.5g alizarin
Layer 4	insulating layer	vinyl shroud	20g DC7900 + 2 mL retarder
MK III			
Layer 1	WE + CE	2 silver strips	5g ESL 1109-S + 0.5 mL ESL#402
Layer 2	WE modifier	alizarin modified graphite pad	10g E423SS + 1.0 mL EGME + 0.5g alizarin
Layer 3	insulating layer	vinyl shroud	20g DC7900 + 2 mL retarder

7.2.1-A STANDARD SPE ANALYSIS PROCEDURE. All measurements using SPEs were made with a new (previously unused) electrode.

Unless specifically stated otherwise the following procedure was used to analyse Al samples with the SPEs. The sample was combined with NH_4Cl/NH_3 buffer, pH 9.0± 0.2 (prepared from NH_4Cl and KOH, both analytical reagent (AR) grade, BDH, in triply distilled water (TDW)), in a volumetric flask and made to volume to give a final buffer concentration of 0.1 M. After standing for at least 2 minutes the buffered sample was contacted with the SPE (quiescent solution conditions) for 3 minutes before scanning. Scanning was performed using a PAR 174a potentiostat in DPV mode (ν = 10 mVs^{-1}, modulation amplitude = 25 mV, clock time = 0.5 s and initial potential = 0.2 V) using a Pt wire counter electrode and a saturated calomel reference electrode. The output was recorded using an *x-y* recorder (Graphtec WX 1200). Digital data for Figure 7.13 was acquired using a PAR 273a potentiostat in combination with the m270 software.

7.2.2 THE OXINE COLUMN.

An enlarged version of the oxine column as described in section 2.5.3 was used.

Solutions were prepared in triply distilled water using the following reagents; glacial acetic acid, ammonium chloride, potassium hydroxide, potassium chloride and tartaric acid, (all were AR grade, (BDH)). Malonic acid (pure) was supplied by Riedel de Haen, oxalic acid (AR grade) by Fissons and Chrome Azural S (CAS) by Aldrich, (65% dye content)

7.2.2-A - STANDARD COLUMN PROCEDURE. The following protocol was used to apply samples to the column in batch mode.

1. The column was cleaned by injecting 1.0 mL of 0.02 M KOH. This was followed by 1.0 mL of pH 4.9 acetate buffer, 0.05 M. Both solutions were adjusted to 0.1 M ionic strength with KCl.
2. Step **1.** was repeated.
3. The sample was injected onto the column. The syringe containing the sample was held in a clamp and pumped by placing a 2.2 kg iron weight upon it. This gave a fixed and reproducible flow rate. The sample was immediately followed by 1.0 mL of the acetate buffer described in step **1.** Both the sample and the following buffer were directed to waste.
4. The column was eluted by performing step **1.** Both the alkali and the following acetate buffer were retained in an appropriate volumetric flask (5-25 mL). Buffer was added and the solution made to volume (the analysis volume).

For solutions analysed spectrophotometrically the final buffer solution added in step 4 was a stock solution of 0.58 mM CAS (an Al sensitive chromophore, [Hawke and Powell, 1994; Hawke *et al.*, 1995]) in 1.25 M acetate buffer. The pH of this stock was adjusted to 4.2 with KOH and the ionic strength adjusted to 2.5 M with KCl. A spike 4% of the flask volume was added. The final pH was 4.9.

For solutions analysed with the SPEs the final buffer solution added in step 4 was a 0.2 M ammonium chloride buffer, pH 9.0. A spike 50% of the flask volume was added to give a final buffer concentration of 0.1 M.

7.2.2-B SYNTHETIC LIGAND SOLUTIONS - These solutions were prepared in 0.005 M acetate buffer, pH 4.5. No KCl was added. Ligands were added at least 2 minutes prior to Al which was introduced as a spike of the $AlCl_3$ stock described in Chapter 3, section 3.2.2. All solutions contained 30 μM Al and between 0 and 100 μM of the appropriate ligand. The pH of each solution was checked against a glass bulb pH meter (calibrated against freshly prepared NBS buffers [Vogel, 1961]), and in no case did it vary beyond 4.45 ± 0.05 pH. All solutions were equilibrated overnight prior to application to the oxine column.

7.3 RESULTS.

7.3.1 ALIZARIN MODIFIED SCREEN PRINTED ELECTRODES.

Figure 7.4 compares the response of the alizarin modified screen printed electrodes to the alizarin CME, as described by Downard et al. (1991). In both cases a large off-scale response for the free ligand is observed, E_{pa} = 0.3 V, followed by a peak at 0.6 V for Al-bound ligand. This indicates that the sensitivity to Al is retained by the SPEs. As for the CME, Al may be quantified by measuring the peak current for Al-bound ligand relative to a tangent.

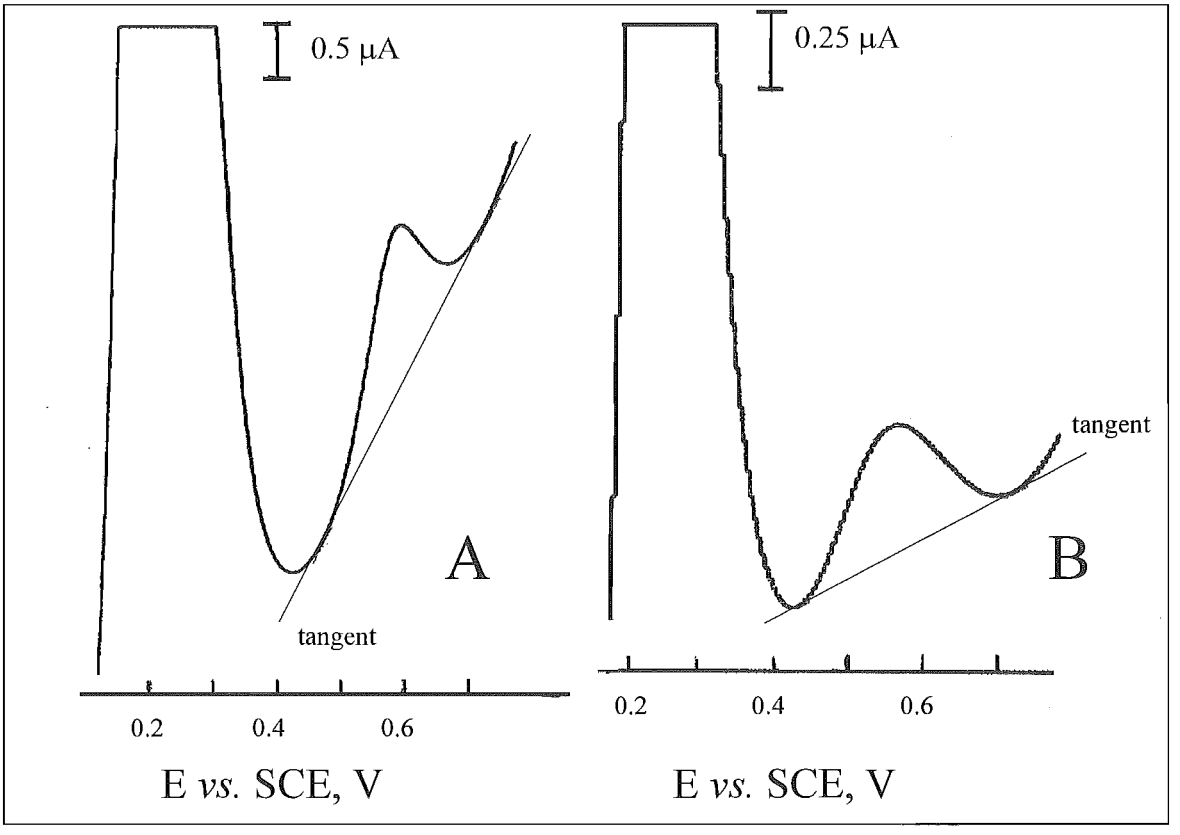

Figure 7.4 Differential pulse scans of A) the alizarin modified graphite CME and B) the alizarin modified SPE (mk. I). [Al] = 5μM. The standard analysis procedure was used. The CME was scanned after 1 minute of contact with the sample and the SPE after 3 minutes.

The effect of pH on the analysis was studied. As indicated in figure 7.5 the largest signal was obtained for pH 9.0 ± 0.2.

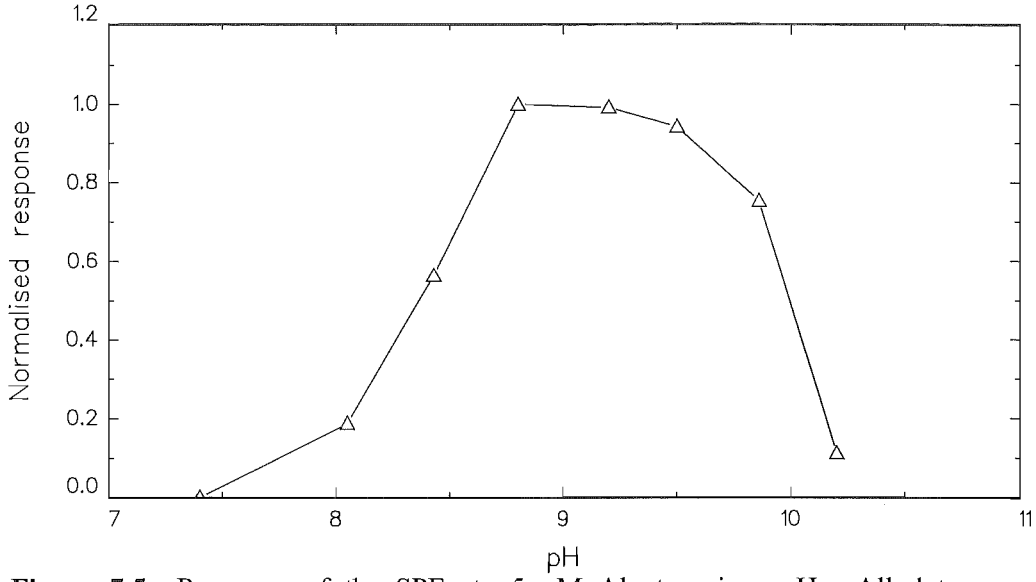

Figure 7.5 Response of the SPEs to 5 μM Al at various pH. All data were normalised to the value for pH 8.8. pH was adjusted by addition of KOH to NH_4Cl/NH_3 buffer. All other parameters were as described in the standard analysis procedure. Mk. I SPEs were used.

In order to produce consistent results it was observed that the contact time between the SPEs and the buffered Al sample must be strictly controlled. Figure 7.6 illustrates the effect of varying this parameter on the response for 5 μM Al. The response increases linearly with contact time (the linear regression fit is plotted). A standard contact time of 3 minutes was adopted as a compromise between sensitivity and speed of analysis.

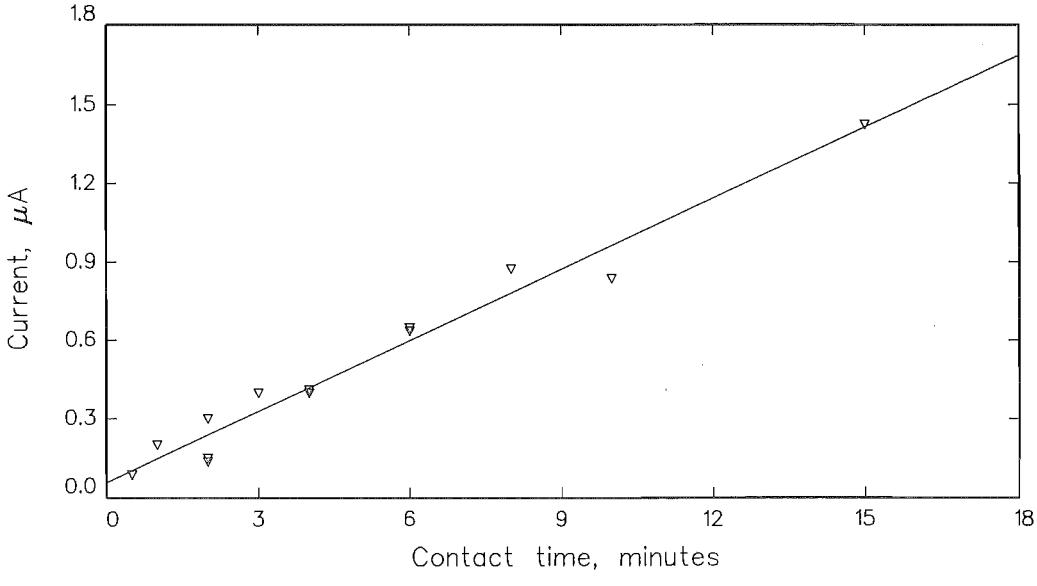

Figure 7.6 Effect of contact time on Al-alizarin peak height. Mk. I SPEs were analysed with the standard parameters. [Al] = 5 μM.

The reasons for the behaviour observed in Figure 7.6 were probed by performing linear sweep analyses at a range of sweep rates upon a solution containing 20 μM Al. The peak currents for the oxidation of both the free and Al-bound alizarin were recorded and are plotted in Figure 7.7 against the scan rate. The Al-alizarin peak currents were directly proportional to the scan rate while the free alizarin peak currents show a parabolic form indicative of a square root relationship with the scan rate. This was confirmed by replotting (not shown) the data against the square root of the scan rate.

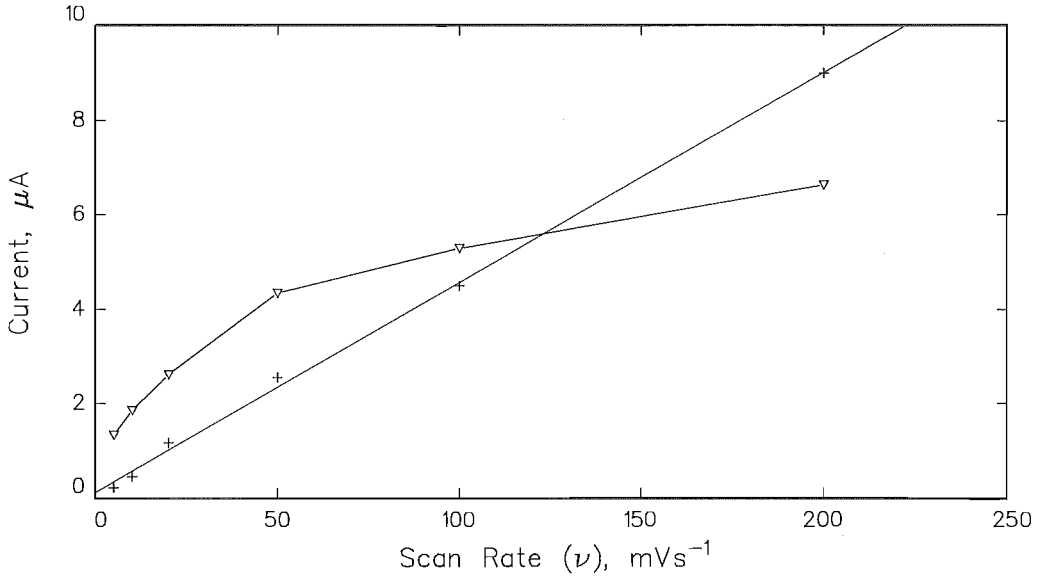

Figure 7.7 Peak currents for free alizarin (▽) and Al-bound alizarin (+) *vs.* linear sweep scan rate. Mk I SPEs were analysed in the standard manner except for a 5 minute contact time and use of the linear sweep waveform. [Al] = 20 μM.

Linear dependencies of peak current on scan rate and (scan rate)$^{1/2}$ are indicative of thin-layer and diffusion controlled behaviour respectively [Bard and Faulkner, 1980, see their equations 6.3.8 and 10.7.17]. Thus it appears that oxidation of uncoordinated alizarin proceeds with diffusion of a solution species to the electrode surface, that is, alizarin dissolves from the electrode surface. In contrast oxidation of Al-bound alizarin has the characteristics of a surface confined process suggesting that the complex precipitates onto the electrode surface (or that coordination occurs before alizarin has dissolved from the surface).

The possibility that stirring the sample during the contact with the SPEs might assist the accumulation of Al was investigated. For stirring times between 15 seconds and 5 minutes the response was constant and slightly greater (~20%) than that for an unstirred

solution. Evidently stirring does not significantly assist the accumulation of Al-bound alizarin at the electrode surface.

7.3.2 ANALYTICAL PERFORMANCE.

Figure 7.8 illustrates a calibration of the SPEs response to Al. A linear working range of 2-16 μM Al was observed. The relative standard deviation (RSD; σ), (n = 6) at 5 μM Al was 5% and at 1μM was 21%. This gave a detection limit of 0.42 μM (2σ at 1μM) and the bottom of the linear working range as 2 μM Al (5 times the detection limit).

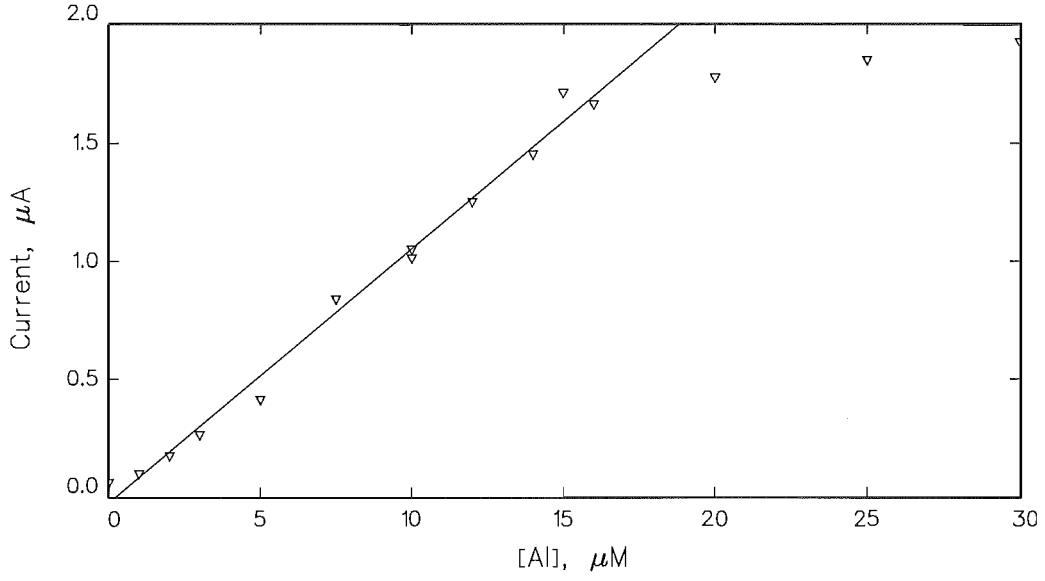

Figure 7.8 Calibration of the SPEs (mk. I). Analysis was performed using the standard analysis parameters. Al concentrations refer to the final concentration in the solution contacting the SPE. Data from 20 μM Al and above were excluded from the linear regression calculation.

7.3.3 PRINTED 3 ELECTRODE ELECTROCHEMICAL CELLS.

The mk. II SPEs contained a complete printed electrochemical cell (3 electrode). The individual electrodes were an alizarin modified graphite working electrode, a graphite counter electrode and a silver electrode to provide a Ag/AgCl reference electrode. Figure 7.9 shows scans of the printed 3 electrode strip in 5 μM Al and of an alizarin SPE in combination with conventional electrodes, ie saturated calomel reference and platinum wire counter electrodes respectively. The only significant difference is the positive potential shift expected [Bard and Faulkner, 1980] for the change in reference electrodes.

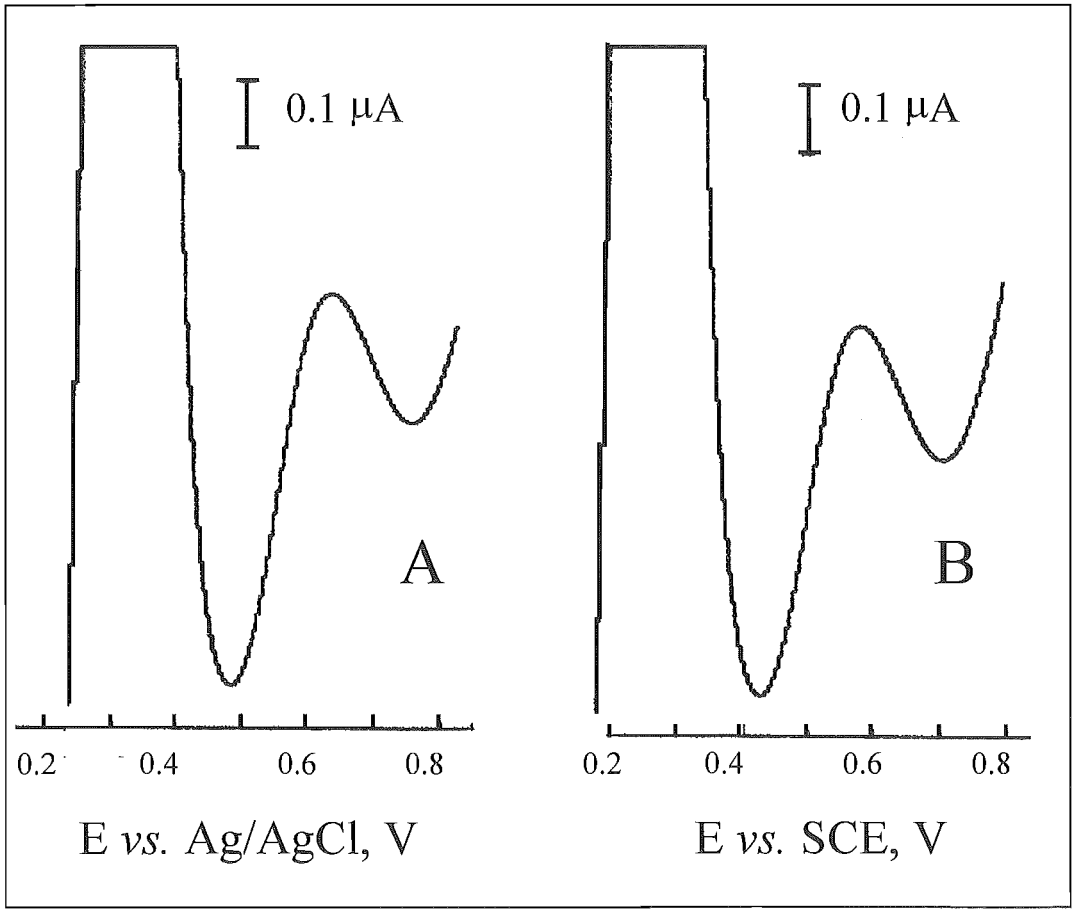

Figure 7.9 DPV scans of A) SPE Mk II, printed electrochemical cell and B) SPE, Mk I, in a conventional electrochemical cell (saturated calomel reference and platinum wire counter electrodes). The Al concentration was 5 μM. The standard parameters of section 7.2.1-A were used.

7.3.7 DEVELOPMENT OF TWO ELECTRODE SPES

In the development of SPEs that can be used in the 2 electrode mode the aim was to be able to obtain and process data using very simple instrumentation. Hence the characteristics of the electrodes were tested using only a DC ramp (linear sweep voltammetry or cyclic voltammetry). This waveform was generated using a potentiostat. For 2 electrode scans the reference electrode and counter electrode leads of the potentiostat were connected together.

Figure 7.10a shows a cyclic voltammetric sweep of the mk. I SPEs in 3 electrode mode (ie SPE working electrode and conventional counter (Pt wire) and reference (SCE) electrodes). This represents a benchmark for scans in the 2 electrode mode. In Figure 7.10b the same type of SPE is scanned in the 2 electrode mode using an unmodified graphite SPE as the counter electrode. Clearly there is a large IR drop factor present with the peak current being reduced and the peak shape flattened so that it is not easily distinguished from the background.

A reduction in this effect was gained by reducing the size of the working electrode and thereby reducing the current passed, Figure 7.10c. A mk. I SPE was used for the working electrode with the area reduced to 10% of the original electrode and the same counter electrode as for 7.10b. The peak for oxidation of Al-bound alizarin is sharper and has moved to a less positive potential with the reduction in IR drop.

In the next step SPEs of a new design, mk. III, were printed. A silver based ink was included in this new design. The manufacturers specifications for the resistivity of the graphite and silver inks is $< 50\ \Omega$/sq and $\leq 0.05\ \Omega$/sq respectively. Clearly the silver ink gives more conductive electrodes. In the mk. III SPEs it was used in the preparation of the counter electrodes. Graphite ink was retained for the working electrode with a silver track underlying the graphite to improve the conductivity. Care was taken to exclude silver from the surface of the working electrode as traces of silver were found to give large oxidation currents. Figure 7.10d illustrates a scan of the mk. III SPEs. This compares well with the 3 electrode scan of Figure 7.10a indicating virtually all IR drop has been eliminated. The peak for oxidation of the Al-alizarin complex occurs at 0.62 V and is very well defined.

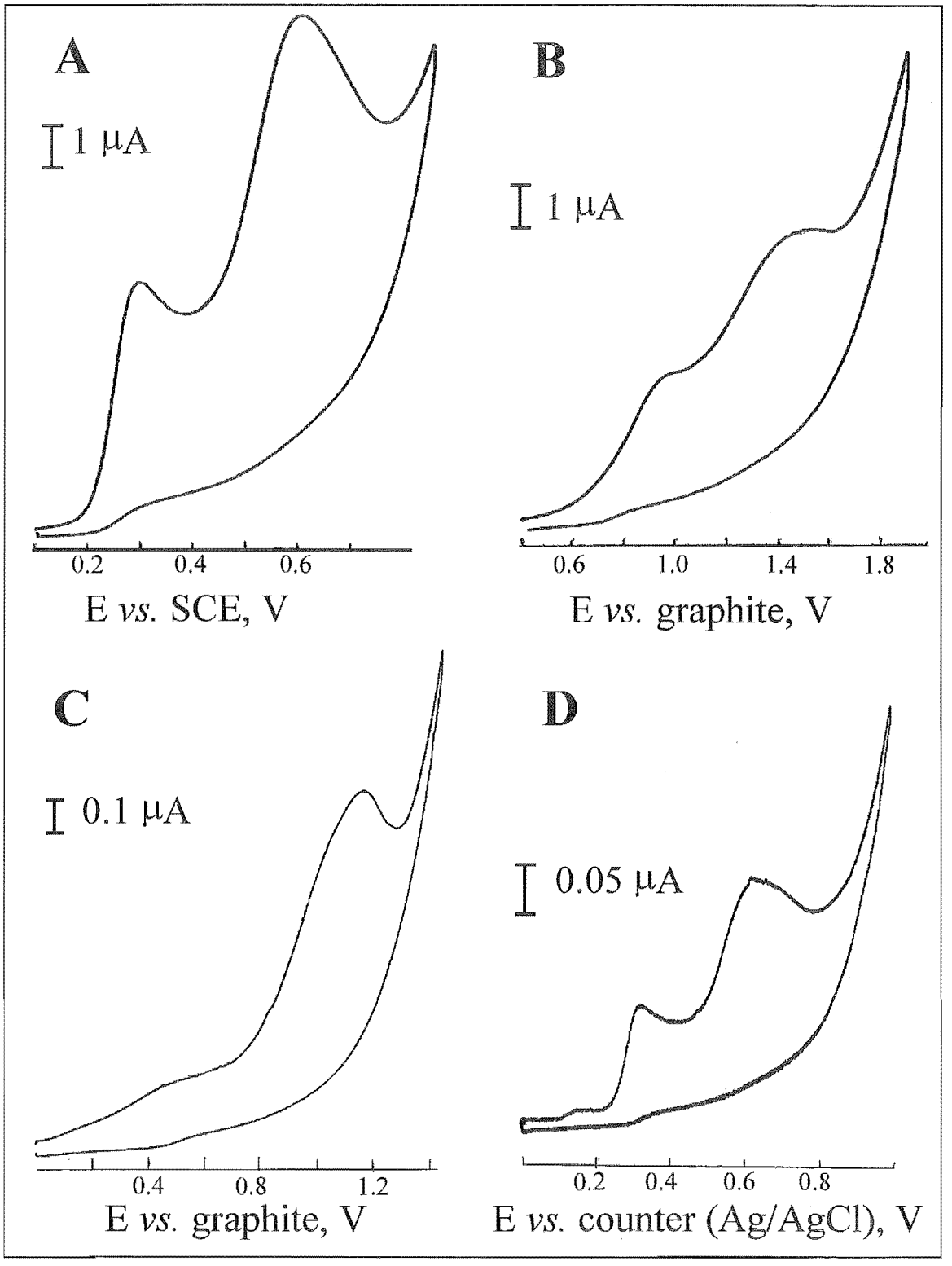

Figure 7.10 Cyclic voltammetric scans (ν = 100 mVs^{-1}) of:
A) Mk. I SPE in 3 electrode mode
B) Mk. I SPE in 2 electrode mode *vs.* an unmodified graphite SPE electrode.
C) As for B) with working electrode area reduced by 90%.
D) 2 electrode scan of mk. III SPE incorporating an Ag/AgCl counter electrode.
[Al] = 20 μM [A-C], 5 μM [D].
A 5 minute contact time was used. Other parameters were as for the standard analysis

Figure 7.11 shows the linear sweep voltammogram (ν = 100mVs^{-1}) obtained for a solution of 1 μM Al with a contact time of 5 minutes. The signal for Al-bound alizarin is significantly improved by taking the derivative of the initial linear sweep data. The large peak at 0.27 V corresponds to oxidation of free alizarin while oxidation of Al complexed alizarin gives the peak at 0.58 V in the differentiated scan.

Differentiation appears to be a useful technique for improving the analytical response in linear sweep voltammetry.

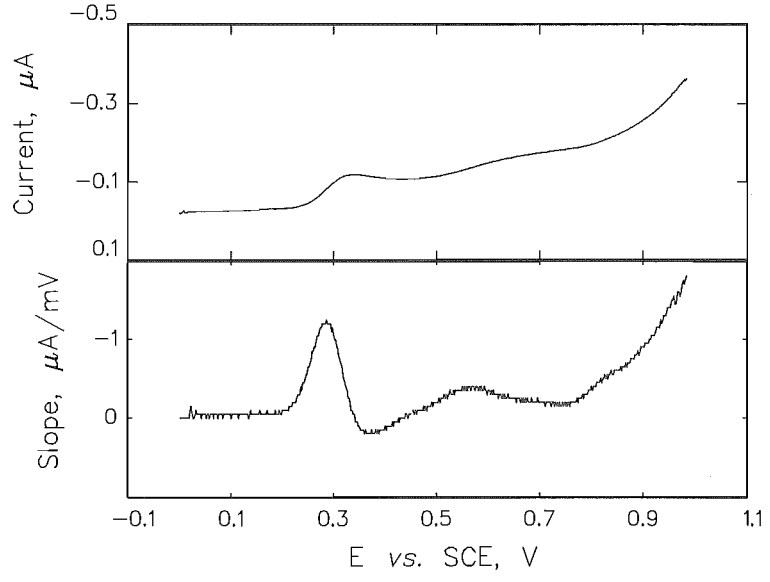

Figure 7.11 Linear sweep scan and the derivative. A mk. III SPE electrode was scanned in the 2 electrode mode. [Al] = 1.0 μM, ν = 100 mVs^{-1}, and contact time = 5 minutes, other parameters were as for the standard procedure.

7.3.4. FRACTIONATION OF Al SPECIES.

In their development of the oxine derivatised gel column Simpson *et al.* (1997) used a flow injection analysis protocol in which the column was placed in line with a flowing carrier stream in order to give reproducible contact times between the column and Al samples. Here the column is used in batch mode. This may change the contact time between the sample and the chelating gel, possibly altering the 'aggressiveness' of the column and changing the fraction of Al species retained by the column. Another difference is that for practical reasons larger sample and eluent volumes are required when operating in the batch mode.

To test out use of the column in batch mode comparisons were made between measured and calculated free Al concentrations in synthetic ligand solutions. Solutions were prepared containing fixed concentrations of Al and varying amounts of the ligands tartaric, oxalic and malonic acid. These ligands were selected to give complexes modelling the organic Al species found in environmental waters [Stevenson and Vance, 1989]. Stability constant data for these ligands and Al have been determined and allow the proportion of free and complexed Al to be calculated for each solution [malonic acid: Powell and Town, 1993; oxalic acid: Sjoberg and Ohman, 1985; tartaric acid: Motekaitis and Martell, 1984b]. The computer program SOLGASWATER [Eriksson, 1979] was used for calculation of reactive Al (assumed to be the sum of Al^{3+}, $AlOH^{2+}$ and $Al(OH)_2^+$) in each solution. Hydrolysis constants for Al were included in the calculations as described in section 3.2.8.

Solutions were applied to the column and the eluted Al was determined spectrophotometrically using the chromophore CAS. The data displayed in Fig. 7.12 show that for all of the Al-ligand systems studied there was a good match between the calculated concentration of reactive Al and that measured. This indicates that the aggressiveness of the column remains the same in transferring from the flow injection analysis to the batch analysis regimes.

Simpson *et al.* (1997) also studied the column's interaction with the Al^{3+} hydrolysis products, finding that only the reactive monomeric species were retained and subsequently eluted. On the basis of the results illustrated in Figure 7.12 this finding is assumed to hold for the batch application of the column also.

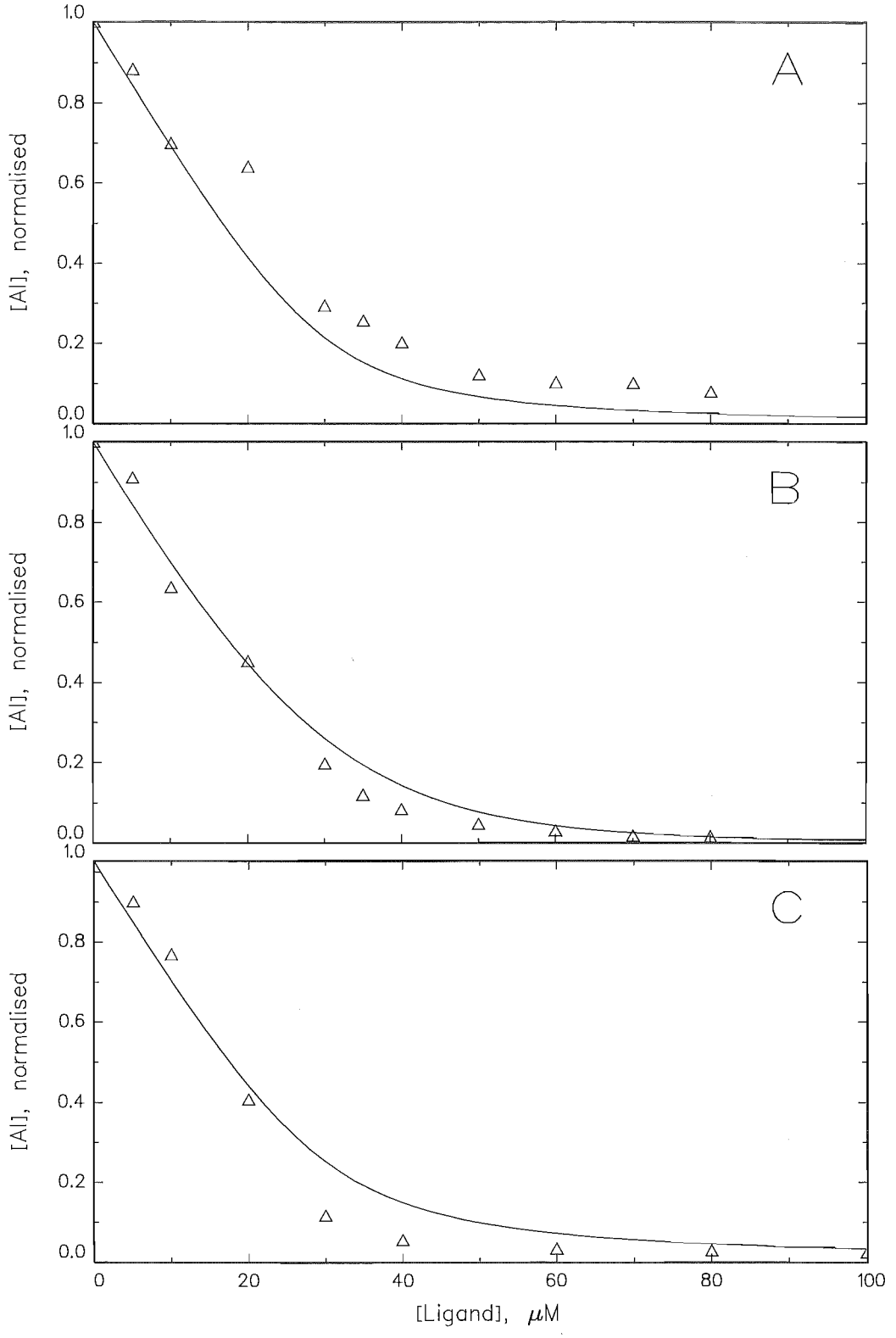

Figure 7.12 Al measured by the oxine column (batch mode) in the synthetic ligand solutions as a function of ligand concentration. Measured Al concentrations (△) are normalised to the value for no ligand present. In all cases the total Al concentration was 30 μM and the pH was 4.5. The solid lines give the calculated concentration of reactive Al

The ligands were **A)** malonic acid, **B)** oxalic acid and **C)** tartaric acid.

7.3.5 ELIMINATION OF INTERFERENCES.

The response of the SPEs to other metals was examined by preparing solutions containing both Al and the potential interferent. As indicated in Table 7.3 the alizarin modified SPEs were found to be susceptible to interference in the analysis of Al, particularly from transition metals and to a lesser extent from the alkaline earth metals Ca and Mg. This is perhaps not surprising considering the rich coordination chemistry of alizarin. A survey of the literature has found that complexes with alizarin have been reported for the following metals; nickel, copper, zinc, palladium, manganese [Bakola-Christianopoulou, 1984], ruthenium [DelMedico *et al.* 1994], iron and hafnium [Liebhafsky and Winslow, 1947] and a mixed chelate with aluminium and calcium [Kiel and Heertjes, 1963; Wunderlich and Bergerhoff, 1994].

The nature of the interference varied with each cation. Some metals (eg. Mn^{2+}) gave a new ligand-based electrochemical process overlapping that for Al. Others such as Ca^{2+} gave no obvious new peak but eliminated the response for Al, presumably by competitively coordinating to alizarin. In all cases pretreatment of samples with the oxine column eliminated the interferences. The factors responsible for this elimination of interference by the oxine column (when used in the flow injection analysis of Al) are discussed in section 5.4.2-B. They are assumed to also be operative in the batch mode of analysis described here. Essentially it is the strong interaction of Al with hydroxide ion to give the aluminate ion, $Al(OH)_4^-$, which allows only Al to be freed in the dilute alkali used for column elution.

Table 7.3 Effects of other cations on the analysis of 5 μM Al in the absence of the oxine microcolumn. Analysis was by alizarin modified SPE (mk. I) using the standard parameters.

	Effect	Cation	Concentration[a]
✹	Al signal reduced, slight change to shape of the free alizarin wave.	Mg^{2+}	100
		Ca^{2+}	1000
✹	New oxidation wave overlying Al-alizarin wave	[b]Fe^{3+}	10
		Mn^{2+}	10
		Co^{2+}	10
✹	Al signal eliminated.	Ni^{2+}	10
		Cu^{2+}	10
		Zn^{2+}	10
		Pb^{2+}	10

[a] concentration of the interfering cation, μM, [b] Fe^{3+}-tartrate complex.

7.3.6 PRECONCENTRATION OF Al SPECIES.

The oxine column captures Al from samples and releases it during a subsequent elution step. By controlling the sample (s) and analysis (a) volumes a dilution or preconcentration of Al can be effected. 'Analysis volume' refers to the volume of the flask in which the column eluent is collected, buffered and made up to volume (see section 7.2.2-A, step 4). The changes in Al concentration may be described by equations 7.2 - 7.3.

$$[Al]_a = F_c * [Al]_s \quad (7.2)$$

$$F_c = \varepsilon \frac{V_s}{V_a} \quad (7.3)$$

F_c = concentration factor.
ε = column efficiency coefficient.
$V_{a/s}$ = analysis or sample volume.

Different F_c values allow Al to be analysed over different linear ranges. F_c may be controlled by varying the parameters V_a and V_s. The coefficient ε describes the efficiency of the column in capturing Al. For the particular column used a value of 0.55 was observed for ε, ie 55% of the free Al standard applied to the column was retained and subsequently eluted. ε is expected to be a function of column geometry and of the 'freshness' of the gel.

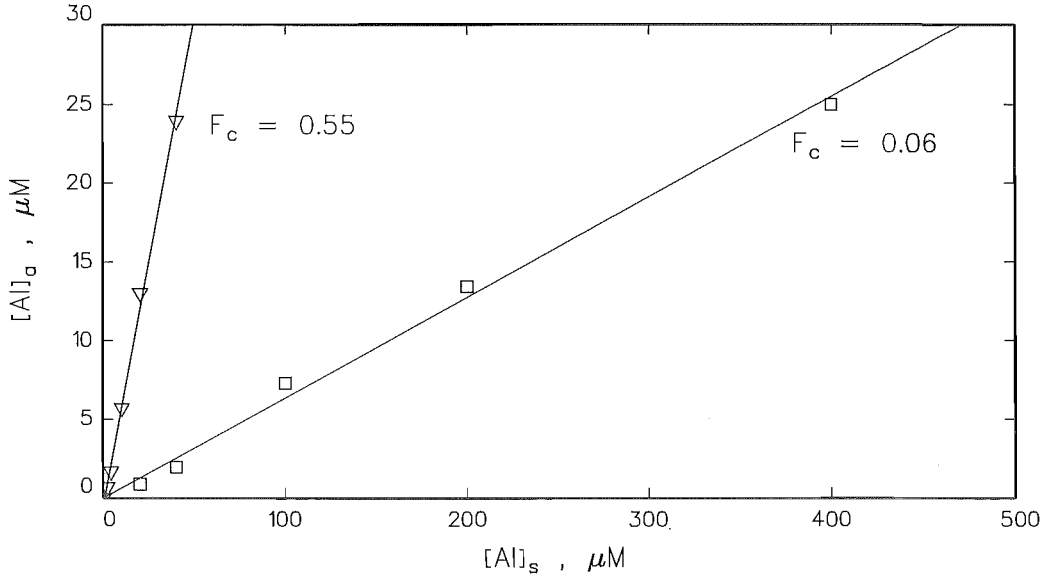

Figure 7.13 Manipulation of the oxine column's preconcentrating effect. $[Al]_a$, $[Al]_S$ and F_C are defined according to equations 7.2 and 7.3. $[Al]_a$ was determined spectrophotometrically with the CAS method.

Figure 7.13 illustrates examples where V_a = 10 mL and V_s = 10 mL and 1.0 mL giving F_c values of 0.55 and 0.06 respectively. $[Al]_a$ was determined using the spectrophotometric CAS method. The data show that by manipulation of F_c samples with widely different Al concentrations can be brought into the desired analysis range.

The calibration curve of Figure 7.8 indicates that the SPEs have a working range of 2 - 16 μM Al. The concentration of Al in the analysis volume, $[Al]_a$, must fall within this range. Surface waters (rivers and lakes) may be expected to contain reactive Al in the concentration range 0.1 - 30 μM [Driscoll and Schecher, 1990]. This corresponds to the expected concentration of Al in the sample volume. Thus in order to measure such samples by the SPEs in combination with the oxine column F_c values of 0.6 to 20 are needed. In Figure 7.14 a range of (synthetic) Al samples were analysed in this manner using a F_c value of 1.1 (V_s = 10 mL, V_a = 5.0 mL).

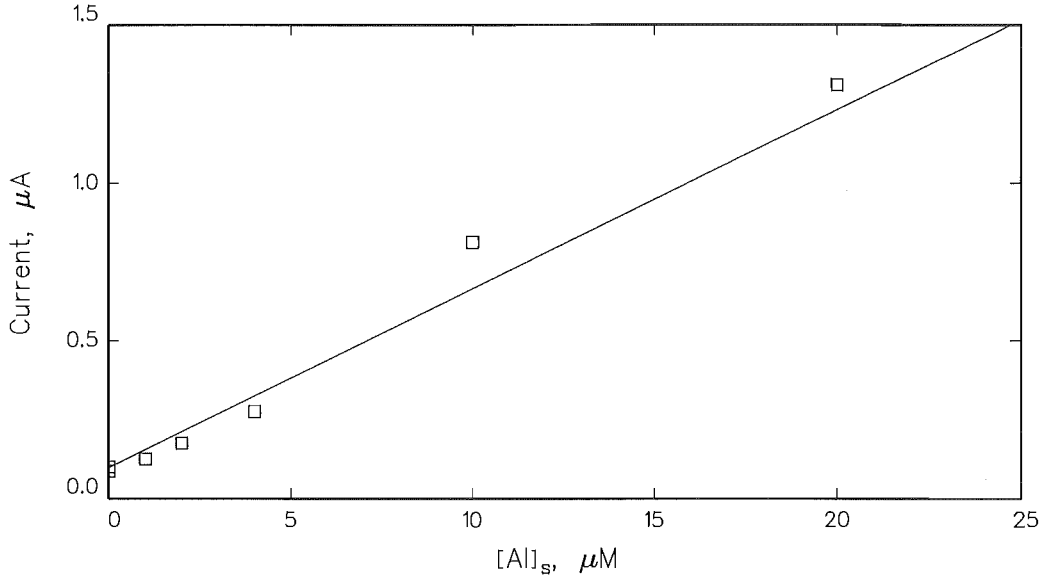

Figure 7.14 SPE analysis of samples after prior treatment with the oxine column. The standard SPE and column procedures were used. F_C = 1.1.

7.4 CONCLUSION.

7.4.1 ALIZARIN MODIFIED SPEs FOR Al ANALYSIS.

The alizarin modified SPE presents a successful development of the alizarin CME. The reactivity to Al is retained with the very simple approach to electrode modification. The modification procedure is reduced from a careful surface cleaning and dip coating process to simply mixing the modifier with the electrode material (ink) prior to printing. This simple approach is shared with the reported SPEs which utilise ligand modifiers [Wang *et al.* 1996; Somasundrum and Bannister, 1993]. It is likely that this is the only feasible approach since SPEs must be produced cheaply so that they may be used disposably. Certainly the elaborate coupling procedures designed to give a covalent attachment of modifiers would not be appropriate.

A difference in the analysis protocol for the alizarin modified SPE and that recommended by Downard *et al.* (1991) for the alizarin CME is that an optimal pH of 9.0 ± 0.2 was found, compared with 8.4 ± 0.2 for the CME. The buffer used in both cases is NH_4Cl/NH_3 and therefore the difference is of very little significance.

The modifier, alizarin, is soluble to millimolar concentrations at pH 9.0. This supports the observation of diffusion controlled voltammetry for the free ligand. Evidently the modifier is leached from the SPE surface into solution where it may freely form complexes with the analyte, Al. In contrast these complexes do not remain in solution but adsorb to the electrode surface. This results in an accumulation of Al at the electrode surface in the form of the alizarin complex. Thus the response of the SPEs increases with increasing contact time.

Stirring was not found to significantly assist the accumulation of the alizarin-Al complex. It may be that alizarin is swept away from the electrode surface before complexation (and precipitation) can occur. Use of quiescent solution conditions is an advantage for field work.

Accumulation of analytes is a common strategy to increase sensitivity in electrochemical analysis [Wang, 1996]. It is also used in the other SPEs described in the introduction for sensing metals and it may be an important requirement for successful sensor function. Accumulation may also function here to increase the response of coordinated ligand relative to free ligand.

7.4.2 DEVELOPMENT OF A FIELD SENSOR.

As a first step towards producing a SPE for use in the field the mk. II design SPEs were fabricated. In these the complete electrochemical cell (3 electrode) was printed. This removed the need for separate electrodes. The sensing elements were contained in a small area (*ca.* 1 cm^2) which allowed samples of a small volume (down to 100 μL) to be analysed. However these SPEs require a potentiostat for scanning because they have separate counter and reference electrodes.

The mk. III SPEs were designed to give printed 2 electrode strips which may be scanned without the need for a potentiostat. They were successfully produced after eliminating the factors contributing to IR drop. They are intended for in-field applications where they would probably be controlled from a laptop computer. In this case digital data would be produced for which taking a derivative is a straightforward matter. This allows the response at low levels of analyte to be more easily separated from the background response.

A number of problems have to be overcome in developing the SPEs for analysis of environmental samples. When used for direct analysis the working range of the SPEs (2-16 μM) is not as wide as that expected for the levels of reactive Al in environmental samples and corresponds to the higher end of the range. The SPEs are highly susceptible to interferences, particularly from the first row transition metals and the environmentally ubiquitous calcium and magnesium. Since the analytical procedure involves buffering samples to pH 9.0 for 3 minutes prior to analysis it is highly unlikely that only reactive Al would be included in the measurement. Rather, the measured Al would approximate to 'total soluble Al'.

These problems have been addressed by the use of a column of oxine-derivatised gel for sample pretreatment. In the original development of this column it was shown to be suitable for fractionation of reactive (toxic) species of Al. In order to combine use of this column with the screen printed electrodes this work has assessed the performance of the column in batch mode, ie using manual injections of sample and eluent. It has been demonstrated that the column's selectivity for reactive Al is retained in this new mode of operation and further it is only Al which is eluted from the column, effectively eliminating all interferences.

The preconcentrating (or diluting) effect of the column allows flexibility in the choice of measurement protocol. The concentration of Al can be adjusted, within limits, to a level convenient for analysis (ie to a range of 2 - 16 μM for measurement by the SPEs).

Chapter 8

CONCLUSION

Work in this project has proceeded along two lines: firstly studies have been directed towards fundamental aspects of the indirect electroanalysis of Al and secondly analytical applications have been developed for the analysis of reactive Al, intended for use both in the laboratory and in the field.

8.1 FUNDAMENTAL STUDIES.

8.1.1 SOLUTION EQUILIBRIA.

The solution equilibria formed between Al and two ligands; DHB and DASA have been characterised.

Al complexation by a catecholamine, DHB, was found to conform to the pattern observed for catechol and for catecholate derivatives with coordination proceeding by the stepwise addition of up to three ligands about the metal centre. An octahedral environment was preserved with the water ligands of hexaquo $Al(H_2O)_6^{3+}$ being substituted by phenoxy donors. Calculation of pM values (the negative logarithm of free metal concentration) revealed that Al is taken up relatively weakly by this ligand. In this respect the ligand was indistinguishable from another catecholamine (epinephrine) and both ligands gave an identical pM curve to catechol suggesting that the *para-* amino substituent plays little or no part in affecting coordination to Al. Unfortunately this relative weakness of interaction meant that DHB was an unsuitable ligand for further development in electroanalytical applications for Al.

The ligand DASA has been applied by several analysts for the electroanalysis of Al. The solution equilibria of the system H^+/Al^{3+}/DASA has been previously investigated by Couturier [1987, 1989] using spectrophotometric methods. In this work potentiometric and spectrophotometric methods were used to re-examine the system. The complexation model has been changed by reassignment of one of the species suggested by Couturier. This was the complex $[Al(DASA)_2OH]^{4-}$ which was determined to be present as a dimer, $[Al_2(DASA)_4(OH)_2]^{8-}$. It is likely that this is the complex formed under the

conditions of many of the published analytical applications of DASA to the electroanalysis of Al [van den Berg, 1986; Downard *et al.*, 1992a; Carrera *et al.*, 1993; Hernandez-Brito *et al.*, 1994]. This shows the advantage of using potentiometry in conjunction with numerical methods of data treatment. It also underscores the importance of bringing independent experimental techniques to bear upon a problem.

The determination of solution equilibria is a useful practice in the evaluation of prospective ligands for the electroanalysis of Al. Further it is useful for the calculation of what species are formed under the conditions of an analytical application.

8.1.2 VOLTAMMETRY.

The voltammetric responses of the ligands catechol, DASA and 4-ncat and their Al complexes have been examined. Complex formation constants are available for each system and were used to determine ideal solution conditions (pH, metal and ligand concentrations) for the formation of each complex.

A theoretical model in the literature which describes the electrochemistry of ligand-based redox systems [Shiu and Harrison, 1989] was shown to be inappropriate for complexes formed with Al. This model assumed that metal-ligand complexes are labile on the electrochemical timescale and that the only interaction of the metal-ligand complex is to limit the concentration of the free ligand. Here it is proposed that coordination systems involving Al are too inert to be described by this model. The shifts in redox potentials which are observed in the presence of the metal are produced by the direct electrode reaction of metal-bound ligand. These shifts are controlled by structural and electronic factors within the complexes.

In each case the oxidation potentials of the complexes were seen to decrease with increasing ligand to metal ratio. This was attributed to decreasing stabilisation of the ligands by Al as the metal's influence is spread over a greater number of ligands. Also it is possible that steric factors lead to a greater rate of ligand dissociation in the complexes of higher stoichiometry. The rate of ligand dissociation is important since the ligands studied here form *ortho*-quinones after oxidation and do not complex Al.

Conclusions may be drawn which are relevant to the electroanalysis of Al. For the application of methods based on monitoring the current due to oxidation of the complex, three results are of particular importance: (i) the shift in redox potential results

from the direct reaction of Al-bound ligand. (ii) The oxidation potential of Al-bound ligand may be expected decrease with increasing ligand to metal ratio. This will give in turn a variation in oxidation potential with pH. This effect may be insignificant in the absence of significant steric interactions (e.g. complexes of catechol and lower stoichiometry complexes of DASA). (iii) the potential for oxidation of a complex does not depend on Al concentration.

8.2 THE DEVELOPMENT OF ANALYTICAL APPLICATIONS.

8.2.1 A FIA SYSTEM FOR THE MEASUREMENT OF REACTIVE Al.

A flow injection system was constructed for the amperometric analysis of reactive Al using the reagent 4-ncat. Strengths of this system were that Al could be measured at micromolar concentrations with precision, minimal sample handling and a high sample throughput.

Use of electrochemical detection in this system is distinctive from most conventional flow systems for Al since these use spectrophotometric detection [e.g. Hawke and Powell, 1994; Royset and Sullivan, 1986]. Electrochemical systems are cheaper, more robust and more readily interfaced with data recording equipment.

Another difference is in the factors which control a particular techniques detection limit. For spectrophotometry these factors are the molar absoptivities of the free and complexed forms of the ligand and the ability of the instrument to discern the light absorption from the complex from the background absorption of the free ligand. For amperometry there is no parameter which is comparable to molar absorptivity. The detection limit is governed by the minimum current from the analyte complex which may be determined in the presence of the capacitance and Faradaic currents which form the amperometric background.

A microcolumn of oxine derivatised gel was incorporated into the manifold. This eliminated the effect of interferences and allowed the selective measurement of reactive Al in a range of natural samples. This was necessary because systems using chelating ligands for the indirect analysis of Al (both spectrophotometric and electrochemical) will rarely be suited for the fractionation of reactive Al. Instead they are optimised towards the detection of Al. Conditions are selected which optimise the formation of a complex between Al and the reagent. For this particular system there is a contact time between the sample and the reagent 4-ncat in the manifold of 15 seconds at

pH 8.9. In this time there would be considerable redistribution of Al between the different species present and an unpredictable proportion of the less reactive species may be included in the analysis. Also a chelating reagent is rarely Al-specific and in this case was susceptible to interference from a wide range of other cations.

The amperometric detector was set at a potential to monitor the free ligand. The signal from Al appeared as a decrease in the oxidation current for free ligand, i.e. the complex formed between Al and the ligand was not directly analysed electrochemically. This was necessary because the complex oxidation potential was higher than that of the free ligand and could not be probed in isolation. As the analytical signal depended on the removal of free ligand by Al a pH was selected for formation of the complex of the highest stoichiometry, $[Al(4\text{-ncat})_3]^{6-}$. This was chosen following speciation calculations using complex formation constants.

A problem arose from the practice of monitoring the free ligand. This required the continuous passing of an oxidation current. Electrode fouling by the oxidation products of the ligand gave rise to an exponential decay in the baseline current. This was largely overcome by incorporating a separate measurement of the baseline current into each analysis.

8.2.2 NOVEL FIA STRATEGIES.

Two novel FIA strategies were developed towards the aim of overcoming the problem of electrode fouling noted in the previous section. Both systems sought to eliminate the response from free ligand so that Al-bound ligand could be measured separately. In the first system a guard reagent was used. This complexed all ligand in excess of the Al complex, rendering it electroinactive. In the second system solvent extraction was used to physically remove excess ligand.

The two systems were successful in removing the electrochemical response of free ligand, leaving only that which is bound to Al for measurement. In the second system this gave the expected decrease in electrode fouling.

The guard reagent system was shown to function correctly, with the guard reagent scavenging free ligand and a signal being observed for Al-bound ligand. Unfortunately the guard reagent was observed to cause even greater electrode fouling than the free ligand. Further development of this system will require identification of a

chemical derivative of the guard reagent which does not cause electrode fouling.

The solvent extraction system was more promising, with complete elimination of electrode fouling. This was achieved by physical removal of excess ligand in combination with an electrochemical pretreatment of the detector electrode.

Strengths of the system were long term stability (at least up to three hours), reasonable throughput of samples (4 minutes each) and detection of micromolar concentrations of Al. These benefits came at the cost of considerable complexity of the system and use of a toxic solvent (chloroform). Also the linear working range was relatively short, covering only one order of magnitude. This may be in part due to the equipment which was available (i.e. the choice of peristaltic pump). In future work this may be overcome by the use of alternative equipment or by developing more complete mixing of the analysis stream prior to its entry into the amperometric detector. Both of these strategies would reduce the incidence of heterogeneous regions in the analysis stream, possibly reducing the baseline noise and lowering the bottom limit to the linear working range.

In most conventional solvent extraction flow systems teflon tubing is used in the extraction coil for its superior inertness and stability. Its use in this system should be investigated.

The solvent extraction system is not limited to electrochemical detection. The reagent used, alizarin, is strongly coloured, especially in the highly alkaline pH of the final reaction coil. An interesting direction for future work may be to connect the FIA manifold to a spectrophotometric detector.

8.2.3 SCREEN PRINTED ELECTRODES.

Some general principles regarding the use of screen printing technology for the fabrication of chemical sensors have been revealed. Electrodes are printed at low cost, allowing them to be treated as disposable. This avoids any problems with electrode deterioration with use and means that irreversible redox agents (e.g. alizarin) may be used. Chemical modification of the electrodes occurs during manufacture, simplifying the analysis protocol. Only a relatively crude method of electrode modification is available, that of incorporating modifiers into the printing inks. For the particular system developed here it was shown that the analyte, Al, was accumulated at the sensor surface. Undoubtedly this assisted in generating a measurable response. It may be true in general that there must be some chemical process present which leads to the accumulation of an analyte at a screen printed sensor.

The alizarin modified SPEs are recommended for the 'in-field' measurement of Al. Their design was modified to allow scanning by a simple linear sweep waveform in the two electrode mode. This allows electroanalysis in the field to be carried out without a potentiostat using, for example, a laptop computer. In combination with the oxine micro-column the alizarin SPEs are suitable for the selective measurement of reactive Al at the levels observed in natural freshwater systems (i.e. soils, rivers and lakes). Use of the oxine micro-column also overcomes problems from interfering cations.

Further development of the SPEs is required to allow their widespread use by the scientific community. The large variability in the electrode's response at low levels of Al (RSD of 21% at 1 μM Al) must be overcome. This may be addressed in part by improved fabrication of the sensors. Fabrication in this project was completed by a novice screen printer (myself!) and was occasionally a 'hit and miss' affair.

Scanning of the electrodes from a laptop computer will require development of an electronic interface to generate the analysis waveform and to report current-potential information. This will require appropriate software.

References

Agren, A., (1955), *Acta Chem. Scand.*, **9**, 49.

Anjo, D. M., Micheal, K. M., Kahr, M., Khodabakhsh, M. M., Nowinski, S., and Wanger, M., (1989), *Anal. Chem.*, **61**, 2603.

Atack, F.W., (1915), *J. Soc. Chem. Ind.*, **34**, 936.

Atkins, P.W., (1987), '*Physical Chemistry*', 3rd. edition, Oxford University Press, first published 1978.

Backes, C.A. and Tipping, E., (1987), *Intern. J. Environ. Anal. Chem.*, **30**, 135.

Backes, C.A. and Tipping, E., (1987), *Wat. Res.*, **21**, 211.

Baes, C.F. Jr., Mesmer, R.E., (1976), '*The hydrolysis of cations.*', (Krieger, Fl) John Wiley & Sons, Inc., USA.

Bakola-Christianopoulou, M.N., (1984), *Polyhedron*, **3**, 729.

Baldwin, R., Christensen, J. and Kryger, L., (1986), *Anal. Chem.*, **58**, 1790.

Bard, A. J. and Faulkner, L. R., (1980), *Electrochemical Methods*, Wiley, New York.

Barnes, R.N., (1975), *Chem. Geol.*, **15**, 177.

Beck, M.T., (1970), '*Chemistry of complex equilibria.*', Van Nostrand Reinhold, London.

Belcher, R., Leonard, M.A. and West, T.S., (1958), *J.Chem. Soc.*, 2390.

Benes, P., and Steinnes, E., (1974), *Wat. Res.*, **8**, 947.

Berggren, D., (1989), *Intern. J. Environ. Anal. Chem.*, **35**, 1.

Berggren, D., Bergkvist, B., Falkengren-Grerup, U., Folkeson, L. and Tyler, G., (1990), *Sci. Total Environ.*, **96**, 103.

Bertsch, P.M., (1989), '*Aqueous polynuclear aluminium species.*', in The Environmental Chemistry of Aluminum., **pp. 87-115.**, Sposito, G. (Editor), CRC press, Florida.

Bixler, J.W. and Bond, A.M., (1986), *Anal. Cem.*, **58**, 2859.

Bjerrum, J., (1931), *Kgl. Danske. Videnskab. Selskab. Mat.-fys. Medd.*, **11**, No.5.

Bjerrum, J., (1932), *Kgl. Danske. Videnskab. Selskab. Mat.-fys. Medd.*, **11**, No.10.

Bjerrum, J., (1934), *Kgl. Danske. Videnskab. Selskab. Mat.-fys. Medd.*, **12**, No.15.

Bjerrum, J., (1941), '*Metal Ammine Formation in Aqueous Solution.*', Haase, Copenhagen.

Blamey, F.P.C., Edwards, D.G. and Asher, C.J., (1983), *Soil Sci.*, **136**, 197.

Bloom, P.R. and Erich, M.S., (1989), *"The quantitation of aqueous aluminum"*, in The Environmental Chemistry of Aluminum., **pp. 1-27.**, Sposito, G. (Editor), CRC press, Florida.

Bloom, P.R., Weaver, R.M. and McBride, M.B., (1978), *Soil Sci. Soc. Am. J.*, **42**, 713.

Bond, A.M., (1980), *Modern Polarographic Methods in Analytical Chemistry.*, Marcel Dekker, N.Y.

Booth, C.E., McDonald, D.G., Simons, B.P. and Wood, C.M., (1988), *Can. J. Fish. Aquat. Sci.*, **45**, 1563.

Brainina, Kh.Z. and Bond, A.M., (1995), *Anal. Chem.*, **67**, 2586.

Brown, P.L., Sylva, R.N., Batley, G.E. and Ellis, J., (1985), *J. Chem. Soc., Dalton Trans.*, 1967.

Cabaniss, G.E., Diamantis, A.A., Murphy Jr., W.R., Linton, R.W. and Meyer, T.J., (1985), *J. Am. Chem. Soc.*, **107**, 1845.

Cai ,Q., and Khoo, S.B., (1993), *Anal. Chim. Acta*, **276**, 99.

Carrera, M.E., Rodriguez, V., Toral, M.I. and Richter, P., (1993), *Anal. Letters*, **26**, 2575.

Cass, A.E.G., Davis, G., Fancis, G.D., Hill, H.A.O., Aston, W.J. Higgins, J., Plotkin, E.V., Scott, L.D.L. and Turner, A.P.F., (1984), *Anal. Chem.*, **56**, 667.

Cha, S.K., Ahn, B.K., Hwang, J-U. and Abruna, H.D.,(1993), *Anal. Chem.*, **65**, 1564.

Christophersen, N., Neal, C., Vogt, R., Esser, J.M. and Andersen, S., (1990), *Sci. Total Environ.*, **96**, 175.

Clark, G.D., Hungerford, J.M. and Christian, G.D., (1989), *Anal.Chem.*, **61**, 973.

Clarke, N., Danielsson, L.-G. and Sparen, A., (1992), *Intern. J. Environ. Anal. Chem.*, **48**, 77.

Cotton, F.A., and Wilkinson, G., (1988), *Advanced Inorganic Chemistry*, 5th Edn., Wiley, New York.

Couturier, Y., (1987), *Bull. Chim. Soc. Fr.*, **6**, 963.

Couturier, Y., (1989), *Bull. Chim. Soc. Fr.*, **6**, 756.

Cronan, C.S. and Schofield, C.L., (1979), *Science*, **204**, 304.

Cronan, C.S., Walker, W.J. and Bloom, P.R., (1986), *Nature*, **324**, 140.

Dahlgren R.A. and Walker, W.J., (1993), *Geochim. Cosmochim. Acta*, **57**, 57.

Deakin, M.R., Kovach, P.M., Stutts, K.J. and Wightman, R.M., (1986), *Anal. Chem.*, **58**, 1474.

Deane, S.F. and Leonard, M.A., (1977), *Analyst*, **102**, 340.

Debye, P. and Huckel, E., (1923), *Phys. Z.*, **24**, 185 and 305.

Delhaize, E. and Ryan, P.R., (1995), *Plant Physiol.*, **107**, 315.

Delamar, M., Hitmi, R., Pinson, J. and Saveant, J.M., (1992), *J. Am. Chem. Soc.*, **114**, 5883.

DelMedico, A., Auburn, P.R., Dodsworth, E.S. Lever, A.B.P. and Pietro W.J., (1994), *Inorg. Chem.*, **33**, 1583.

Denison, R.B., (1912), *Trans. Faraday Soc.*, **8**, 20.

Downard, A.J., Lenihan, R.J., Simpson, S.L., O'Sullivan, B. and Powell K.J., (1997)a, *Anal. Chim. Acta*, **395**, 5.

Downard, A.J., Money, S.D. and Powell, K.J., (1997)b, *Anal. Chim. Acta*, **349**, 111.

Downard, A.J., Powell, H. K. J. and Xu, S., (1991), *Anal. Chim. Acta*, **251**, 157.

Downard, A.J., Powell, H. K. J. and Xu, S., (1992)a, *Anal. Chim. Acta*, **256**, 117.

Downard, A.J., Powell, H. K. J. and Xu, S.,(1992)b, *Anal. Chim. Acta*, **262**, 339.

Downard, A.J., Roddick, A.D. and Bond, A.M.,(1995), *Anal. Chim. Acta*, **317**, 303.

Downard, A.J., O'Sullivan, B. and Powell, K.J., (1996), *Polyhedron*, **15**, 3469.

Driscoll, C.T. and Schecher, W.D., (1990), *Environ. Geochem. and Health.*, **12**, 28.

Driscoll, C.T., (1984), *Intern. J. Environ. Anal. Chem.*, **16**, 267.

Driscoll, C.T., Baker, J.P., Bisogni, J.J. and Schofield, C.L., (1980), *Nature*, **284**, 161.

Du pont de Nemours (E.I. & Company.), Electronic products division, (1970), *'Thick film handbook.'*, also published under the title *'The thick film microcircuitry handbook.'*, E.I. Du pont de Nemours & Company, Electronic products division, Wilmington, Delaware 19898, U.S.A.

Eriksson, G., (1979), *Anal. Chim. Acta*, **112**, 375.

Favero, G. and Jobstraibizer, P., (1996), *Coord. Chem. Rev.*, **149**, 367.

Florence, T.M., (1962), *Anal. Chem.*, **34**, 496.

Florence, T.M., and Belew, W.L., (1969), *J. Electroanal. Chem.*, **21**, 157.

Florence, T.M., Miller, F.J. and Zittel, H.E., (1966), *Anal. Chem.*, **38**, 1065.

Forsling, W. and Wu., L., (1992), *Acta Chem. Scand.*, **46**, 418.

Furrer, G., Trusch, B. and Muller, C., (1992), *Geochim. Cosmochim Acta*, **56**, 3831.

Galan-Vidal, C.A., Munoz, J., Dominguez, C. and Alegret, S., 1995, *Trends Anal. Chem.*, 14, 225.

Gans, P., Sabatini, A. and Vacca, A., (1985), *J. Chem. Soc. Dalton Trans.*, **6**, 1195.

Gelado-Caballero, M.D., Hernandez-Brito, J.J., Herrea-Melian, J.A., Colldo-Sanchez, C. and Perez-Pena, J., (1996), *Electroanalysis*, **8**, 1065.

Gherini, S.A., Mok., L., Hudson, R.J.M., Davis, G.F., Chen, C.W. and Goldstein, R. A., (1985), *Wat. Air Soil Pollut.*, **26**, 425.

Goto, K., Ochi, H. and Okura, T., (1958), *Bull. Chem. Soc. Jpn.*, **31**, 783.

Gran, G., (1952), *Analyst,* 77, 661.

Green, M.J. and Hilditch, P.I., (1991a), *Anal. Proc.*, **28**, 374.

Green, M.J. and Hilditch, P.I., (1991b), *Analyst*, **116**, 1217.

Gregor, J.E., (1987), '*Metal organic complexing in soil systems.*', Ph.D thesis, University of Canterbury, New Zealand.

Gregor J.E., and Powell, H.K.J., (1986), *J. Soil Sci.*, **37**, 577.

Griffith, W.P., White, A.J.P. and Williams, D.J., (1996), *Polyhedron*, **15**, 2835.

Häkkinen, P., (1984a), *Finn. Chem. Lett.*, 151.

Häkkinen, P., (1984b) *Finn. Chem. Lett.*, 59.

Häkkinen, P., (1984c), *Finn. Chem. Lett.*, 9.

Häkkinen, P., (1985), *Finn. Chem. Lett.*, 17.

Hart, J.P. and Wring, S.A., (1994), *Electroanalysis*, **6**, 617.

Hartwell, B.L. and Pember, F.R., (1918), *Soil Sci.*, **6**, 259.

Havel, J. and Meloun, M., (1985), '*Strategies for solution equilibria studies with specific reference to spectrophotometry.*', chapter 2, pp. 19-36, in '*Computational Methods for the Determination of Formation Constants.*', Leggett, D.J., (Ed.), Plenum Press, New York.

Havelkova, L. and Bartusek, M., (1969), *Collec. Czech. Chem. Commun.*, **34**, 2772.

Hawke, D.J. and Powell, H.K.J., (1994), *Anal. Chim. Acta*, **299**, 257.

Hawke, D.J. and Powell, H.K.J., (1995), *Aust. J. Soil Res.*, **33**, 611.

Hawke, D.J., Powell H.K.J., and Sjöberg, S., (1995), *Polyhedron*, **14**, 377.

Hawke, D.J., Powell, H.K.J. and Gregor, J.E., (1996), *Mar. Freshwater Res.*, **47**, 11.

Henry, R.P., Prue, J.E., Rossotti, F.J.C. and Whewell, R.J., (1971), *Chem. Commun.*, 868.

Henshaw, J.M., Lewis, T.E., and Heithmar, E.M., (1988), *Intern. J. Environ. Anal. Chem.*, **34**, 119.

Hernández-Brito, J.J., Gelado-Caballero, M.D., Pérez-Peña, J., and Herrera-Melián, J.A., (1994), *Analyst*, **119**, 1593.

Hodges, S.C., (1987), *Soil. Sci. Soc. Am. J.*, **51**, 57.

Ingman, F., (1973), *Talanta*, **20**, 135.

Jardine, P.M. and Zelazny, L.W., (1986), *Soil Sci. Soc. Am. J.*, **50**, 895.

Job, P., (1928), *Ann. Chim. Phys.*, **9**, 113.

Johnson, K.E. and Treble, R.G., (1993), *Can. J. Chem.*, **71**, 824.

Joseph, M.H., (1985), *J. Chromatogr.*, **342**, 370.

Kapel, M. and Selby, D.W., (1969), *Talanta*, **16**, 915.

Karlberg, B. and Thelander, S., (1978), *Anal.Chim. Acta*, **98**, 1.

Karpiuk, M., Politowicz, M., Stryjewska, E. and Rubel, S., (1995), *Fresenius J. Anal. Chem.*, **351**, 693.

Kennedy, J.A. and Powell, H.K.J., (1985), *Aust. J. Chem.*, **38**, 659.

Kennedy, J.A., Munro, M.H., Powell, H.K.J., Porter, L.J. and Yeap Foo, L., (1984), *Aust. J. Chem.*, **37**, 885.

Kiel E.G. and Heertjes, P.M., (1963), *J. Soc. Dyers and Colourists.*, **79**, 21.

Killa, H.M., Mercer, E.E and Philip, R.H. Jr., (1984), *Anal. Chem.*, **56**, 2401.

Kinraide, T.B., (1991), *Plant Soil*, **134**, 167.

Kiss, T., Sovago, I. and Martin, R.B., (1989), *J. Am. Chem. Soc.*, **111**, 3611.

Koryta, J., (1962), *Progress in Polarography*, **Vol. 1**, Interscience, New York, p. 295.

Kramer, J.R., Hummel, J. and Gleed, J., (1986), *'Speciation of aluminium and its toxicity to fish.'*, **In**: 'Proceedings of the international conference on chemicals in the environment.' (**Ed.:** Lester, J.N., Perry, R. and Sterritt, R.M.), Selper Ltd, London.

Lalande, H. and Hendershot, W.H., (1986), *Can. J. Fish. Aquat. Sci.*, **43**, 231.

Landing, W.M., Haraldsson C., and Paxeus, N., (1986), *Anal. Chem.*, **58**, 3031

Lanza, P., (1997), *Anal. Chim. Acta*, **341**, 91.

Larson J. and Zink, J.I., (1990), *Inorg. Chim. Acta*, **169**, 71.

LaZerte, B.D., (1984), *Can. J. Fish. Aquat. Sci.*, **41**, 766.

LaZerte, B.D., Chun, C., Evans, D. and Tomassini, F., (1988), *Environ. Sci. Technol.*, **22**, 1106.

Lee J., and Pritchard, M.W., (1984), *Plant Soil*, **82**, 101.

Lee, S.K., Kim, H. and Chung, T.D., (1997), *Electroanalysis*, **9**, 527.

Leggett, D.J., (1985), '*Computational Methods for the Determination of Formation Constants.*', Plenum press, New York.

Leonard, M.A. and West, T.S., (1960), *J. Chem. Soc.*, 4477.

Liebhafsky, H.A. and Winslow, E.H., (1947), *J. Am. Chem. Soc.*, **69**, 1130.

Lucy, C.A. and Yeung, K.K.C, (1994), *Anal. Chem.*, **66**, 2220.

Matthews, D.R., Holman, R.R., Bown, E., Steemson, J., Watson, A., Hughes, S. and Scott, D., (1987), *Lancet*, **1**, 778.

May, H.M., Helmke, P.A. and Jackson, M.L., (1970), *Chem. Geol.*, **24**, 259.

McCahon, C.P., Brown, A.F., Poulton, M.J. and Pascoe, D., (1989), *Wat. Air Soil Pollut.*, **45**, 345.

McCreery, R.L., (1991), *Electroanalytical Chemistry,* A.J. Bard (Editor), **Vol 17**, Dekker, New York, pp. 337.

Meulenhoff, J., (1925), *Rec. Trav. Chim*, **44**, 150.

Millero, F.J. and Schreiber, D.R., (1982), *Am. J. Sci.*, **282**, 1508.

Miyasaka, S.C., Buta, J.G., Howell, R.K. and Foy, C.D., (1991), *Plant Physiol.*, **96**, 737.

Mllakar, M., Culjak, I., Dakovic, S. and Branica, M., (1997), *Electroanalysis*, **9**, 63.

Mookherji, S. and Floyd, M., (1991), *Plant Soil*, **136**, 25.

Motekaitis, R. J., and Martell, A. E., (1984), *Inorg. Chem.*, **23**, 18.

Neuhold, C.G., Wang, J., Cai, X. and Kalcher, K., (1995a), *Analyst*, **120,** 2377.

Neuhold, C.G., Wang, J., Nascimento, V.B. and Kalcher, K., (1995b), *Talanta*, **42**, 1791.

Nordstrom, D.K. and May, H.M., (1989), '*Aqueous equilibrium data for mononuclear aluminium species.*', in The Environmental Chemistry of Aluminum., **pp. 29-53.**, Sposito, G. (Editor), CRC press, Florida.

Öhman, L.O., Sjöberg, S. and Ingri, N., (1983), *Acta Chem. Scand.*, A **37**, 561.

Öhman, L.O. and Sjöberg, S., (1983), *Polyhedron*, **2**, 1329.

Ohsaka, T., Oyama, N., Takahira, Y., and Nakamura, S., (1988), *J. Electroanal. Chem.*, **247**, 339.

Ohsaka, T., Takahira, Y., Hatozaki O., and Oyama, N., (1989), *Bull. Chem. Soc. Jpn.*, **62**, 1023.

Okura, T., Goto, K. and Yotuyanaga, T., (1962), *Anal. Chem.*, **34**, 581.

Ostromysslensky, J., (1911), *Ber.*, **44**, 268.

Palmer, D.A. and Wesolowski, D.J., (1992), *Geochim. Cosmochim. Acta*, **56**, 1093.

Parker, D.R., Kinraide, T.B. and Zelazny, L.W., (1988), *Soil Sci. Soc. Am. J.*, **52**, 438.

Parker, D.R., Kinraide, T.B. and Zelazny, L.W., (1989), *Soil Sci. Soc. Am. J.*, **53**, 789.

Pettit, L.P., (1984), *Pure and Applied Chem.*, **56**, 247.

Pichet, P. and Benoit, R.L., (1967), *Inorg. Chem.*, **6**, 160.

Playle, R.C. and Wood, C.M., (1989), *Can. J. Fish. Aquat. Sci.*, **47**, 1558.

Playle, R.C. and Wood, C.M., (1989), *J. Comp. Physiol. B*, **159**, 539.

Poon, M. and McCreery, R.L., (1986), *Anal. Chem.*, **58**, 2750.

Powell, H.K.J. and Town, R.M., (1993), *Aust. J. Chem.*, **46**, 721.

Proudfoot, G.M. and Ritchie, I.M., (1983), *Aust. J. Chem.*, 36, 885.

Resing, J.A. and Measures, C.I., (1994), *Anal. Chem.*, **66**, 4105.

Rice, R.J., Pontikos, N.M. and McCreery, R.L., (1990), *J. Am. Chem. Soc.*, **112**, 4617.

Rogeberg, E.J.S. and Henriksen, A., (1985), *Vatten*, **41**, 48.

Rosseland, B.O., Blaker, I.A., Bulger, A., Kroglund, F., Kvellstad, A., Lydersen, E., Oughton, D.H., Salbu, B., Staurnes, M. and Vogt, R., (1992), *Environ. Pollut.*, **78**, 3.

Rossotti, F.J.C. and Rossotti, H., (1961), '*The Determination of Stability constants and other Equilibrium Constants in Solution.*', McGraw-Hill, New York.

Royset, O. and Sullivan, T.J., (1986), *Intern. J. Environ. Anal. Chem.*, **27**, 305.

Russell, J.M.R., (1977), Ph.D Thesis, University of Canterbury.

Ryan, M. D., Yeuh, A. and Chen, W.-Y., (1980), *J. Electrochem. Soc.*, **127**, 1489.

Scampavia, L.D., Blankenstein, G., Ruzicka, J. and Christian, G.D., (1995), *Anal. Chem.*, **67**, 2743.

Schnitzer, M. and Khan, S.U., (1972), *Humic substances in the environment.*, Marcel Dekker, New York, **pp. 372**

Seddon, B.J., Shao, Y. and Girault, H.H., (1994), *Electrochimica Acta*, **39**, 2377.

Seip, H.M., Muller, L. and Naas, A., (1984), *Wat. Air Soil Pollut.*, **23**, 81.

Shann, J.R. and Bertsch, P.M., (1993), *Soil Sci. Soc. Am. J.*, **57**, 116.

Shiu, K.K. and Harrison, D.J., (1989), *J. Electroanal. Chem.*, **260**, 249.

Simpson S.L., Powell, K.J. and Nilsson, N.H.S., (1997), *Anal. Chim. Acta*, **343**, 19.

Sjoberg, S. and Ohman, L.O., (1985), *J. Chem. Soc. Dalton Trans.*, 2665.

Smith, R.W., (1971), *Adv. Chem. Ser.*, **106**, 250, (Am. Chem. Soc., Washington DC).

Somasundrum, M. and Bannister, J.V., (1993), *Sensors and Actuators B*, **15-16**, 203.

Stevenson, F.J., and Vance, G.F., (1989), *"Naturally occurring Aluminium-organic complexes"*, in The Environmental Chemistry of Aluminum., **pp. 117-116.**, Sposito, G. (Editor), CRC press, Florida.

Stutts, K. J., Kovach, P. M,. Kuhr, W. G. and Wightman, R. M., (1983), *Anal. Chem.*, **55**, 1632.

Tikhonov, V.N., (1973), *'Analytical chemistry of aluminium.'*, John Wiley & Sons, New York, **Chap. 2**.

Turner, R.C., (1969), *Can. J. Chem.*, **47**, 2521.

Valcarcel, M. and Gallego, M., (1989), *Practical Spectroscopy*, 7, 157.

van den Berg, C.M.G., Murphy, K. and Riley, J.P., (1986), *Anal. Chim. Acta*, **188**, 177.

Vogel, A.I.,(1961), *A Textbook for Quantitative Inorganic Analysis*, 3rd Edn. Longmans, London.

Vogt, R., Seip, H.M., Christophersen, N. and Andersen, S., (1990), *Sci. Total Environ.*, **96**, 139.

Vukomanovic, D.V., Page, J.A. and Vanloon, G.W., (1991), *Can. J. Chem.*, **69**, 1418.

Wang, E. and Liu, A., (1991), *Microchem. J.*, **43**, 191.

Wang, J. and Freiha, B.A., (1985), *Anal. Chem.*, **57**, 1776.

Wang, J. and Hutchins, L.D., (1985), *Anal. Chim. Acta*, **167**, 325.

Wang, J. and Tian, B., (1992), *Anal. Chem.*, **64**, 1706.

Wang, J. and Tian, B., (1993), *Anal. Chim. Acta.*, **274**, 1.

Wang, J., (1994), *Analyst*, **119**, 763.

Wang, J., (1996), *"Electrochemical Preconcentration"*, in Laboratory Techniques in Electroanalytical Chemistry., **pp.719.**, Kissinger, P. T. and Heineman, W. R. (Editors), Marcel Dekker, Inc., NY.

Wang, J., Farias, P.A.M., and Mahmoud, J. S., (1985), *Anal. Chim. Acta*, **172**, 57.

Wang, J., Lu, J., Tian, B. and Yarnitzky, C., (1993), *J. Electroanal. Chem.*, **361**, 77.

Wang, J., Nascimento, V.B., Lu, J. Park, S.S. and Anges, L., (1996), *Electroanalysis*, **8**, 635.

Waring, C.P. and Brown, J.A., (1995), *Fish Physiol. and Biochem.*, **14**, 81.

Watteau, F. and Berthelin, J., (1994), *Eur. J. Soil Biol.*, **30**, 1.

Willard, H.H. and Dean, J.A., (1950), *Anal. Chem.*, **22**, 1264.

Williams, R.J.P., (1996), *Coord. Chem. Rev.*, **149**, 1.

Wood, C.M., Playle, R.C., Simons, B.P., Goss, G.G. and Mcdonald, D.G., (1988), *Can. J. Fish. Aquat. Sci.*, **45**, 1575.

Wright R.F., Lotse E. and Semb A., (1988), *Nature*, **334**, 670.

Wunderlich, C.-H. and Bergerhoff, G., (1994), *Chem. Ber.*, **127**, 1185.

Zelazny, L.W. and Jardine, P.M., (1989), *'Surface reactions of aqueous aluminium species.'*, in The Environmental Chemistry of Aluminum., **pp. 147**, Sposito, G. (Editor), CRC press, Florida.

Zhang, J. and Anson, F.C., (1993), *J. Electroanal. Chem.*, **353**, 265.

Zhang, J., Lever, A.B.P. and Pietro, W.J., (1994), *Inorg. Chem.*, **33**, 1392.

Zittel, H.E. and Florence, T.M., (1967), *Anal. Chem.*, **39**, 320.